Optical and Other Methods for the Assessment of Arterial and Venous Insufficiency

Paul. T. Williams

A thesis submitted to the School of Engineering, Cardiff University for the degree of Doctor of Philosophy

Institute of Medical Engineering and Medical Physics

June 2011

Declaration and Statements

This work has not previously been accepted in substance for any degree and is not being concurrently submitted in candidature for any degree.

Signed …….(candidate)
Date ……

Statement 1

This thesis is the result of my own investigations, except where otherwise stated. Other sources are acknowledged by footnotes giving explicit references. A bibliography is appended.

Signed ……...(candidate)
Date ……...

Statement 2

I hereby give consent for my thesis, if accepted, to be available for photocopying and for interlibrary loan, and for the title and summary to be made available to outside organisations.

Signed ……..(candidate)
Date ……..

Acknowledgements

I would like to thank ArjoHuntleigh UK for financing this project and particularly to Dr N. Gough for his help and support throughout this work.

My heartfelt thanks go to the patients and also to the staff of the Medical Physics and Clinical Engineering Department, who kindly acted as volunteers, some of whom gave up their evening to support this project.

I am also sincerely thankful to Dr N. Pugh and Dr D. Coleman for taking the time to listen to my many Friday afternoon presentations and to their advice and guidance writing this thesis.

I am indebted to Dr R. Morris and Dr C. Wells for listening to my wild ideas and my many requests for help and assistance, on too many occasions, and for giving me the confidence to carry on.

A special thanks to Professor J.P. Woodcock who has given me nothing but support over the 23 years I have known him and who gave me the chance to enter a profession that looked out of reach. I would also like to thank Professor P. Wells who stepped in as my supervisor towards the end and gave me valuable help and advice.

As always I would like to thank my friends and family for their unending support over a long and tortuous educational route, particularly to my mother and father who never stopped believing in me, to Carol and Bob who countless times have been there when I have not, to my children, Jessica and Jacob, for keeping me young and finally to my darling wife, Hilary, who is my life.

Paul.

Abstract

There are a number of different techniques used to diagnose vascular insufficiency ranging from expensive hospital based equipment to less expensive devices used in primary care centres. Currently, some of these devices are unsuitable for use on patients with diabetes or DVI and have poor sensitivity for detecting moderate PAD patients. Additionally, some of the tests, particularly for DVI, require tourniquets or the patient to perform postural changes which some may find difficult. This may extend testing time. The study investigated 2 groups of patients, one with PAD and the other with DVI. The arterial group consisted of 46 controls and 57 patients. PPG probes were placed on the index finger and great toe. The venous group consisted of 24 controls and 25 patients and PPG probes were placed behind the knee and 10 cm above the medial malleolus. Duplex ultrasound was used as the gold standard to assess the arteries and veins in the lower limbs. The aim was to investigate whether signals acquired from patients at rest using Photoplethysmography (PPG) could be used as a screening tool. Pulse wave transit time (PWTT) and shape analysis techniques were used on the pulses from the patients with PAD, while time base and spectral analysis techniques were used on the waveforms of patients with DVI. PWTT and shape analysis techniques achieved sensitivities and specificities of 82% and 84% respectively. Accuracy dropped to 70% for detecting patients with moderate PAD. Spectral analysis techniques gave the best results for detecting patients with DVI achieving sensitivities and specificities of 69% and 80% respectively. In conclusion, reducing the signal acquisition time on patients with PAD did not significantly reduce the sensitivity and specificity. Without any patient movement it was difficult to separate patients with DVI from healthy normals.

Contents

List of Figures

List of Abbreviations

AAA	Abdomen aortic artery
ABPI	Ankle brachial pressure index
AC	Alternating current
A-mode	Amplitude modulation
ANN	Artificial neural network
APG	Air plethysmography
ATA	Anterior tibial artery
AUNP	Area under normalised pulse
AVP	Ambulatory venous pressure
B-mode	Brightness modulation
CDI	Colour duplex imaging
CDM	Complex demodulation
CEAP	Clinical etiological anatomical patho-physiological
CFA	Common femoral artery
CFD	Colour flow duplex
CFI	Colour flow imaging
CFV	Common femoral vein
CIV	Common iliac vein
CTA	Computer tomography angiography
CVI	Chronic venous insufficiency
DC	Direct current
DFT	Discrete Fourier Transform
DPA	Dorsal pedis artery
DVS	Deep venous system
DVT	Deep venous thrombosis
ECG	Electrocardiogram
EDV	End diastolic velocity
EF	Ejection fraction
EIA	External iliac artery
EIV	External iliac vein
EV	Expelled volume
FFT	Fast Fourier Transform
FN	False negative
FP	False positive
GP	General Practitioner
Hb	Reduced haemoglobin
HbO_2	Oxyhaemoglobin
IC	Intermittent claudication
IIA	Internal iliac artery
IPPG	Impedance plethysmography
IR	Infra-red
IVC	Inferior vena cava
LD	Laser Doppler
LDF	Laser Doppler flow
LSV	Long saphenous vein

MRA	Magnetic resonance angiography
NIMH	Nickel metal hydride
$PaCO_2$	Partial pressure of carbon dioxide
PAD	Peripheral arterial disease
PaO_2	Partial pressure of oxygen
PAOD	Peripheral arterial occlusive disease
Patrium	Central venous pressure
PFA	Profunda femoris artery
PFV	Profunda femoral artery
Phydro	Hydrostatic pressure
PI	Pulsatility index
Pocc	Pressure through outflow obstruction
POH	Post occlusive hyperaemia
PPG	Photoplethysmography
PSV	Peak systolic velocity
PTA	Posterior tibial artery
PTS	Post thrombotic syndrome
PV	Perforator vein
Pv	Venous resting pressure
PWTT	Pulse wave transit time
PWV	Pulse wave velocity
RF	Refill time
RI	Resistance index
RI	Reflection index
RMSE	Root mean square error
ROC	Receiver operator curve
SFA	Superficial femoral artery
SFJ/I	Saphenous femoral junction incompetence
SFV	Superficial femoral vein
SGPPG	Strain gauge plethysmography
SI	Shape index
SPJ/I	Saphenous popliteal junction incompetence
SpO_2	Saturated partial pressure of oxygen
SSV	Short saphenous vein
SVS	Superficial venous system
$tcpCO_2$	Transcutaneous partial pressure of carbon dioxide
$tcpO_2$	Transcutaneous partial pressure of oxygen
THM	Traube Hering Mayer
TN	Test negative
TP	True positive
USB	Universal serial bus
VI	Venous insufficiency
VO	Venous pump power
VOT	Vein occlusion test
VRT	Venous refill time
VV	Venous volume

1 Introduction and Background:

Peripheral vascular disease does not have a precise meaning, but in general refers to diseases that affect the arterial, venous and lymphatic systems of the lower limbs (Fowkes, 2004).

Vascular disease can be a very debilitating condition. With peripheral arterial disease (Meissner et al.) as arteries narrow, the blood supply to the lower limbs becomes compromised and patients can experience pain on walking, called intermittent claudication (IC) (Meissner et al., 2007). Progression of the disease can lead to critical limb ischaemia and possible amputation (Ouriel, 2001). Chronic venous insufficiency (CVI) affects the superficial venous system (SVS), the deep venous system (DVS) or both. CVI can be caused by primary abnormalities of the vein walls and valves or secondary changes due to a previous venous thrombosis. This can obstruct venous outflow from the lower limbs or damage the valves leading to reflux and subsequent failure to correctly return blood back to the heart. Over time, this may result in a variety of symptoms such as tired legs, oedema and in more advanced cases leg ulcers that are uncomfortable or distressing for the patient (Nicolaides, 2000).

Intermittent claudication affects 5% of those between 55 to 75 years, with the incidence of critical limb ischaemia estimated at 500-1000 per million population per year (Fowkes, 2004). Peripheral vascular disease is a considerable burden on the health care system with significant cost implications. The population most at risk from this disease are people of advanced age (>50yrs), smokers and diabetics. Other

risk factors for PAD include hypertension, hyperlipidemia, male sex, prior myocardial infarction and history of stroke (Ouriel, 2001). Claudicants have a two to three fold increase in mortality compared with non-claudicants, mainly due to associated coronary heart disease. Fifty percent of amputee patients from PAD die within 5 years (Fowkes, 2004).

Venous disease also has a high economic impact with spending of between 1% and 2% of the European health budget. In the United States of America between 1.9 and 2.5 billion dollars per year are devoted to venous disease (Callejas and Manasanch, 2004).

An early diagnosis of PAD and CVI would be advantageous as the earlier they are diagnosed the quicker treatment can begin, also there is a strong link of PAD and future cardiovascular events such as myocardial infarction or stroke (Dachun et al., 2010).

Current hospital based techniques used to assess patients for PAD and CVI include angiography and colour duplex imaging (CDI). However these imaging methods are relatively expensive and require a skilled operator to perform and interpret the images. Other less expensive technologies used to assess patients with PAD and CVI such as plethysmography and laser Doppler, provide the clinician with less information as to the nature and extent of the disease, compared to CDI, but they require less user training and are a fraction of the cost.

Primary care uses less expensive hand held Doppler technology to assess patients for PAD, but this is unsuitable for diabetics and has poor sensitivity when identifying patients with moderate lower limb disease (Stein et al., 2006). Plethysmographic techniques used to assess patients with CVI require pneumatic cuffs or tourniquets fitted to the lower limbs which can be time consuming, ill fitting and an infection control risk. Other methods require patients to perform certain manoeuvres which some may find difficult to execute due to their physical condition or age. Therefore these methods are only used in specialist vascular laboratories and not in primary care setting.

A General Practitioner, (GP) at present will take a family history and perform a clinical examination as the first step of diagnosing a patient's condition. If the clinical signs and symptoms are clearly vascular in nature, then the primary care clinician can send the patient to hospital or a specialist vascular clinic for further investigation as to the nature, extent and severity of the disease,. However, if the clinical signs and symptoms are ambiguous, then the clinician may use a non-invasive technique, such as a hand-held Doppler device to supplement the clinical examination and thereby provide additional evidence as to the nature and cause of the patient's condition. However at present, these non-invasive techniques can be cumbersome and time consuming.

If these existing non-invasive technologies could be used to assess for vascular disease without the need for cuffs or patient movement and give a simple yes or no diagnosis for the presence of vascular disease, then this would be an advantage over

current screening methods. This might potentially reduce the number of patients sent for further investigation for suspected vascular insufficiency

The aims of this thesis are to:

- Identify a technology that could be used to screen for vascular disease in primary care that requires minimal user training and is relatively cheap.

- Investigate a technique using that technology that requires minimal time minimal patient intervention and minimal patient effort.

2 Anatomy and Physiology of the Circulatory System:

2.1 Arteries

The heart is the organ responsible for pumping blood to the major parts of the body, such as the head, arms and lower limbs. Blood transports oxygen to the tissues of the body, it leaves the left ventricle of the heart and enters the aorta, the largest artery in the body. The aorta has two principal branches, namely the ascending and descending aorta, and it the latter that provides the lower part of the body with blood. Branches of the aorta progressively become smaller as they travel distally, becoming arterioles and eventually capillaries, where the transfer of oxygen into the tissue takes place. Arterial anatomy is described in more detail below

2.1.1 Anatomy

In more detail, the aorta is split into four main sections: ascending aorta, aortic arch, thoracic aorta and the abdominal aorta. The abdominal aorta continues to the 4th lumbar vertebra where the vessel bifurcates into the common iliac arteries (Bernardi et al.). These two vessels feed the lower limbs and split further into the internal iliac artery (IIA) and external iliac artery (EIA). The internal iliac supplies the bladder, rectum and reproductive organs, while the external supplies the lower pelvis and leg. At groin level the external iliac becomes the common femoral artery (CFA), which then bifurcates into the superficial femoral artery (SFA) and the profunda femoris artery (PFA). The PFA feeds the thigh, while the SFA continues distally, gradually

becoming deeper until it reaches the distal adductor region, just above the knee. The SFA then joins the popliteal artery at knee level. The popliteal artery trifurcates into three principal tibial arteries: Anterior tibial artery (ATA), which feeds the front of the lower leg, Posterior tibial artery (PTA), which feeds the back of the lower leg and the peroneal artery, which feeds the medial lower leg. As the ATA travels onto the trough it becomes the dorsalis pedis artery (DP) (Scanlon, 1997).

2.1.2 Structure and Function:

Investigations have revealed that arteries are not simple passive conduits that only transport blood to different parts of the body, but are intricate adaptive vessels that can change their diameter in response to acute internal or external stresses. They are also affected in the long term by chronic conditions such as hypertension, obesity and cigarette smoking. Arteries age by becoming dilated and stiffer, due to the cyclical change in diameter from the 2 billion heart beats on average in a person's lifetime. Arteries have several layers to be able to withstand these different states, and these are described in more detail below (Rutherford, 1995).

When we see an artery in cross section it has three distinct layers: tunica intima, tunica media and the tunica externa (adventitia). The tunica intima is the inner most layer, which extends from the luminal surface to the internal elastic lamina. It consists of endothelial cells that are extremely smooth, which helps to prevent blood clotting. The middle layer, the tunica media is composed of smooth muscle and elastic connective tissue. Both of these help in the maintenance of normal blood pressure, particularly diastolic blood pressure when the heart is relaxed. The outermost layer,

the tunica externa consists of fibrous connective tissue. This needs to be strong to prevent the artery rupturing at high pressures during the systolic phase of the heart beat (Scanlon, 1997). Arterioles have a smaller lumen diameter and practically no outer coating of elastic fibres. They consist mostly of endothelial cells and smooth muscle fibres, which allows them to produce more active tension by dilation or contraction. This has the affect of changing the lumen diameter of the vessel and so controlling the amount if blood entering the vascular bed (Burton, 1965).

Depending on their function within the body, arteries can be subdivided into two main groups: elastic or muscular. The large central arteries in the body such as the aorta and its immediate proximal branches are called elastic arteries because there is a greater extent of thick and closely packed elastic fibres than smooth muscle cells within the tunica media. This allows for greater compliance and recoil of the vessel wall during pulse propagation after a cardiac beat. Distal to the large elastic central arteries are the muscular arteries (Femoral, brachial and radial) so called because they contain relatively less collagen and elastin and more smooth muscle cells, therefore enabling them to change their diameters quickly by constricting or dilating. This allows them to adapt to any acute haemodynamic changes occurring within the body (Rutherford, 1995).

2.1.3 Disease

Arterial disease can be split into two main categories: that which narrow the lumen of the vessel and therefore obstruct the blood flow, and secondly, that which weaken the walls of the vessel and cause it to dilate. The intracranial, abdominal aorta and popliteal arteries are the common places where dilation of the blood vessels can

occur. Localised dilation of a main artery such as the abdominal aorta, termed an abdominal aortic aneurysm (AAA), can be life threatening if not operated on quickly, after reaching a certain diameter. However, obstructive disease can affect many arteries in the body including the carotid, coronary and many of the lower extremity arteries. There is an increased risk of Cardiovascular and cerebrovascular events, including death by myocardial infarction and stroke with this type of arterial disease. Peripheral arterial disease is a term used to describe obstructive arterial disease external to the coronary and intracranial vessels and technically includes the extracranial carotid circulation, upper limb arteries and the mesenteric and renal circulation. However this thesis will only focus on obstructive disease in the abdominal aorta, the iliac vessels and the arteries of the lower limbs (Ouriel, 2001).

2.2 Veins

The venous anatomy of the lower limbs in some respects is more complicated and varied than its arterial counterpart. However, to aid our understanding the venous system has been divided into a number of different subsystems: Deep, superficial, communicating and perforator veins.

2.2.1 Anatomy of the lower Extremity Veins

The veins in the lower extremities can be categorised according to the compartment in which they travel. Two compartments are created by a thin layer of tissue, called the fascia that travels the entire length of the leg. The superficial compartment consists of the tissue between the skin and the fascia, and the deep compartment includes all tissue between the fascia and the bone (Figure 1).

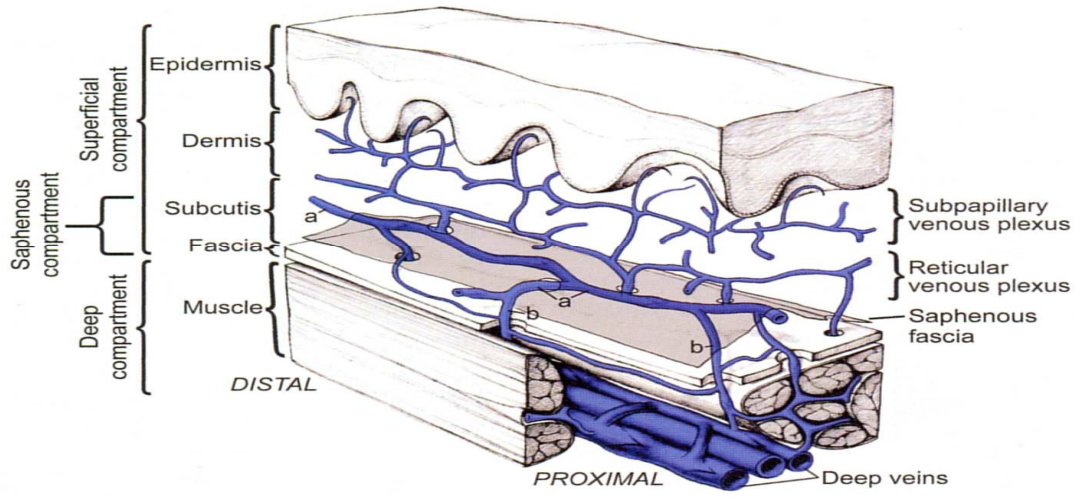

Figure 1 Relationship between fascia and veins in the lower extremity (Bergan, 2006).

A third major category consists of veins which connect the superficial and the deep veins. These veins pierce the fascia which separates the two compartments and are therefore called perforating veins. Communicating veins connect veins within the same venous subsystems.

2.2.1.1 Superficial and Perforator Veins

The Subpapillary and Reticular venous plexus are drained by small superficial veins, which form bigger tributaries that eventually all connect into the saphenous veins. From the ankle the Long Saphenous Vein (LSV) travels medially to the knee (Figure 2). Proximal to the knee the LSV ascends on the medial side of the thigh and enters the fossa ovalis, where it ends at the confluence of the superficial inguinal veins (saphenofemoral junction) joining the Common femoral vein (CFV).

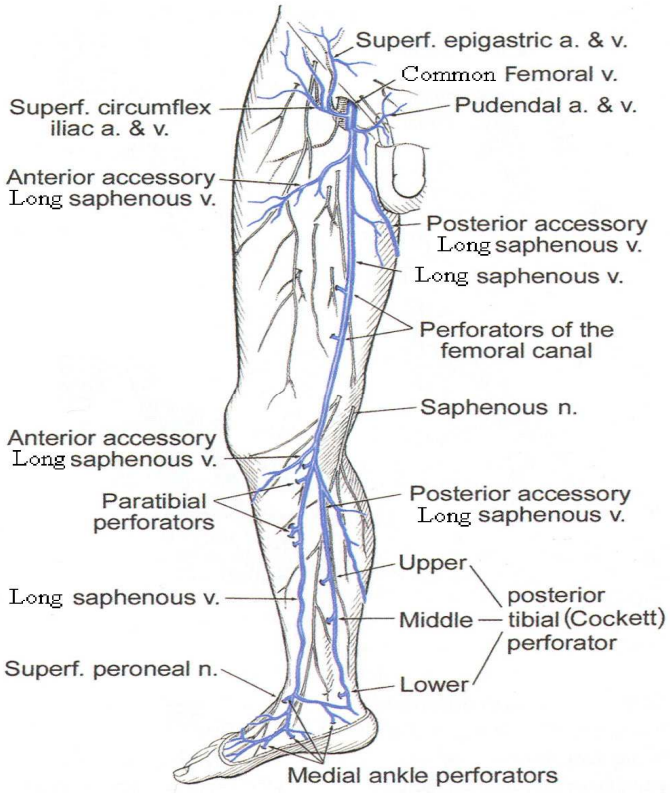

Figure 2 Superficial and perforating veins of the leg. Adapted from (Bergan, 2006).

The Short Saphenous vein (SSV) lies lateral to the Achilles tendon in the distal calf. It ascends posterior, firstly running in the subcutaneous fat and then piercing the fascia and eventually joining the deep popliteal vein approximately 5cm proximal to the knee crease. Perforating veins act as a conduit between the deep and superficial venous systems by crossing the muscular saphenous facia that separates them (Meissner et al., 2007). There can be greater than 100 perforating veins (PVs) in the lower extremities, however only a small number of these are clinically relevant. Of particular importance are the medial calf perforators and these have two groups: posterior tibial and paratibial PVs. The posterior tibial PVs can be further divided into Cockett I-III which connects the posterior accessory LSV to the PTVs. The paratibial perforators drain the LSV into the posterior tibial veins.

Superficial veins usually have their valves located at the termination of major tributaries. Some valves are robust, while others are more delicate in their structure. In the LSV there are approximately 6 valves, with more located below than above the knee. Common to most people, the LSV has a valve 2-3cm distal to its confluence with the SFV. Valves in the SSV are closer together than in the LSV. Valves in communicating branches between the SSV and the LSV are orientated to direct blood from the SSV to the LSV.

2.2.1.2 Deep Veins

On the dorsum of the trough the pedal vein drains the deep dorsal digital veins through the dorsal metatarsal veins. The pedal vein continues in the anterior tibial veins.

There are three pairs of deep veins in the calf, with their associated arteries: the peroneal, posterior and anterior tibial veins. These join at just below knee level to form the popliteal vein, which meets the short saphenous vein (SSV), a superficial vein. The gastrocnemius and soleal veins drain venous sinuses in the calf muscle and also join the popliteal vein. Venous sinuses are closely related to deep veins and can hold large amounts of blood which is pumped proximally, with the contraction of the calf muscles, by the action of walking. As the popliteal vein continues it passes into the adductor canal where it becomes the superficial femoral vein (SFV, superficial only in name, it is still classified as a deep vein). The popliteal and SFV are frequently duplicated. The SFV travels proximally and joins the deep femoral also know as the profunda vein and long saphenous veins (PFV and LSV respectively) in the groin, where it now becomes the common femoral vein (CFV). After passing under the inguinal ligament it becomes the external iliac vein (EIV), which then joins with the internal iliac vein (IIV) to become the common iliac vein (CIV), which joins with the contralateral CIV in the inferior vena cava. Frequently the femora-popliteal segment communicates with the profunda vein through a large collateral, providing an important alternative for venous drainage in case of a femoral vein occlusion.

Similar to superficial veins, deep veins have more valves in the calf than in the thigh. The tibial veins are densely packed with valves in contrast to the poplieal vein where there are only one or two valves. There are three to five valves in the SFV, with one located just distal to the junction of the profunda vein. There is usually one valve in the CFV. There are one to three valves all located below the level of the fascia and these ensure that venous blood is directed toward the deep veins. Small PVs are usually valveless (Bergan, 2006).

2.2.2 Circulation

The purpose of the heart is to pump arterial blood to different parts of the body, ensuring that the organs and tissues receive the oxygen and nutrients they require in exchange for carbon dioxide and waste products that need to be removed from the tissue. Deoxygenated blood that leaves the capillaries and enters the venous system is 'pumped' back to the heart, by two mechanisms:

The calf muscle pump effectively pushes blood up from the lower extremities by compression of the muscles in the calf, which are activated when walking. This action decreases the pressure in the deep veins and allows higher pressure venous blood in the superficial system to flow into the deep venous system via perforating veins; whose valves are arranged to prevent blood flowing back into the superficial system. While walking this cycle continues, reducing high pressure which builds up in the calf while at rest; which can reach pressures as much as 100mmHg when standing.

Respiration, and the subsequent action of the diaphragm, causes the pressure within the abdomen to increase and decrease which controls the flow of venous blood back to the heart. During inspiration the ribcage expands causing the diaphragm to descend into the abdominal cavity. This action decreases the pressure within the thorax, increases the pressure within the abdomen and subsequently there is an increase in pressure gradient along the Inferior Vena Cava (IVC) (Figure 3). Therefore any venous blood in the abdominal IVC is encouraged back to the heart. At this time there is minimal venous return from the lower limbs. During expiration, minimal pressure gradient along the IVC results in minimal flow here. However, the recoil of the diaphragm reduces the pressure in the abdomen and therefore the abdominal IVC

refills with venous blood from the lower limbs (Figure 4). Therefore venous return to the heart from the lower limbs exhibits a phasicity that is maximum during expiration and minimum during inspiration (Oates, 2001).

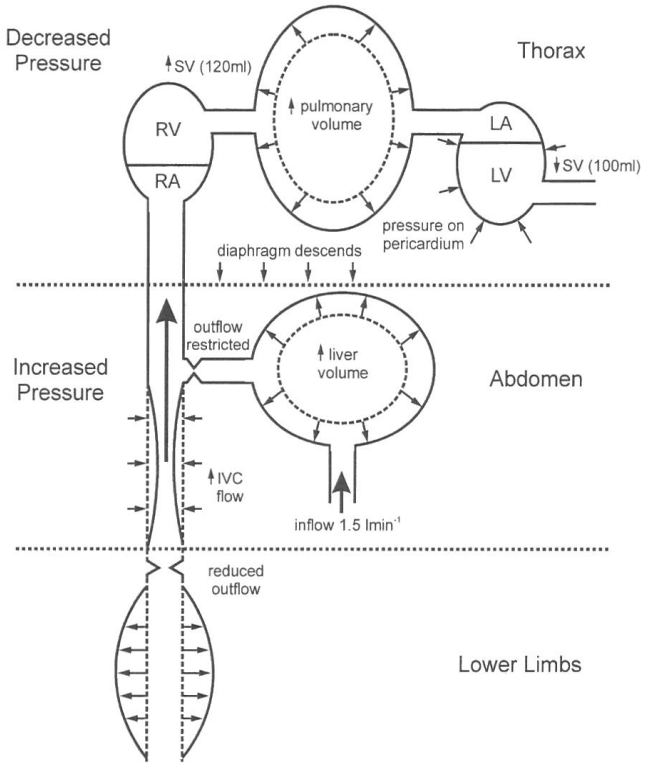

Figure 3 The respiration pump during inspiration (Oates, 2001).

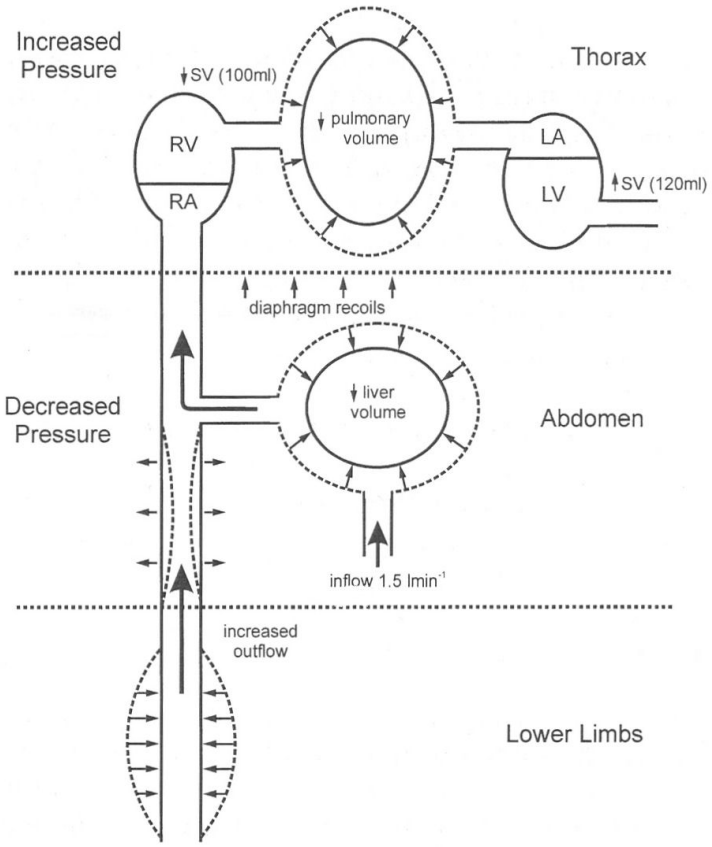

Figure 4 Respiration pump during expiration (Oates, 2001).

2.2.3 Venous Disease

Venous anatomy and physiology must be thoroughly understood by the clinician if an accurate diagnosis is to be made, therefore ensuring that the subsequent treatment and therapy is appropriate and timely. Venous anatomy consists of two main networks, a superficial and a deep venous network and these are interconnected at certain points by a system of perforating veins. Any one or a combination of these networks can fail, termed venous insufficiency (VI), either primarily from vein wall weakening and valve dysfunction, or from secondary pathologies caused by a venous thrombosis, which can lead to reflux, obstruction or both. When either the superficial or the deep venous system fails, leading to sustained venous hypertension, the resulting clinical condition, known as chronic venous insufficiency, (CVI), can have mild or more

severe symptoms. These venous systems are described below with particular attention being paid to CVI caused by a previous DVT and the associated clinical signs and symptoms known as the post-thrombotic syndrome (PTS).

Primary varicose veins alone, which are the result of vein wall weakness and valvular dysfunction without significant skin changes, are not sufficient for a diagnosis of CVI. Primary varicose veins are more often the result of incompetent valves at the junctions where the superficial veins join the deep veins, typically examples being the sapheno-femoral junction (SFJ/I) or the sapheno-popliteal junction (SPJ/I). They are generally visible and are more of a cosmetic problem that can often be corrected by surgery. A hand-held continuous wave Doppler unit can be used in a GP surgery to confirm the site of reflux, however, further ultrasound investigation is required if a complete and thorough diagnosis is needed, as many other sites of potential reflux can not be established with a hand-held device because the veins are too deep.

Chronic venous insufficiency is a broader term that involves structural and functional abnormalities of the superficial venous system (SVS) or the deep venous system (DVS) or both (Nguyen, 2005). The signs and symptoms of CVI are the result of ambulatory venous hypertension. This is defined as the failure to reduce venous pressure with exercise. Normally a combination of calf muscle pump and vein valves help to reduce the venous pressure in the lower extremity veins, which can reach venous pressures of 90 to 100mmHg when standing (Burton, 1965). When the valves are functioning correctly, venous blood travels distal to proximal and from superficial to deep veins. If the calf muscle pump fails either due to outflow obstruction from chronic thrombus, or valve failure, the venous pressure remains abnormally high. If

the valves in the deep veins are incompetent, the blood in the lower limbs pool and there is no reduction in pressure. Prolonged abnormally high venous pressure in the lower extremities is termed chronic venous hypertension and can result in a range of pathological effects of the skin and subcutaneous tissue. Sustained venous hypertension can lead to the signs and symptoms of CVI. However in some cases the perforator veins can act as conduits for the high pressure deep venous blood to escape into the lower pressure superficial veins. In this case venous blood travels from the deep to superficial veins, which is the reverse direction of normal lower limb venous blood flow. The superficial veins then act as collaterals for the deep venous blood in an attempt to lower the abnormal high venous pressure, but in-doing so the superficial veins become a higher pressure venous system. Since the superficial veins do not have a muscular support, unlike the deep veins, they become varicosed. When superficial veins act as collaterals the progress of CVI can be delayed (Nicolaides, 2000).

Symptoms of CVI include, aching, heaviness, leg tiredness, cramps, itching, sensation of burning and swelling. Signs include telangiectasia and reticular veins (spider veins), varicose veins, oedema. Additionally, the skin can change in appearance, also known as trophic changes, such as eczema, (erythematous dermatitis or reddening of the skin), hyper-pigmentation, (a brownish darkening of the skin), lipodermatasclerosis, (localised chronic inflammation and fibrosis of the skin), and ulceration. The significance of trophic changes is a sign of more severe CVI.

Of particular importance to this study is the development of CVI due to a previous acute DVT, known as the post-thrombotic syndrome (PTS). Approximately one third of patients with a previous acute DVT will develop PTS within 5 years (Bernardi and

Prandoni, 2000). However the precise incidence of PTS varies among published studies between 20 and 100%; although in recent studies the incidence has reduced to approximately 30 to 60%, probably due to increased diagnostic accuracy (Bergan, 2006). The post-thrombotic syndrome can progress from mild signs and symptoms of pain, slight swelling and cramp to severe cases of lipodermatosclerosis, hyper-pigmentation and in certain cases of recurrent DVT, ulceration. The incidence of patients going on to develop ulcers is approximately 3 to 8%. This severe form can occur in one quarter to one third of patients with PTS and it is therefore costly to society and is a cause of substantial patient morbidity (Kahn and Ginsberg, 2004). A recent study however revealed that a quarter of limbs they tested with trophic changes to the skin did not have functional venous disease. In the same study 26% of limbs with oedema were normal functionally, with no varicose veins or trophic changes (Criqui et al., 2003). In most cases CVI is clinically apparent particularly with associated varicose veins, however a number of other diseases have similar clinical features such as cellulitis, periarteritis nodosa, ruptured Baker's cyst, rheumatoid arthritis, gout, arterio-venous malformation of the calf muscles, limb pain and swelling from adverse drug reactions and numerous other dermatological conditions. Mixed arterial and venous pathologies, particularly in the elderly, can mask some venous symptoms. Since approximately 30% of DVTs are silent or asymptomatic, further development of the PTS will not have any obvious underlying source. In addition, a DVT following trauma or surgery can be hidden under the symptoms of post-operative pain.

CVI and its associated signs and symptoms are a considerable and costly burden on society, in western countries in particular due to its high prevalence, cost of

investigations and loss of working days. Varicose veins are present in 25% to 33% of females and 10% to 20% in male adults. The prognosis of venous leg ulcers is poor, only 50% heal in 4 months, 20% remain open at 2 years and 8% remain open at 5 years. In the United Kingdom the annual cost of venous ulcers has been estimated to be £400 to £600 million and greater than 1 billion dollars for the United States (Nicolaides, 2000).

A history and clinical examination will often not give the full nature and extent of the abnormality, therefore a number of diagnostic techniques have been developed to help the clinician make a more informed diagnoses of CVI.

2.3 Microcirculation

The large and muscular arteries serve as vessels solely for the distribution of oxygenated blood to the tissues. The major veins serve to take deoxygenated blood back to the heart. Between these are the arterioles, capillaries and venules which make up the microcirculation. Here and particularly in the capillaries, oxygen and nutrients are exchanged for carbon dioxide and other waste products from the tissue. The follow section describes the microcirculation in more detail, explaining the anatomy and then how it is controlled.

2.3.1 Anatomy of the Microcirculation

The diameter of arterioles range from 5-100μm and they have three distinct layers; a thick smooth muscle layer, a thin adventitial layer and an endothelial lining. Arterioles feed directly into capillaries that have diameters in the range of 5-10μm

and are the smallest blood vessels in the body. In some tissue metarterioles of diameter 10-20μm feed capillaries directly or they bypass the capillary bed completely, known as arterio-venous shunts (AV shunts) and directly feed the venules. Because of their smooth muscle wall, arterioles, also known as resistance vessels, are able to alter their diameter thereby controlling the amount of blood entering the capillaries. The amount of capillaries in tissue depends on its metabolic activity. Cardiac and skeletal muscles have numerous capillaries but less active tissue, such as subcutaneous tissue has fewer. Blood flow through capillaries may be random or have a rhythmic flow caused by the contraction and relaxation of the smooth muscles of the precapillary vessels. A difference in the intravascular pressure and the extravascular pressure, known as the transmural pressure can also cause the precapillary vessels to alter their diameters and therefore control capillary blood flow. Capillaries can alter their shape in response to certain chemical stimuli, but this is a passive response to changes in precapillary or postcapillary changes in resistance and is not an active change that controls blood flow. On leaving the capillaries the blood drains into the venules. These are generally larger than the arterioles but they have weaker vessel walls. These venules merge to form larger and larger veins and in doing so conduct the deoxygenated blood back to the heart (Scanlon, 1997).

2.3.2 Control of the Microcirculation.

Control of blood flow through the microcirculation can be split broadly into two main control mechanisms; local control from conditions in the immediate area of the blood vessels and central control via the nervous system. These will be explained in more detail below.

2.3.2.1 Local Control

Changes in perfusion pressure or metabolic activity of the surrounding tissue elicit autoregulatory mechanisms that maintain blood flow by altering the tone of the smooth vascular muscle and which in-turn controls total peripheral resistance. These mechanisms are:

1. Myogenic control of the diameter of the arterioles in response to an increase in perfusion pressure. An initial passive increase in vessel diameter and therefore increased blood flow is followed by a contraction of the vessel and a return to previous blood flow levels.
2. Endothelial control is prompted from the rapid blood flow through the vessel which produces vasoactive factors that regulate the vessel diameter. Vasodilation is caused by nitric oxide which is released from the endothelial cells.
3. Increased metabolic activity or a reduction of oxygen in the surrounding tissue produces vasodilatory substances that increase blood flow. Conversely, a decrease in metabolic activity reduces the amount of vasodilatory substances and increases peripheral resistance and thereby reduces blood flow. It is unclear from current literature which substance is primarily involved.

2.3.2.2 Extrinsic or Central Control

Alteration of tissue blood flow can be controlled by local mechanisms as mentioned above or globally from nervous regulation by the brain. Nervous regulation is controlled by the autonomic nervous system and the part of this that controls the micro-circulation is called the sympathetic nervous system. The parasympathetic

nervous system regulates heart function but has little effect on the micro-circulation. Nervous control of the micro-circulation is described below.

Several regions in the brain, when activated, influence cardiovascular activity. One of these regions, called the vasomotor centre, controls vasoconstriction. Fibres connected to this region travel down the spinal cord eventually joining with the peripheral sympathetic nerve fibres which innervate the arterioles and venules and veins. The micro-vessels that are not sympathetically controlled are the capillaries, metarterioles and the pre-capillary sphincters. During rest, the tone of the micro-vessels is altered by stimulating or inhibiting the vasoconstrictor area of the brain. Stimulation causes the vessels to constrict and therefore impede blood flow, while inhibition causes vasodilation. Sympathetic activity is altered rhythmically by altering the frequency of impulses passing along the sympathetic nerves that join with the micro-circulation. These rhythmic changes are evident as oscillations in pulse pressure at respiration frequencies called Traube-Hering waves (0.15 to 0.4Hz) and also occur at even lower frequencies called Meyer waves (Levy, 2005).

Under normal stimulating conditions the micro-vessels are in a state of mild contraction, which is called vasomotor tone (Hall, 2005).

When there is a need for rapid adjustment of blood pressure, there are a number of vascular reflexes that feedback impulses concerning the physiological activity of the body to the vasomotor centre of the brain. These impulses travel along neural fibres from baroreceptors, chemoreceptors, hypothalamus, cerebral cortex and the skin (Levy, 2005).

Baroreceptors also know as stretch receptors can be found at specific points in the walls of a number of major systemic vessels, for example at the carotid sinus and the aortic arch,. The receptors respond to increases in blood pressure, which stretch the walls of the vessel and this has the affect of inhibiting the vasomotor centre. This results in peripheral vasodilation and therefore a lowering of blood pressure. When arterial pressure falls, the inhibitory effect of the baroreceptors is lost and blood pressure rises. Because baroreceptors respond rapidly to changes in blood pressure they have limited effect controlling it over prolonged periods of time. Baroreceptor impulse frequency is set to a new basal rate if the mean arterial pressure drifts higher or lower than previous levels.

Chemoreceptors are located at the carotid sinus and in the region of the aortic arch. They are specialised cells that respond to changes in arterial blood tension (PaO_2), CO_2 tension ($PaCO_2$) and hydrogen ion excess (Pasternak et al., 2004). A reduction in PaO_2 or an increase in $PaCO_2$ stimulates the cells. The carotid and aortic bodies respond by increasing the frequency of the nerve impulses to the vasomotor centre in the brain. The result is an increase in tone of the resistance and capacitance vessels and a subsequent increase in blood pressure. Chemoreceptors have a strong influence over the vasomotor centre only when arterial blood pressure falls below 80mmHg. In addition they play a far greater role in respiratory control than in pressure control.

Core-body temperature is controlled within a narrow range by the hypothalamus, the thermostat of the body, which is located at the base of the brain. The temperature of the blood perfusing through the pre-optic region of the brain is considered the body's

ultimate core temperature and monitoring of this region by the hypothalamus is performed to regulate core body temperature. However, receptors in other parts of the body also help regulate body temperature. The hypothalamus also receives temperature sensory information from receptors in the skin. Part of the hypothalamus is responsible for skin-temperature regulation of the body via sympathetic nerve pathways that innervate the micro-vessels of the skin. These receptors detect peripheral temperature fluctuations, but because there are more cold receptors than warm receptors the skin is more sensitive to a decrease in temperature. When the skin detects these changes a number of reflexes take place that increase body temperature, one of those being peripheral vasoconstriction. However, when the body becomes too hot, vasodilation of the peripheral vessels takes place to reduce body temperature.

Intrinsic and extrinsic control of peripheral vessels do not occur in isolation but they act together to form a comprehensive system of vascular regulation. Together they supply blood to areas of the body that need it and divert blood away from areas that do not. However different types of tissue will need different proportions of each control type. For the brain and heart to function at optimal performance, they need a constant blood supply and so this is largely intrinsically controlled; in the skin however, extrinsic control is dominant as sympathetic and hypothalamic activity controls vasoconstriction of the cutaneous vessels. Nevertheless, central control of the resistance and capacitance vessels can be over-ridden by intrinsic mechanisms due to local changes in skin temperature. In resting skeletal muscle sympathetic control is dominant, but with the onset of exercise, local regulatory mechanisms take over as the demand for nutritive blood supply increases. Vasodilation occurs in vessels feeding active muscles, while vasoconstriction occurs in vessels supplying inactive muscle

tissue. Initially, sympathetic constrictor impulses will be sent to the active muscle tissue in an attempt to bring blood flow within normal limits, but this will be overridden by local metabolic control which will dilate the vessels (Scanlon, 1997).

3 Vascular Diagnostic Methods

Before any invasive or non-invasive vascular investigation is undertaken, the clinician will carry out a clinical evaluation which will entail a patient history and a physical examination.

The most common clinical presentation for peripheral arterial disease is intermittent claudication. This is pain experienced in the calf when walking and which is relieved when the patient rests. If this is left untreated the condition may progress to a point where the patient experiences pain even when stationary, called rest pain. This condition can progress to ulceration and gangrene. The physical examination encompasses palpation of the lower extremity pulses, generally at the ankle, knee or groin level. The pulses can be graded as normal, bounding, weak or absent. Hair loss, skin colour and trophic skin changes may also be noted as potential signs of arterial disease.

As with arterial insufficiency, a venous clinical evaluation starts with a patient history and physical examination. A visual inspection will reveal any skin changes such as atrophy, healed ulcers, oedema and pigmentation changes. Any visible vessels should be categorised as telangiectasias, reticular, phlebectasias or varicose veins. Their distribution should also be noted (Nguyen, 2005). This clinical assessment can form part of a more comprehensive venous classification system called CEAP. This system organises information into clinical, etiologic, anatomic and pathophysiologic (CEAP) categories. The venous assessment above, forms part of the clinical assessment in the

CEAP classification; the anatomic and pathophysiological categories would be assessed using duplex ultrasound at a specialist vascular clinical. More details of the CEAP classification system can be found in appendix B.

To help the clinician diagnose arterial or venous insufficiency, a number of different technological methods have been developed. Most are hospital or specialist vascular clinic based and can be separated broadly into a number of different categories:

X-ray Techniques:

- Angiography
- Phlebography

Optical and Other Techniques:

- Duplex Ultrasound (DU)
- Photoplethysmography (PPG)
- Impedance plethysmography (IPPG)
- Strain-gauge plethysmography (SGPPG)
- Air plethysmography (APPG)
- Laser Doppler (LD)
- Tissue Oxygen Saturation (SPO_2)
- Transcutaneous pressure O_2/CO_2 Tension (tc-PO_2/CO_2)
- Ankle Brachial Pressure Index (ABPI)
- Ambulatory Venous Pressure (AVP)
- Segmental Pressures

In general the invasive procedures give the clinician anatomical information, while the non-invasive procedures give hemodynamic information. As the name suggests invasive procedures can be very uncomfortable for the patient, often relying on the use of a needle or catheter inserted into an artery or vein. A contrast medium is then injected into the body which can be tracked as it passes through the vascular system of the body high-lighting the arteries and veins of interest to the clinician. The expense and discomfort of these procedures limits their application to patients with the most severe conditions or where the results of non-invasive procedures are equivocal. In contrast non-invasive procedures are relatively pain-free, normally relying on cuffs to measure arterial blood pressure at certain sites, such as the ABPI procedure, or tourniquets to occlude lower limb veins to distinguish between superficial or deep venous incompetence. Other non-invasive procedures use light to penetrate the tissue and estimate superficial blood volume beneath the probe from measuring the amount of back scattered light, as in PPG. Tc-pO_2/CO_2 and SpO_2 measurement technique can locally assess the body's ability to deliver oxygen to the tissue and remove carbon dioxide from it (Baumbach, 1986). The above techniques are described in more detail below.

3.1 X-ray Techniques

These techniques are hospital based and can be uncomfortable or stressful for the patient. They are utilised if the results of non-invasive techniques are equivocal.

3.1.1 Angiography:

Angiography and certain types of non-invasive imaging modalities, such as duplex ultrasonography, computed tomography and magnetic resonance angiography (MRA) have gained wide acceptance in recent years due to their diagnostic accuracy. However it is angiography that is still considered to be the gold standard by which all other vascular imaging modalities are judged (Nicolaides, 2000). In its basic form angiography consists of radiographic exposure of a sheet of x-ray film. An anatomic region of interest is positioned between an x-ray source and the film while a relatively radio-opaque agent is passed through the vessel of interest. In modern angiography a catheter is passed to the area of interest, in particular the arteries of the lower limbs, a radio-opaque agent flows through the catheter and into the arteries. X-ray images are taken and displayed on a monitor, which acts as a guide for the surgeon. Certain procedures can now be performed such as dissolving a clot with certain drugs or opening a partially blocked artery with a balloon (Rutherford, 2005).

3.1.2 Phlebography

Phlebography relies on injecting a contrast medium into an appropriate vein in the body and subsequently tracking its path by fluoroscope. The method is used to demonstrate patency of the veins and to detect reflux in the superficial or deep venous systems. The patient is placed during the procedure on a tilting table in the semi-erect or standing position. The disadvantages of phlebography are that it is invasive, costly and has potential complications due to possible patient reactions to the contrast medium. With the advent of non-invasive technologies such as duplex scanning, the demands for phlebograms have reduced (Nicolaides, 2000).

3.2 Optical and Other Techniques

These techniques are non-invasive and so are generally less painful or stressful for the patient. Most of the techniques as they are currently used involve cuffs, tourniquets or require the patient to perform manoeuvres that they may find difficult to perform considering their condition. Additionally, techniques such as duplex ultrasound require extensive user training. Also any physiological data gathered from a procedure that requires the patient to perform repeated movements may be inconsistent.

3.2.1 Ultrasound

As the name suggests ultrasound is above the range of human hearing. The consensus of opinion regarding the lower frequency limit for ultrasound is 20 kHz. Ultrasound is a form of energy which consists of mechanical vibrations that travel through a medium in the form of a longitudinal pressure wave. This wave disturbs the particles of the medium in a backwards and forwards manner, which has the effect of transmitting the energy in the wave in a direction parallel to that of the oscillation of the particles.

Common to most applications is brightness or B-mode imaging, also known as gray-scale sonography, however other disciplines such as echocardiography use motion mode also, while ophthalmology can use amplitude or A-mode. The following section will concentrate on B-mode imaging, which is the basic imaging technique use in ultrasound, and then go on to describe the various Doppler techniques.

Echo amplitude is represented by the brightness or grey scale on a visual display. A single line of the B-mode scan yields information about the position of the echo, given by

$$d = ct/2 \qquad \textbf{Equation 1}$$

where d is the distance from the transducer to the target; t is the time it takes for the pulse from the transducer to the target and back; and c is the sound velocity in tissue, which is assumed to be constant at $1540ms^{-1}$. The single lines of the B-mode scan are electronically combined to generate an ultrasound B-mode image of approximately 30 frames per second for modern scanners (Shung, 2006). This enables real time imaging of structures within the body. Distances can be measured and viewed on screen using the calliper tool. This is calculated by using the timing information stored within the memory matrix to measure anatomical structures such as the size of Abdominal Aortic Aneurysms (AAA), the diameters of arteries or veins.

When an ultrasound beam is fired at a moving target, such as blood, the reflected beam is shifted in frequency by an amount proportional to the velocity of blood. This effect is common throughout nature, where a source of sound energy moves in relation to an observer, and is called the Doppler Effect. For a target moving towards the transducer, the frequency of returning echoes, f_r, will be higher than f_t, or the transmitted frequency, and for a target moving away from the transducer, f_r will be lower than f_t. When measuring the velocity of blood however, the direction of blood flow will not generally be directly towards the transducer, but at some angle to it, called the Doppler Angle, and therefore the frequency relationship between the transmitted and received signals is

$$f_d = \frac{2vf_t \cos\theta}{c} \qquad \textbf{Equation 2}$$

where f_d is the Doppler shift in frequency between the transmitted and reflected wave, c, is the speed of sound in the blood, which is $1570ms^{-1}$ and θ is the angle subtended between the ultrasound beam and the direction of blood flow (angle of insonation) (Oates, 2001).

A convenient and informative way of displaying the Doppler signal over time is by a Doppler spectral display, or simply Doppler spectrum. This gives a complete visual description of changes in flow velocities occurring within the sample volume of the ultrasound beam. The range of velocities over time is shown on the x and y axes, and the brightness of the grey scale trace showing the level of the backscattered power at that frequency. It is important to note that the absolute velocity on the spectral display can only be calculated provided the angle of insonation is known. Without this the display shows just changes in Doppler frequency over time.

Pulsed wave Doppler uses a spatially well defined sample volume, which is able to detect local flow velocity phenomena, and can be narrowly adjusted and precisely focussed. Haemodynamical effects of any vessel narrowing can be assessed from the Doppler frequency spectrum as it changes its shape and amplitude. The degree of arterial narrowing or stenosis can be quantified by using the change in amplitude, and whether there is proximal or distal disease by changes in waveform shape (Hennerici, 1998).

Continuous wave Doppler uses a continuous beam of ultrasound, with overlapping ultrasound fields, from a transducer containing two piezoelectric elements, the transmitter and receiver. Due to this arrangement, no exact information about depth

can be obtained, and since the sample volume of the ultrasound beam is fixed, movement within any overlapping vessels is heard together making isolation of the vessel of interest more difficult.

Scanners are able to combine B-mode real-time imaging with Doppler so that anatomical information as well as blood flow data can be displayed at the same time; this is called duplex imaging. In this mode of operation, the display is normally split into two parts; the B-mode image and the Doppler spectrum image, with a cursor line superimposed onto the B-mode image to indicate the direction of the Doppler beam.

An alternative mode of operation is called colour flow imaging (CFI). A colour display is superimposed onto the B-Mode image to show areas within the image which are Doppler shifted. Conventionally, the colour red is used to indicate blood flow toward the transducer, and blue for blood flow away from the transducer. Different hues of colour will indicate different velocities of blood flow. Changes in velocity can occur for example due to normal changes in vessel calibre, due to a narrowing of the vessel lumen because of a stenosis or, changes in vessel angle with respect to the transducer. CFI will give the operator qualitative information about the degree of a stenosis, however, quantitative information can be obtained by using a third mode of operation called triplex or colour flow duplex (CFD). Here, qualitative information regarding haemodynamic flow is displayed on one part of the screen with CFI, while quantitative information regarding blood flow velocities is displayed separately. Both the CFI and the Doppler Spectral waveform are used together to obtain a complete picture of the area of interest, with regard to anatomical and haemodynamical information (Oates, 2001; Shung, 2006).

The Doppler arterial waveform can be separated into two distinct cardiac phases: the systolic and diastolic phase. The systolic phase occurs when the ventricles of the heart contract causing blood to be pushed out into the circulation. The diastolic phase occurs when the aortic valve closes and the ventricles are refilling. The diastolic phase can be divided further into two phases which are described below. A typical Doppler waveform of a healthy person taken from the lower limbs will look like that shown in Figure 5.

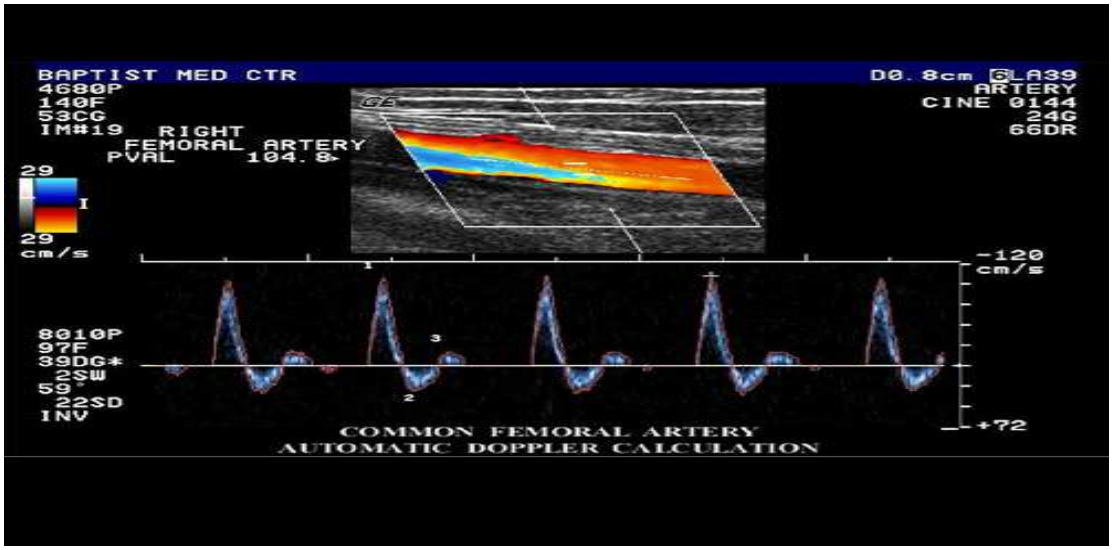

Figure 5 Triplex image showing Doppler signal (lower image) of blood flow from sampled arterial flow (top image). Triplex flow in the Doppler signal referring to three phases of flow: forward; reverse and finally forward flow.

This type of waveform is called triphasic, as there are three distinct phases during the cardiac cycle. Phase one is the forward flow during systole where there is a steep systolic ascent, a narrow peak, and a quick descent. In the second phase there is a short period of reverse flow caused by the primary pulse wave being reflected from the peripheral arterial tree. In the third phase, the reflected wave continues proximally through the arterial system and is reflected again at the aortic valve, where it then proceeds peripherally and causes the second forward peak. Phases two and three are

part of the diastolic phase. Therefore the shape of the Doppler waveform from a healthy individual is in most part due to the primary systolic wave being reflected from some distal arterial site. This site of reflection is the part of the arterial tree where there are high impedance terminal vessels, namely the arterioles (Oates, 2001; Nichols and O'Rourke, 2005). The peak systolic velocity in healthy individuals measured using duplex sonography from the muscular arteries of the lower can range from approximately $50cms^{-1}$ to $120cms^{-1}$ (Hennerici, 1998).

3.2.2 Doppler waveform Measurements

The full spectral waveform contains much information, but can be simplified by taking the maximum velocity at each point in time along the Doppler waveform; this is known as the peak velocity envelope. If the Doppler waveform is presented in this way it can more clearly show the changes in shape from different locations around the body and changes in shape from the presence of disease. However, where the Doppler angle is unknown, several quantitative indices have been formulated that enable the angle in the Doppler equation to be eliminated.

Pulsatility index (PI) is a measure of how pulsatile a waveform is and is particularly appropriate for waveforms that are pulsatile in nature, for example waveforms from the lower limbs, and for Doppler waveform measurements it is the difference between the peak systolic and minimum diastolic velocities divided by the mean value of the peak velocity envelope over the cardiac cycle. The more pulsatile the waveform the higher the PI value will be, Equation 3, therefore damped waveforms will have a low PI (Oates, 2001).

$$PI = \frac{\text{peak to peak value}}{\text{Mean value of peak velocity envelope}}$$

Equation 3 Pulsatility index

The resistance index (RI) is defined as shown in Equation 4. This equation is also independent of the Doppler angle. Since this index is dependent on the changing relationship between the end-diastolic velocity (EDV) and the peak systolic velocity (PSV), then changes in peripheral resistance to flow will affect RI. An increased peripheral resistance lowers EDV and therefore produces a higher RI. This index is more appropriate for waveforms that normally have a continuous forward flow throughout diastole, for example the carotid arteries.

$$RI = \frac{PSV - EDV}{PSV}$$

Equation 4 Resistance index

Duplex ultrasound scanning has been used in a clinical setting to diagnose arterial or venous insufficiency for the past 30 years. The technology has advance considerably in that time and at present it can provide anatomical information as well as visualisation of blood flow as well as its direction. The B-mode image can be used to subjectively assess the echogenicity of thrombus within arteries or veins and pulsed Doppler can be used to objectively grade the degree of arterial narrowing with a overall diagnostic accuracy of 90% (Baxter and Polak, 1992).

3.2.3 Laser Doppler Flowmetry

Over the last 15 years laser Doppler Flowmetry (LDF) has developed from a scientific research tool into a promising clinical diagnostic instrument giving comparable results to other non-invasive devices. LDF can be used to assess blood flow in either large vessels or to assess skin perfusion. These two methods use different technologies but only the instrumentation used to assess the micro-circulation will be considered in this section. Many instruments use laser light that is produced from helium-neon gas or gallium-aluminium arsenide elements. This produces a weak beam of laser light that penetrates the skin to an approximate depth of 1-2mm and has minimal metabolic disturbance on the tissue. At this depth blood constitutes only a small proportion of the tissue volume and most of the back scattering of the beam will be from small particles and stationary tissue. Light scattered from moving particles (blood cells) within the sample volume will experience a Doppler shift in the light frequency. To distinguish the Doppler shifted signal due to blood cells from interference from other sources such as electronic noise, complex electronic processing and filtering are performed on the photo-detected signal. The signal now represents a meaningful quantity that varies linearly with the blood flow in the sample volume. However as there are still some calibration issues, clinical investigations tend to look at relative changes from before and after interventions, such as measurements pre and post hyperaemia when investigating vascular diseases (Serup, Jermec and Grove, 2006).

LDF technology can measure blood flow in the skin at depths of only 0.1 to 0.05mm where the capillary beds and the blood flow within them are the site of nutritional exchange with the tissue; it can also penetrate further into the sub-papillary layer, 0.05 to 2mm, where thermoregulation takes place. However as approximately 90 to 95% of

blood flow in the microcirculation occurs at this depth and only 5 to 10% in the more superficial skin layer, the LDF signal is composed mainly of the thermoregulatory component and only a small component of nutritional flow. The high frequency response of the system permits recordings of the pulsatile nature of the microvascular signal (Bernstein, 1985).

LDF technology has developed over the years from just an experimental lab-based research tool to a potentially useful and practical clinical diagnostic instrument. However there are still a number of issues which the technology needs to overcome if it is to become a useful tool in the primary care setting. There are standardisation and calibration issues as well as the transducers not being as robust as some other non-invasive transducers. The average cost of a LDF system is higher than a PPG system.

3.2.4 Transcutaneous Oxygen Monitoring ($tcPO_2$)

Monitoring of transcutaneous partial pressure of oxygen ($tcPO_2$) provides the clinician with trend information regarding the body's ability to deliver oxygen to the tissue. Because $tcPO_2$ is measured through the skin, the value obtained is a measure of the oxygen tension in the capillary beds. The reason for measuring $tcPO_2$ is to obtain information regarding the patient's arterial oxygen level (PaO_2) and to indicate the level of peripheral perfusion. This is achieved by elevating the skin temperature in order to dilate the peripheral capillaries, increase superficial blood flow and therefore oxygen diffusion to the skin. $TcPO_2$ and PaO_2 values differ from each other because some oxygen is absorbed by the dermal layer during its passage to the skin's surface. Therefore if the patient is haemodynamically stable $tcPO_2$ correlates well with PaO_2.

$TcPO_2$ transducers consist of an anode a cathode and an electrolyte solution as they operate on a polargraphic cell principle. A membrane, which is permeable to oxygen, fits over the transducer surface and encloses the electrolyte solution. This transducer technology requires periodic maintenance to ensure that: the electrolyte solution does not dry out over time; there is minimal drifting of sensitivity due to electrochemical deposits on the transducer surface and as the membrane is only a few micrometers thick that routine use has not damaged the permeable membrane.

As the skin temperature is elevated within 42 to 45^{o}C, there is a danger of burning the patient's skin surface, particularly if the transducer remains in one place too long (Baumbach, 1986).

3.2.5 Tissue Oxygen Saturation (Pulse Oximetry)

Pulse oximetry uses the difference in the absorbance spectra for reduced haemoglobin (Hb) and oxyhaemoglobin (O_2Hb) within red and infrared wavelengths to calculate oxygen saturation levels. These wavelengths are used because they readily penetrate tissue and light emitting diodes (LEDs) are widely available at these frequencies. The pulse oximeter can be found in many hospital departments where there is a need to monitor desaturation or hypoxia. It has also been used to assess patients for lower limb arterial or venous insufficiency. However there are a number of limitations of pulse oximetry: calibration assumptions, optical interference and signal artefact. Additionally, this technique displays a single number to represent the tissue oxygen saturation of the patient only. Other information such as blood volume flow to the tissue is not displayed, therefore missing important diagnostic information (Tremper, 1989; Sinex, 1999).

3.2.6 Ankle Brachial Pressure Index

Ankle brachial pressure index (ABPI) is the ratio of the ankle to brachial systolic blood pressure. A value of <0.9 indicates the presence of flow limiting arterial disease affecting the limb. A value between 0.9 and 1.2 is considered normal, any greater indicates hardening of the tibial artery walls or medial sclerosis. This type of disease is more common in patients with diabetes and can cause the ABPI to give high and therefore misleading readings. The ABPI is non-invasive and can be performed in a vascular laboratory or a GP surgery. For a cut-off point of 0.9 the sensitivity is reported to be between 75 to 100%, and the specificity between 80 to 100%. Sensitivities and specificities of 90% and 98% respectively have been reported for the detection of leg artery stenosis >50% (Doobay and Anand, 2005). In order to calculate ABPI, firstly the patient is placed supine and an appropriately sized cuff is placed around the ankle of the patient just above the medial malleolus. Locate the dorsalis pedis artery with a hand-held Doppler unit. Inflate the cuff until the signal can no longer be heard, then slowly deflate the pressure in the cuff and record the pressure at which the signal returns. This is the systolic pressure in the posterior tibial artery. Repeat this procedure for the posterior tibial artery. The next step is to measure the brachial systolic pressure and this is done in the same way as for the ankle pressures. Repeat this for the other arm and use the higher of the two brachial pressures with the highest of the ankle pressures to calculate the ABPI for that leg. Repeat the procedure to measure the ankle pressures for the contra-lateral leg.

The ability of ABPI to detect significant arterial peripheral disease is well documented with high sensitivities and specificities reported (Yao, Hobbs and Irvine,

1969; Ouriel et al., 1982). However the lack of a standardized methodology and the inherent limitations in the ABPI technique make interpretation and comparison of studies difficult. In particular, studies use different ABPI threshold values to distinguish normal from patients with PAD; normal threshold values have been used ranging from 0.8 to 1.3 depending on the required sensitivity. Further studies employ subjective measures, such as the patient's clinical history, to determine the extent and severity of PAD and so group patients according to the presence or absence of lower limb symptoms. Criqui et al (1985) reported that relying on a clinical history in this way would underestimate the prevalence of PAD by a factor of two to five. Similarly palpating pedal pulses also underestimates the prevalence of disease. Marinelli et al (1979), Allen et al (1996) concluded that ABPI is biased towards detecting more severe disease and reported a reduction in sensitivity when identifying moderate PAD against duplex ultrasound. Stein et al (2006) also concluded that resting ABPI technique was poor at detecting low grade stenotic disease and that nearly half of all patients with symptoms of PAD had a normal resting ABPI.

A number of studies evaluated the use of stress testing using a treadmill to investigate if the increased blood during the exercise would detect early or low grade disease in patients. Ouriel et al (1982) studied patients with early disease, selecting those patients with asymptomatic limbs with contra-lateral symptomatic disease. They concluded that stress testing did not significantly increase the sensitivity of resting ABPI to detect low grade disease. As with any treadmill exercise the ability of the test to uncover moderate PAD in the asymptomatic limb will depend on the distance the patient can walk and this will be decided by the worse limb or symptomatic limb. Also many patients will be unable to perform the treadmill exercise due to co-

morbidity such as cardiac or respiratory disease or disability and the availability of space required for a treadmill, particularly in a primary care setting.

3.2.7 Segmental Pressures

This type of technique helps to determine the degree of arterial occlusive disease. Pressure cuffs are placed on the arms, thighs below the knees and above the ankles. Arterial pulses are then obtained distal to the cuff using continuous wave Doppler. The cuff is then inflated to a pressure that occludes the relevant artery and therefore the Doppler signal disappears. Generally the top thigh pressure is approximately 30mmHg above the brachial pressure. Adjacent pressure levels in the lower limb should differ by less than 20mmHg; a difference greater than this suggests some degree of arterial narrowing between the cuffs. Brachial pressures should be recorded from each arm using continuous wave Doppler, and the difference between these pressures should be less than 20mmHg. The higher of the two pressures will be used for calculating all relevant indices.

Ankle brachial pressure indices (ABPI) are calculated for each segmental level in both lower extremities. The ABPI calculated at each segment will indicate the ongoing arterial disease process. An ABPI of between 0.9 and 1.2 is considered normal; <0.9-0.5 indicates moderate narrowing disease; and <0.5 indicates possible critical limb ischaemia and potential trough of limb loss. An ABPI greater than 1.2 may indicate that the walls of the arterial vessels are non-compressible. This is consistent with wall calcification. This type of disease is more common in people with diabetes (Kerstein and Reis, 2001).

3.2.8 Ambulatory Venous Pressure

Ambulatory venous pressure (AVP) measurements provide haemodynamical information that can supplement the anatomical information provided by Phlebography. Venous pressure in the trough decreases during walking and gradually returns to normal when the subject rests. These observations were first recorded in the 1940s and soon the technique was widely adopted by different institutions so that by the 1970s and 1980s AVP measurements had become the haemodynamic gold standard.

The method uses a needle that is inserted into a vein in the dorsum of the trough and which is then connected to a pressure transducer, amplifier and recorder. The patient then performs 10 tip-toe movements or knee bends at the rate of one per second, which is the standard exercise. On completion of the exercise the patient then rests while the pressure returns to the pre-exercise baseline level, which is recorded in seconds. Performing the 10 tip-toe or knee bend activates the calf muscle pump which squeezes the venous blood out of the lower leg. Healthy people's refilling takes place from the arterial side and can take approximately 18 to 40 seconds to return to baseline levels, however in patients with valvular incompetence the damaged or non-functioning valves can not prevent venous blood, which was ejected from the lower limb, from travelling back down into the lower leg. Venous filling in this way occurs more quickly, approximately 5 to 18 seconds. If reflux is suspected, due to a quick refill time, the exercise is repeated with a 2.5cm wide cuff placed at the ankle to occlude the superficial veins. If the refill time is not affected by the cuff and remains abnormally short then deep venous reflux is suspected. If however the reflux time returns to normal then just superficial venous reflux is suspected.

The measurements which are regarded as the most useful are the pressure at rest (Baxter and Polak, 1992), the mean steady state pressure (P10) at the end of the 10 tip-toe movements, the calculated pressure difference (Po-P10) and the refill time (RT). AVP is the best method for assessing venous hypertension and the parameter P10 is considered to measure its severity irrespective of its pathophysiology. However because AVP is invasive it can not be used a screening tool. Other disadvantages with using this technique are not all patients would be physically able to carry out 10 tip-toe movements or knee bends over 10 seconds and also it has been suggested that erroneous errors may occur if there is a competent valve in the trough. Also, on standing, muscle artefact can become a problem, particularly in the rest phase of the procedure, and so the patient uses an orthopaedic frame to support themselves with their weight supported on one leg. The use of cuffs also introduces further sources of potential errors as the cuff width is critical; too wide and it will tend to compress deep as well as superficial veins (Nicolaides, 2000).

Because of these short comings non-invasive methods have been developed which address some of the problems mentioned above.

3.2.9 Plethysmography

Plethysmographs are devices that measure volume change. A number of these devices have been used clinically over the past 50 years that employ completely different principles. These are described below.

3.2.9.1 Strain Gauge Plethysmography (SGP)

This device measures circumference of a selected limb segment. Circumference is related to segment cross-sectional area and cross-sectional area multiplied by length is volume. In using SGP the following assumptions are made. Blood volume is the only significant variable with time; also, arterial blood volume change is small compared to venous blood volume changes. The device is made by utilising a small hollow elastic tube filled with mercury and an electrical circuit that can measure voltage across the length of the tube. The length of the elastic tube changes for alterations in limb circumference due to venous blood volume changes. The voltage is measured and displayed by the circuit. By measuring circumference as a function of time, venous blood volume as a function of time may be measured.

This method can be used to detect acute deep vein thrombosis as well as venous valvular incompetence. SGP has some advantages over other methods: it is far less cumbersome than water-filled plethysmography, and it is more sensitive than air-filled plethysmography (Bernstein, 1985). The test basically consists of

1. measurement of calf volume expansion in response to a standard venous congestion pressure
2. Measurement of the rate at which blood flows out of the leg after the congestion pressure has been released
3. Measurement of rate and volume of venous reflux flow in response to sudden inflation of a thigh cuff
4. Measurement of the rate of calf volume expansion after the venous blood has been displaced by exercise.

The first two tests are used to detect deep venous thrombosis (acute or chronic) and the second two are designed to evaluate venous valvular incompetence. Considering the first two tests:

3.2.9.1.1 Venous Outflow Obstruction

With the patient in the supine position the leg is elevated to empty the deep venous system. The transducer is then placed on the widest part of the calf and the system is then balanced and calibrated electronically. A pneumatic cuff is placed around the thigh and inflated to a pressure of approximately 30 to 50mmHg, which will occlude the venous return; the calf now begins to expand. After approximately 2 minutes the calf expansion slows considerably, but not completely due to an increase in capillary pressure and the subsequent loss of fluid into the interstitial spaces, and a new equilibrium is reached where the venous outflow equals arterial inflow. At this point the venous pressure distal to the cuff equals the pressure in the cuff. After stabilisation the pneumatic cuff pressure is released quickly and the rate of change of calf circumference is recorded. This change in circumference or volume is related to the total venous outflow, which can also be related to the inflow during the initial phase of the test with venous occlusion. The venous outflow maybe expressed in millilitres per minute per 100ml of calf tissue. Patients suffering with chronic venous insufficiency, who may have much of their venous outflow from the lower limb occurring via the superficial veins, will have the test repeated with the application of a tourniquet to ensure venous blood returns via the deep venous system.

Venous outflow obstruction assessed by SGP is useful for three main reasons; firstly it quantifies the severity of chronic venous outflow obstruction, secondly longitudinal

follow up studies can show the degree of resolution of venous obstruction, and thirdly, objective documentation of increased venous outflow obstruction in the late post-thrombotic period may be an indirect clue to the development of recurrent active venous thrombosis (Nicolaides, 2000). Considering the second two tests:

3.2.9.1.2 Venous Valvular Incompetence

This test may be carried out with the patient in the supine position or with the patient standing and performing 10 tip-toe movements. With the patient in the supine position calf volumetric changes, due to proximal pneumatic cuff compressions, are monitored. A tourniquet placed proximal to the cuff prevents venous blood reaching the lower leg via the superficial venous system. If the valves in the deep venous system are competent then these will prevent the proximal blood from reaching the lower limb. However if the valves are incompetent then the transducer in the calf will register volume changes, which will be proportional to the incompetence of the deep venous valves, due to the proximal blood reaching distal parts of the leg.

3.2.9.1.3 Ambulatory Strain Gauge Plethysmography (ASGP)

Calf volume changes during exercise can be monitored and related to the extent and severity of chronic venous insufficiency. The patient performs 10 tip-toe movements, knee bends (20 at 60º flexion) or treadmill exercise. Normally the calf volume initially decreases and then increases during exercise. After cessation of exercise the calf volume returns to normal within a short period of time. In patients with deep venous insufficiency the calf volume increases rapidly after cessation of exercise. This method of recording calf volume changes allows calculation of venous refill time (RT), and expelled volume (EV) (Meissner et al., 2007). By application of a below

knee compression cuff inflated to approximately 70mmHg, isolated superficial venous reflux can be determined as this compression will normalise the venous return time. The positive predictive value for the presence of CVI was 100% for both RT and EV, and the negative predictive value for the absence of CVI was 94% for RT and 75% for EV. When compared to the gold standard AVP, the coefficient of correlation for ASGP was 0.91 ($P<0.001$) for RT and 0.41 for EV ($P<0.05$). ASGP may be able to differentiate between superficial from deep venous insufficiency, but it can not precisely localise the site and extent of the reflux or obstruction in either system (Nicolaides, 2000).

3.2.9.2 Air Plethysmography

This instrument consists of three major components: the first is a transducer, which is a closed air bladder used to surround the limb of interest; the second is a pressure sensor that measures the pressure in the cuff as a function of time; and thirdly, an electrical circuit that controls the pressure and displays the measured results.

Venous hypertension is the result of impaired venous return due to reflux, venous obstruction or poor calf muscle pump function. Air plethysmography is able to measure all three of these venous disorders by having the patient perform certain exercises. Firstly a 35-cm-long air chamber is fitted to the lower limb and pressurised to approximately 6mmHg. This ensures an adequate fit without unduly compressing any of the underlying venous vessels. A syringe is connected to the air circuit and is used for calibration purposes. Therefore, with this set-up volume changes in the lower limb, from venous empting or filling, affect the pressure in the air-chamber, and so

these changes in pressure can be read-off as volume changes of the lower limb in millilitres according to the calibration.

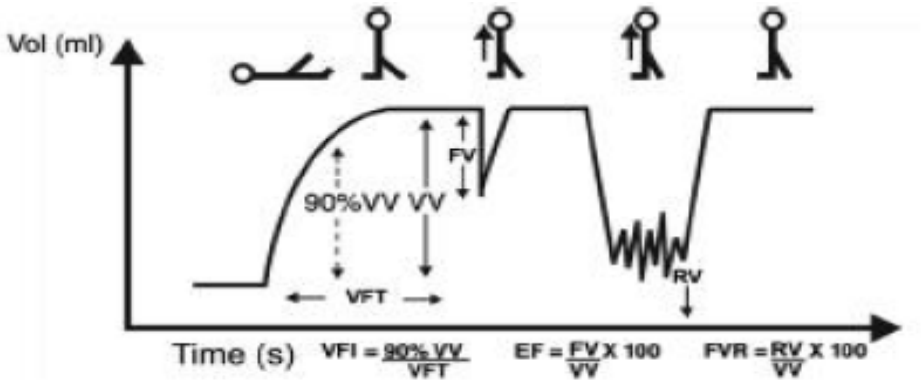

EF = ejection fraction; RVF = residual volume fraction; VFI = venous filling index; VFT = venous filling time; EV = ejection volume; RV = residual volume; VV = venous volume.

Figure 6 Plethysmographic curves with corresponding exercises (Nicolaides, 2000).

3.2.9.2.1 Venous Reflux

To be able to measure the extent of venous reflux the patient first has to lay supine with the leg elevated 45º, with the knee slightly flexed to empty the veins. When this has been accomplished the patient stands with their weight on the opposite leg and the examined leg flexed. The increase in leg volume is due to venous filling, and the functional venous volume (VV) in normal patients is approximately 80 to 150ml but up to 400ml in patients with CVI. Because it is difficult to find exactly when a plateau is reached on the recorded signal while the patient is standing, the venous filling index has been defined. This is the ratio of 90% of VV (90% VV) by the time taken for 90% filling (VFT90), VFI = 90%VV/VFT90%. This is a measure of the average filling rate expressed in ml s^{-1} (Figure 6). In normal limbs the VFI is < 2ml s^{-1} with the veins filling slowly from the arterial side. In patients with severe reflux this increases up to 30ml s^{-1}. A VFI of > 7ml s^{-1} has 73% sensitivity, 100% specificity and a 100% positive predictive value of identifying limbs with venous ulceration (Nicolaides,

2000). A further study by Harada, Katz and Comerota (1995) was conducted to evaluate the sensitivity and predictive value of VFI as a predictor of phlebographically demonstrated critical venous reflux. This study found that VFI greater than 7 showed 73% sensitivity and 100% positive predictive value of identifying critical venous reflux.

3.2.9.2.2 Ejection Capacity of the Calf Muscle Pump

To carry out this part of the test the patient is asked to perform one tip-toe movement with weight on both troughs and to return to the initial rest position. From this we can define the ejection fraction EF = (EV/VV*100), where EV represents the expelled volume as a result of the tip-toe movement. EF is > 60% in limbs without venous disease, 30% to 70% in patients with primary varicose veins and possibly as low as 10% in limbs with deep venous disease. EF is an important parameter to measure in the assessment of CVI because a EF > 60% is associated with low prevalence of ulceration despite marked reflux, and an EF < 40% was found in limbs with minimal reflux but ulceration in the limbs. In combination EF and VFI measurements have good correlation with the incidence of ulceration.

The overall performance of the calf muscle pump, which is assessed from measuring the combined contribution of reflux, obstruction and ejection capacity, can be calculated from the residual volume fraction (RVF). This is measured through the patient performing 10 tip-toe movements and recoding the residual volume of venous blood immediately after the final movement. The residual volume fraction is then calculated as follows: RVF = (RV/VV)*100. For normal patients RVF is in the range of 5% to35% and 20% to 70% in limbs with primary varicose veins and up to 100% in patients with deep venous disease (Browse et al., 1999).

3.2.9.2.3 Evaluation of Venous Outflow

With this technique the patient is placed in the supine position and a thigh cuff is fitted proximally and inflated to 80mmHg. This will occlude the venous system underneath the cuff and the leg will start to increase in volume. The pressure in the cuff transducer will reflect this changing volume which is being recorded. When the volume reaches a plateau the proximal thigh cuff is suddenly deflated and the venous outflow (VO) curve is recorded. From this outflow curve the outflow fraction at 1 second (OF_1) can be calculated. This is the VO in terms of the percentage of the total venous volume. The procedure is then repeated after occlusion of the long saphenous vein. When used in a clinical setting an OF_1 of > 38% is considered to be indicative of the absence of any functional obstruction; in the range of 30% to 38% indicates moderate obstruction, and an OF_1 <28% indicates severe obstruction.

3.2.9.2.4 Venous Resistance Measurements

The venous outflow curves can also be used with simultaneous pressure measurements to calculate the resistance to venous outflow. Pressure is measured by inserting a 21 gauge butterfly needle into a vein in the trough, and volume by inflating a thigh cuff to 80mmHg for 2 minutes and then deflating it suddenly. By calculating the tangent at a number of different points on the venous outflow curve, venous flow can be estimated at different times. The resistance to venous outflow can then be calculated by using the measured pressure at those same times. By plotting the calculated resistance against pressure it is possible to produce curves which show their relationship. By performing this over a large number of patients without and with varying degrees of obstruction, a range of pressure-resistance curves can be produced that can be used by a clinician to help with grading of obstructive disease.

Air-plethysmography provides information derived from the entire leg, as opposed to continuous Doppler which gives information concerning individual vessels. Because the measuring cuff encompasses the entire calf and therefore includes all the muscles from the calf to the knee, it avoids errors due to muscle movement during exercise, which otherwise would interfere with other methods such as segmental devices. Because air plethysmography can measure all three disorders (reflux, obstruction and calf muscle pump dysfunction), it has the potential to give a complete quantitative haemodynamical analysis of a patient, and therefore isolate the particular CVI disorder from which the patient is suffering (Nicolaides, 2000).

3.2.9.3 Photoplethysmography(PPG)

Photoplethysmographs are not true plethysmographs as the measure they provide is qualitative and can not be used to determine volume. Due to the depth of penetration of the transmitted signal, the measurement area is limited to the microcirculation.

A simple PPG sensor consists of an infrared light emitting diode (LED) and a photo detector, placed in a small plastic housing. Figure 7 shows the approximate depth of penetration of infra-red light into the tissue. There are two types of PPG probe construction; both the light source and photo-detector are on the same side of the tissue, this is called reflection PPG; and transmission PPG where light source and photo-detector are on opposite sides of the tissue. Figure 7 shows the reflection type probe.

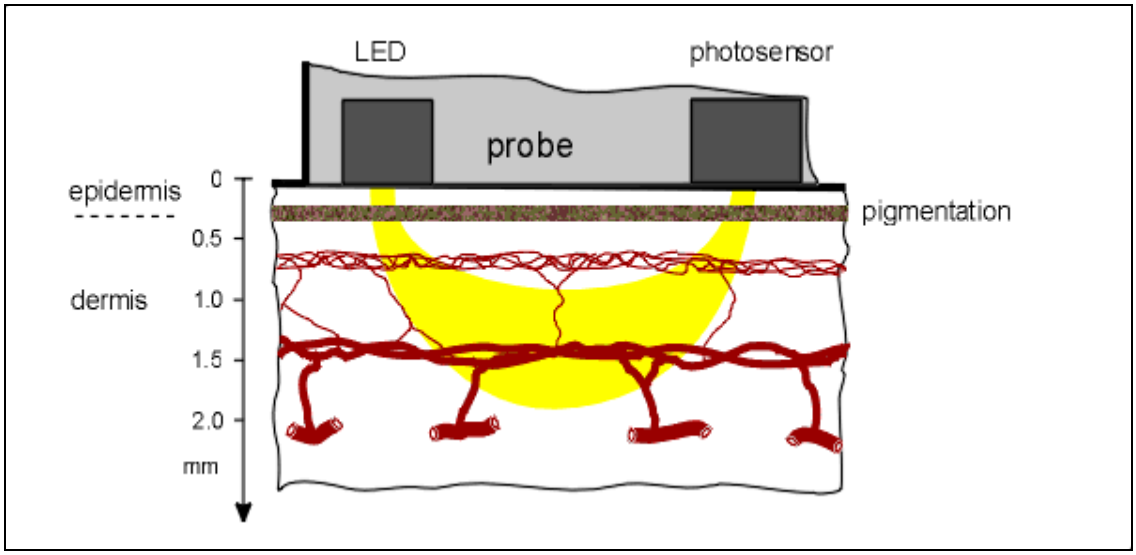

Figure 7 Depth of penetration of typical PPG probe (Blazek and Schultz-Ehrenburg, 1996).

The disadvantage of the transmission type probe is that it can only be used on parts of the body where light can penetrate all the way through the tissue to the photo-detector. It can therefore only be used on sites such as the ear-lobe or the digits. Alternatively, due to the construction of the probe, reflection mode PPG can be placed on most parts of the body, such as the sole of the trough or on the ankle. In this thesis only reflection PPG will be considered. The sensor is placed on the skin, preferably where there is a concentration of subcutaneous blood vessels. And as the volume of blood within the skin layer underneath the sensor increases and decreases with differing physiological mechanisms (heart rate, respiration etc) so the amount of reflected light measured by the photo detector will change. More subcutaneous blood, the less infrared light gets reflected (Blazek and Schultz-Ehrenburg, 1996).

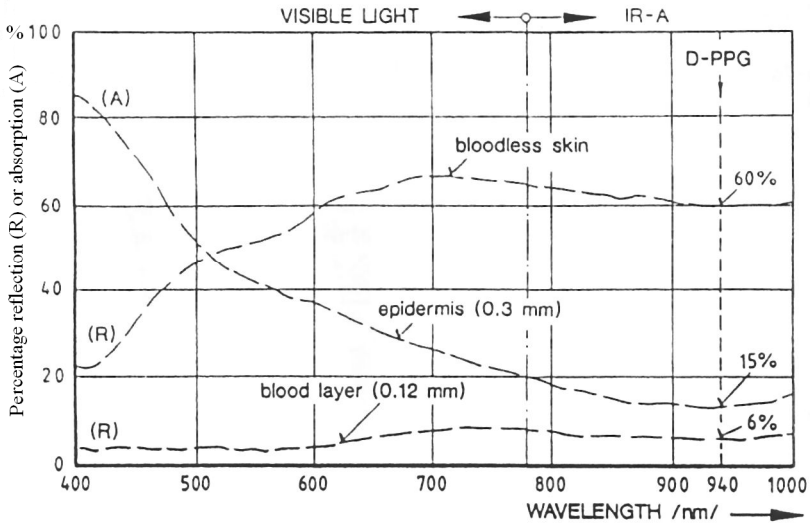

Figure 8 Optical properties of the skin (Blazek and Schultz-Ehrenburg, 1996). (A)- percentage absorption; (R)- percentage reflection. To the left of the vertical line at 800nm the diagram shows the visible spectrum of light; to the right the infra-red portion of the spectrum (IR-A).

The detected PPG signal is composed of reflections from the bloodless epidermis and from the layer of tissue containing blood vessels. Figure 8 shows the light reflection (R) and the absorption (A) properties of the blood layer and the bloodless human skin. The large reflected signal from the bloodless skin can easily be filtered from the signal in the post-processing stage. Therefore most of the IR signal is absorbed by the blood layer, as can be seen from Figure 8, where the blood layer has only a small reflected component. Between approximately 800 to 900nm there is a narrow measurement band where the IR light penetrates the epidermis with little attenuation and there is also a relatively large separation between reflective properties of the bloodless skin and the vessels filled with blood

Changes in oxygen concentration in the blood can influence PPG signal. It is therefore important to know how the absorption spectrum of oxygenated and de-oxygenated blood varies with the wavelength of light used; otherwise changes in oxygen concentration in the blood could be mistaken for blood volume changes.

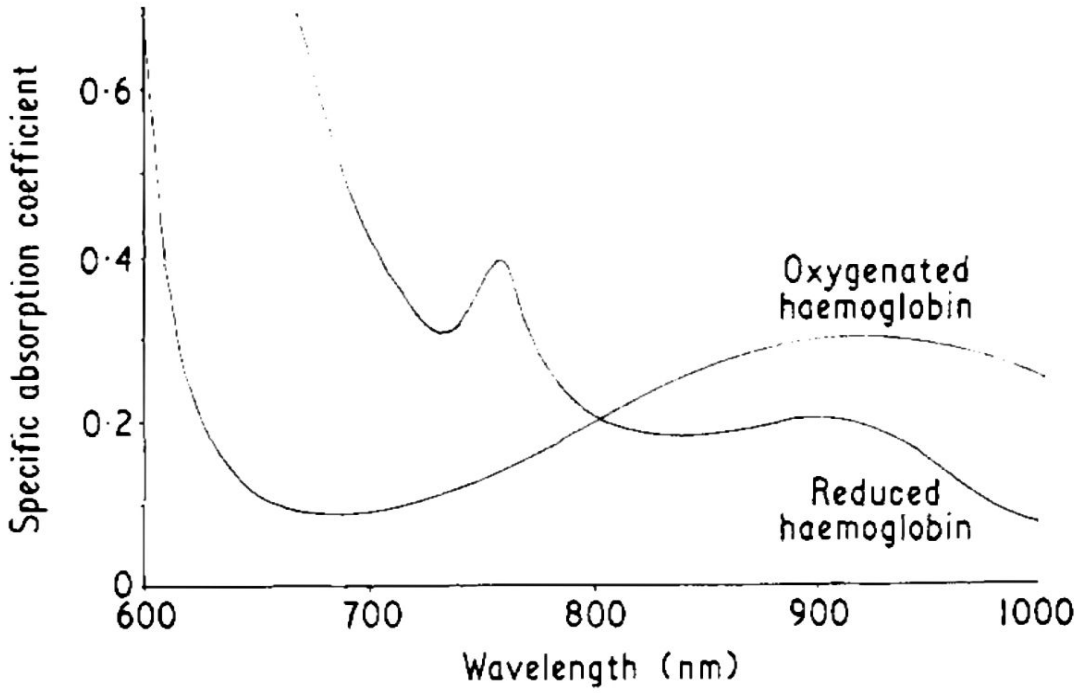

Figure 9 Absorption spectra of haemoglobin (Challoner and Ramsay, 1973). The intersection of the two curves, i.e. the isobestic point, 805nm, is where the absorption difference between oxyhaemoglobin and reduced haemoglobin is minimal. This point is utilised in the PPG technique

Figure 9 shows the absorption spectra of haemoglobin. As can be seen there is a point on the graph where the absorption co-efficient of oxygenated haemoglobin and deoxygenated haemoglobin are the same. This is known as the isobestic point for haemoglobin and occurs at a wavelength of 805nm. Using this wavelength overcomes the difficulties mentioned above (Challoner and Ramsay, 1973).

Since 90% of the reflected PPG signal comes from the tissue, 10% from the venous blood and 0.1% from the arterial blood volume, separation of the reflected PPG signal into its component parts, i.e. the venous and arterial signal can be accomplished. The signal is then comprised of a large signal offset, from tissue, a slowly changing venous portion (quasi d.c.) and a pulsating arterial signal (a.c. signal).

A major disadvantage of the PPG system is the affect that skin colour and thickness have on the reflected signal. The same blood volume change can produce different PPG amplitudes under different skin conditions. The advances of the electronics industry into the digital age have enabled PPG systems to perform automatic self-calibration, which is microprocessor controlled. This involves adjusting the intensity of the emitted light until the amount of reflected light reaches a defined level, Ro. The maximum reflected signal, Rmax, is also stored. Therefore defining Ro allows a constant starting value which is valid and reproducible for every skin type and is performed before each measurement. One of the advantages of this self-calibrating technique is that a quantified PPG signal amplitude in PPG % can be used, defined by

$$PPG\% = ((R\max - Ro)/Ro \times 100) \quad \textbf{Equation 5}$$

Additionally, inter-individual comparison of PPG signals is possible.

3.2.9.3.1 Evaluation of Venous Reflux and Calf Muscle Pump Test.

The probe for this test is placed approximately 8cm proximal to the medial malleolus or on the dorsum of the trough. After baseline and zero have been achieved, emptying of the calf venous blood is produced by repeated dorsiflexion and plantar flexion of the trough (Figure 10).

Figure 10 Calf exercises during calf muscle pump test

This can be performed in a chair or with the patient standing and performing 10 tip-toe exercises. However, if the patient is standing, it is essential that they hold on to an orthopaedic frame or a table so that artefacts from the leg muscles are minimised during the refilling period. Better separation was found for patients in the standing rather than sitting position (Nicolaides and Miles, 1987). As the patient carries out this exercise the venous blood gets squeezed upwards and out of the lower limb. This reduces the amount of blood beneath the sensor causing the PPG signal to rise.

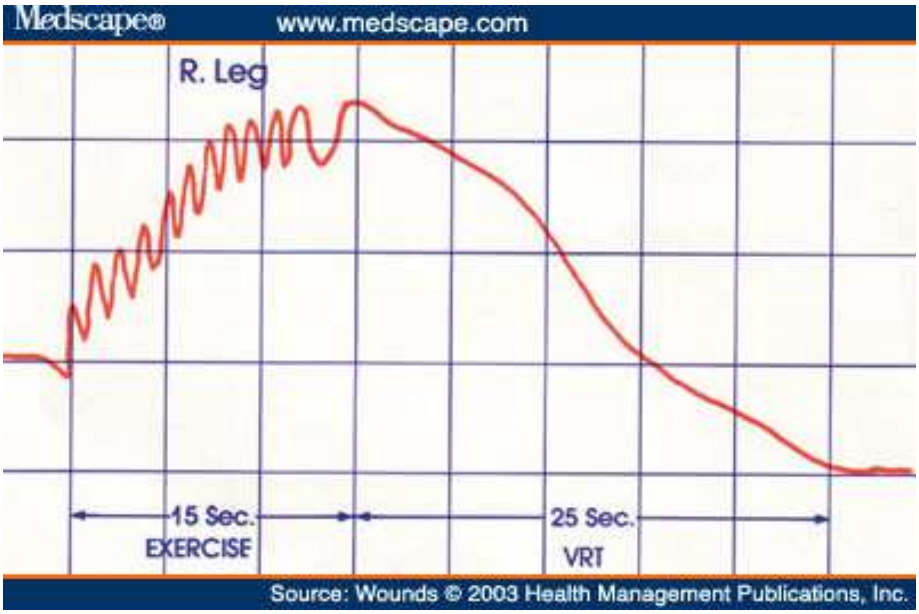

Figure 11 Typical graph of volume flow signal using a PPG probe. The first 15 seconds show the dorsa-flexion phase of the test, where the venous blood 'empties' from the calf. The time to complete the remaining rest phase, (VRT), venous filling, indicates whether the patient has an abnormal or normal venous refill time. The vertical axis is PPG% and the horizontal axis is time in seconds

In healthy patients the competent valves do not allow the blood to travel back down the leg, but the leg refills gradually from arterial inflow. This makes the PPG signal fall back towards its initial value. However, patients with valvular incompetence can not stop the ejected blood falling back down the leg due to gravity and filling the subcutaneous vessels. This reduces the Venous Refill Time (VRT). From this test a graph of volume flow over time is produced (Figure 11). Two important parameters can be calculated from this graph, namely, VRT and Venous Pump Power (Vo), which is the peak height the signal reaches during the exercise period, from the steady state value at the beginning of the of the test and is measured in %PPG. If VRT is abnormally short (<20 to 25 seconds in the sitting position or 18 in the standing position) then the test is repeated, but this time with a tourniquet around the ankle or knee to occlude the superficial veins. If this does not affect the VRT and return it to within normal range then this suggests deep venous insufficiency or perforator

incompetence. Normalisation of the VRT suggests insufficiency is confined to the superficial venous system and that the deep veins are competent.

Three degrees of insufficiency are used internationally to evaluate the muscle pump function:

- Normal VRT greater than 25 s
- Stage 1 VRT 20s to 24s
- Stage 2 VRT 10s to 19s
- Stage 3 VRT less than 10s

Although not yet decided internationally, venous pump power, Vo, has been separated as below:

- Normal Vo greater than 4 PPG %
- Equivocal Vo from 3 to 4 PPG %
- Abnormal Vo lower than 3 PPG %

The muscle pump test can be used for the diagnosis of the following venous disorders:

- Varicose veins of any type with or without junctional saphenous incompetence
- Varicose veins of any type with or without incompetent perforator veins
- Post thrombotic syndrome or other forms of deep venous insufficiency
- The differential diagnosis of venous leg ulcers
- Deep venous thrombosis

3.2.9.3.2 PPG Vein Occlusion Test: Evaluation of Venous outflow (VOT).

Evaluating venous outflow utilising PPG technology is carried out in much the same way as measuring it using strain gauge or air plethysmography mentioned previously. The patient lies supine, with the leg under investigation raised, and a pneumatic cuff is placed around the thigh. The PPG probe is placed on the inner or outer aspect of the lower leg and the cuff is inflated to approximately 80mmHg for 2 minutes. The PPG signal recorded will reflect the blood volume changes occurring in the superficial layer of the skin. On release of the cuff pressure blood will be forced out of the lower leg, due to the pressure build up, and this outflow will be recorded for approximately 30 seconds. Among other parameters which are calculated from this outflow curve are: venous capacity in PPG% and VO in PPG%/min. VO is defined over the 1 to 2 seconds after the release of the occlusion cuff. In healthy subjects this change is > 30%/min. The VOT is a test for venous obstruction rather than specifically for venous thrombus. Therefore the test can not differentiate between

1. Acute thrombus
2. Post thrombotic occlusions
3. External compressions

3.2.9.3.3 PPG Vein Pressure Test

For healthy people in the supine position venous resting pressure (Pv) is approximately 10mmHg. However this can be altered by additional components as shown below:

$$Pvp = Pv + Phydro + Pocc + Patrium \qquad \textbf{Equation 6}$$

where:

Pv = venous resting pressure

Phydro = additional hydrostatic pressure

Pocc = pressure through outflow obstruction

Patrium = central vein pressure

The vein pressure test is measured with the patient supine. A small pneumatic cuff is placed around the base of the great toe and a PPG sensor is placed on the tip of the great toe. The pressure in the cuff, Po, is electro-pneumatically increased at a constant rate (4mmHg s^{-1}). The PPG signal will rise as soon as the pressure in the cuff reaches the venous resting pressure, Pv. After approximately 20 to 30 seconds the cuff is suddenly deflated.

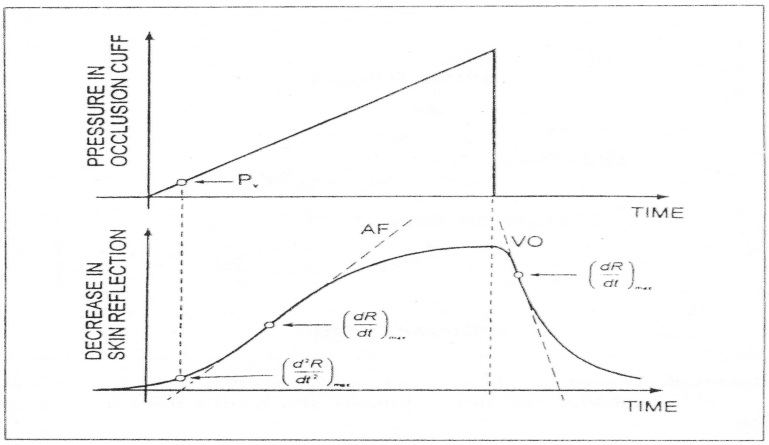

Figure 12 Relationship between cuff pressure and PPG curve (Blazek and Schultz-Ehrenburg, 1996).

With this examination method a number of parameters can be calculated by using the air pressure and PPG volume curves produced. Figure 12 shows the relationship between the cuff pressure and the PPG curve. Figure 13 shows the results of an experiment carried out on patients with a simulated DVT by way of a pneumatic cuff used to occlude the veins in the lower limb.

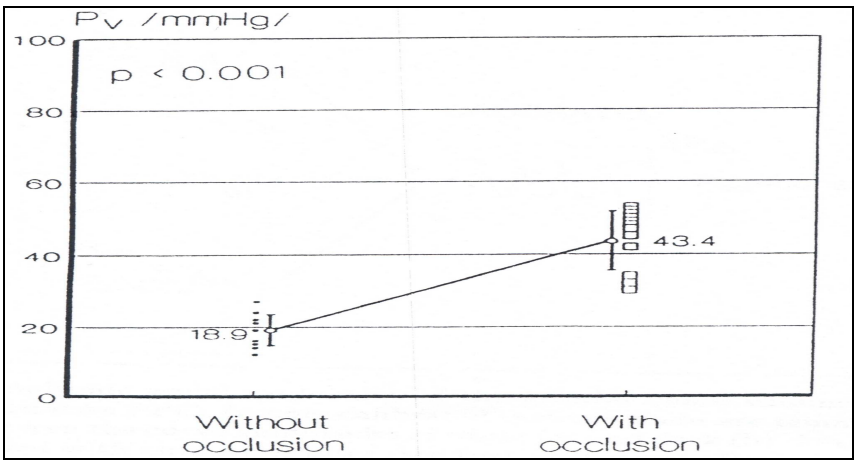

Figure 13 Mean values of peripheral venous pressure for patients with and without occlusion (Blazek and Schultz-Ehrenburg, 1996).

As can be seen from Figure 13 the mean value of Pv is 43.4mmHg with a cuff simulating an occlusion and just 18.9mmHg without a cuff. Both conditions could be discriminated with High significance ($p < 0.001$) (Blazek and Schultz-Ehrenburg, 1996).

The technologies described previously for assessing patients with vascular disease are predominantly used in a hospital or specialist vascular clinic. However, as some require extensive user training or are relatively expensive, others require more patient intervention or effort, and so are unsuitable as a screening tool in a primary care setting. Therefore the technology and method used should meet the time and cost constraints of a GP practice. Because of these reasons, researchers have investigated a number of alternative techniques of assessing patients with vascular disease.

Optical techniques such as Photoplethysmography and Laser Doppler are relatively cheap to purchase when compared to duplex ultrasound. They record local skin blood flow changes, which is composed of an arterial and venous component. Appropriate signal conditioning can isolate these components and so can be analysed separately. The arterial component, due to its dynamic nature, has been characterised and analysed to assess patients with PAD and the venous signal has been used to assess patients with venous insufficiency.

The following section will considered how the PPG signal is generated, its shape and how it is altered by physiological and pathophysiological mechanisms.

3.3 Peripheral Pulse Wave characteristics

The peripheral pulse wave is generated when blood is ejected from the heart during opening of the aortic valve. As the pulse propagates towards the periphery, along individual arteries, it changes in shape and temporal characteristics. These changes are the result of the complex relationship between left ventricular output and the capacitance of the vascular tree (Murray and Foster, 1996). The peripheral pulse has been recorded and analysed extensively as a pressure wave using tonometry. To measure the peripheral pulse, tonometry can be used on the wrist to measure the radial pulse or on the neck to measure the carotid pulse. Applanation tonometry requires the artery to be applanated (flattened) underneath the sensor. The pressure is then transmitted from the vessel to the sensor and recorded (O'Rourke, Pauca and Jiang, 2001). If measured at the wrist the vessel needs to be supported by the radial bone. Blood volume changes in the microvascular bed have also been recorded and analysed by PPG. The PPG blood volume pulse has similarities with the blood pressure pulse. However, the tonometry technique is relatively expensive compared to PPG and requires a skilled operator to obtain accurate pulse recordings, therefore the peripheral pulse will be described from research using PPG technology.

A typical PPG signal obtained from the finger or toe is shown in Figure 14. The signal is produced by shining infrared light into the skin and recording the amount of reflected light coming back to a receiver. The amount of reflected light will ultimately depend on the amount of blood directly under the transducer

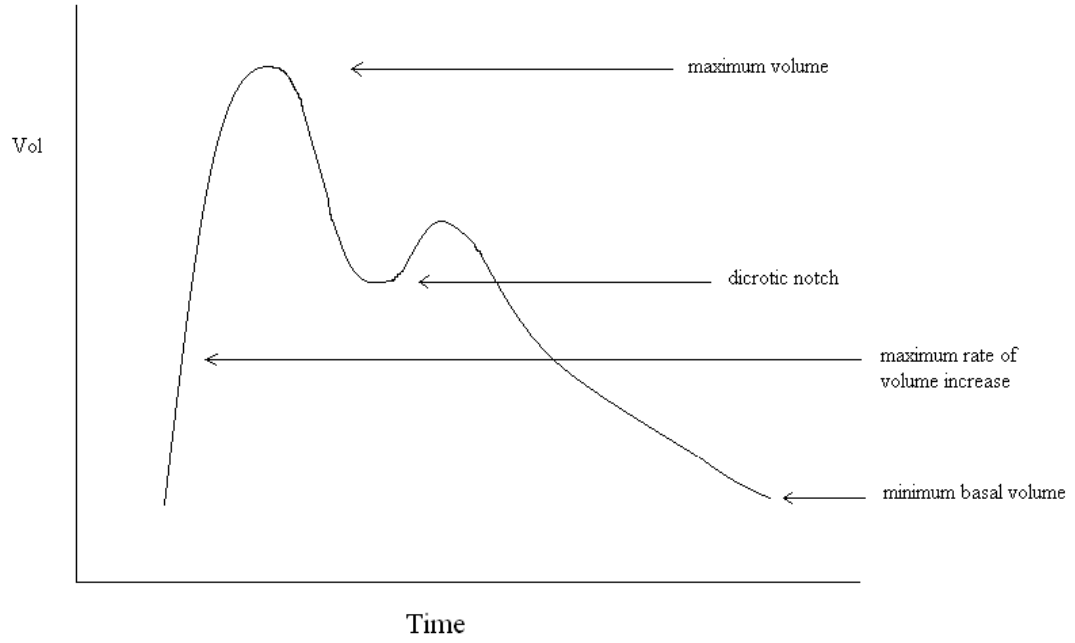

Figure 14 Example of a normal PPG waveform (Murray and Foster, 1996).

Following each heart beat, a bolus of blood travels along the arterial tree eventually entering the arterioles. This bolus causes distension of tissue which is seen as a rising deflection of the PPG trace associated with the systolic phase of the heart beat also known as the anacrotic phase. During the resting or diastolic period of the heart beat also known as the catacrotic phase the trace returns to baseline level. During this catacrotic phase a dicrotic notch is usually seen in patients with healthy compliant arteries. This notch has been associated with pulse wave reflections from the periphery. The position of this notch or incisura on the descending slope of the PPG waveform can change, rising towards the systolic peak during vasoconstriction or towards the baseline during vasodilation. Figure 14 shows the pulsatile component of the PPG waveform also known as the 'AC' component. Figure 15 shows this AC

component sitting on a large quasi-DC component that relates to the tissue and the average blood volume.

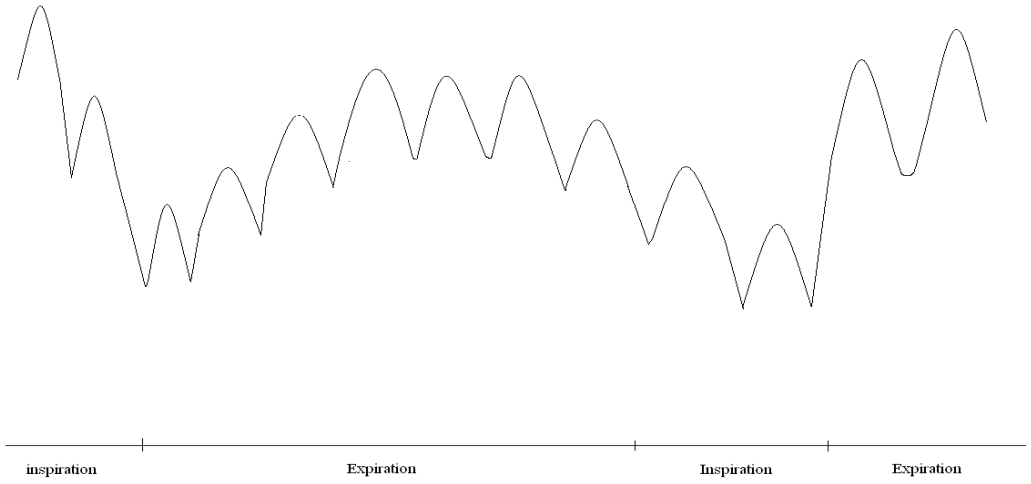

Figure 15 The effect of respiration on the PPG signal (Murray and Foster, 1996).

This DC component is affected by respiration, vasomotion, Traube Hering Mayer (THM) waves (see 2.3.2.2) and thermoregulation. Allen and Murray (2000b) also showed that these pulse wave characteristics are also body site dependent.

Certain features of the PPG waveform, such as pulse wave transit time (PWTT), amplitude and pulse shape, have been investigated as a potential technique for assessing vascular disease or clinical physiological monitoring. PWTT refers to the time taken for a pulse wave to travel between any two arterial points. In non-invasive studies the reference point used to measure PWTT to different parts of the body has been the ECG R-wave. PWTT to different parts of the body, such as the ears, fingers and toes has been measured using this method and a normal range of values for each

site recorded (Allen and Murray, 2000a). The measurement points used in these studies are shown Figure 16.

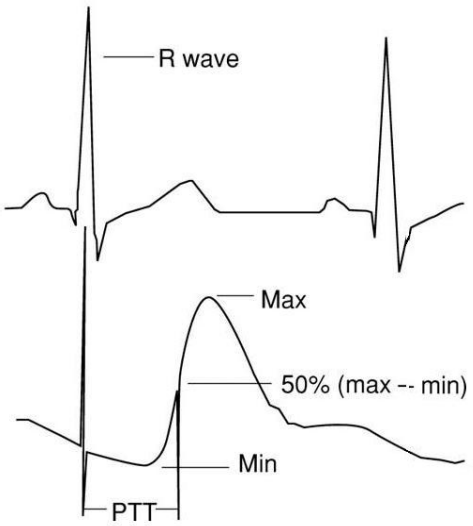

Figure 16 An example of how PWTT can be measured (Smith et al., 1999). The upper figure shows the ECG waveform and the lower figure a typical PPG signal taken from a peripheral site, such as the finger or toe.

This method of measuring PWTT although convenient, and the R wave being easily identified with ECG leads, has one disadvantage; there is a delay between the ECG R wave and opening of the aortic valve. Therefore the measurement of PWTT using this method overestimates the true value, which is the time taken for the pulse to travel from the aortic valve to the periphery (Smith et al., 1999).

PWTT is proportional to blood pressure. As the vascular tone increases from acute rises in blood pressure the artery walls become stiffer and this increases PWTT, conversely, when the artery walls relax as vascular tone decreases, PWTT decreases. The normal aging process also has the affect of stiffening artery walls which therefore

affects PWTT and to a lesser extent PWTT is also affected by patient height and heart rate (Allen and Murray, 2002).

PWTT is also affected by the presence of atherosclerotic disease. This disease is more prevalent as we age especially in the fourth and fifth decades in life. It impedes blood flow by narrowing vessel lumen and a subsequent drop in pressure distal to the stenosis. This narrowing in the lumen of the vessel has the tendency to increase the transit time of the pulse (Erts et al., 2005). When the PWTT to the great toe was measured in two separate groups, a healthy and a patient group with low and high grade disease, from the ECG R wave to pulse peak sensitivity and specificity of 64% and 91% respectively were achieved (Allen et al., 2005). A comparison between healthy controls and patients with lower limb unilateral stenosis was conducted by Erts et al (2005); they found that the PWTT recorded at the periphery of the stenotic leg when compared to those of the healthy leg were delayed. The average PWTT delay reported was 23ms, with full specificity at 32ms.

The pulse shape and how it is affected by certain physiological mechanisms has also been widely studied. Age related changes in shape of the peripheral pulse at various body sites have been studied by Allen and Murray (2003). By normalising the pulse in amplitude and time they were able to show subtle, gradual and significant changes in pulse shape at all sites between the different age groups, with elongation of the systolic rising edge and damping of the dicrotic notch. The frequency content of the signal has also been analysed by Sherebrin and Sherebrin (1990) and they found a decrease in power of harmonic frequencies of the peripheral pulse wave at the finger with age.

As reported previously, respiration and sympathetic nervous system activity affect the amplitude of the peripheral pulse, but this has little effect on the overall pulse shape or contour. Local thermal stimulation or infusion of vasodilator drugs increases local blood flow and amplitude of the PPG signal, but has little impact on its shape (Millasseau et al., 2006). This suggests that the contour of the peripheral volume pulse is primarily influenced by characteristics of the systemic circulation.

PPG pulse shape has also been investigated as an assessment tool for lower limb stenotic disease. As well as a delay in transit time to the periphery the volume pulse also becomes more damped as the disease becomes more severe (Figure 17).

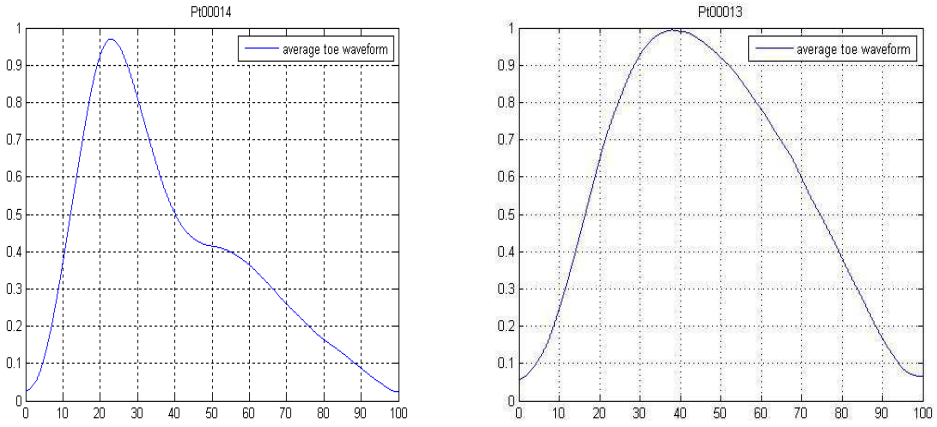

Figure 17 Examples of PPG toe pulses from a healthy patient (left) and a patient with significant lower limb arterial occlusive disease. Both patients of similar age.

Various aspects of the pulse have been measured to distinguish healthy from patients with different levels of arterial disease, from moderate, significant, to occlusive stenotic disease. The systolic rise time was investigated by (Allen et al (2005), and they found that it had 91% specificity and 64% sensitivity for detecting unilateral low grade and high grade disease when using ABPI as the gold standard. However in the same study, Allen et al (2005) used a shape index to assess the same group of patients

and found this to have a better diagnostic performance than the systolic rise times with specificities and sensitivities of 90% and 88% respectively.

In 2000 Allen and Murray (2000a) studied the blood volume pulse from 40 subjects with no known vascular disease. PPG probes were placed at the ears fingers and toes and the aim of the study was to determine the similarity in the right to left pulse characteristics with pulses obtained simultaneously from the 6 peripheral sites. By studying the pulses obtained, important information about the peripheral circulation can be extracted, such as pulse wave transit time (PWTT), the strength and shape and their variation over time. Also, a normative range of pulse data can be collected with which specific vascular patient groups can be compared. Data were gathered over a 5minute period while the patient rested on a measurement couch.

Similarities in the pulse waveform shape at the three segmental levels were found using two types of analysis: Root Mean Square Error (RMSE) provides a measure of differences and the cross correlation analysis provides a measure of the degree of similarity. The study showed that pulses from the left and right sides of the body from normal subjects are highly correlated at each segmental level.

Allen and Murray (2002) investigated the age related changes in the peripheral pulse timing at the three segmental levels, i.e. the ears, fingers and toes using PPG. The aim of the study was to determine how the PWTT changed between 116 normal healthy volunteers whose age ranged between 13 to 72 years. These were divided into 5 decade age groups. Additional effects such as differences in subject height, systolic blood pressure and heart rate were also investigated. It is generally accepted that older

subjects PWTT to the extremities decreases due to increasing arterial stiffness. However it is less clear in younger subjects. PWTT was determined with reference to the electrocardiogram R-wave.

It was found that age was the strongest contribution to PWTT at the 3 sites and the greatest effect could be seen at the toes. Right to left sides showed to be highly similar. Systolic blood pressure was also an important contributor to PWTT at all sites. Height was significantly and independently related to PWTT at the fingers and toes. Allen and Murray (2002) concluded that age effects decrease linearly with age from the second to the seventh decades, showing the effect of changes in the arterial stiffness can be detected from an early age.

Using the same normal healthy subjects and the 3 segmental levels Allen and Murray (2003) investigated the age related changes in the characteristics of the photoplethysmographic pulse shape. Arterial stiffness in older subjects changes the propagation of the blood volume pulse to the periphery, which therefore changes the pulse shape and timing. However it is less clear in young subjects and for different peripheral sites. Subjects were divided into 4 decades: <30yrs, 30-39, 40-49, >50yrs. Pulse shapes were calculated at the three sites for the whole subject group and for the subjects within each age group. Differences in pulse shape relative to the oldest group were also calculated. In particular two distinct regions of interest were used from the peripheral pulse to use as indicators of disease; they were the systolic rising edge and the dicrotic notch. The study concluded that, minimal, moderate and significant changes in pulse shape were found at all sites, with elongation of the systolic rising edge and damping of the dicrotic notch.

Allen et al (2005) compared pulse timing, amplitude and shape characteristics of PPG signals taken simultaneously from the great toes of 63 healthy subjects and 44 patients with suspected lower limb arterial disease. Pulse wave analysis extracted pulse timings, amplitude and shape characteristics. Pulse timings and shape analysis were calculated as in previous studies respectively (Allen and Murray, 20022003). These were taken from both toes and for the right and left toe differences. Normative ranges were then calculated for healthy subject groups. The aim of the study was to calculate the relative diagnostic value of the different pulse features for detecting lower limb arterial disease, which were referenced to the ankle brachial pressure index (ABPI) measurement. Signals were recorded for 2.5 minutes. The patient group was divided into 2 subgroups according to their ABPI result: lower grade arterial disease were patients with an ABPI of between $0.9 < ABPI \geq 0.5$ and higher grade disease with an $ABPI < 0.5$. All healthy subjects had an $ABPI \geq 0.9$.

When individual great toe measurements of pulse timings, amplitude and shape features were ranked in order of diagnostic performance, shape index (SI) performed the best with a >90% accuracy. PWTT produced a diagnostic accuracy of 78%, while amplitude had a diagnostic accuracy of 79%. Bilateral differences showed that PWTT had a diagnostic accuracy of 87% and shape index an accuracy of 82%.

Nitzan, Khanokh and Slovik (2002) measured the PWTT to the toe and fingers of 44 normotensive male subjects by PPG and ECG. This method is related to pulse wave velocity (PWV) which in turn is a measure of arterial distensibility. However PWV assessment, by measuring the appearance time of a pressure pulse in two sites along

an artery and the distance between the two sites, is complicated and inaccurate. The difficulties in measuring PWV can be overcome by measuring the delay in arrival of the cardiac induced volume pulse at two peripheral sites on the body, such as the finger and toe.

In particular, two parameters which are related to PWV were tested: the time delay between the ECG R-wave and the arrival time of the pulse at the toe (E-T PWTT) and the difference in the transit time of the blood pressure pulse between the toe and the finger (T-F PWTT). The results showed that both E-T PWTT and T-F PWTT decreased as a function of age and systolic blood pressure (SBP), but they were not statistically significant with diastolic blood pressure (DBP). The study also concluded that the decrease of PWTT with age was attributed to the direct structural decrease of arterial compliance with age and not the functional effects associated with the increase of blood pressure with age.

Erts et al (2005) studied the PWTT delay between the finger and toe of 20 healthy control subjects and 45 patients with diagnosed arterial stenosis in a leg. Both groups had parallel measurements of local blood pressures by means of the oscillatory method of both upper arms and on the upper and lower thighs and slightly above the ankles. Subsequent ABPIs were calculated and the healthy groups assigned ABPIs of 1-1.1 which indicates that there is no significant narrowing or blockage of blood flow. In this study patients with an ABPI below 0.95 were assigned to the patient group. However the study did not indicate if these patients were further subdivided into moderate or significant disease. The study did however indicate that an ABPI of 0.25 or below is related to severe limb-threatening peripheral vascular disease.

The study showed a correlation between bilateral differences in local blood pressure and in the corresponding PWTT delay, as well as between PWTT delay and ABPI. They also reported that the average PWTT value of leg stenosis diagnostic threshold was 23ms +/- 9ms. The range of patients PWTT were 20-80ms, while in the case of healthy subjects the leg PPG signals arrived without delays or with PWTT delays not exceeding 14ms. Patients were not included in this study if they had bilateral stenoses.

A study which investigated the reaction of 5 flow motion frequency bands to post occlusive hyperaemia by laser Doppler technique was conducted by Rossi et al (2005). Baseline readings of the 5 flow motion frequency bands: 0.007-0.02Hz, 0.06-0.2Hz, 0.2-0.6Hz and 0.6-1.8Hz were recorded in 20 healthy subjects and 20 patients with stage II peripheral arterial obstructive disease (PAOD). General wavelet Analysis (GWA) was used to calculate mean and peak powers in the different frequency bands. These were then recalculated after skin post occlusive hyperaemia (POH). During POH the mean peak power of the flow motion wave increased significantly in healthy subjects with respect to baseline, with the exception of the frequency band 0.02-0.06Hz. In the PAOD patients compared to baseline, the amplitude of the flow motion waves did not significantly change during POH. Rossi et al (2005) concluded that patients with stage II PAOD, the leg skin perfusion is not impaired during baseline because of the compensatory mechanisms related to the increased endothelial, myogenic, and sympathetic activities. However, during reactive hyperaemia these mechanisms appear to be exhausted.

3.4 Clinical Pathway

A clinical pathway for a patient is the possible treatment options available to the clinician when managing their care after suspecting a disease condition. Figure 18 illustrates the possible route a patient would take suspected of having arterial or venous insufficiency, if they were to enter the healthcare process at primary care level. The techniques above the red line would be performed at the primary care level or the specialist vascular clinic; below the red line the techniques are hospital based. Initially, the GP takes a history and performs a clinical examination, which may include using a hand-held Doppler device to 'listen' to arterial blood flow at ankle level. If arterial insufficiency is suspected, an ABPI may be taken before referring the patient for a hospital based duplex ultrasound examination to confirm the diagnosis and also to identify the arterial segment or segments affected. If the ultrasound scan is equivocal then further investigations are available, however these may be more invasive, such as an MRA or CTA.

If venous insufficiency is suspected, the GP can confirm the site of reflux by again using a hand-held Doppler instrument. If further information is required such as the functional impact of venous reflux the clinician has the option of sending the patient to a specialist vascular clinic to undergo a plethysmographic investigation, which has been described earlier in 3.2.9. Both of these techniques can be performed in primary care or a specialist vascular clinic. Alternatively, the GP could request a duplex ultrasound scan that will detect if the insufficiency is just superficial, deep or

Figure 18 Clinical Pathway

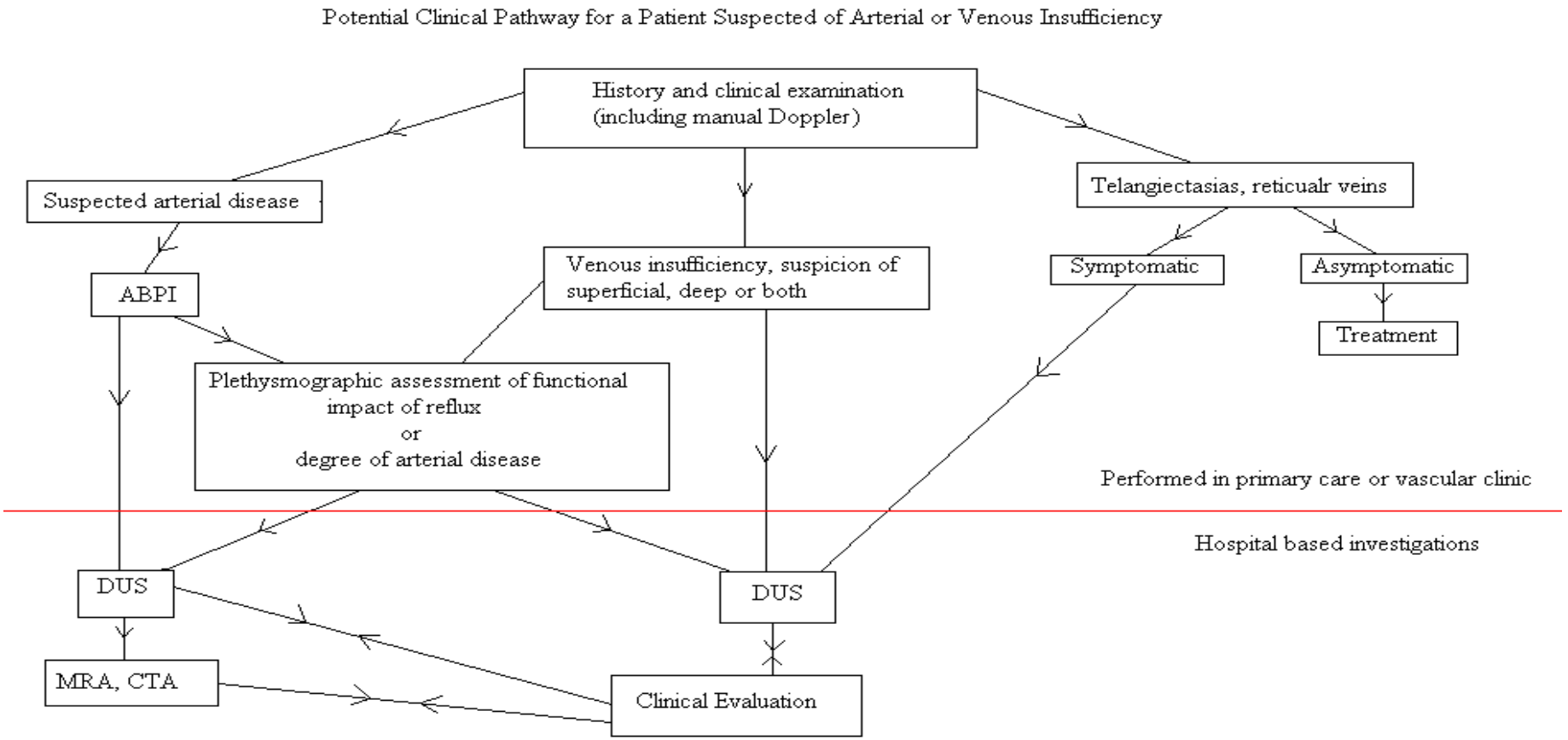

both and report the sites of reflux. Again this would be performed at the local hospital.

The aims of the techniques available to the clinician are to ascertain the nature, position and extent of the arterial or venous insufficiency present in the lower limbs. The physician is then able to make an informed decision as to the appropriate level of patient care need.

3.5 Disadvantages of Current Vascular Techniques

The disadvantages of hospital based x-ray techniques to investigate vascular insufficiency are self evident as they are invasive and so can be painful or distressing for the patient and because of this were never intended to be used as a screening tool for vascular disease. However these techniques are generally only used if the results of the non-invasive procedures are equivocal.

As mentioned previously the GP will decide whether a patient has arterial or venous insufficiency by taking a clinical history and performing an examination. This examination may be just visual if the clinical signs are obvious, such as varicose veins. If the aetiology of the patient signs or symptoms is not obvious the GP can utilise a handheld pocket Doppler or use plethysmographic techniques to distinguish different levels of arterial or venous disease. However only superficial venous insufficiency can be examined with a handheld pocket Doppler and also the device is inappropriate for use on diabetic patients with arterial disease. In addition the ABPI technique used for detecting lower arterial disease uses cuffs and so is relatively time consuming to perform and can be uncomfortable for the patient. Plethysmographic techniques used to investigate venous insufficiency are also relatively time consuming to perform and again require the use of cuffs or a tourniquet. The technique also requires the patient to perform certain lower limb manoeuvres which some patients may find

difficult to execute in their condition. Duplex ultrasound, although non-invasive and has the ability to identify patients with arterial or venous insufficiency, it is relatively expensive to purchase and currently not within the purchase costs of most GP surgeries. It also requires a specialist user to operate and interpret the images.

The methods used in this thesis are intended to be used with an appropriate existing technology. Therefore a device that is cheap to purchase, requires minimal user training and that can be used to investigate arterial or venous insufficiency without the need of cuffs or tourniquet, or requires the patient to perform any manoeuvres would be advantageous to a primary care centre. The technique is intended to supplement the clinical examination and give the clinician more confidence in diagnosing vascular disease. The test is intended to be used at the clinical examination stage giving the clinician a simple yes if there is vascular insufficiency present or no if there is not. If there is vascular insufficiency present the clinician can then put the patient forward for further testing to investigate the extent and severity of the insufficiency, however if the signs and symptoms are not vascular in origin, then an alternative investigation can be performed thereby reducing the number of inappropriate vascular scans.

Various methods and aspects of assessing arterial and venous insufficiency have been considered. Some methods of assessing vascular disease are not suitable as a screening tool because they are too expensive to purchase, use potentially harmful x-ray technology, or they require extensive user training. Other techniques are more appropriate as a screening device for the assessment of vascular disease. Certain optical techniques such as laser Doppler and Photoplethysmography are relatively cheap to purchase in comparison to for example, duplex ultrasound, and they require minimal user training. However as described in section 3.2,

optical techniques used at present, to assess arterial and venous insufficiency, are still cumbersome to perform for the patient and user. However optical technology appears to have the most potential to be used as a simple vascular screening device by a GP at the clinical evaluation stage as it meets most of the criteria set out in the background section of this thesis. The following literature search examines laser and photoplethysmography techniques and investigates if they can be used in this way to assess vascular disease

4 Literature Review

This chapter comprises an historical review of the developments of laser Doppler and Photoplethysmography, which are the two main lab-based non-invasive optical methods used to assess arterial and venous blood flow, and a critical analysis of recent developments in the clinical and experimental use of Photoplethysmography.

4.1 Laser Doppler- Historical review

A laser Doppler instrument generates monochromatic light at one particular wavelength, typically 632.8nm, but other wavelengths have been used, 780nm, if slightly deeper penetration is required. At these wavelengths and the low powers used (1-15 mW) the emitted light penetrates the skin to a depth of about 1-2 mm. This reaches the thermoregulatory skin blood flow as well as flow in the capillaries. The laser Doppler signal is derived from the Doppler shift of reflected laser light which is caused by the moving blood corpuscles. This makes laser Doppler suitable for monitoring changes in skin perfusion. While laser Doppler and Doppler ultrasound utilise the Doppler shift to visualise blood flow, laser Doppler can only estimate micro-circulatory blood flow, where as Doppler ultrasound can penetrate further into the tissue and therefore measure blood flow in larger individual vessels.

One of the earliest working lasers was developed by Maiman (1960) using the material ruby. Only a few years later Cummins and Yeh (1964); Yeh and Cummins (1964) measured localised fluid flow in flow tubes filled with small reflective targets using a laser spectrometer to examine the Doppler shifts in the Rayleigh scattered light.

Early experiments in the use of laser light to measure blood flow in the retinal arteries of rabbits were carried out by Riva, Ross and Benedek (1972). Initially the optical and electronic system was set-up by firing a Helium Neon laser at polystyrene spheres in distilled water inside a glass capillary tube. This was connected to a syringe pump which was set to different flow rates. The spectral distributions observed were in agreement with the set pump flow rates. Next, similar measurements were made with the glass capillary tube filled with rabbit's blood. Similar spectral distributions were obtained, but the presence of multiple scattering by red blood cells affected the shape of the spectrum. However the narrow high frequency peaks in the spectrum did vary proportionately to the rate of flow of the syringe driver. Finally the flow of blood in the retinal artery of an albino rabbit was measured. The experiments showed that the spectral distribution of laser light backscattered from the retinal arteries of a rabbit permits reasonable estimates of the flow velocity. And since the spectrum was sensitive to deviations in the parabolic velocity profile, Riva et al (1972), suggested that information concerning the pathological state of vessels may be obtained.

In 1974 Tanaka, Riva and Ben-Sira (1974) took this procedure a step further and measured the blood velocity profiles in human retinal vessels. These results were in agreement with in-vitro experiments, showing that the technique could be easily adapted for monitoring retinal circulation in a clinical setting. However it was not until 1975 that laser Doppler blood perfusion measurements were performed to assess the microcirculation before and after external stimuli. A 15mW He-Ne laser was used by Stern (1975) to illuminate a small area of skin of a fingertip. He confirmed that the Doppler signal received from the finger is caused by blood flow. This was accomplished by placing a blood pressure cuff over the arm and comparing the change in the Doppler frequency before and after occlusion of the brachial artery. Secondly to demonstrate the pharmacological effects on the microvasculature a

vasodilator was administered over a 15 minute period. This showed discrete increases of flow in the superficial vessels. This work indicated that laser light could detect relatively rapid changes in blood flow in the microcirculation and in different micro-vascular compartments.

Important work on the advancement of the instrumentation into a practical and portable system was conducted by Holloway and Watkins (1977); Watkins and Holloway (1978). Previous optical coupling systems used a single central transmitting fibre with a surrounding annulus of receiving fibres. Watkins and Holloway (1978) used a fibre-optic catheter construction which was composed of separate transmitting and receiving fibres. Separating the transmitting and receiving fibre in this way increased the signal to noise ratio of the system. Additionally, a photodiode instead of a photomultiplier was used in the sensing circuit, which eliminated the need for a high voltage source and decreasing the size of the instrument overall. However, they experienced problems caused by mode interference in the laser cavity when taking measurements in low blood flow areas. This work compared the laser optical technique to ^{133} xenon radioactive clearance technique in the forearms of normal volunteers subjected to UV induced erythema. A good linear relation was demonstrated between these two methods. Further positive comparisons of laser Doppler spectroscopy with ^{133} xenon clearance method were performed by Stern et al (1977). This method provided continuous monitoring of blood flow fluctuations, including the pulsatile component.

Problems encountered by Watkins and Holloway (1978) regarding mode interference in the laser cavity were addressed by Nilsson, Tenland and Oberg (1980b). Instead of using a single photo-detector, a differential detector technique was used. This reduced common mode noise to a negligible level, increased the signal to noise ratio and significantly improved the sensitivity of the instrument. This resulted in a highly stable system from which continuous

recordings of regional blood flow variations could be performed. Further problems encountered in the early development of the laser Doppler technique were revealed by Boggett, Blond and Rolfe (1985). Their investigations revealed that over the audio range of reflected Doppler signals produced, particularly up to a few hundred Hertz, much of the signal appears to be non-Doppler in origin. They reported that the source of this interference were low frequency signals being generated by optical fibre movement, particle number fluctuations in the scatter volume and changes in the intensity of the laser light. However they concluded that most of the processed signal is due to Doppler shifts derived from interactions with moving blood cells and careful selection of a low noise laser will keep low frequency interference problems to a minimum.

The effects of oxygen pressure changes on the laser Doppler signal have been explored (Nilsson, Tenland and Oberg, 1980a). They found the level of blood oxygenation to have only a minor influence on the Doppler signal and proposed that other factors such as haemoglobin content and tissue pigmentation may play a larger role in effecting the signal. He suggested the use of an infrared laser may overcome these difficulties.

Laser Doppler measurements have also been compared against a number of other blood flow techniques such as strain-gauge plethysmography and electromagnetic flowmeter. Laser Doppler closely correlates with these methods, although variations in the signal have been found between subjects. These studies suggested that laser Doppler flow provided a good estimate of tissue blood flow, however variability among subjects and uncertainties in the value at zero made calibrating and quantifying results difficult (Johnson et al., 1984; Smits, Roman and Lombard, 1986).

Most of the early research exploring the use of laser light to monitor changes in microvascular blood flow used a laser wavelength of 632.8nm (Stern, 1975; Holloway and Watkins, 1977; Nilsson et al., 1980b). Later research was conducted using laser diodes with a wavelength of 780nm. This had the advantage of deeper penetration and is also insensitive to changes in oxygen saturation of tissue.

4.2 Photoplethysmography- Historical Review

Photoplethysmography is a non-invasive method of detecting blood volume pulsations that travel to the periphery of the body. The method can be used to detect a number of different conditions, but this thesis will concentrate on the identification of arterial and venous insufficiency.

Palpation of pulses to determine the presence of significant vascular disease has been used for centuries (O'Rourke et al., 2001), however, by the 1930s various plethysmographic techniques had begun to be used to provide more objective measures of the extent of disease.

Hertzman (1938) was a pioneer in the development of PPG as a tool for measuring the superficial circulation. The device consisted of a pencil flashlight bulb that emitted light at a broad frequency and a photocell used to detect the returning signal. His work investigated the blood flow in the skin of healthy male individuals at various positions on the body at rest, such as the arm, leg, hand and trough. In these early experiments a filter was used in an attempt to quantify the PPG signal; variations in the blood content of the skin volume under observation are compared with the deflections of the PPG trace caused by the insertion of a filter into the light path. The amplitude of the PPG signal is then calculated in filter units. Hertzman (1938) validated his PPG measurements with previous studies that used

mechanically recorded plethysmograms. These recordings were in complete agreement at rest and during conditions of physiological stress such as cold, amyl nitrate, voluntary apnea and valsalva manoeuvres. He also explored the effects of reducing oxy-haemoglobin in the skin vessels and found the PPG recordings responded to these changes and therefore concluded that these alterations in blood oxygen levels could be a possible source of error that may invalidate the PPG signal.

However he did discover sources of error, a number of which were due to his experimental set up. There were the difficulty in keeping the relative movement between the skin and the sensor/light source to a minimum, due to respiration, probe contact pressure with the skin caused a drift in the signal, and variations in the spectrum of the light source, which was an incandescent bulb, caused more significant problems than alterations in light intensity. Other unknowns were the size of the vascular area under observation. Most of the changes in the PPG signal he suggested were due to alterations in the skin blood volume directly beneath the light source; however, backscattered light from surrounding tissue outside the probe area could have an impact on the signal, but suggested that this would be minimal.

By investigating the changes in the amplitude of the PPG waveform from different physiological tests and also on participants with Raynaud's disease, Hertzman (1938) indicated the potential use of this technique for investigating arterial pathology.

Burton (1939) examined the blood flow in human fingers using a mechanical plethysmographic method. However, it was this work into the range and fluctuations of blood flow in peripheral vessels, and the excellent correlation found between the amplitude of the mechanically recorded volume pulses and blood flow in the finger that led Hertzman and

Dillon (1940b) to investigate the possibility of separating the arterial from the venous flow. The method involved a combination of resistive and capacitive coupled amplifiers which could record changes in the blood volume and volume pulse amplitude. The capacitive coupling allowed a more accurate identification of the volume pulses. However, attempts at calibrating the volume pulse to filter units as before failed due to discharge characteristics of the capacitors. Separate recordings of finger volume and finger volume pulses showed excellent correlation when monitoring respiratory and vasomotor activity. They associated these changes in volume and volume pulse with the controlling arteries and therefore concluded that the recording of the volume pulse alone was all that was needed for information on the condition of the arteries.

Distinction of the venous component in the plethysmogram proved to be more difficult and no definite conclusions were drawn regarding venous flow.

Earlier research had identified movement artefact between the sensor and the skin as a major source of error in the PPG signal. So, elaborate positioning rigs were developed to keep this error to a minimum. Hertzman and Dillon (1940a) were one of the earliest teams to apply the photoelectric plethysmographic technique to peripheral vascular disease. They observed the spontaneous activity in the blood flow to the fingers of normal subjects and a patient with Raynaud's syndrome and found there was a marked difference between the two participants and the affected fingers. In addition a male patient suffering with intermittent claudication of both legs was investigated over a number of months. Waveforms were recorded on various positions on the troughs on both legs at various times and on some occasions using a vasodilator. Overall they concluded that the PPG technique was capable of providing objective evidence regarding the superficial circulation in patients with vascular disease.

A qualitative and quantitative correlation between the cutaneous blood flow and the mechanically recorded pulse in the finger measured by changes in skin temperature or venous occlusion technique had been demonstrated earlier by two independent studies (Burton, 1939; Goetz, 1945). Hertzman, Randall and Jochim (1945) attempted to show that this correlation existed between photoelectrically recorded cutaneous volume pulse and cutaneous blood flow. Arbitrary filter units were used as before to quantify the PPG signal and compare this with blood flow in different parts of the finger. Inequalities in these measurements invalidated the procedure, which were assigned to physical differences in the blood flow over the surface of the finger. Some correlation was found in any one subject if mechanically measured blood flow and the PPG signal are measured in the same area of skin. However, overall a single usable calibration factor was unobtainable.

Hertzman and Randall (1948) explored further the regional differences in rates of cutaneous blood flow at various points over the entire body by PPG in two young adult males. Measurements were taken from various parts of the hand, trough, trunk and head, and further recordings from the arm leg and thigh. Individual blood flow rates were calculated for each body location and these were summed to obtain a total cutaneous blood flow. They found that the rates of cutaneous blood flow are considerably higher in the palm and the plantar surfaces and in the skin of the face and head than in the trunk, arms and legs.

At this point a major step forward was taken towards a more compact and user friendly design that would greatly reduce one of the major problem with PPG signal acquisition i.e. movement between sensor and patient. Weinman and Manoach (1962) used a photocell as the detector instead of a photoemissive cell which were large and insensitive to changes in blood

flow, but were the best available up to this time. Special plaster of paris casts had to be made to attach the photoemmisive cell and light source to the patient. This made recordings susceptible to the slightest movement between tissue and device. The introduction of the photoconductive cell changed the construction greatly allowing a more compact design. The cells operate by converting changes in light energy into changes of electrical resistance. Therefore a simple, small and low cost circuit could be built to convert these changes in electrical resistance into fluctuating voltages to drive a recorder. The photoconductive cells were also more sensitive to changes in light levels than photoemissive cells and are simply attached to the area of the body under investigation by adhesive tape. The compact design allowed the photocell and light source to be constructed as one unit, which was not possible up to this point. They also highlighted the importance of matching the correct light source and photodetector.

PPG signal changes were studied in individual minute vessels in animals with a special arrangement of microscope, light and recorder by D'Agrosa and Hertzman (1967). They found pulses in the arteries down to arteriolar size, but an absence in capillaries and veins. The origin of the photoelectric signal was also investigated. It was concluded that the pulse in arterial vessels does not appear to be volumetric in origin, but the factors contributing to the arterial pulse are related to the orientation of the erythrocytes during pulsations in flow.

Challoner and Ramsay (1973) used a fibre optic light guide to transmit light to the skin surface in conjunction with infra red filters to overcome earlier problems of the light source heating the skin tissue and therefore affecting the PPG signal. To compensate for any local temperature changes a thermistor was fitted. Also to account for and reduce the influence that changes in oxygen content in the blood have on the recordings, a near infra-red filter was

placed between the photocell and the skin. By carefully selecting a photocell at a particular wavelength, the combined optical response of the photosensor can be predicted and made to operate at the isobestic wavelength. Thereby ensuring that the signal is largely unaffected by changes in blood oxygen saturation.

An important advance in the interpretation and origin of the reflected photoelectric plethysmographic signal was made by Nijboer and Mahieu (1981). They investigated the phase and amplitude of the reflected PPG signal in-vitro and in-vivo and found that the variations in the reflected signal were in-phase with the volume pulsations produced by the specially constructed jig and pump. However, in-vivo the reflected light is in anti-phase with the volume pulses. It was suggested that the difference between the two experiments could be explained by the reflecting and absorbing properties of the erythrocytes and how those properties could be affected by the optical properties of the surrounding tissue. They concluded that the reflected plethysmographic signal is in anti-phase to the volume pulsations because the absorbing property of the erythrocytes dominates the reflective property. Thereby an increase in blood volume produces a decrease in reflected light.

With the recent developments in semi-conductor technology, such as light emitting diodes (LEDs), photodiodes and phototransducers, and their narrower operating frequency, the effects of altering light intensity and incident wavelength on the tissue and to the reflected signal have been investigated (Ugnell and Oberg, 1995; Murray and Marjanovic, 1997). Careful selection of light source operating wavelength will allow the user to penetrate different depths of the tissue for the same optical intensity. Blue light for example penetrates the skin four times less than red light which reaches between about 0.5mm to 1.5mm (Jones, 1987). The correct selection of the wavelength of optical radiation is also important because

tissue is mainly composed of water, which absorbs light strongly in the ultraviolet and longer infra-red wavelengths. Melanin, a pigment which is found in the epidermis, also strongly absorbs light in the shorter wavelengths. There is however, a region in the absorption spectrum of water that allows red and infra-red light to penetrate the skin more easily. Therefore red and infra-red light are often chosen to follow changes in blood volume in the skin (Allen, 2007).

4.3 Photoplethysmography- Current Use

4.3.1 Assessment of Blood Flow

Blood flow to the periphery has been assessed long before the advent of Photoplethysmography. Palpation of the pulse was carried out in ancient times to determine physical health. With the invention of the sphygmograph in1860, the palpation of the peripheral pulse by mechanical means could be performed. This instrument, by means of a pressure plate placed over the artery, traced out the contour of the peripheral arterial pressure pulse (Balthazar, 1866). This instrument was the fore-runner of modern electronic tonometry systems. The first investigations into the peripheral pulse using PPG were not performed until much later (Hertzman, 1938). Therefore much of our early knowledge of pulse wave characteristics and the effect of physiological and pathological mechanisms are based on work investigating the pressure pulse. Consequently, much work has been done comparing the PPG pulse to the pressure pulse.

As the pressure wave moves towards the periphery it changes in shape and temporal characteristics, which are produced mainly from reflection of the pulse wave from the periphery. Differences in pulse wave reflection have been attributed to such physiological

phenomena as growth and development, aging, physical fitness, food, heart rate, exercise, body height and gender and to disease conditions such as hypertension, and heart failure. Vasodilator drugs also appear to effect waveform characteristics. However, in a number of studies, analysis of pulse wave reflections do not appear to be able to distinguish between populations with different levels of atherosclerosis or from sections of the population with diabetes mellitus (Megnien et al., 1998; O'Rourke et al., 2001).

A number of studies have investigated the relationship between the pressure pulse and the PPG pulse (Millasseau et al., 2000); (Avolio, 2002); (Allen and Murray, 1999). It is understood that the peripheral pressure pulse obtained from the finger or radial artery is affected by pulse wave reflections mainly from the lower body. If these reflections are reduced by using a vasodilator such as nitroglycerine, then marked changes to the contour of the pressure pulse are seen. The PPG signal also shows changes in temporal characteristics in response to nitroglycerine, however, it was not known whether the signals were influenced by similar mechanisms. Millasseau et al (2000) quantified the relationship between the digital volume pulse and the peripheral pressure pulse by investigating changes to these waveforms from different patient groups. They concluded that the peripheral pressure pulse can be predicted from the digital volume pulse and has a linear relationship across a wide range of normotensive and hypertensive subjects and over large changes in both pressure and volume. They also concluded that both the peripheral pressure and volume pulse are influenced by the same vasodilatory mechanism. However even though the PPG and peripheral pulse are related to one another by similar mechanisms, the wave contour is not the same. They also found that in the frequency domain the volume pulse does not contain some of the higher harmonic frequencies as does the pressure pulse and so its contour is relatively more damped. Allen and Murray (1999) employed artificial neural network analysis, as well as other

techniques, to model the linear and non linear relationships between peripheral pressure pulse and the blood volume pulse in normal healthy subjects. They found the ANN using the chosen identification techniques could simple describe their relationship.

The PPG signal is produced from fluctuations in the intensity of the back-scattered light due to changes in blood volume flow in the micro-circulation. The signal can be basically separated into two main components: A quasi D.C component which reflects the total red cell volume below the skin, and superimposed onto this is an A.C component that is produced by the fluctuations in blood volume directly beneath the sensor. Therefore the A.C component reflects relatively fast temporal changes, while the D.C component traces relatively slow temporal changes in blood flow (Kamal et al., 1989). As early as 1937 Hertman and Spealman (1937) described the appearance of the A.C. component of the PPG signal as two phases: The rising edge of the pulse called the anacrotic phase and the falling edge known as the catacrotic phase. Physiologically, the first phase is produced by the systolic period of the cardiac cycle and the second phase produced during the diastolic or resting period of the cardiac cycle. The diastolic phase is particularly affected by wave reflections from the periphery and in patients with healthy compliant arteries; there is normally a dicrotic notch present on the falling or catacrotic phase.

The D.C and A.C. components are affected by a number of different physiological mechanisms which have been attributed to low frequency activity of the sympathetic and parasympathetic nervous systems and thermoregulation. In particular the amplitude of the pulsatile component (A.C component) and the tissue blood volume below the skin (D.C. component) fluctuate in the low frequency region, due to vasomotor activity, while fluctuations in the period of the signal appear to be more intense in the high frequency region,

i.e. respiration (Nitzan et al., 1998); (Nitzan et al., 1995; Nitzan, Babchenko and Khanokh, 1999); (Nitzan et al., 1995); (Hyndman, Kitney and Sayers, 1971).

An additional parameter used to assess blood flow and has been studied extensively is pulse wave transit time. With each heart beat, a pressure pulse radiates to the peripheries and the effect of this wave can be detected as changes in blood volume under the skin by PPG. The time it takes for the pulse to reach the peripheral sites, such as the ear lobes, fingers or toes, is significantly influenced by age, blood pressure, height and arterial disease. Some studies have used the ECG R wave as the timing reference point and then measured the time between this and the onset of the pulse trough or peak (Allen and Murray, 2000b2002; Jeong, Yu and Kim, 2005). Other studies have used the delay in the arrival of the pulse between the finger and toe. This therefore does away with the need for ECG leads (Erts et al., 2005); (Nitzan et al., 2002).

The repeatability of unilateral and bilateral PWTT measurements made at the ears, fingers and toes within sessions and between sessions was studied by Jago and Murray (1988). They found that is was important to account for and control such factors as body position, temperature, and acclimatisation as these affected PWTT measurements. This study also highlighted that the arrival time of the pulse depends on site of measurement; the pulse arriving at the ears first and the toes last. The variability in taking bilateral PWTT and amplitude measurements was investigated by Allen and Murray (2000b). A significant difference between the right and left sides was found only for PWTT to the toes, which was accounted for in the asymmetry between the iliac arteries. Their study provided a normative set of amplitudes and PWTT measured at different peripheral sites and showed the bilateral symmetry in pulse characteristics. In the same year, Allen and Murray (2000a) investigated

the similarity in the pulse shape between the right and left sides of the body at the ears, fingers and toes. They found that the pulse shapes from the right and left sides are highly correlated at each segmental level. The disadvantages of PWTT measurement are blood pressure and age, which are major confounders when assessing PAOD.

Autonomic control of blood flow in skin micro-vessels has also been investigated by spectral analysis techniques (Bernardi et al., 1996). They found a high coherence between fluctuations in blood pressure, PPG and the ECG signals. They concluded that skin vessels are under central as well as local control.

Because PPG is a simple non-invasive low cost technique, it has been widely used as a means of monitoring changes in a number of physiological and cardiovascular parameters. It has been used to monitor changes during anaesthesia (Dorlas and Nijboer, 1985), and for observing continuous changes in blood pressure, respiration and heart rate (Jeong et al., 2005); (Linberg, Ugnell and Oberg, 1992). PPG has also been used to monitor blood volume to control hydration during haemodialysis (McMahon et al., 1996).

4.3.2 Assessment of disease

The potential of photoplethysmography as a means of estimating the effects of various disease conditions on peripheral blood flow has been recognised for many years. Hertzman and Dillon (1940b) investigated the reduction in skin blood supply in patients with Raynaud's disease and on a patient with intermittent claudication. Visual inspection of the pulsatile component and the quasi D.C component of the PPG signal showed a decrease in amplitude, which was explained as evidence of arterial constriction. However at that time they were

unable to apply any more objective or sophisticated analysis techniques to the signals, therefore the information was limited.

4.3.2.1 Arterial Assessment

Much work has been done more recently investigating the changes in shape of the PPG signal over different physiological conditions and pharmacological effects. As mentioned previously the PPG signal is affected by respiration, the sympathetic nervous system and other locally controlled influences such as vasomotion, however these largely produce changes to the amplitude of the PPG and leave the shape of the pulse mostly unchanged. Chowienczyk et al (1999) infused vasodilatory drugs into the forearm of minimal concentrations such that it produces no systemic reaction, but only local stimulation showed that the amplitude of the PPG increased but had little effect on the shape of the waveform. They concluded that this observation suggested that the contour of the PPG signal is influenced by characteristics of the systemic circulation. An important study by Lax, Feinberg and Blake (1955) classified the finger signal into five different groups according to the change in shape of the pulse, in particular the gradual disappearance of the dicrotic wave. The change in waveform shape, from a pronounced dicrotic notch in young individuals to no notch in older participants is interpreted as the early arrival of the pressure wave reflected from the peripheral circulation, due to increasing stiffness of the conduit arteries. Sherebrin and Sherebrin (1990) investigated how the pulse shape changed in the finger as a function of age using spectrum analysis. They found that there was a significant decrease in the power of the second harmonic frequency as a function of age. This results in a gradual disappearance of the dicrotic notch with age and a general rounding of the pulse. However, for these changes to be of clinical use more objective measures have to be developed.

The effects of aging on the contour of the peripheral pulse have been studied using indices made up of various parameters from the volume pulse. Millasseau et al (2002); Millasseau and Kelly (2003) proposed a Shape index (SI) and a reflection index (RI) as a measure of vascular aging and their response to vasoactive drugs. The indices used timings and amplitudes of different parts of the pulse contour as an estimate of large artery stiffness. Their results revealed that SI was strongly correlated with age and pulse wave velocity (PWV), but was not significantly affected by vasoactive drugs. Alternately, RI was weakly correlated with age, but showed dose dependent increase with vasoactive drugs. They concluded that SI was a more reliable index of vascular aging than RI.

Factors which influence the dynamics of the peripheral pulse have been investigated using the second derivative of the PPG waveform. The second derivative or the acceleration waveform enables inflection points in the anacrotic or catacrotic phases of the signal to be visualised with greater confidence and consists of a number of peaks and troughs corresponding to these inflection points. Five points on the acceleration waveform have been used as indices of certain physiological mechanisms and pathological conditions. Particular indices have been shown to correlate with age and blood pressure in a hypertensive population (Hashimoto et al., 2002). However their success at detecting arterial compliance related to atherosclerosis is unclear (Takazawa et al., 1998; Bortolotto et al., 2000).

Examining the change in shape and characteristics of the PPG signal for the diagnosis of lower limb peripheral vascular disease (PVD) has been investigated. Analysis and classification of the PPG pulse from the great toe in patients with atherosclerotic disease has been performed using artificial neural networks (Meissner et al., 2007). A single normalised toe pulse was used as the input to the ANN and the outputs represented the diagnostic

classification, i.e. normal, significant PVD or major PVD as trained by the ankle to brachial pressure indices (ABPI). The results showed a high diagnostic accuracy of 90% and showed that a ANN can be trained to distinguish between PPG pulses from normal and diseased lower limb arteries (Allen and Murray, 19931995).

Age related changes of pulse shape characteristics and pulse transit times (PWTT) measured using PPG at ears, fingers and toes was examined by Allen and Murray (2002, 2003). They found that age was the strongest contributor to PTT measurements at all sites, referenced to the ECG R-wave. Systolic blood pressure also significantly contributed to PTT measurements and height contributed to just the finger and toe times. The change in shape to the peripheral PPG signal was determined by measuring changes to the systolic rising edge and damping of the dicrotic notch. They found subtle, gradual and significant changes to the systolic rising edge and to the damping of the dicrotic notch and concluded that age matched normal range must be considered when evaluating pulses from patients with vascular disease.

With the normative sets of data gathered regarding PWTT and pulse shape Allen et al (2005) compared patient pulse data with these normative ranges with the intention of estimating the accuracy of pulse timings, amplitude and shape of the PPG signal at the toe for detecting lower limb arterial disease. A shape index (SI), different from the shape index produced by Millasseau et al (2002), was developed to quantify changes in contour of the great toe signal. Bilateral as well as unilateral differences in PWTT and SI from patients with low or high grade arterial disease were compared with healthy subjects using ABPI as the gold standard. PWTT, amplitude and SI were ranked according to their diagnostic value for detecting lower limb PVD. They found that for individual great toe measurements, SI performed the best at detecting peripheral arterial occlusive disease (PAOD) with a diagnostic accuracy of 90% and

pulse wave transit time to the great toe performed the worst with a diagnostic accuracy of 78%. For bilateral differences in great toe pulses, pulse wave transit time performed the best with a diagnostic accuracy of 88% and SI had an accuracy of 82%. They concluded that PWTT and their derived SI could be used to detect PAOD with confidence.

Bilateral PPG study of one-sided arterial stenotic leg disease was conducted by Erts et al (2005). In particular they measured the difference in the arrival of the blood volume pulse at the toes, between the right and left legs for patients with unilateral stenosis and compared these PWTT with healthy subjects. They found a significant increase in the time delay between bilateral measurements of PWTT on patients with PAD when compared to bilateral PWTT measurements on healthy subjects. In this study they also noted a significant change in shape of the PPG signal taken from the toe between bilateral measurements from patients with unilateral stenosis. There was no equivalent significant change in shape in healthy subjects.

A number of PPG studies looking at the alteration of blood volume pulsations in the toes before, during and after changes in limb position have been conducted. These studies take advantage of locally mediated myogenic vasodilator responses or more centrally controlled responses from the autonomic nervous system. These regulatory controls respond to the pressure changes at the periphery induced by the leg elevation. Perfusion pressure at the trough is reduced if the trough is raised above the heart. This triggers local compensatory mechanisms mentioned above in an effort to maintain adequate blood flow to the tissues. In patients with PAD or diabetes mellitus it is suggested that these local regulatory actions will already be in effect. Therefore further demands for increases in blood flow to the tissue from changes in pressure due to alterations in leg position will be partially or completely

ineffective. This effect is manifested in the PPG signal and can be compared with equivalent signals from healthy controls as a means of screening for PAD (Alnaeb et al., 2007).

The change in amplitude of PPG derived toe pulses and their correlation to toe systolic blood pressures has been investigated in the assessment of the severity of peripheral arterial disease and critical limb ischaemia (Carter and Tate, 1996). They found that the toe systolic blood pressures were lower in patients with PAD when compared to healthy controls and that the amplitude of the PPG pulses was also correspondingly low. They concluded that the addition of pulse wave recording by PPG and specifically low toe pulse amplitude was related significantly to increased risk of amputation and death in patients with PAD (Carter and Tate, 1996, 2001). The change in shape of PPG toe measurements in a patient group consisting of lower limbs with varying degrees of arterial stenosis was analysed by Oliva and Roztocil (1983). They analysed the toe pulses by splitting the waveform into thirds and producing an index base on the width of the pulse one third down from the peak and the pulse length. When they compared the amplitude ratio of stenotic limbs to young healthy individuals the results showed 80.8% sensitivity, and rose to 100% when comparing legs with complete occlusions. However the sensitivity dropped to 69.8% when comparing healthy individuals with an average age of 50 years, but they still found 100% sensitivity for completely occlusive legs.

4.3.2.2 Venous Assessment

Since the first direct measurement of venous pressure in the lower limb by Barber and Shatara (1925) many investigations have been conducted analysing the venous haemodynamics of healthy subjects and patients with venous pathology. Venous pressure measurements have functioned as the gold standard as they can demonstrate the presence of

venous insufficiency, quantify its severity and determine the relative contributions from deep or superficial valvular dysfunction (Nicolaides and Zukowski, 1986). However since this is an invasive procedure, involving the insertion of a needle into a vein on the dorsum or medial aspect of the trough, it has not been widely accepted as a routine clinical test. Since plethysmography and in particular photoplethysmography, is a non-invasive procedure which can be used to investigate blood volume changes in the skin, numerous PPG investigations of venous haemodynamics and disorders have been conducted. Many of the early investigations examined the correlation of PPG derived signals with venous pressure measurements. Light reflected signals were recorded at medial malleolus level as studies had shown that this was the best position to achieve the best separation between healthy controls and patients with venous insufficiency (Rosfors, 1990; Rashid, 1996).

Initial tests concentrated on measuring the venous refill time (VRT). This utilises the quasi-D.C part of the PPG signal, which represents the slowly changing venous portion of the signal. A zero or baseline level is achieved with the subject at rest either sitting or standing. They then perform a predetermined number of dorsiflexions, approximately 10 within a certain specified time approximately 15 seconds. During this exercise, a pressure drop in the deep veins encourages blood in the venuoles and superficial veins to drain into the deep venous system. This emptying of the superficial veins causes the baseline of the PPG signal to increase in the positive direction. This continues until a maximum emptying of the superficial veins occurs, whereby the deflected signal begins to return to the baseline level after completion of the exercise programme. Slow refilling of the veins ordinarily occurs only as a result of arterial inflow. However, patients with valvular dysfunction experience venous reflux which refills the veins by gravity before they are filled by normal inflow from the arterial side, therefore reducing the venous refill phase. If there is an abnormally short venous

refill time the procedure is repeated with a pneumatic cuff inflated to a pressure that occludes the superficial veins, but not the deep veins. If the refill time is now normal then the patient suffers from superficial venous incompetence, however if the refill time is still abnormally short then the patient has deep venous incompetence. This method however is severely limited by the ability of often elderly patients to perform the exercise adequately. However, a series of simple calf compression squeezes can overcome this problem.

PPG venous refill times have been shown to correlate well with venous pressure recovery times (Abramowitz, Flinn and Bergan, 1979; Nicolaides and Miles, 1987; Williams, Barrie and Donnelly, 1994). Nicolaides and Miles (1987) though, found that PPG refill times could provide a good separation between normal subjects and patients with venous insufficiency when the test was performed in the standing position, but not the sitting position. They also concluded that the test is qualitative because of a lack of correlation between the short refilling times with deep venous insufficiency and ambulatory venous pressure.

An investigation by Norris, Beyrau and Barnes (1983) explored a technique which used quantitative PPG. This was achieved by adjusting the gain of the recorder between the sitting and standing positions so that the recorder measures maximum deflection. This maximum deflection then corresponds to the measured distance between the right atrium and the position of the PPG transducer. The calibrated PPG signal was then validated against ambulatory venous pressures (AVP) measured at ankle level. Quantitative PPG correlated closely with AVP.

A major advancement in the technological side of PPG measurements came in the 1990s with the development of an automatic optoelectronic signal calibration procedure. Blood volume

changes measured by PPG are influenced by a number of factors such as damping of the optical signal from skin thickness and pigmentation level, and the degree of skin perfusion affects the initial blood volume under observation. However the major problems that affected non-calibrated PPG systems were skin thickness and colour. Different skin conditions, such as those mentioned above, could produce differences in PPG signal amplitude for the same blood volume change. Quantitative plethysmographic systems adjust the intensity of the emitted light until the reflected signal reaches a defined level. Therefore every skin type has a constant starting value. This brings a number of advantages such as intra-individual comparison of PPG signals, quantified PPG signal amplitude in PPG% and different quantitative PPG units can be compared (Blazek and Schultz-Ehrenburg, 1996; Ulrich Schultz-Ehrenburg, 2001).

With the advantages of quantitative PPG, a number of additional and more elaborate venous tests were developed with a number of active or passive tests that involved the patient standing, sitting or supine. The tests also involved the use of tourniquets or cuffs at a number of positions on the lower limbs to occlude venous outflow. The graph recorded is then examined and divided into an emptying and filling phase with various points on the graph corresponding to functional parameters that can be used to assess venous function. The three main venous tests used are: Muscle Pump Test; Vein Occlusion Test and the Vein Pressure Test. These tests used parameters such as venous filling times, venous outflow, venous capacity and venous pressure measures to quantify venous function (Fronek, Minn and Kim, 2000; Ulrich Schultz-Ehrenburg, 2001).

The three basic tests have been used extensively to investigate and assess a number of venous disorders such as varicose veins, post thrombotic syndrome and deep vein thrombosis (Thomas et al., 1991; Abbott, Diggory and Harris, 1995; Sproule, 1997).

The tests described so far have in some way required the use of cuffs, tourniquets or some patient movement to assess the condition of the venous system. This limits the applicability, both in the range of patients and ease of use; however a number of studies have investigated vasomotion in patients with chronic venous insufficiency using laser Doppler technology (Cheatle et al., 1991; Chittenden et al., 1992; Hafner et al., 2009; Heising et al., 2009). In these studies no cuffs or tourniquets were used and the patients remained supine throughout the study. Some of them performed local skin heating to investigate the different effect this may have on healthy patients and patients with CVI. The results of the studies showed a statistically significant difference in the amplitude and frequency of vasomotive waves between the healthy and patient group. Cheatle et al (1991) were able to show a statistically significant difference between all three patient groups: lipodermatosclerotic, uncomplicated varicose veins and controls. Hafner et al (2009); Heising et al (2009) used more advanced wavelet analysis to investigate laser Doppler vasomotion in patients with CVI. In particular, Heising et al (2009) separated the laser Doppler derived skin blood flow signal into its dynamic frequency components: myogenic 0.06-0.16 Hz; respiration 0.16-0.6 Hz; and heart rate 0.6-1.6 Hz. They found that there was a significant difference between patients and healthy subjects in these frequency intervals and further more, the main energy peak height in these frequency intervals increased with the severity of venous disease.

5 Equipment and General Methods

This chapter is an overview of the general methods employed and a description of the equipment used to conduct the research study. The data were collected using three different modalities: ultrasound imaging to assess the lower limb vessels for arterial and venous disease, pressure measurements at the ankle and upper forearm to assess for any pressure changes due to stenotic disease (arterial methods only) and photoplethysmography (PPG) to measure intensity of the reflected infra-red signal, which is proportional to blood volume flow.

This study was given ethical approval by the South East Wales Research Ethics Committee – Panel D on 2 May 2006. (ref: 06/WSE04/25) Informed consent was obtained from all volunteers.

5.1 Study Design

Subjects in the healthy, arterial and venous disease groups were taken from people visiting the Doppler Department at the University Hospital of Wales for an ultrasound investigation. These comprised of GP referrals and organised outpatient appointments. If after the ultrasound examination they were found not to have arterial or venous insufficiency, then they were placed in the healthy group. Firstly, visitors to the department had an ultrasound scan performed to learn whether they were suitable candidates for the study. If appropriate, potential candidates were asked if they would like to participate. Subjects were excluded from the arterial study if they had significant stenotic disease of the upper limbs, if they had Raynaud's disease or if they had previous lower limb graft surgery. Subjects were excluded from the venous study if they were diagnosed as having an acute DVT, previous venous

stripping or limb tremor. Volunteers were then taken to a temperature controlled room where they were asked to expose their lower limbs. Subjects in the arterial study were asked to lie down, while subjects in the venous group were asked to sit in a chair. Additional information was then gathered while the patient rested for a period of 10 minutes. This was to ensure a level of cardiovascular stability. Following this, PPG signals were acquired and stored for later analysis. Once the PPG signals had been obtained, a further ABPI measurement was taken for the arterial group only.

All five types of scans, arterial PPG, venous PPG, ABPI and lower limb arterial B-mode and lower limb venous B-mode were performed following the standard clinical protocols which are described in more detail in section 5.3. All subjects in the arterial group were over 40 years of age. This age criterion was set so as to obtain a similar age range for the cases and for the healthy group. The age range in the venous study comprised the normal volunteer group: 8 under 40yrs and 16 over 40yrs; the patient group: all over 40yrs.

Once the waveforms were obtained from the normal and patient groups, they were processed and conditioned using Matlab software so that they could be analysed later and relevant parameters taken from the waveforms. Once the effective parameters were found a program was written in Matlab which classified the waveforms into predetermined groups.

5.2 Equipment

All the subjects in the trial had ultrasound scans of the lower limbs and PPG signals recorded for comparison and later analysis. Subjects in the arterial study had a further ABPI test performed. Further details of each test are outlined:

5.2.1 Toshiba Xario System

The Toshiba Xario system is routinely used for clinical measurement of vascular disease in the Doppler Ultrasound Department at UHW. It is a sophisticated colour flow duplex system, optimised for the assessment of peripheral vascular disease and has a range of transducers available for different vascular imaging applications. Patients with certain types of body composition and differing levels of adipose tissue can be difficult to scan. Because the structures of interest can be at different depths within the tissue, probes of different fundamental frequencies can be used to optimise the image. Harmonic imaging is an additional technique which uses the harmonic frequencies of the reflected ultrasound signal to enhance the contrast and grey scale image. For this study, the lower limb vessels were assessed using the PLT-604AT linear probe employing tissue harmonic imaging at 6.6MHz, which is the optimal frequency for imaging the vessels in the lower limbs, (the depth of the vessels range from approximately 2 cm to 6cm) and pulsed wave Doppler at 4 MHz fundamental frequency. For the arterial study iliac arteries were assessed using the PVT-375BT curvilinear probe employing tissue harmonic imaging at 4MHz (the iliac vessels travel deeper in the abdomen than the vessels in the lower limbs, reaching 8-10cm in some cases) and pulsed wave Doppler at 1.8MHz fundamental frequency.

5.2.2 Arterial Equipment

All subjects in the arterial study had blood volume measurements taken using both a Huntleigh Assist and pocket Doppler. Further details are given below.

5.2.2.1 Huntleigh Assist

The Huntleigh Assist is a portable vascular assessment tool, (Figure 19), with the ability to measure and record dual arterial and dual venous PPG signals, a pulse volume recording and

Doppler colour spectrum waveform analysis. The unit has connectors for two probes and this allows it to be used in single or dual probe configuration. Each probe houses an infrared emitter (LED) that emits light at a wavelength of 940nm and a photodetector. The probes are attached to the skin by a transparent double-sided sticky pad. The signal detected by the probe is sent to the main unit where it is displayed and stored for later use. The data can also be transferred to an external memory device for further analysis.

Figure 19 Huntleigh Assist

5.2.2.2 Huntleigh Pocket Doppler

The Huntleigh Pocket Doppler provides bidirectional blood flow information. Clinically it may be used to assess patients for sites of venous incompetence, or used to assess patients for arterial insufficiency of the lower limbs when taking ankle brachial pressure indices (ABPI). In this thesis it was used in the latter. There is a choice of 8 MHz or 5 MHz probes and pneumatic cuffs to fit limbs of different diameters.

5.2.3 Venous Equipment

The Assist assesses venous insufficiency by performing the Muscle Pump Test, (section 3.2.9.3.1). Therefore it is programmed so that the subject performs certain manoeuvres in a predetermined order specified by metronomic timing; these last for approximately 45 seconds. For these reasons the Assist is unsuitable for the venous tests in this thesis.

The venous unit used in this study is a four channel photo plethysmography (PPG) system. The unit was manufactured by ArjoHuntleigh UK but is not commercially available as a product at present. The system main components are:

- Main unit including analogue opto-transmitter and receiver circuits, A/D convertor with USB interface and rechargeable batteries.
- Four opto-transducers with integrated pre-amplifier
- Laptop P-C & software
- Mains battery charger

The main unit electronics are contained within a standard multi-purpose aluminium instrument housing. The system includes four PPG opto-transducers. Each transducer incorporates an infra red LED of wavelength 890nm and a matching photodiode. Also included is a miniature printed circuit board containing an infra red pre-amplifier circuit. In order to transmit and receive light to and from the patient tissue, the LED and photodiode protrude a small way through the front of the plastic housing. The opto-components and the amplifier circuit are enclosed in a circular plastic housing. The main unit contains two 12V NiMH re-chargeable battery packs. The batteries are charged from a regulated 20V supply within the external charger.

One PMD-1608FS from Measurement Computing is provided in order to convert the analogue PPG signals to digital and transfer them via a single USB cable to the laptop personal computer. The four analogue PPG signals are connected to analogue to digital converter input channels. The converter is a 16-bit successive approximation type, and it derives its power from the USB port. The bandwidth of the unit is 0.06Hz to 50Hz maximum The PPG unit is interfaced to the PC via its USB output. Continuous PPG data is transferred to the PC and is stored for analysis off-line.

5.3 General Methods

5.3.1 Lower Limb Arterial Ultrasound Scan

When scanning the lower limb arteries, the patient lay supine on the scanning couch with the lower limbs exposed. The distal CFA was imaged and the Doppler waveform was assessed visually for any loss of triphasic flow or rounding of the waveform due to significant iliac disease. If the Doppler waveform showed indications of this then the iliac arteries were assessed for the presence of artherosclerotic disease using the curvilinear probe and the Abdominal Vascular setting. The scan continued distally from the CFA assessing the SFA and popliteal arteries in the longitudinal plane, using the linear probe and the lower limb arterial scan pre-set. The extent and severity of any arterial disease was assessed using triplex mode by measuring the peak systolic velocity (PSV) from the Doppler waveform just proximal to and through the stenosis. The severity of the disease could then be classified using the following standard criteria given in Table 1 . Once the lower limb arterial scan was complete, both upper limbs were scanned for evidence of any arterial stenotic disease

PSV Ratio	% Stenosis
<2	Not haemodynamically significant
2	50% (moderate)
>3	>70% (tight)
No colour flow	Complete occlusion

Table 1 shows how the stenoses were graded according to PSV ratio of velocities

A complete occlusion was confirmed by reducing the colour scale and/or using power Doppler.

The data from the patient group were classified according to the level of artherosclerotic disease present by triplex imaging. Patients with at least one stenosis in the lower limbs of between 50-70% were classified as having moderate disease and placed into the moderate disease group; patients with at least one stenosis between 70-99% were classified as having significant disease and placed into the significant group and patients with an occlusion were placed in the occlusive group.

A total of 46 normal subjects (27 males) and 57 patients (32 males) with lower limb peripheral arterial disease were included in the study, with age ranges of 40-83 and 40-86 years, respectively. There were no lower limb amputees, giving toe pulse data from 66 legs in the normal group and a total of 66 legs in the patient group. Using the duplex classification of arterial disease shown in the table above the patient group had 20 legs in the moderate disease group; 25 legs in the significant disease group; 21 legs in the occlusive disease group.

5.3.2 Arterial PPG Method

Arterial subjects lay with their lower limbs exposed and a blanket over the troughs to reduce heat loss for a period of 10 minutes before any signals were recorded. During this period, relevant patient details were obtained and recorded. Next the two Assist PPG probes were placed on the volunteer's right hand side of the body, at the great toe and index finger, ensuring that both sites were clean and dry, (Figure 20 and Figure 21). Subsequently, blood volume recordings were taken for the pre-set recorded time of 10 seconds into the dual channel Assist. This procedure was repeated for the left side of the body.

Figure 20 Probe placement and subject position for data acquisition

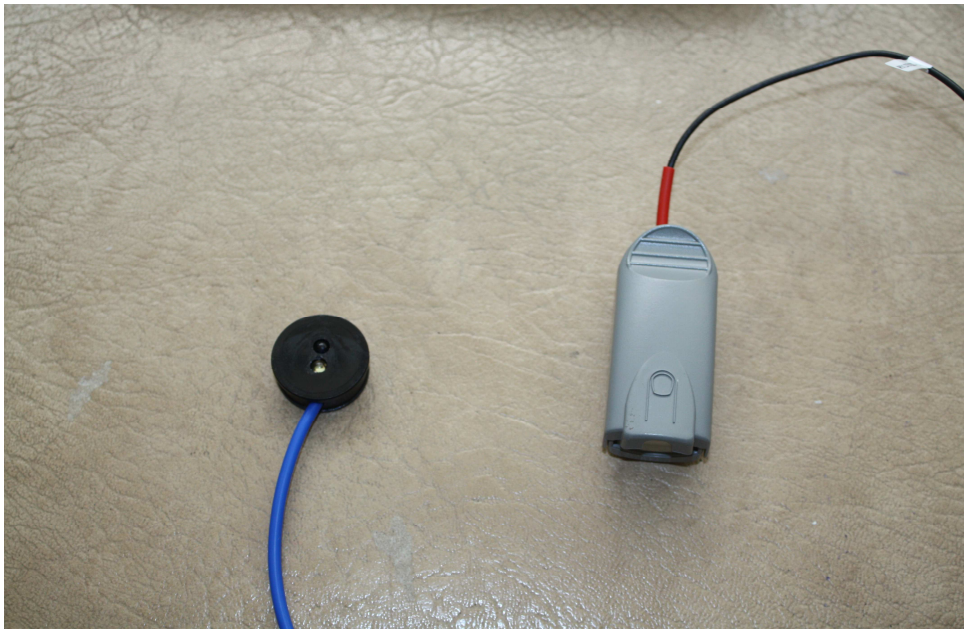

Figure 21 Both APPG probes used in the study. Great toe probe (left), finger probe

5.3.3 Ankle Brachial Pressure Index (Arterial Subjects Only)

With the patient lying supine, an appropriate sized pneumatic cuff was placed around the volunteer's ankle. A Doppler probe was positioned over the dorsalis pedis artery and the cuff inflated to a supra-systolic pressure so that the arterial pulse could no longer be heard. Slowly the pressure in the cuff was decreased until the arterial pulse resumes, at this point the pressure was noted, and was identified as the peak systolic pressure. This procedure was repeated for the posterior tibial artery located posterior to the medial malleolis. The procedure was repeated for the other leg. Next a cuff is placed around the upper arm and a Doppler probe is placed over the brachial artery until the brachial pulse was audible. The cuff was inflated to a pressure that occluded the artery and then the pressure in the cuff was reduced until the audible pulse resumed. This was the brachial systolic pressure. This procedure was repeated for the other arm. To obtain the volunteer's right ABPI, the higher peak systolic pressure at the right ankle is divided by the higher systolic pressure between the right and left

arms. Similarly the volunteer's left ABPI, the higher systolic pressure at the left ankle is divided by the higher systolic pressure between the arms.

5.3.4 Lower Limb Venous Ultrasound Scan

Firstly, potential venous subjects were scanned to exclude the possibility of an acute DVT, as many of the patients referred to us from GPs have these signs and symptoms. This protocol is written below. Once a DVT has been excluded, a lower limb venous assessment is conducted to assess the deep, superficial and perforator veins for reflux greater than one second. This assessment is explained later.

The assessment for above knee DVT was performed with the subject supine. The CFV was imaged so that volume flow changes due to respiration could be detected. If no changes were detected, this would indicate significant iliac venous disease and so the veins in the abdomen would be assessed for any obstruction. If however phasic flow was detected, scanning would continue distally observing any phasic flow in the SFV and popliteal vein. If spontaneous venous flow due to respiration changes was not seen then venous blood flow was augmented by manual compression of the subject's leg with the operator's free hand. Flow in the vein would be evident on the ultrasound scanner as colour filling and therefore indicate that portion of the vein was patent. A widely accepted method of excluding thrombus is vein compression with the ultrasound transducer. This method was used if manual compression by squeezing the subject's leg did not initiate colour filling. Scanning would continue in this manner assessing the patency of the deep venous system. The assessment for below knee DVT was performed with the patient sitting and legs dependent. The deep tibial veins were assessed for patency.

The deep and superficial venous system was assessed for competency with the subject standing. Venous incompetence was classified as reflux greater than 1 second (Evans et al., 1998) in the veins associated with each venous system in accordance with the CEAP classification system, (Appendix B). However the generally accepted value is 0.5 seconds.

5.3.5 Venous PPG method

Before the test commenced, subjects sat with lower limbs exposed and their details were taken while they rested for a period of 10 minutes. The PPG probes were placed 10cm above the medial malleolus and behind the knee on both right and left legs. The subject was told to breathe normally, and to sit in a chair as still as possible for the duration of the six minute test. Even though signals were recorded from both lower limbs simultaneously, only the signals from a single leg were taken forward for further analysis. After completion of the test, the trace was visually inspected on the PC screen and if there were any obvious major deviations in the amplitude of the signal from normal, then the test was repeated.

5.4 Statistical Tests

In the remaining sections of this thesis a number of different statistical tests were performed to compare data groups or to evaluate a diagnostic test against a ‘gold standard’ test, which, in this case, is duplex ultrasound. An explanation of the meaning and reasoning behind these tests follows.

5.4.1 Scatter Diagrams

Scatter diagrams are used to show the relationship between two continuous variables. Additionally, data that are separated into groups can be compared, which is useful to check the assumptions of some analytical methods. See section 6.3.

5.4.2 Box-plots

Sometimes we want to summarise a frequency distribution in a few numbers for ease of reporting. A five figure summary can be used composed of the median, quartiles, maximum and minimum to describe the data. The median is the central value of the distribution. The quartiles divide the distribution into four equal parts and for example the second quartile is the median. The box shows the distance between the first and third quartiles, with the median marked as a line and the vertical bars show the extremes. An observation that is 1.5 times or more the length of the box may be called an outlier. See section 7.4.

5.4.3 Q-Q Plots

The purpose of the quantile-quantile plot is to determine whether the data collected is drawn from a specific distribution, in this case a Normal distribution. If the distribution of the data is

from a Normal distribution the plot will be close to linear. The reference line on the graph represents the corresponding quantiles of the theoretical Normal distribution. The plotted data points represent the quantiles of the sample data. If the data are not from a Normal distribution then the line will not be straight, but a curve.

5.4.4 Sensitivity and Specificity

Sensitivity and specificity are the most widely utilised statistics used to describe a diagnostic test. The diagnosis and the test results are considered to be either positive or negative. True negative (TN) results are those in which both the diagnostic test and the gold standard test are negative; true positive (TP) results are those in which both the diagnostic test and the gold standard test are positive. False negatives (FN) are those in which the diagnostic test is negative, but the gold standard test is positive indicating the presence of disease. False positive (FP) results are those in which the diagnostic test is positive, but the gold standard is negative, indicating the absence of disease.

$$\text{Sensitivity} = \frac{TP}{TP + FN} \qquad \textbf{Equation 7}$$

$$\text{Specificity} = \frac{TN}{TN + FP} \qquad \textbf{Equation 8}$$

Sensitivity is the ability if a test to recognise the presence of disease and this is calculated by dividing the number of true positive results by the total number of positive results obtained by the gold standard. Specificity is the ability to recognise the absence of disease and is calculated by dividing the number of true negative results by the total number of negative results obtained with the gold standard.

5.4.5 Receiver Operator Characteristics

The results of diagnostic tests may not be as easily classified as positive or negative. For example the degree of arterial narrowing can range from none to total occlusion. Additionally, a threshold level or cut-off point must be selected to divide positive from negative results. Where this cut-off point is set will have an effect on the sensitivity and specificity of the test. ROC curves can be used to compare the accuracy of tests at various thresholds. They are constructed by plotting the sensitivity against (1-specificity) at various thresholds.

5.4.6 Hypothesis Testing On Means

Hypothesis testing involves deciding between two possible hypotheses: H_0 or the Null Hypothesis where there is no difference between the means of the populations from which our samples were drawn and H_1 the Alternative Hypothesis, the case where there is a true difference between the population means. To decide if H_0 or H_1 is true a probability or p-value is calculated. The p-value is the probability the difference observed between the sample means is a chance finding due to sample variation. A large p-value indicates there is a high probability that an observed difference is due to sample variation; a small p-value indicates there is a low probability that an observed difference is due to chance. Therefore small p-values indicate a real or significant difference between the means. It is common practice to reject H_0, or the Null hypothesis when $p<0.05$ or not to reject H_0 when $p>0.05$. The lower the p-value, the stronger is the conclusion that H_0 should be rejected.

To test the difference between the means a t-test is performed. The type of t-test performed will depend on whether the data are paired, i.e. repeated data on the same group e.g. before and after treatment, or whether the data are un-paired, i.e. independent groups e.g. males and females. The t-test however makes certain assumptions about the data: for paired data the

differences are normally distributed; for un-paired the variable of interest is normally distributed. Tests performed on data that follows a Normal distribution are called parametric tests. When we have small samples or non-normally distributed data alternative non-parametric tests can be used. These do not make assumptions about the distribution of the data, but are less powerful. The non-parametric tests on paired data is the Wilcoxon Signed Rank Test; for un-paired data there is the Mann-Whitney U test.

6 Arterial Research

This chapter is divided into three main sections: the first explains the methods used to sort and process the signals before any analysis is performed; the second section explains the methods used in a preliminary study conducted on a subgroup of arterial subjects to investigate which measurement parameter to use for further analysis; and the final section reports the main arterial results.

6.1 Arterial Patients and methods

The patient group consisted of 57 subjects, 32 men and 25 women (mean age 67 years), with an age range of 40-86 years. This provided a total of 66 legs with stenotic disease between moderate and occlusive disease. The moderate group consisted of 20 legs; the significant group consisted of 25 legs and finally the occlusive group consisted of 21 legs. A group of 27 men and 19 women (mean age 62 years,) were chosen as the control group, with an age range of 40-83 years. Both patient and control groups underwent a duplex ultrasound scan; the control group to rule out any stenotic arterial disease and the patient group to classify the location and severity of stenotic arterial disease present. The distribution and severity of arterial stenotic disease is shown in Table 2. As can been seen the majority of

	Moderate	Significant	Occlusive
Iliac	2	12	2
Femoral	16	12	18
Popliteal	1	1	1
Tibial	1		

Table 2 shows the location and severity of stenotic lesions in lower limbs of patient group

stenoses were confined to the femoral artery; however there were a number of significant iliac lesions. The legs were categorised according to location and severity of stenotic disease present. If more that one stenosis was present, then the leg would be categorised according to the more severe disease present.

Once the data were transferred into Matlab, the data were organised into 4 separate groups based on degree of arterial disease present. These 4 groups were: Controls; moderate disease only, significant disease only; occlusive disease only. A further 2 groups were produced, combining different diseased groups namely: significant and occlusive disease and finally moderate, significant and occlusive disease, (Table 3).

No	**Separate Non Disease and Disease Groups**
1	Controls
2	Moderate
3	Significant
4	Occlusive
	Combined Disease groups
5	Significant and Occlusive
6	Moderate, significant and occlusive

Table 3 Table showing individual and combined disease groups

In general the data were analysed in three different ways. Firstly, PWTT were calculated for each healthy control and patient from the 10s strip of PPG data obtained. Secondly, total area under the normalised PPG pulse was calculated on the same subject groups using the same

10s strip of PPG data. Once these parameters were obtained sensitivities and specificities could then be calculated and the two methods compared. And thirdly, combining PWTT and total area calculated previously to consider if this could improve on individual results.

The following section is a more detailed description of how these parameters were calculated, firstly looking at PWTT, then area and lastly a combination of the two.

6.1.1 Preliminary Data Processing

The D.C offset was removed from each toe and finger waveform. Following this, the breathing component was removed by using a Filt-Filt function in Matlab. This function operates by filtering the input signal twice, once in the forward direction and then reversing the output and passing it through the filter once more. The output from this stage is then reversed, giving the required filtered signal. This filtering procedure is carried out to eliminate any phase differences between the input and output filtered signal that would otherwise be introduced by a single pass filtering process. The Filt-Filt function operates on the co-efficients produced from a second order infinite impulse response high pass Butterworth filter whose 3dB cut-off was set to 0.6Hz. Any noise on the toe and finger signals was then removed using a 100 point unsymmetrical moving average filter. This operates by averaging a number of points of the input signals, in this case 100, to produce each point in the output signals. Unsymmetrical averaging uses only the data points to one side of the output point, as opposed to symmetrical averaging which uses the data points symmetrically either side of the output point. Unsymmetrical averaging was chosen because it meant for easier programming, however it does introduce a relative shift between the input and output signals. But as this relative shift occurs to both finger and toe waveforms, both signals are equally affected, therefore the time delay between the finger and toe waveforms

did not alter. The moving average filter conditions the signals and therefore makes identification of the signal peaks and troughs easier. Figure 22 shows a block diagram of the signal conditioning process.

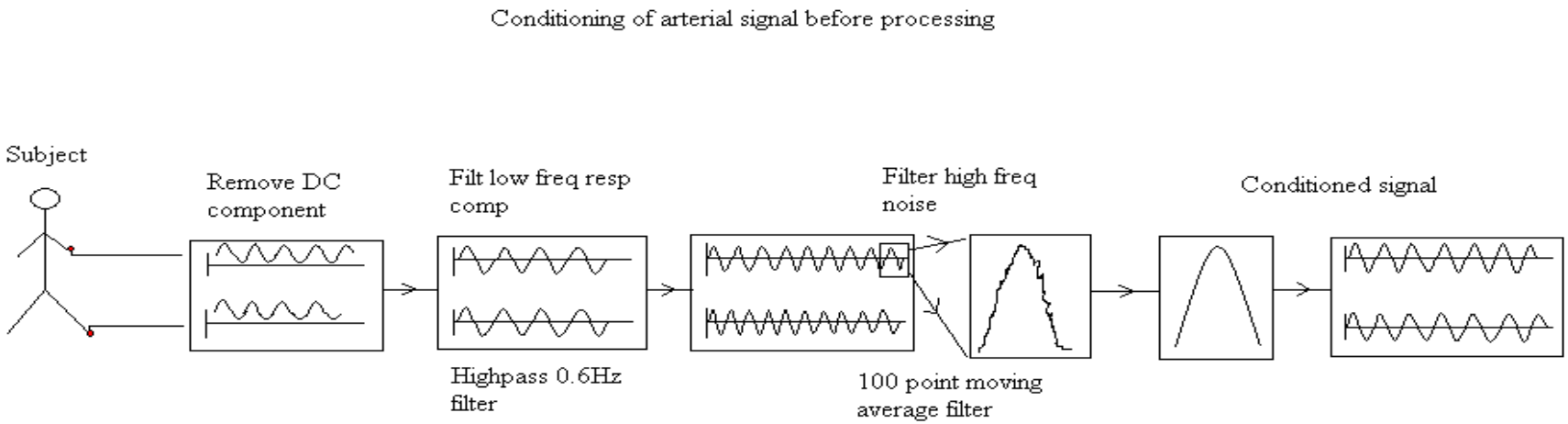

Figure 22 Signal conditioning process.

6.1.2 PWTT Analysis

Before pulse wave transit times could be calculated between the finger and toe waveforms, the pulse troughs and pulse peaks were identified. This was done by calculating the gradient between successive points on the anacrotic phase of each of the PPG pulses. The zero cross-over positions of the subsequent gradient points were used to locate the pulse troughs and pulse peaks of the toe and finger waveforms. The correct identification of these points can be seen in Figure 23.

The peaks and troughs of the finger and toe waveforms were identified by plotting the gradient of these pulses. The points where the graph of the gradient passes through the x-axis indicates where the gradient of the toe and finger pulses were zero. These points correspond to the troughs and peaks of each of the pulses that make-up the toe and finger waveforms. Since only the positive going part of the toe and finger pulses is required to identify the trough and peak only the positive part of the gradient plot was needed, therefore the negative half was discarded. Next, the maximum value of each peak in the gradient plot was stored in a rectangular matrix so that this could be used to identify the peak of each pulse in the toe and finger waveforms. Following this, the overall maximum peak pulse could be identified. To eliminate any incorrectly indentified pulse peaks which may be due to noise, a range of threshold-hold values were tested. Subsequently, any pulse peaks less than 45% of the maximum pulse amplitude were discarded.

Once the main peaks from the gradient plot were identified, they were used to locate where the peaks of the toe and finger pulses occurred in time. With this time information, the program counted back from the peak in the gradient plot to the zero value to obtain the

location of the trough, then counted forward to the zero value to locate the peak of the toe or finger pulse.

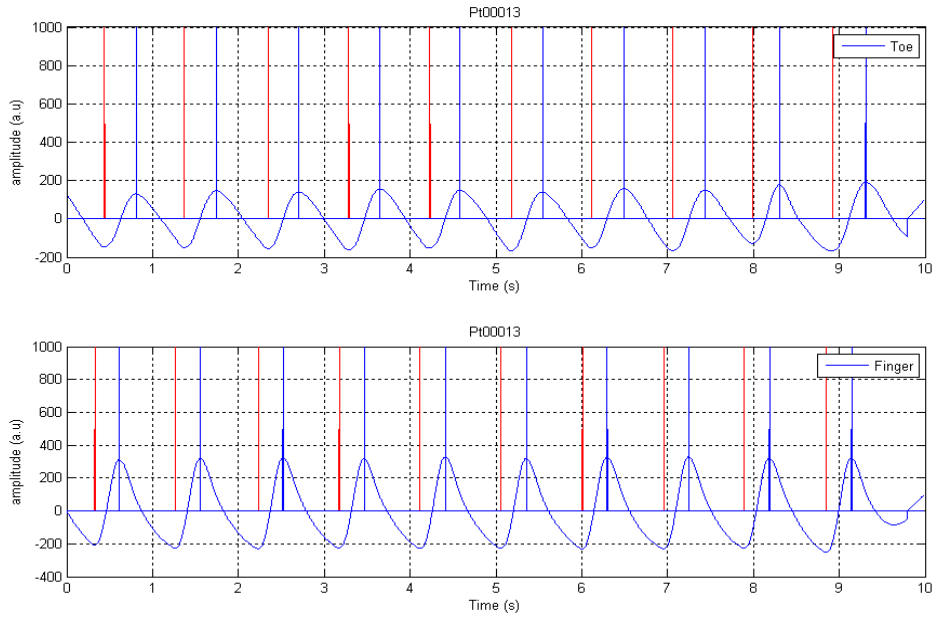

Figure 23 Location of troughs and peaks on finger and toe waveforms.

Once identified the troughs and peaks of the finger waveforms need to be matched in time to the troughs and the peaks of the toe waveforms. This ensures that with each heart beat the corresponding pulses at the finger and toe are compared in time and not pulses from different heart strokes. This was achieved automatically as the program calculated the number of beats per minute in the signal. From this the frequency and hence the period of the waveform was computed and a time threshold of half this was used to match the finger and toe pulses in time. Therefore if the difference in time between the peaks of the toe and finger pulses was greater than half the period, the pulses were not matched in time. This was repeated for the troughs of the pulses. Once this was accomplished, the delays between corresponding finger and toe pulses could be calculated. This was achieved by summing individual pulse delays between the trough of each finger and toe waveform. However, as the delays varied between

successive beats of the heart an average delay was calculated that would represent the delay for that subject. Therefore successive delays were totalled for each individual and this was divided by the total number of delays. This gave the average delay for that individual (Figure 24).

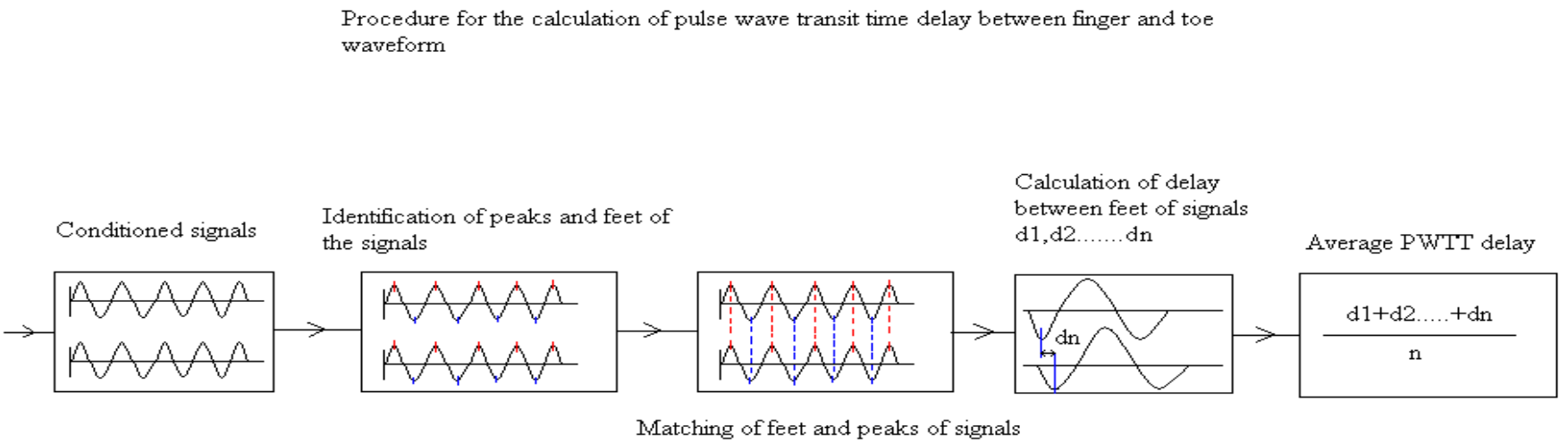

Figure 24 Block diagram showing procedure for the automated identification of the pulse peaks and troughs and subsequent calculation of PWTT

6.1.3 Area Analysis

Before we can compare the areas between controls and patients, the waveforms were scaled in amplitude and normalised in time. Each individual's finger and toe waveform data were scaled in amplitude to the maximum peak detected out of the 10 second recording. Therefore the amplitude of each pulse and that of the average pulse will be a fraction of the maximum amplitude of the signal (Figure 25). The next step was to normalise the waveforms in time. This was achieved by determining the length of each pulse (trough to trough) in the pulse train. A new x-axis for each pulse was produced from 0 to 100 which was then divided by each pulse width. This produced a normalised x-axis which could then be interpolated. A Piecewise Cubic Hermite Interpolating Polynomial (PCHIP) was used to interpolate the pulse from 0 to 100 in steps of 0.01, giving the total number of points at 10,000, and thereby giving each pulse the same number of data points in order that the normalised pulses could be added together and then averaged. This was performed for each pulse in the toe and finger waveforms.

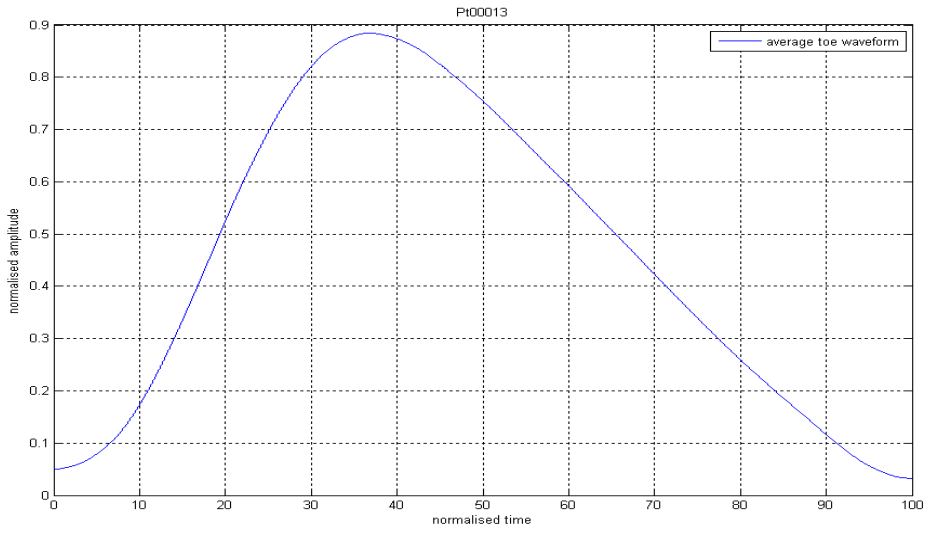

Figure 25 Average normalised toe waveform

When this was completed an average normalised pulse was calculated from each individual volunteer. An example is shown in Figure 25. This would be used as a representative toe or finger waveform for that individual volunteer. The next step was to identify the peak of the average normalised waveform and then identify the pulse trough. These would be used as markers to calculate the area under different parts of the waveform. Figure 26 shows the identified pulse peaks and troughs of the average normalised toe waveform.

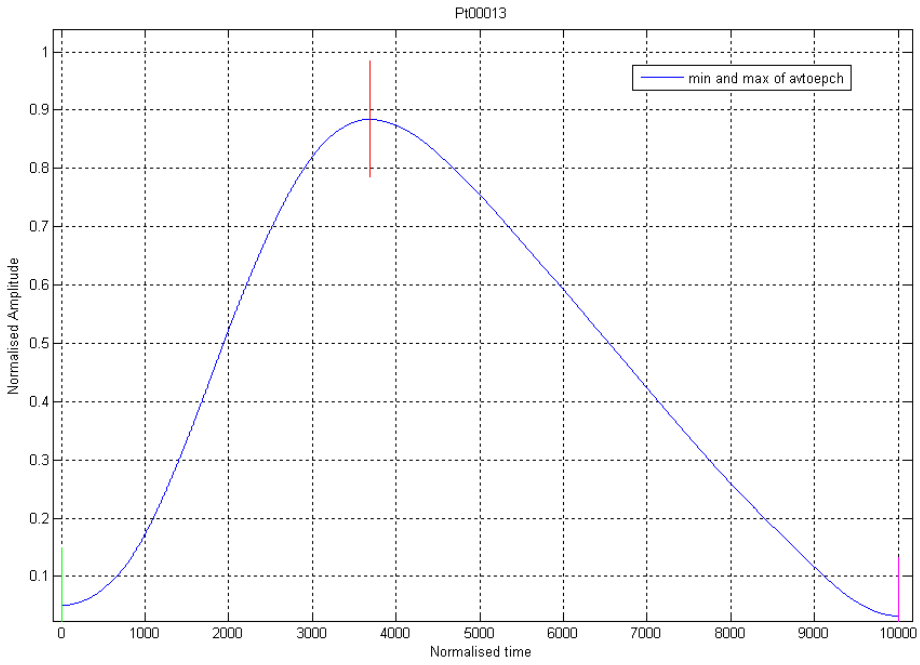

Figure 26 Average normalised toe waveform showing the pulse peak and pulse trough markers used to calculate areas under the waveform.

Once the peak and troughs markers were identified different sections of the average normalised toe waveform could be determined. By identifying distinct segments within the waveform, a number of separate areas could be calculated. This was performed on the toe pulses from both the control and patient groups so that a comparison of areas could be made between normal and pathogenic waveforms. Figure 27 shows a block diagram of the automated toe pulse normalisation and area calculation procedure.

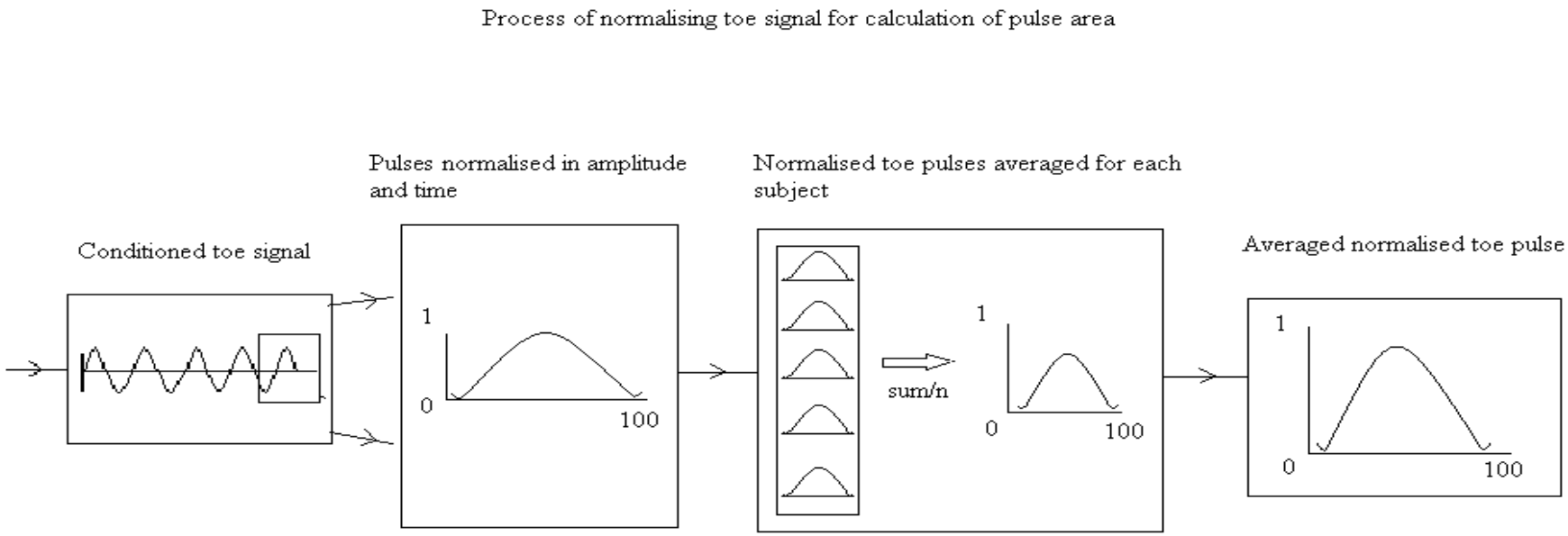

Figure 27 Process of normalising toe signal for calculation of pulse area.

6.1.4 PWTT and Area Combined Analysis

A Matlab code was written to investigate whether combining the tests of PWTT and area would increase the sensitivity and specificity scores as opposed to their individual scores.

Sensitivity and specificity scores were calculated for each patient group, i.e. moderate only, significant only, significant and occlusive only and finally moderate, significant and occlusive. Threshold levels were set as for previous individual PWTT and individual area tests. Each patient scored a '1' if they were test positive for individual PWTT measure and individual area measure, however, the patient scored a '0' test negative. These scores were then stored in individual PWTT and area vectors. The same procedure was carried out for the control subjects. With these scores stored in vectors, sensitivities and specificities were calculated as follows:

If by summing the individual PWTT and area vectors for each patient their score was $\geq$ '1' then that patient was recorded as test positive; if the sum came to '0', the patient was recorded as test negative. The proportions of test positives were then employed to calculate the sensitivities at each threshold level and for each patient group. This method was repeated for the control group to calculate specificities. From this data, ROC curves were produced for each disease group.

6.2 Preliminary Research

This next section presents the results of a preliminary study that investigated which sections of area of the normalised PPG toe pulse best reflected the difference between healthy and diseased groups. The section of area which showed the best result was taken forward and

used in further analysis. A total of 20 legs were chosen, 10 normal subjects and 10 patients, 5 with significant disease and 5 with occlusive disease. The study group age ranges were normals: 48-76yrs (mean 62.4yrs), patients: 41-76 (mean 63.0yrs).

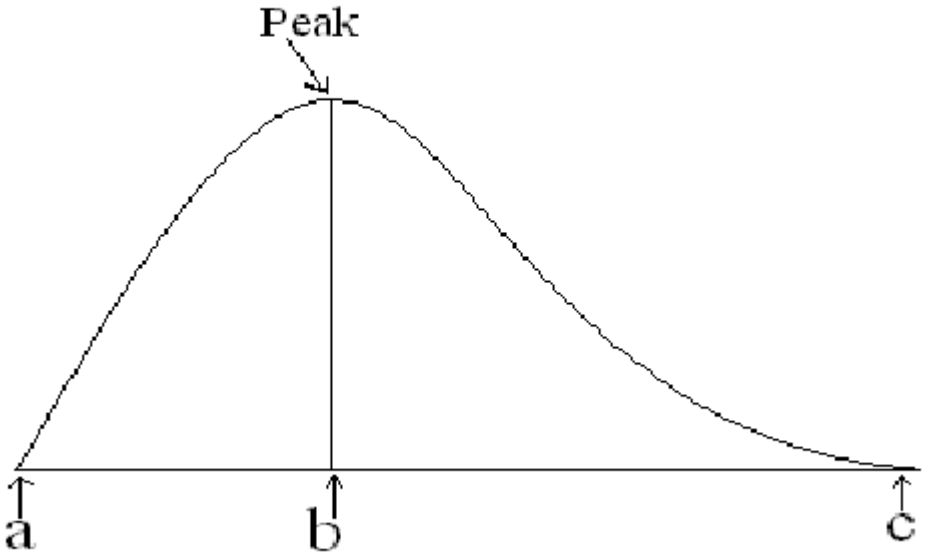

Figure 28 shows a typical normalised toe waveform

The areas considered are explained with reference to Figure 28. Points a - b represent the pulse trough to pulse peak area under the curve, while the points b - c represent the pulse peak to distal pulse trough area. An area index was also calculated by dividing area b - c by a - b. Finally the complete area under the curve from a - c is used. A number of different area thresholds were used for each of the 4 different areas of the normalised pulse to calculate the range of sensitivity and specificity values. A graph of these results is shown in the ROC curves of Figure 29. The area a-b and the complete area a-c under the normalised PPG toe pulse have similar ROC curves and have a better range of sensitivities and specificities overall than area b-c and the index of area (b-c/a-b). These curves deviate below the 90% sensitivity level. However, both area calculations have 90% sensitivity and specificity and

further more, have 100 % sensitivities and 70% specificities. However one of these techniques for calculating the area had to be taken forward. The anacrotic and catacrotic phases of the PPG pulse are affected by certain physiological conditions; the anacrotic phase can be used as an indicator of the force of ventricular contraction and the catacrotic phase is affected by the capacitance of the vascular tree (Murray and Foster, 1996). Therefore relying on just one of these phases of the PPG pulse to indicate lower limb stenotic disease may be unreliable. Therefore the whole area of the pulse, (a-c), was chosen as the area parameter for further analysis. Any change in one of the phases due to the physiological conditions mentioned above, may have less affect on the change in the whole area under the PPG pulse due to arterial stenotic disease.

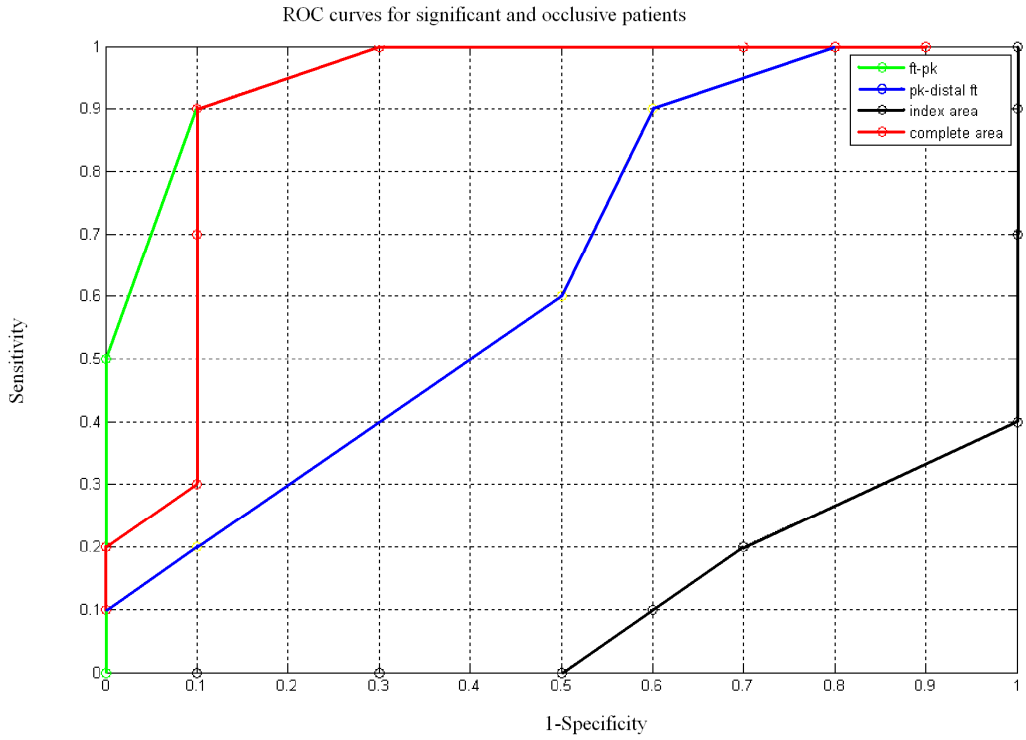

Figure 29 ROC curves for the four areas used in preliminary testing

6.3 Main Arterial Results

This chapter presents the results of the main arterial work and has been separated into three subsections according to the analysis technique used: Pulse wave transit time (PWTT); area under the normalised toe pulse; combined PWTT and area under normalised pulse (AUNP). Statistical tests were performed on the arterial data and the results are reported in the text for each arterial group. Parametric t-tests on un-paired data were performed; see section 5.4.6 for further information. PWTT and area data for the control and patient groups can be found in appendix C.

6.3.1 Pulse Wave Transit Time

PWTTs for the three disease groups, moderate, significant and occlusive, were compared individually to the healthy control group, then significant and occlusive disease groups were combined and compared against the control group and finally all three diseased groups were compared against the control group. The results are shown in the following sections.

6.3.1.1 Moderate Disease

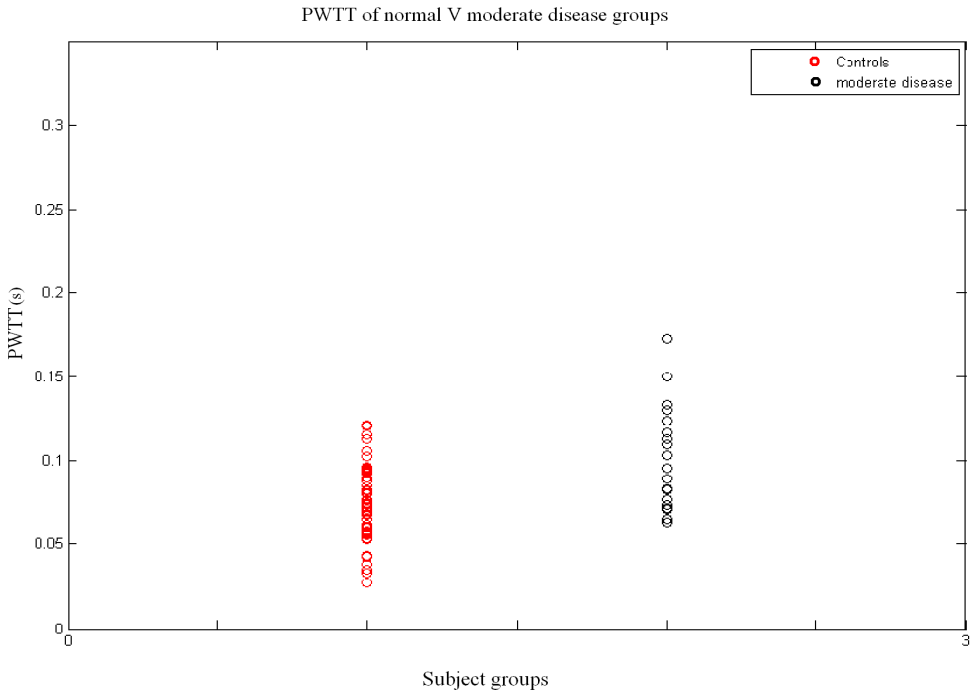

Figure 30 Pulse wave transit time of Normal Group against Moderate disease group

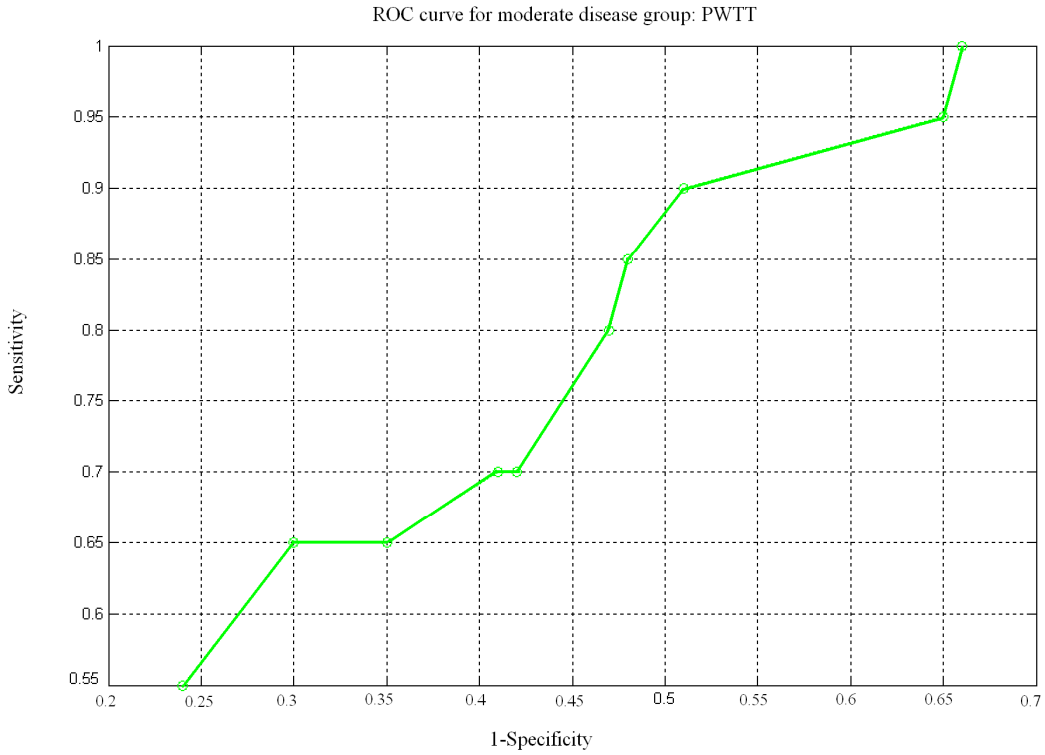

Figure 31 ROC curve for moderate disease group

Statistical analysis showed there to be a statistically significant difference between the mean PWTTs of the moderate disease and control groups at the 5% level. Referring to Figure 30, PWTT in the healthy group ranged from 27ms to 121ms where as PWTT ranged from 63ms to 172ms in the moderate disease group. Using threshold values from 62ms to 88ms produces the ROC curve as shown in Figure 31. The lower threshold value of 62ms produced a maximum sensitivity of 100% and a specificity of 34% where as the 88ms threshold value produced a sensitivity of 55% and a specificity of 76%.

6.3.1.2 Significant Disease

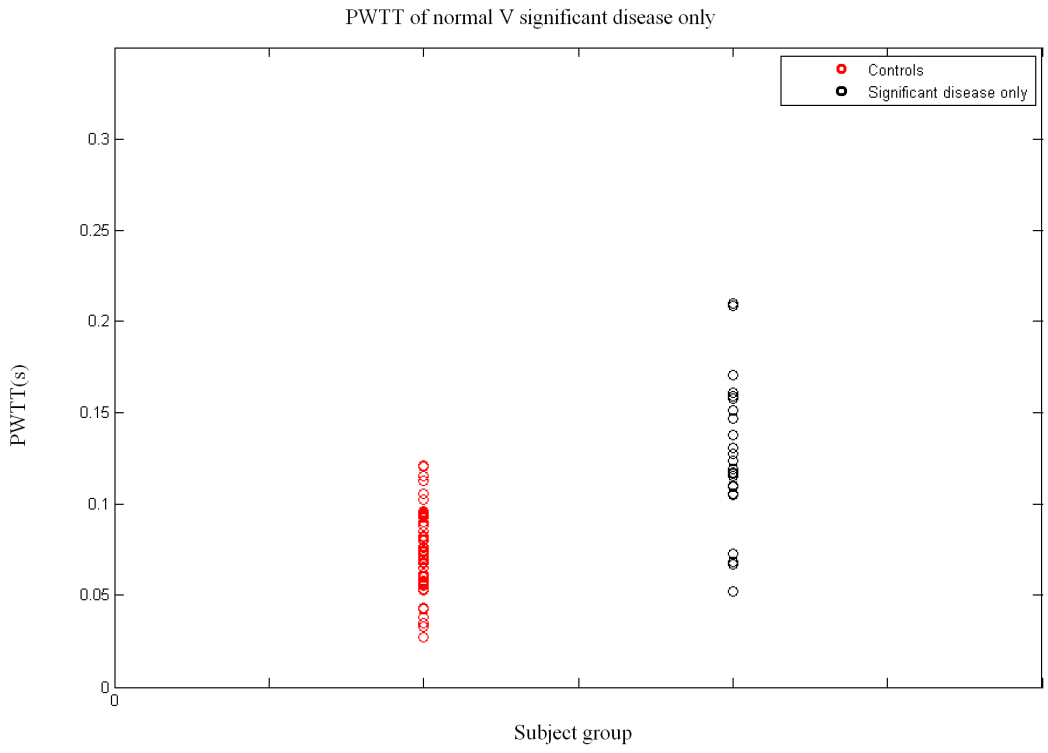

Figure 32 Pulse wave transit time of Normal group against significant disease group

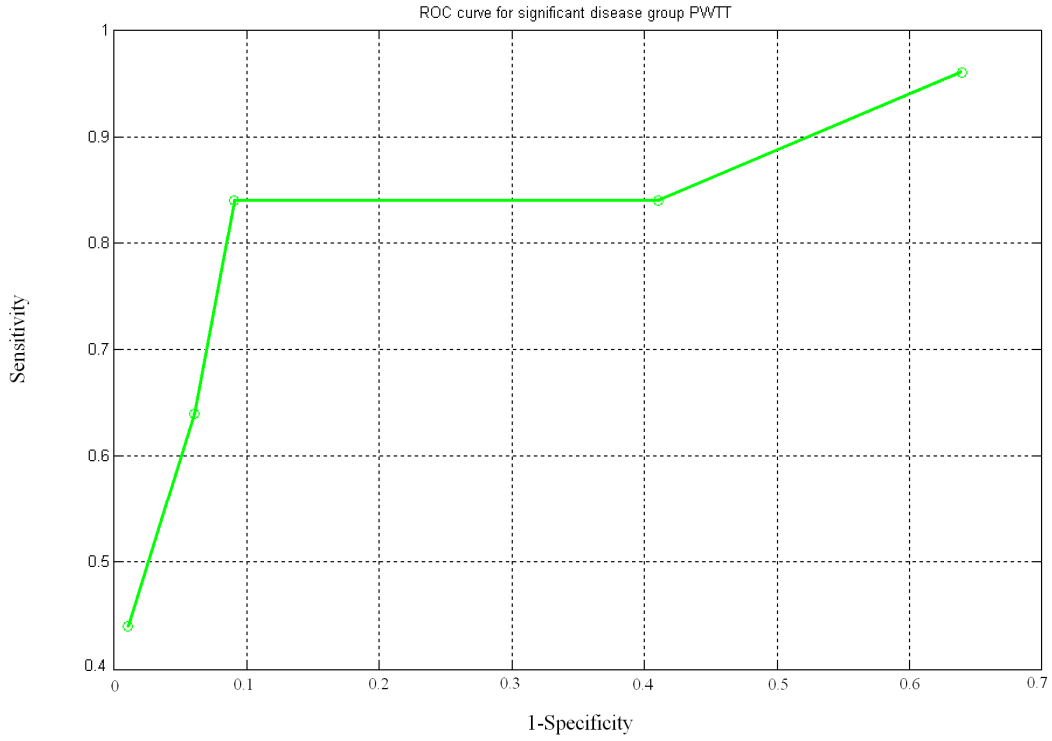

Figure 33 ROC curve for significant group

There was a statistically significant difference between the mean PWTTs of the significant disease and control groups at the 5% level. As indicated in Figure 32 the PWTT of the significant disease group ranged from 52ms to 209ms. Using a PWTT threshold value of 66ms produced a sensitivity of 96% and a specificity of 36%. Using a PWTT threshold of 125ms produced a sensitivity of 44% and a specificity of 99% and shown by the ROC curve in Figure 33.

6.3.1.3 Occlusive Disease

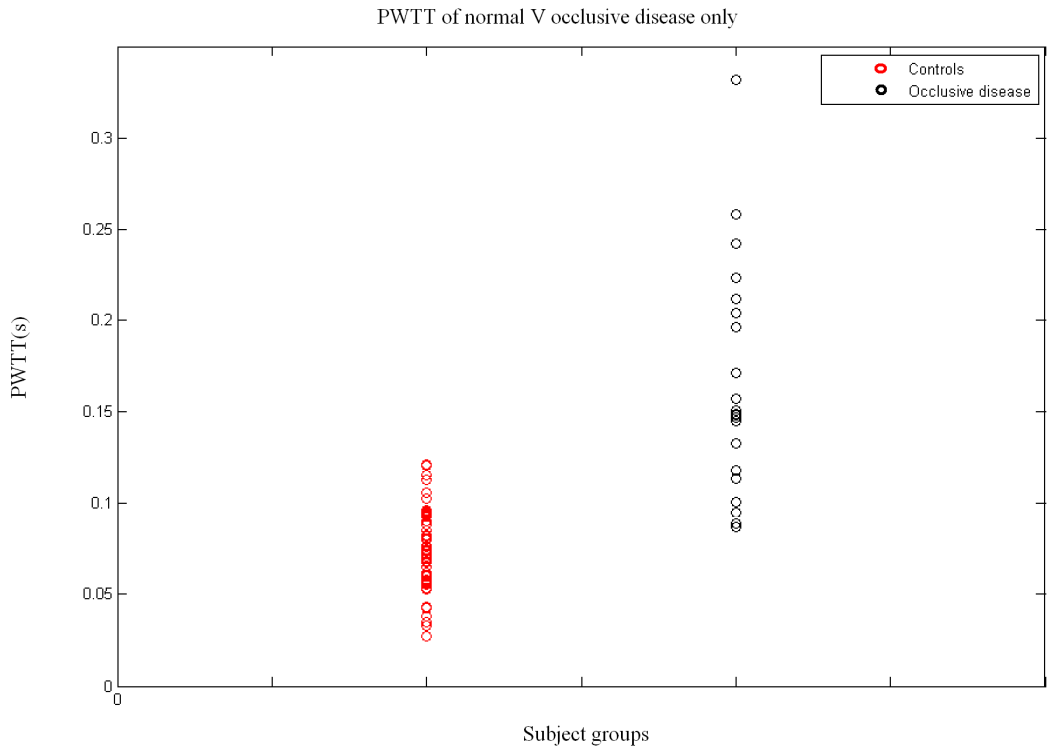

Figure 34 Pulse wave transit time of Normal against occlusive disease group

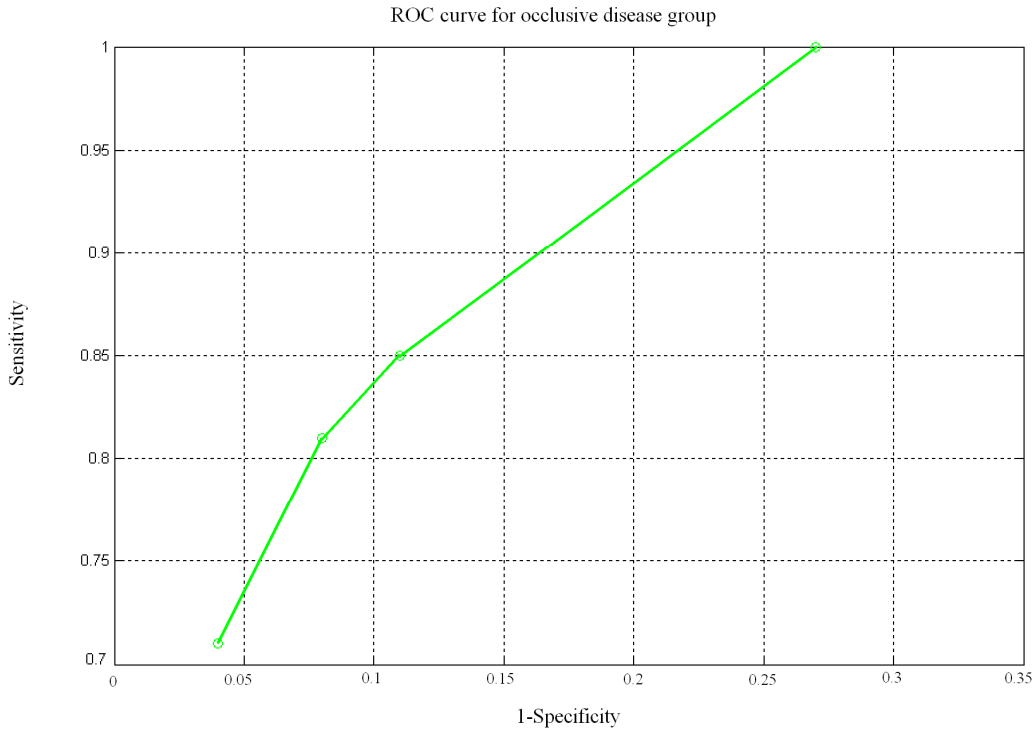

Figure 35 ROC curve for Occlusive Disease

Statistical analysis showed there was also a statistically significant difference between the mean PWTTs of the occlusive disease and control groups at the 5% level. Referring to Figure 34, PWTT for the occlusive disease group ranged from 86ms to 331ms. Taking threshold values from 86ms to 130ms produces a sensitivity of 100% (83ms threshold) and a specificity of 74% and sensitivity of 71% and a specificity of 96% (130ms threshold) as shown by the ROC curve in Figure 35.

6.3.1.4 Significant and Occlusive Disease

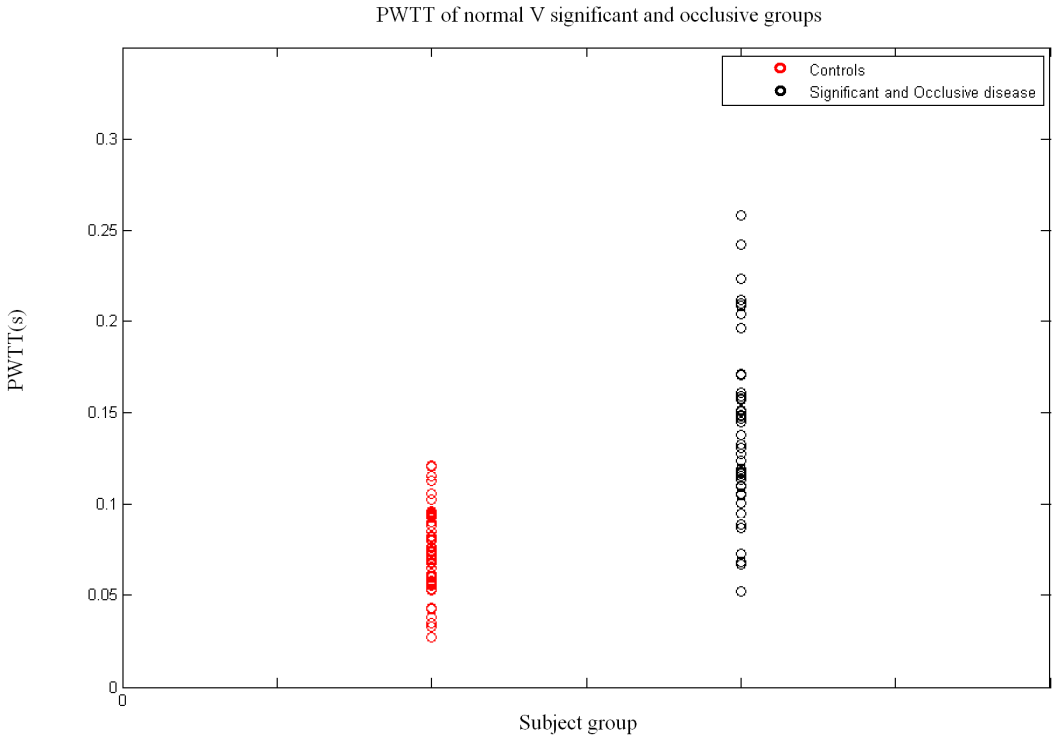

Figure 36 Pulse wave transit time of Normal against significant and occlusive disease group

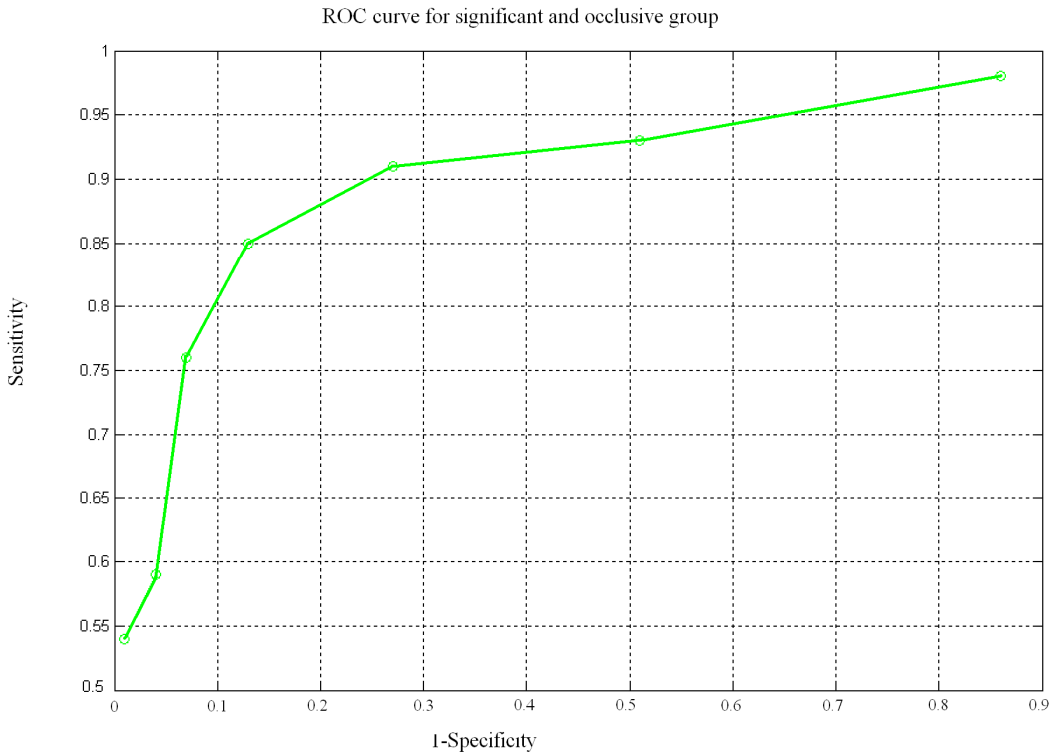

Figure 37 ROC curve for significant and occlusive groups

Combining the significant and occlusive disease groups gives the separation as shown in Figure 36. Statistical analysis showed there to be a statistically significant difference between the mean PWTTs of the significant and occlusive disease group and control group at the 5% level. The range of PWTT in this group is from 52ms to 331ms. As indicated by the ROC curve in Figure 37, using a PWTT threshold of 55ms gives a sensitivity of 98% and a specificity of 15% and using a PWTT threshold of 331ms gives a sensitivity of 54% and a specificity of 99%.

6.3.1.5 Moderate, Significant and Occlusive Disease

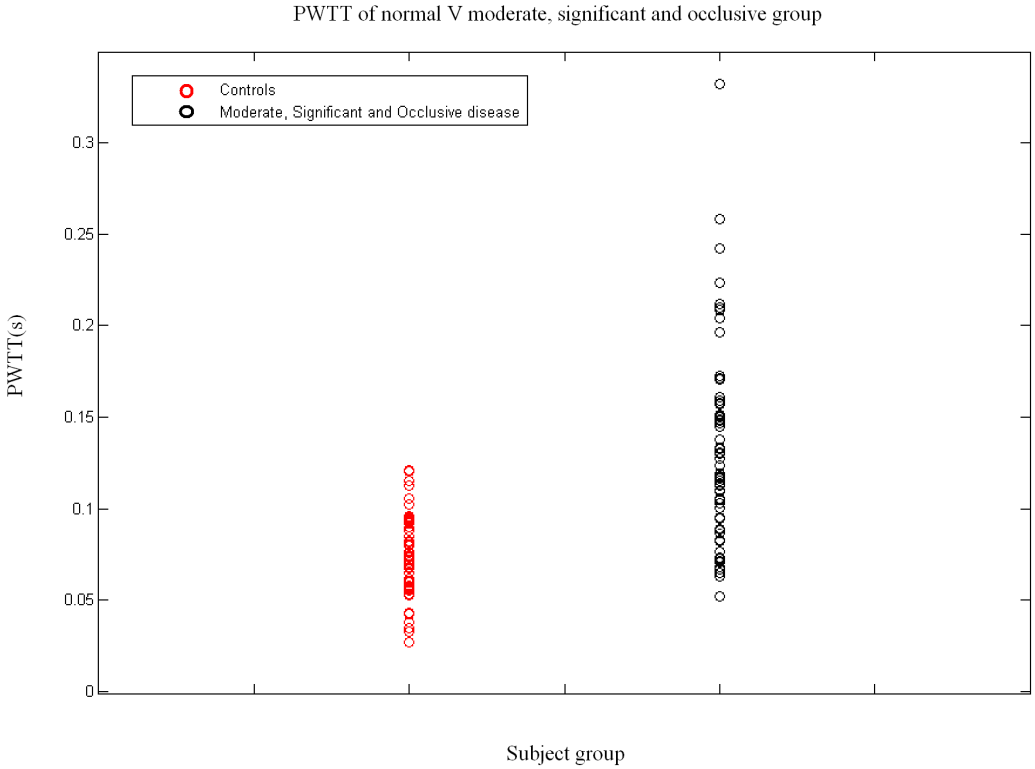

Figure 38 Pulse wave transit time of Normal against moderate, significant and occlusive disease group

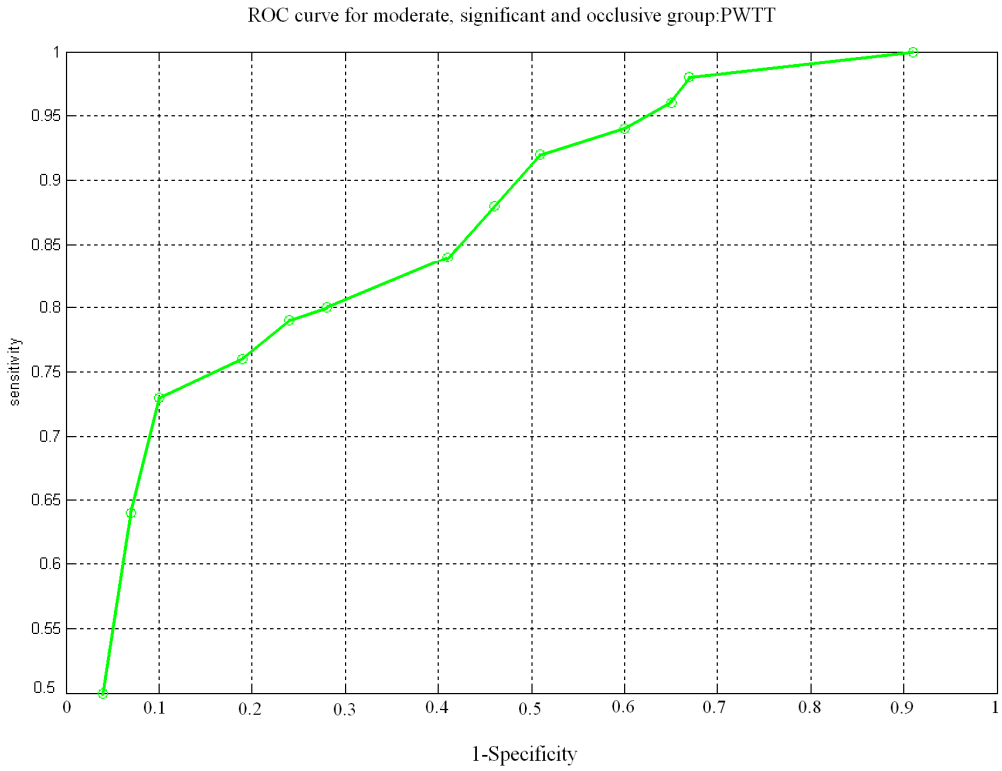

Figure 39 ROC curve for moderate, significant and occlusive groups

A comparison all 4 groups; the three disease groups, moderate, significant and occlusive and the healthy control group can be seen in Figure 38. Statistical analysis showed there to be a statistically significant difference between the mean PWTTs of the moderate, significant, occlusive disease group and control group at the 5% level. PWTT threshold values ranging from 52ms to 120ms were used to produce the ROC curve shown in Figure 39. As the ROC curve shows, a maximum sensitivity of 100% gives a specificity of 10% and a maximum specificity gives a sensitivity of 50%. Figure 40 shows the general PWTT trend of all 4 groups.

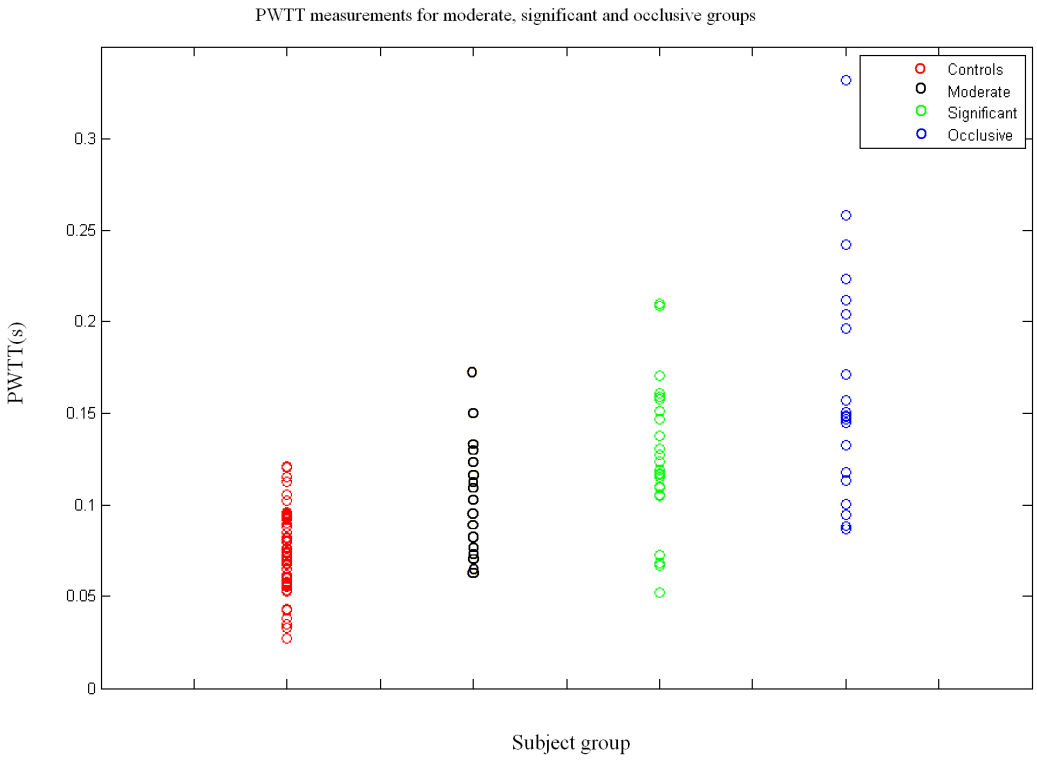

Figure 40 Comparison of PWTT of all four groups: normal, moderate, significant and occlusive

6.3.2 Area Under the Normalised PPG Toe Pulse

The comparison of groups is repeated using the complete area under the normalised PPG toe pulse

6.3.2.1 Moderate Disease

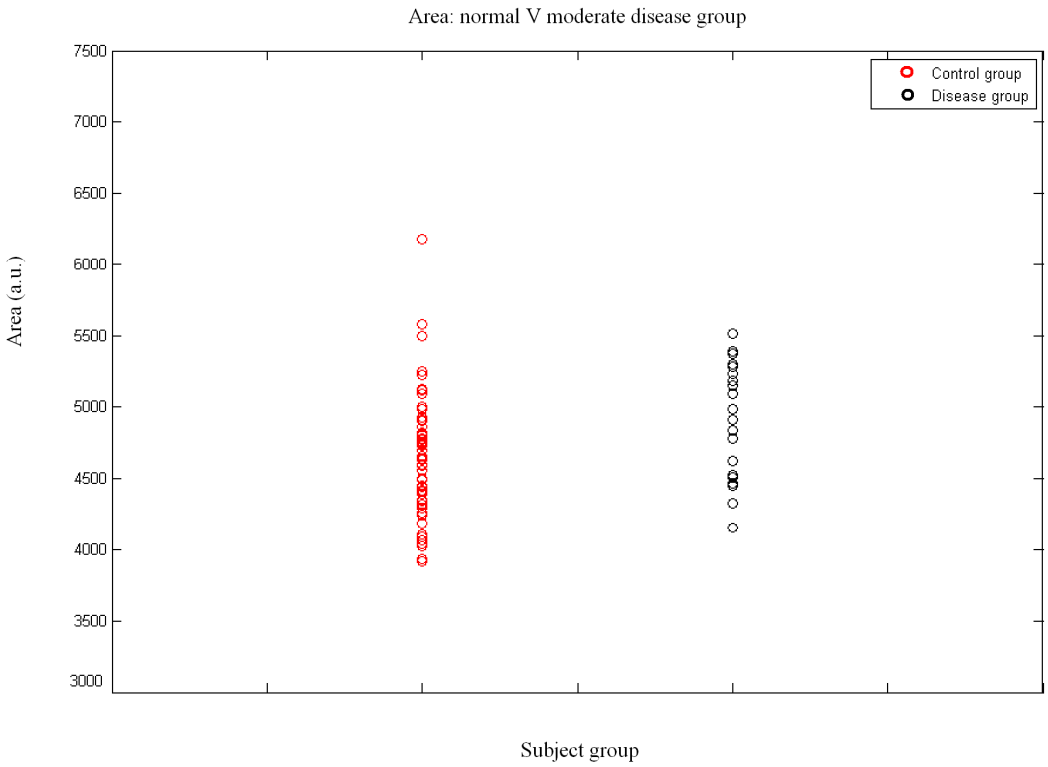

Figure 41 Area of Normal against moderate disease group

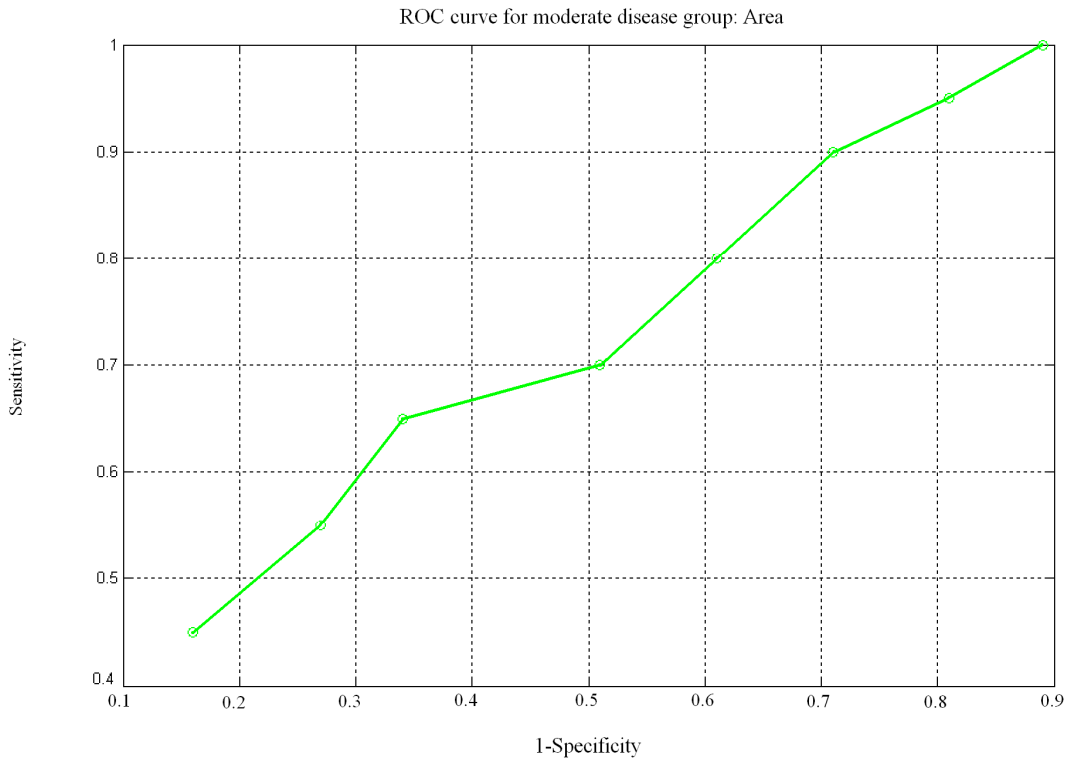

Figure 42 ROC curve for moderate disease group

Statistical analysis showed there to be a statistically significant difference between the mean areas of the moderate disease and control groups at the 5% level. However there is a greater range of toe pulse area for the control group. With reference to Figure 41 the control group area range is 3920 – 6120 au (arbitrary units) and the moderate disease group area range is 4169 – 5510 au. Using a range of area thresholds, sensitivities and specificities of 100% and 12% at 4140 au and 45% and 85% at 5000au respectively were obtained. The intermediate values are shown in the ROC curve of Figure 42.

6.3.2.2 Significant Disease

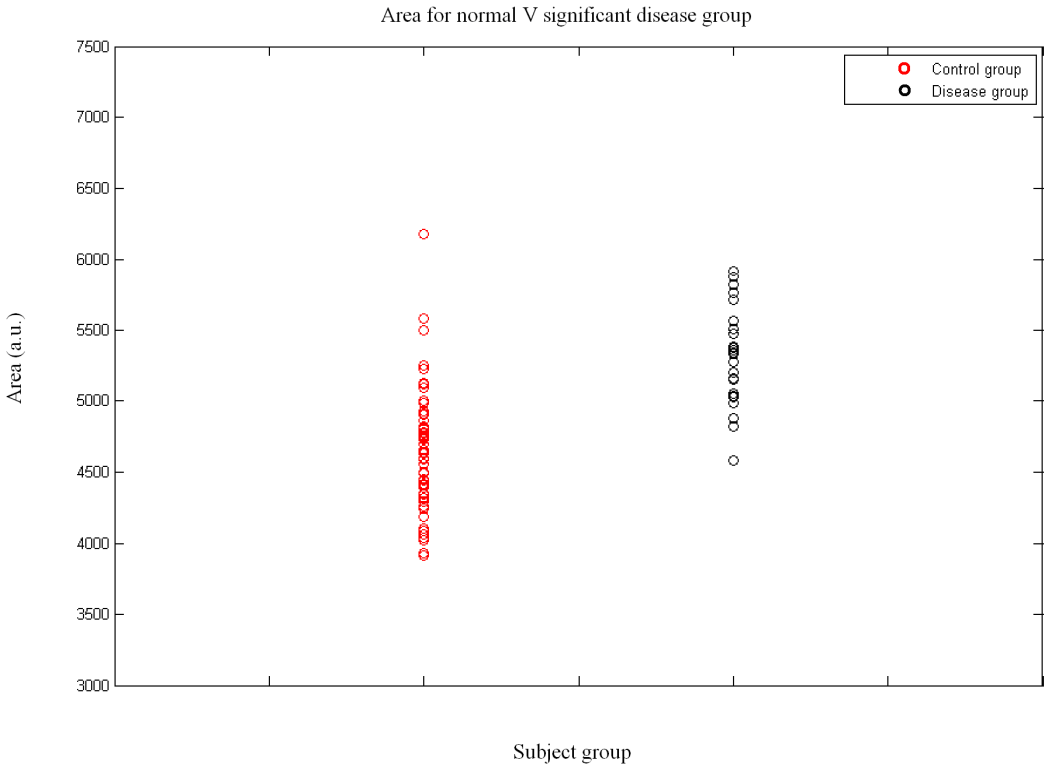

Figure 43 Area of normal against significant disease group

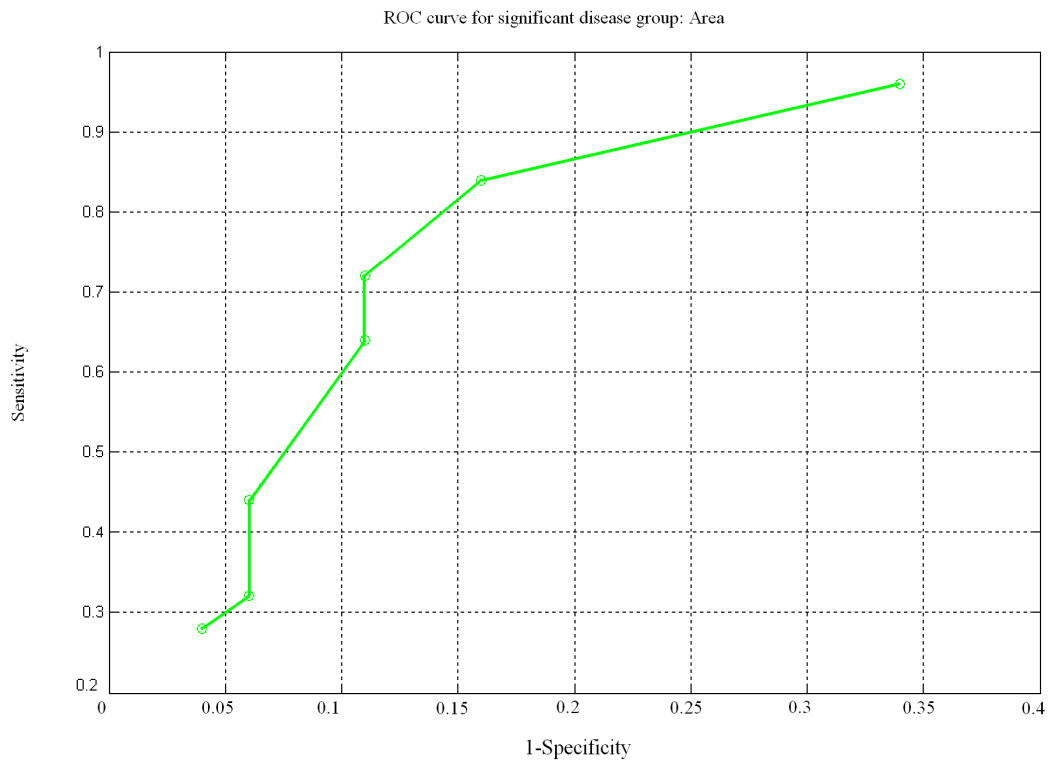

Figure 44 ROC curve for significant disease group

The range of areas calculated for the significant disease group are between 4580 – 5920 a.u. as indicated in Figure 43 and again statistical analysis showed there to be a statistically significant difference between the mean areas of the significant disease and control groups at the 5% level. The ROC curve of Figure 44 shows 96% sensitivity and 66% specificity at an area threshold value of 4780 a.u. and 28% sensitivity and 96% specificity at an area threshold of 5500 a.u.

6.3.2.3 Occlusive Disease

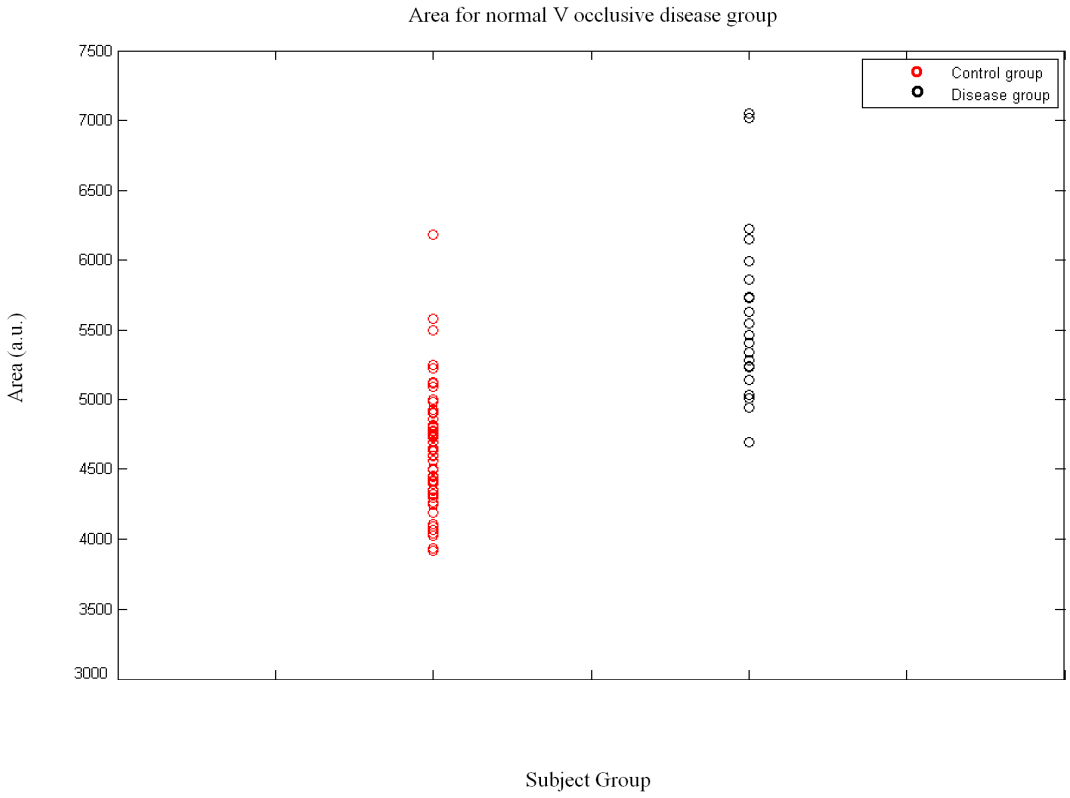

Figure 45 Area of normal against occlusive disease group

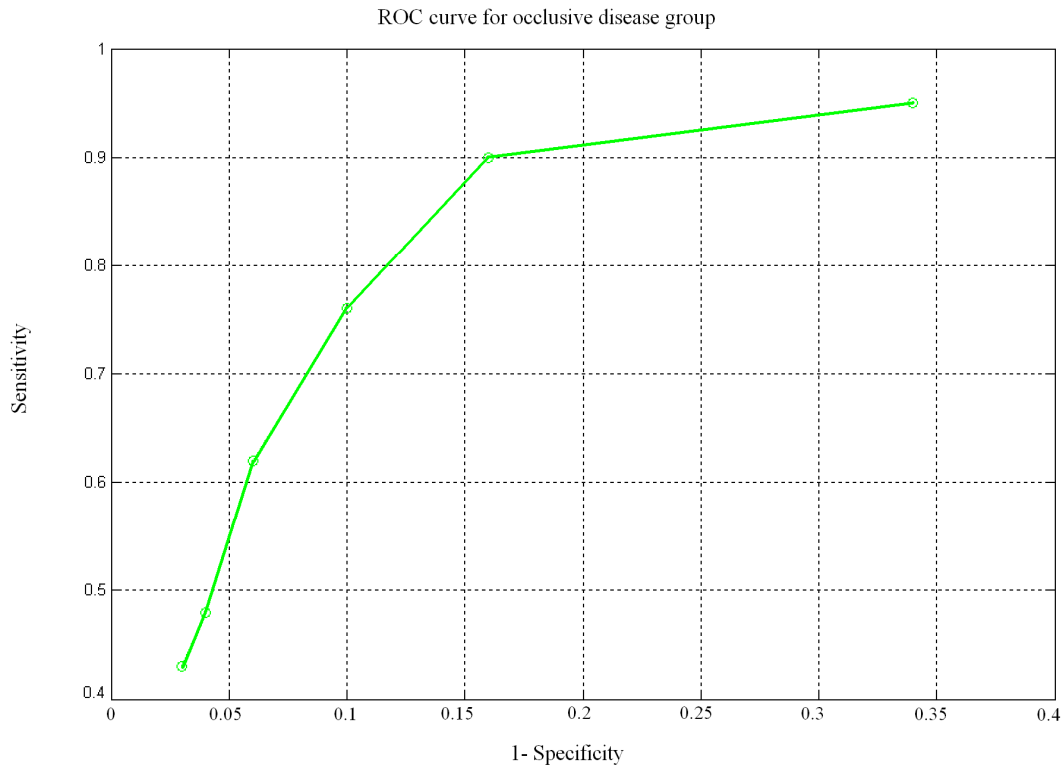

Figure 46 ROC curve for occlusive disease group

The range of areas calculated for the occlusive group range from 4700 – 7050 a.u. as indicated in Figure 45. There was a statistically significant difference between the mean areas of the occlusive disease and control groups at the 5% level. The ROC curve in Figure 46 shows sensitivity and specificity of 95% and 66% respectively for an area threshold of 4780 a.u. and sensitivity and specificity of 43% and 97% respectively for an area threshold of 5600 a.u.

6.3.2.4 Significant and Occlusive Disease

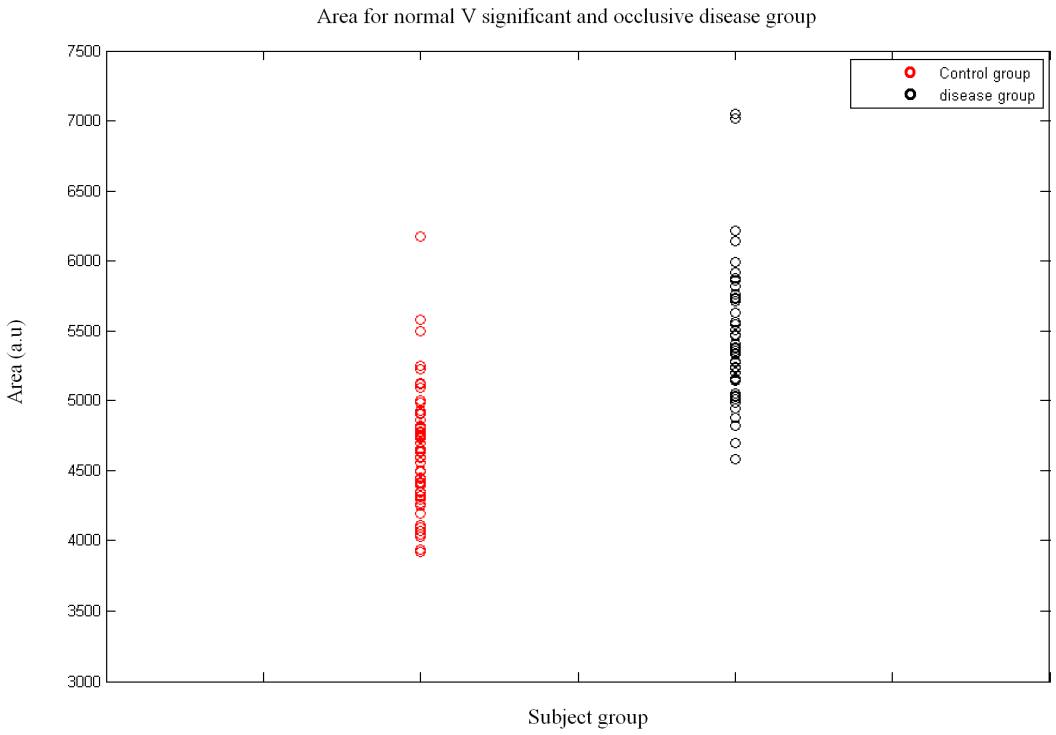

Figure 47 Area of normal against significant and occlusive disease group

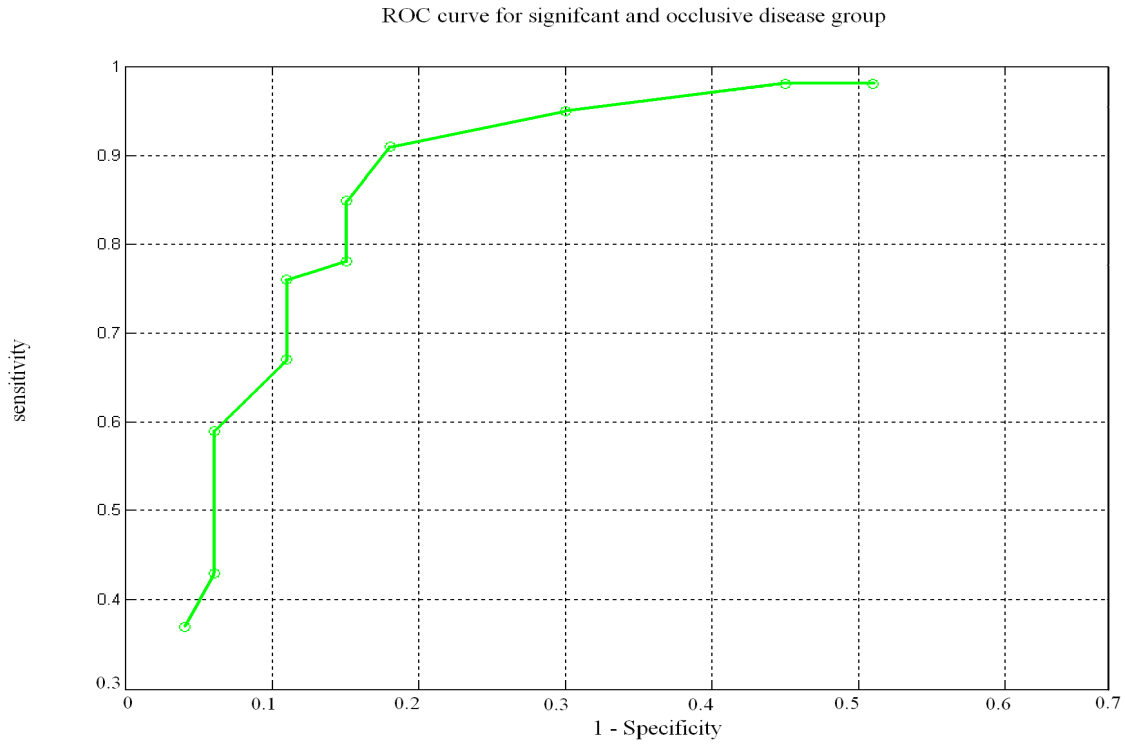

Figure 48 ROC curve for Significant and occlusive disease groups

Combining the significant and occlusive disease groups gives a range of normalised areas of 4580 – 7050 a.u. as can be seen in Figure 47. Statistical analysis showed there to be a statistically significant difference between the mean areas of the significant and occlusive disease group and control group at the 5% level. Using a threshold value of 4600 a.u. the ROC curve of Figure 48 shows sensitivity of 99% and specificity of 49%, while using a threshold of 5500 a.u. the sensitivity and specificity are 37% and 97% respectively.

6.3.2.5 Moderate, Significant and Occlusive Disease

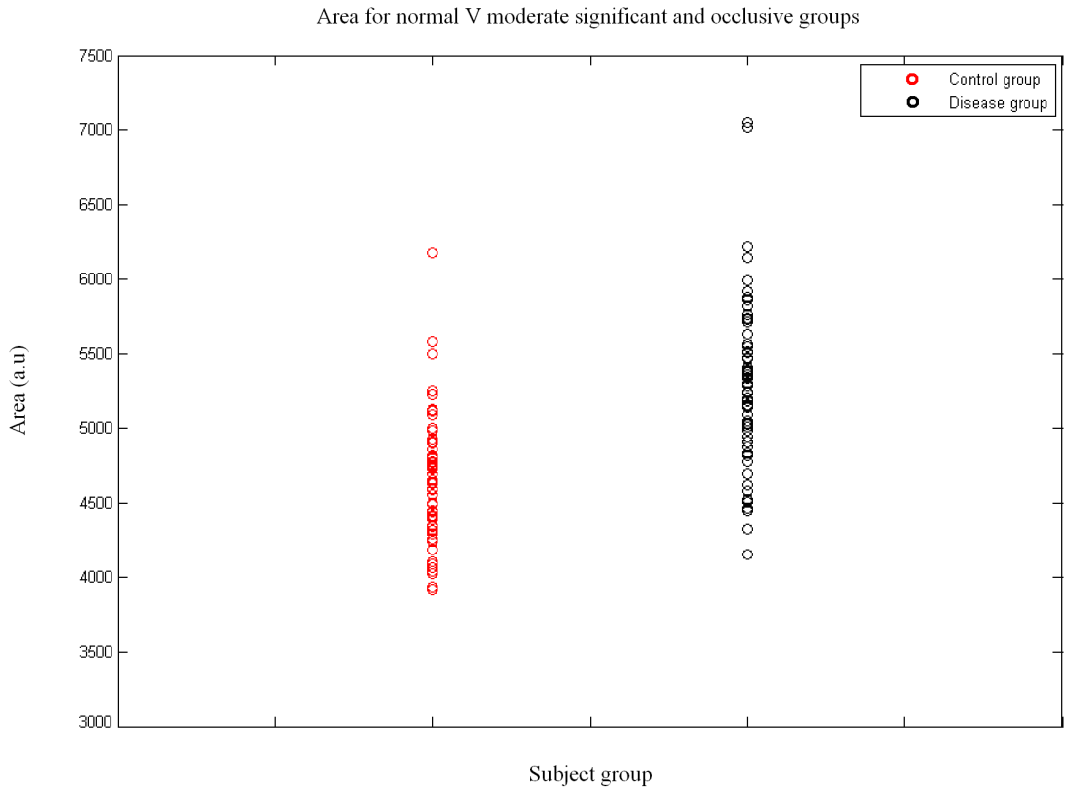

Figure 49 **Area of normal against moderate, significant and occlusive disease group**

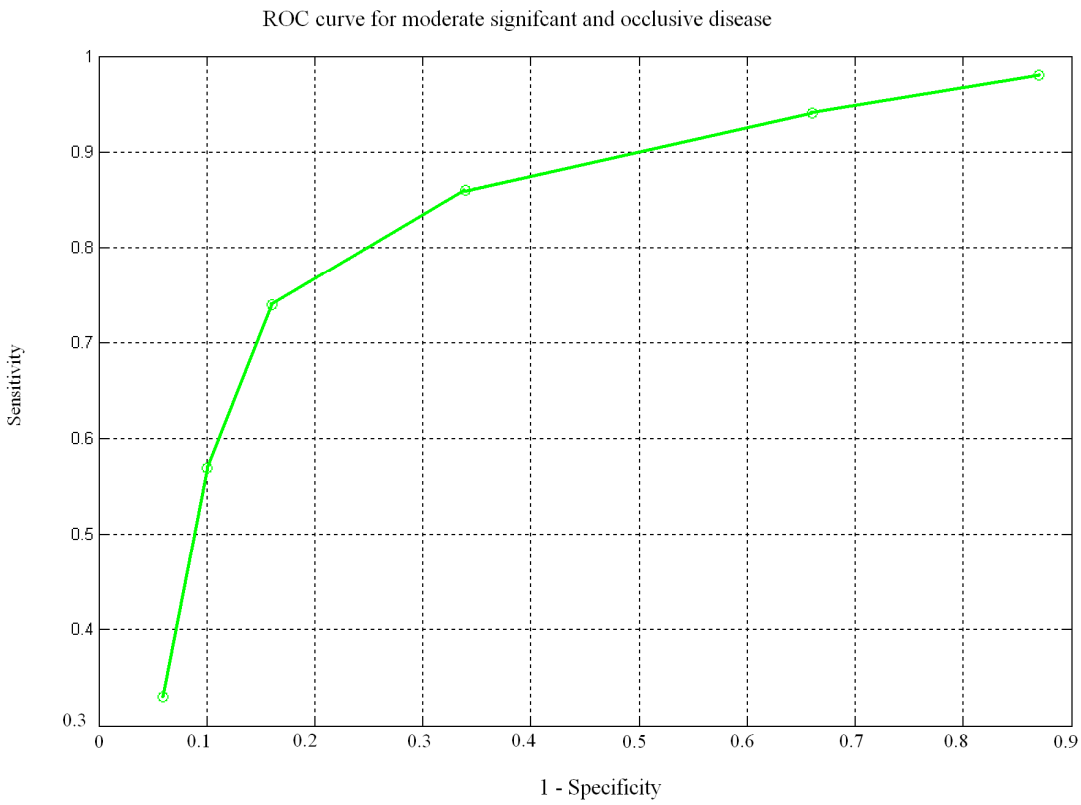

Figure 50 ROC curve for moderate, significant and occlusive disease groups

Statistical analysis showed there to be a statistically significant difference between the mean areas of the moderate, significant, occlusive disease group and control group at the 5% level Combining all three disease groups produces a normalised area range of 4160 – 7060 a.u. as shown in Figure 49. Using a threshold value of 4200 a.u. the ROC curve of Figure 50 shows sensitivity of 98% and specificity of 13% and with a threshold value of 5400 a.u. the sensitivity is 33% and specificity of 94%.

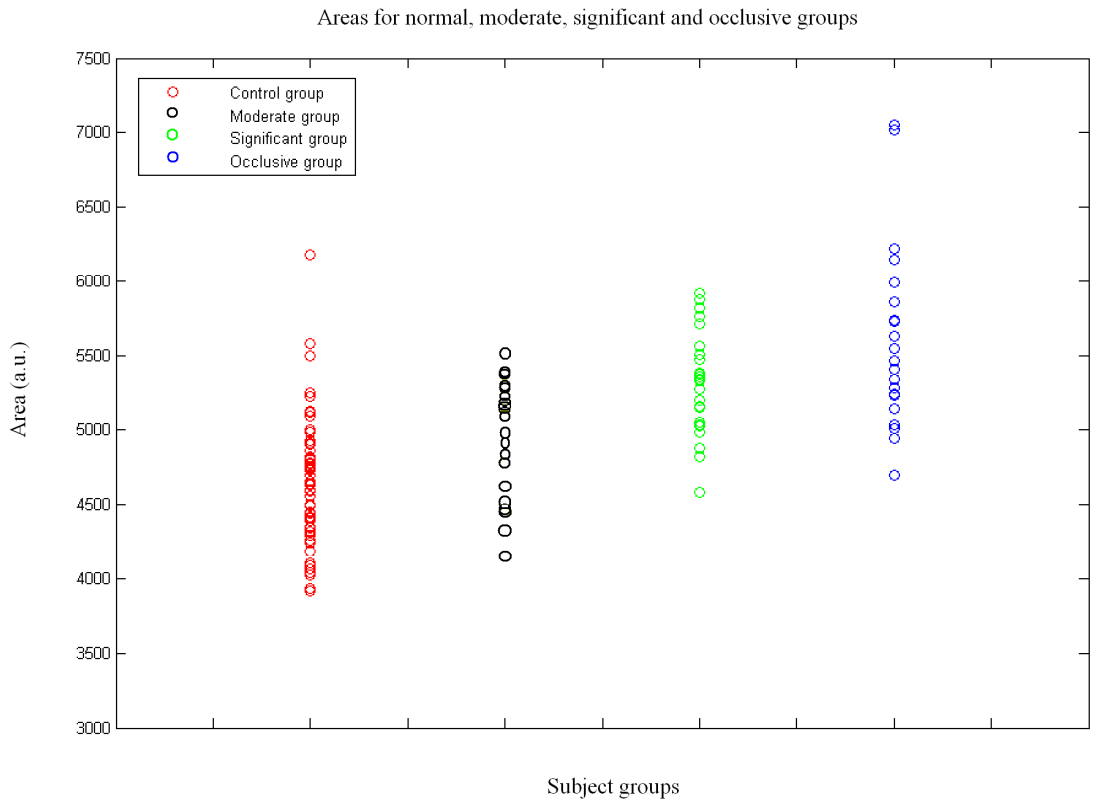

Figure 51 Comparison of all four groups: normal, moderate, significant and occlusive

Figure 51 compares the range of normalised areas for all four groups, showing a trend of increasing area for increasing disease level.

6.3.3 Comparison of Area, PWTT, Combined PWTT and Area for Each Disease Group.

When combining PWTT and area as an analysis technique, a sequence of tests was performed for each disease group, (moderate; significant; occlusive; significant and occlusive; moderate, significant, and occlusive). A series of ROC curves were produced in order to investigate which of these to take forward when comparing all three analysis techniques. A number of different PWTT thresholds were selected and each one was kept constant while a number of different area thresholds were varied throughout the disease group. Each PWTT threshold

produced a single ROC curve which could be compared against the other PWTT thresholds to produce a family of curves. These were then examined and the best ROC curve was selected for that disease group. See appendix A. These chosen curves were then compared against the two other analysis techniques for each disease group.

Combining the techniques of PWTT and area, the results for each group are presented below.

6.3.3.1 Moderate Disease

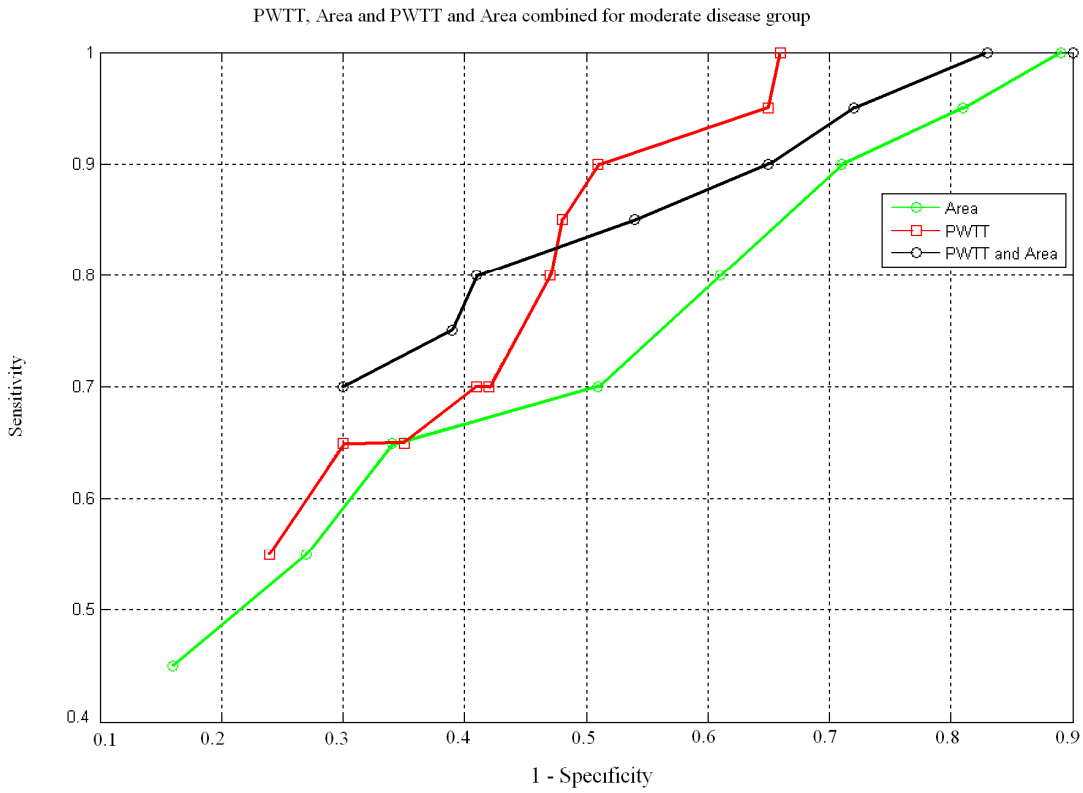

Figure 52 ROC curves of PWTT, Area and combined PWTT and Area for moderate disease group

A comparison of all three measuring techniques for the moderate disease group shows that at maximum sensitivity PWTT has a higher specificity; although, as the sensitivity decreases, the overall sensitivity and specificity scores stay higher when the two measuring techniques

are combined. As indicated in Figure 52 at a sensitivity of 100% the PWTT has specificity of 35%, while for PWTT and area combined the sensitivity and specificity are100% and 18% respectively. Conversely, at a sensitivity and specificity of 80% and 60% respectively, PWTT and area combined has the highest score compared to a sensitivity and specificity of 70% and 60% respectively for PWTT only and 67% and 60% sensitivity and specificity respectively for area only.

6.3.3.2 Significant Disease

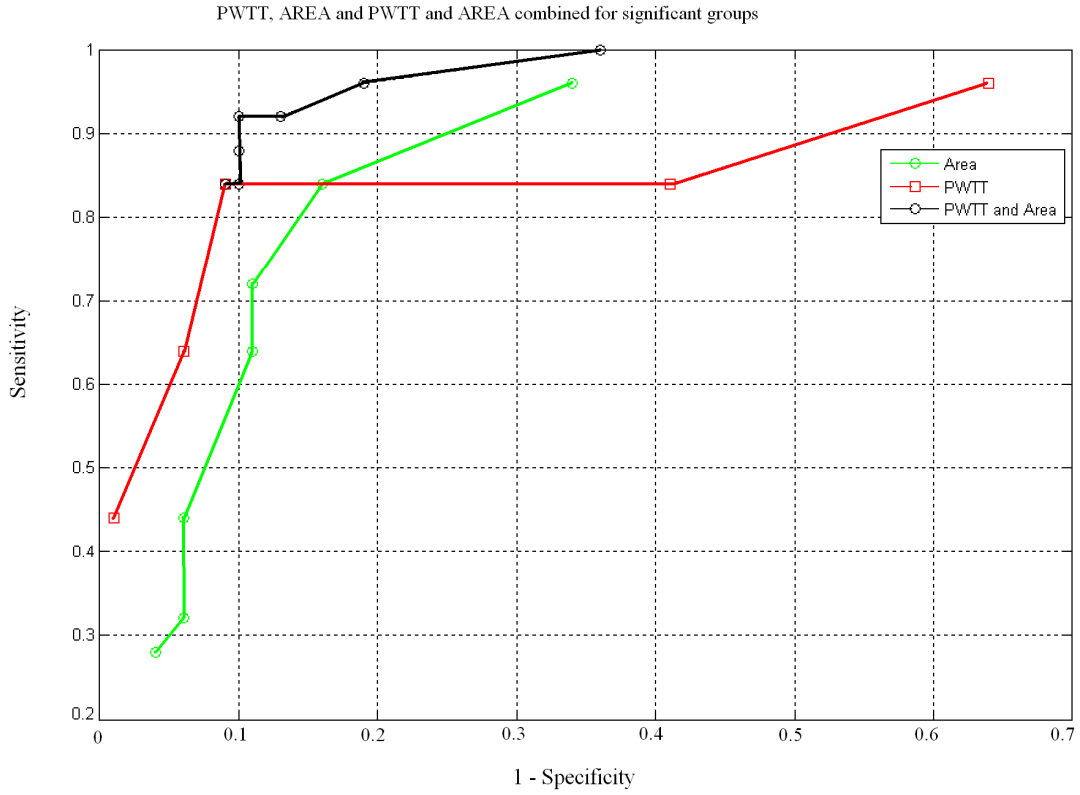

Figure 53 curves of PWTT, Area and combined PWTT and Area for significant disease group

PWTT and area combined for the significant disease group only, shows the best separation for sensitivity and specificity. As indicated in Figure 53 from a sensitivity of 100% through to 85% the specificity remains between 65% and 92%, while the comparable results for area only, the sensitivity ranges from 98% to 71% and the corresponding specificity ranges from

66% to 89%. The sensitivity stays flat at 85% while the specificity ranges from 59% to 91% for PWTT only.

6.3.3.3 Occlusive Disease

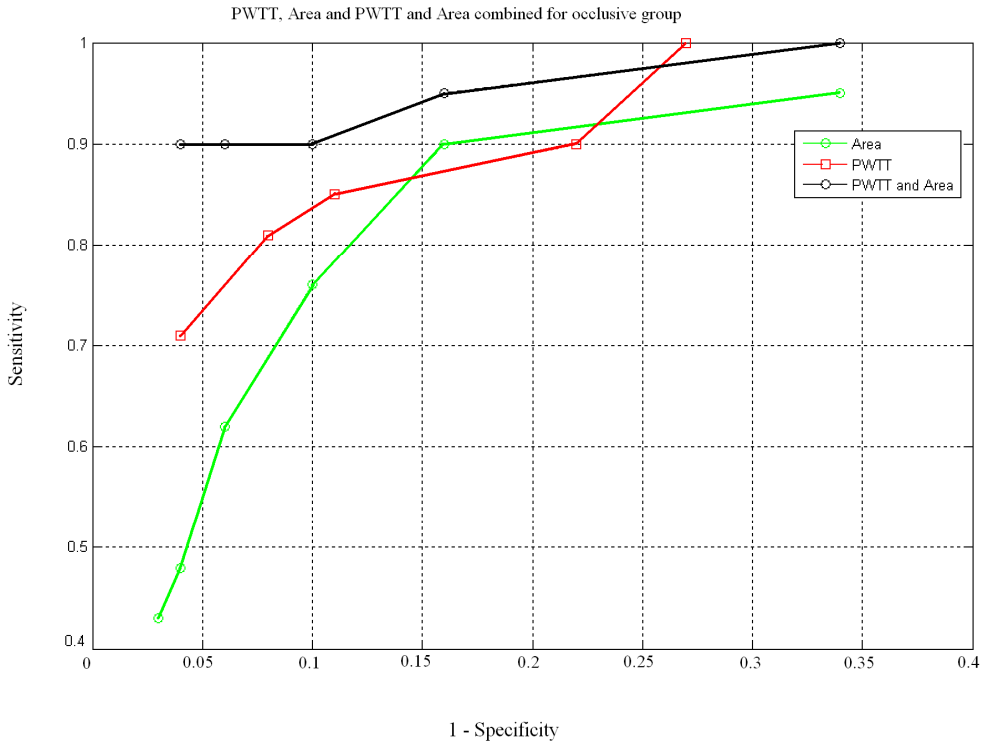

Figure 54 ROC curves of PWTT, Area and combined PWTT and Area for occlusive disease group

Combining the PWTT and area measurement techniques for the occlusive disease group appears overall to maximise the sensitivity and specificity scores when compared to PWTT and area. As indicated in Figure 54 the sensitivity scores for the combined method range between 100% and 90% and the specificity ranges between 66% and 96%. Alternately PWTT and area consistently score lower.

6.3.3.4 Significant and Occlusive Disease

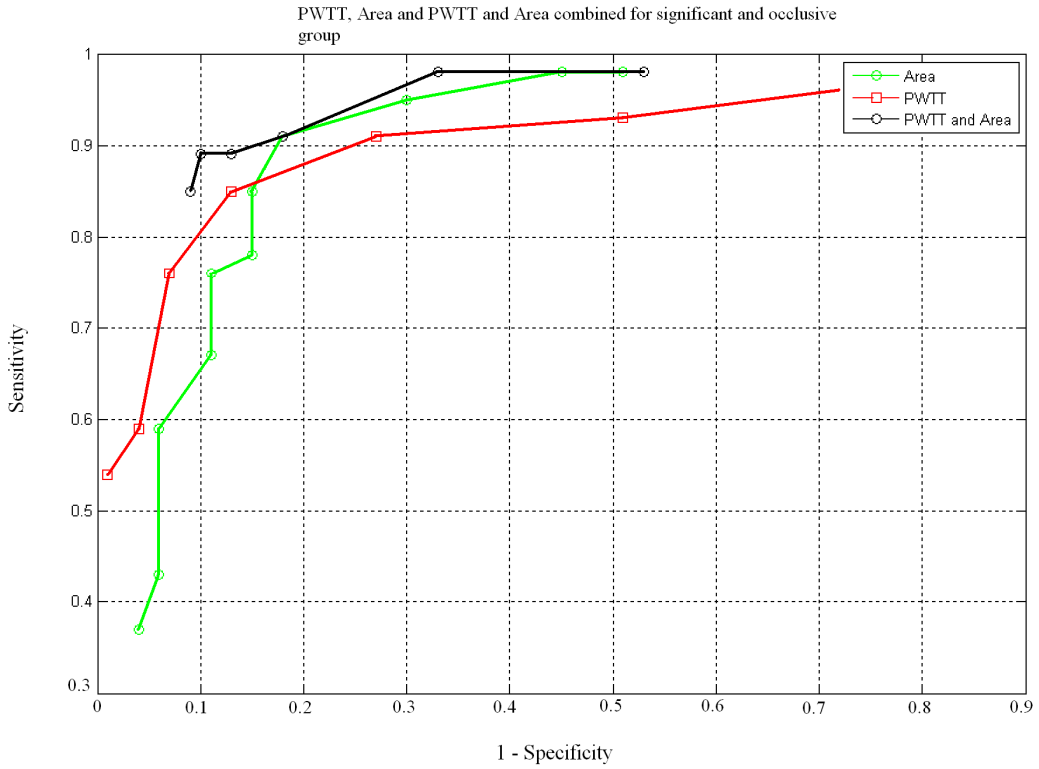

Figure 55 ROC curves of PWTT, Area and combined PWTT and Area for significant and occlusive disease group

Figure 55 compares the three measurement parameters when the significant and occlusive disease groups are combined. Over the sensitivities and specificities calculated, PWTT and area combined is constantly higher than PWTT and area separately giving a maximum sensitivity and specificity of 90% and 90% respectively.

6.3.3.5 Moderate, Significant and Occlusive Disease

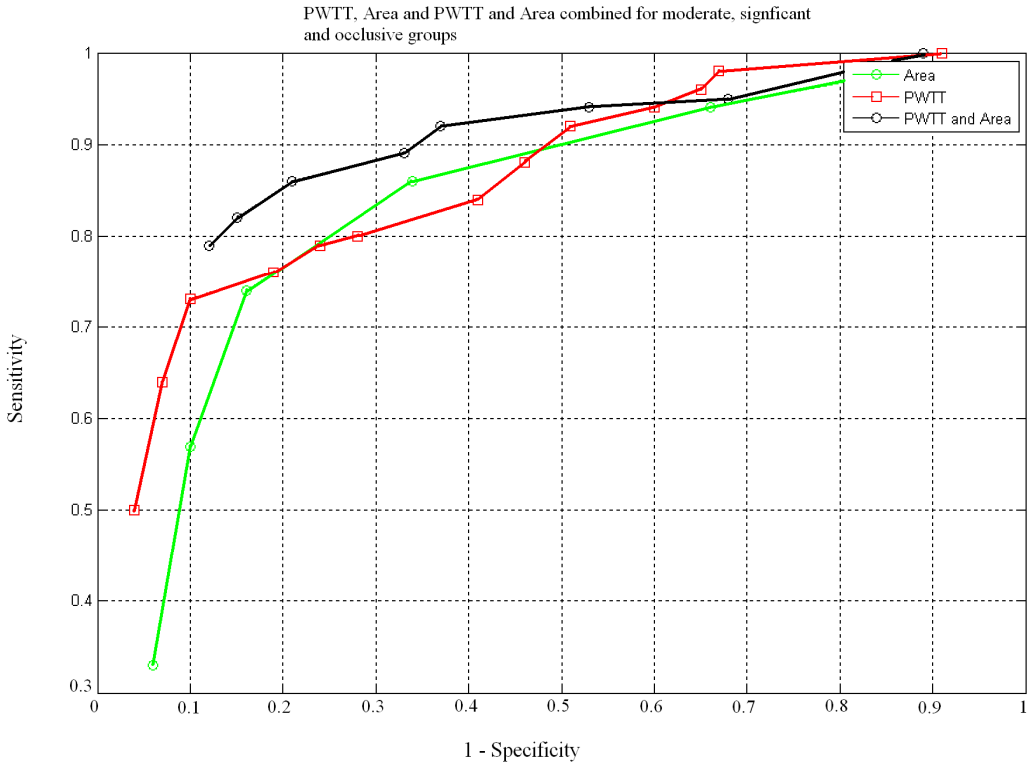

Figure 56 ROC curves of PWTT, Area and combined PWTT and Area for moderate, significant and occlusive disease group.

Combining all three diseased groups, Figure 56 shows that over the sensitivities and specificities calculated PWTT and area together is consistently best, giving 90% sensitivity and 70% specificity. PWTT and area show at an equivalent specificity, sensitivities of 80% and 83% respectively.

6.4 Arterial Threshold Levels

The sensitivity and specificity of ABPI for detecting significant lower limb PAD range from 90% to 100% (Fowkes, 1988; Doobay and Anand, 2005). However if moderate disease is included then the accuracy reduces to approximately 83% ($0.6 \leq ABPI \leq 0.9$) and 76% (normal $ABPI \geq 0.9$) (Allen et al., 1996). Therefore, to determine whether the techniques employed in this thesis are as accurate as ABPI for detecting lower limb arterial insufficiency, sensitivity and specificity levels need to be approximately 80% or more. If the values of the technique used are lower, then the sensitivity and specificity closest to 80% are chosen. If both sensitivity and specificity are above 80%, and to ensure that comparisons are consistent between the groups, the sensitivity data point on the ROC curve nearest to 80% was selected and hence the equivalent specificity point was recorded. Table 4 summarises the sensitivity and specificity scores and lists the threshold levels used for the different disease groups and for the different techniques used.

Disease level (Ultrasound)	PWTT			Area			PWTT and Area		
	T.H	sens	spec	T.H	sens	spec	T.H	sens	spec
Moderate	82ms	65	70	4780au	65	65	88ms 5000au	70	70
Significant	105ms	84	91	5000au	83	84	105ms 6000au	84	91
Occlusive	110ms	81	92	5000au	90	84	130ms 5300au	90	96
Significant and Occlusive	95ms	85	86	5020au	85	85	110ms 5500au	85	91
Moderate, significant and Occlusive	88ms	79	76	5000au	74	84	100ms 5200au	82	84

T.H threshold

Table 4 sensitivities and specificities for the different disease groups, for PWTT only; Area only and combining the two diagnostic tests

In the moderate disease group, combining both measurement techniques raised the sensitivity from 65% to 70% when compared to PWTT and area techniques individually. This level of sensitivity and specificity was achieved by setting PWTT and area thresholds of 88ms and 5000au. Combining both measurement techniques for the significant disease group showed an increase in specificity of 7% from 84% achieved when using area only, however, there was no increase in sensitivity or specificity scores when using PWTT only at a threshold of 105ms. There were also marginal increases in both sensitivity and specificity scores for the occlusive disease group when combining both tests using PWTT and area thresholds of 130ms and 5300au respectively. There was an increase in specificity to 91% for the significant and occlusive disease group when PWTT and area parameters were combined, but no increase in sensitivity from individual measures. In the final group, which consisted of

patients with moderate, significant and occlusive disease, both sensitivity and specificity increased marginally when PWTT and area parameters were combined as compared from their individual measures. Considering the ABPI threshold levels discussed above, these results compare favourably with ABPI for both the moderate disease group and for the higher levels of disease i.e. the significant and occlusive group. The sensitivity and specificity levels achieved for the moderate disease group, at 70%, are lower than those achieved with ABPI. However, as referred to in section 3.2.6 ABPI is possibly biased towards detecting more severe disease and resting ABPI technique was poor at detecting low grade stenotic disease. This would suggest that there is a disparity between a moderate disease group as defined by duplex ultrasound and one as define by ABPI. Indeed, this would indicate that moderate disease groups as identified by ABPI, contain subjects that would be classified as significant with duplex ultrasound and therefore would partly explain the higher sensitivity and specificity achieved with ABPI on a supposedly moderately disease group. Further more, studies have suggested that a proportion of subjects with moderate disease as identified by duplex ultrasound are misclassified with the ABPI technique, implying that ABPI sensitivity and specificity scores could be lower than 80% and therefore reducing the accuracy between PPG and ABPI for detecting lower grade disease (Stein et al., 2006). Therefore if just the significant and occlusive disease group is considered, which would be a better comparison to ABPI of disease level, all parameters i.e. PWTT, area and PWTT and area combined have sensitivities and specificities comparable with ABPI i.e. 80% or higher.

6.5 Results of test Group

The test group consisted of 8 patients and 8 normal controls. In the patient group there were 3 patients with occlusive disease, 3 patients with significant stenotic disease and 2 patients with moderate stenotic disease. The thresholds calculated from each test as shown in Table 4 were used on the test group. The sensitivity and specificity results are shown in the following tables:

Table 5 Moderate disease group:

	Threshold	Sens(%)	Spec(%)
PWTT	82ms	50	87.5
Area	4780(au)	50	50
Combined	88ms, 5000(au)	50	75

Table 6 Significant disease group:

	Threshold	Sens(%)	Spec(%)
PWTT	105ms	66	100
Area	5000(au)	66	75
Combined	105ms, 5000(au)	66	100

Table 7 Occlusive disease group:

	Threshold	Sens(%)	Spec(%)
PWTT	110ms	100	100
Area	5000(au)	100	66
Combined	130ms, 5300(au)	100	100

Table 8 Significant and Occlusive disease group:

	Threshold	Sens(%)	Spec(%)
PWTT	95ms	100	100
Area	5020(au)	83	75
Combined	110ms, 5500(au)	83	100

Table 9 Moderate Significant and Occlusive disease group:

	Threshold	Sens(%)	Spec(%)
PWTT	88ms	87.5	87.5
Area	5000(au)	75	75
Combined	100ms, 5200(au)	75	87.5

The results of the test group show that PWTT and area combined performs marginally better than area only at detect lower limb arterial disease. However, it does not perform better than PWTT measured in any of the disease groups. The combined measure is equal to PWTT in the significant disease and occlusive disease groups, i.e. Table 6 and Table 7, but PWTT performs better in the remaining groups. The moderate, significant and occlusive disease group i.e. Table 9 shows a sensitivity and specificity of 75% and 87% respectively, although PWTT had a higher sensitivity. If the moderate disease group is removed, as in Table 8, both sensitivity and specificity increase to 83% and 100% respectively for PWTT and area combined, however PWTT achieved 100% for both sensitivity and specificity. With the moderate disease patients removed, the significant and occlusive disease group contains the more severe disease and so as discussed in 3.2.6 closely resembles a patient group classified according to the ABPI method. The sensitivity and specificities achieved in this group match those ABPI for detecting lower limb arterial disease. Since there were such a small number of

patients in each test group it is difficult to be statistically confident about the results. However the results of the test groups indicate that there may be some merit in combining PWTT and area.

6.6 Comparison of ABPI Measurements

Table 10 categorises subject's legs according to duplex ultrasound disease level and compares this with the same legs categorised according to ABPI disease level.

Duplex Disease Level	No of legs	ABPI Disease Level			
		Norm 0.9	Mod 0.5-<0.9	Sig <0.5	Total
Normal	66	57	5	0	62
Moderate	20	15(9D)	5(2D)	0	20
Significant	25	1(1D)	19(5D)	5(2D)	25
Occlusive	21	0	20(5D)	1	21
Total	132	73	49	6	128

D- diabetic leg

Duplex Grading of Disease:

Moderate Disease: PSV ratio = 2-3 (50%-70% narrowing in diameter)
Significant Disease: PSV ratio > 3 (70%- 99% narrowing in diameter)
Occlusive Disease: complete occlusion of lumen of vessel.

ABPI Grading of Disease:

Normal: >0.9-<1.3
Moderate: <0.9->0.5
Significant: <0.5

Table 10 Comparison of duplex disease categories against ABPI Disease categories for bilateral stenosis

If the significant disease category by duplex ultrasound is considered, then of these 25 legs, 1 was classified as normal, 19 were classified as moderate and 5 were classified as having a significant level of disease by the ABPI technique. Similarly for the occlusive disease group

by ultrasound; none out of the 21 legs were classified as normal, but 20 were classified as moderate and 1 was classified as having significant disease by the ABPI technique. Diabetic patients were not excluded from this study and so classifying the legs of diabetic patients with PAOD into the appropriate ABPI disease categories will be difficult as described in 3.2.6. However, as indicated in Table 10, many of the patients did not have diabetes but their duplex ultrasound and ABPI disease levels are not in agreement. Specifically, a number of legs classified by duplex ultrasound as having moderate disease were actually classified as normal by the ABPI technique. This suggests that duplex ultrasound is more sensitive than the ABPI technique, using the generally accepted threshold level of 0.9, for identifying more moderate arterial disease. Furthermore, it could be argued that a certain level of disease classified by the ABPI technique would contain patients with more severe disease than their equivalent level in duplex ultrasound, when categorising arterial disease according to Table 1.

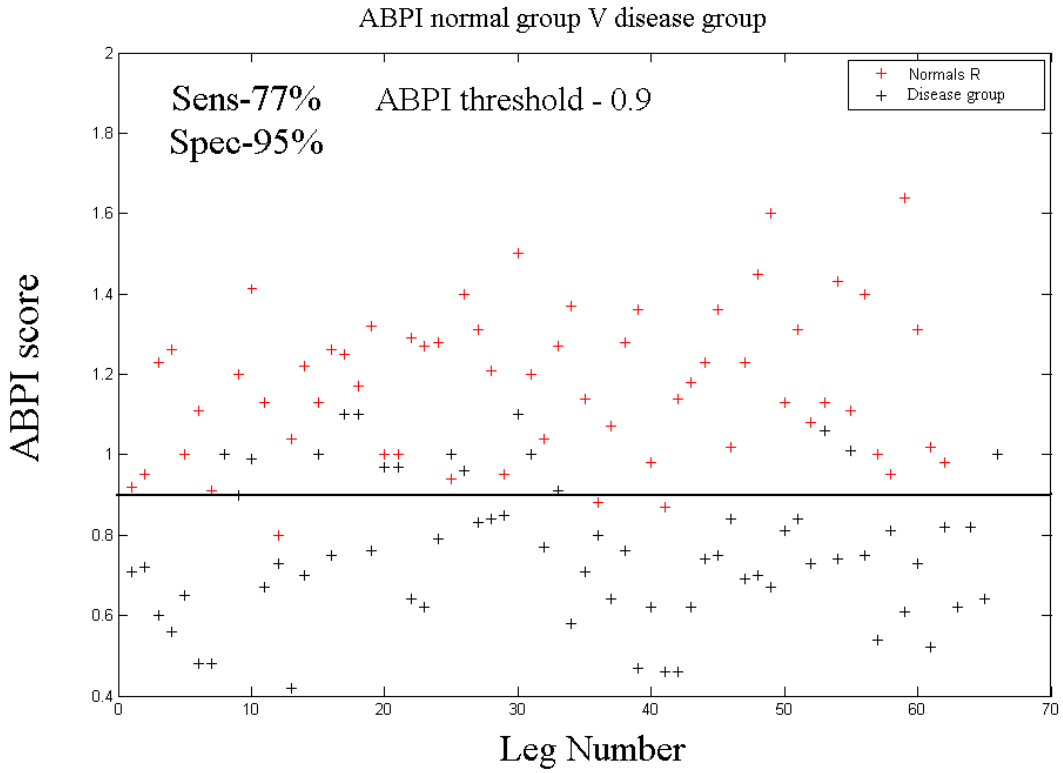

Figure 57 **Scattergram of ABPI scores for normal group and disease group (ABPI: 0.4-1.6)**

Figure 57 shows a scattergram of ABPI scores for the normal and disease group with sensitivity and specificity scores of 77% and 95% respectively, when using 0.9 as the threshold level for disease. The disease group shown in Figure 57 contains the moderate, significant and occlusive disease levels. The equivalent disease group in Table 4 i.e. the bottom row shows sensitivity and specificity scores of 82% and 84% respectively when PWTT and Area are combined.

6.7 Arterial Summary and Discussion

From the results it would seem that combining PWTT and area as a measure of arterial insufficiency could increase sensitivity and specificity scores, than if they were used individually. However the increase is only marginal. As expected it is more difficult to separate patients with more moderate arterial insufficiency from healthy normals than it is to separate patients with more severe disease. This is indicated in Table 4 by the decrease in sensitivity and specificity scores for decreasing disease levels.

If the more severe disease group is considered, i.e. the significant and occlusive group, then combining PWTT and area achieves sensitivities and specificities of 85% and 91% respectively. This is marginally lower than the sensitivity and specificities achieved with ABPI, which are reported to be >90%. Considering the moderate disease group, combining PWTT and area achieved sensitivities and specificities of 70%, a marginal increase from PWTT or area only. This again is lower than the sensitivities and specificities reportedly achieved by ABPI i.e. >80%. However, the lower accuracy scores are compensated by the quicker testing time of 10seconds compared to 5 minutes it takes to obtain an ABPI. Additionally, ABPI uses cuffs, where this PPG method does not.

Similarly work by Erts et al (2005) investigated patients with unilateral stenosis of the lower limbs by comparing bilaterally recorded PPG pulses at the periphery. Their study recorded and examined the delay in the arrival of the PPG pulse at the toe between a healthy and stenotic leg and as a reference bilateral PPG signals detected at the fingertips. Erts et al (2005) also measured bilateral segmental pressures and ABPI. They found convincing correlations between pressure differences between healthy and stenotic legs and the PPG time delay. A similar correlation was found for ABPI results. This thesis records the delayed arrival between the PPG pulses at the index finger and concomitant great toe and so it is difficult to make a direct comparison between PWTT delays. However the study did not report sensitivity or specificity scores or if the patients were grouped according to disease levels. Additionally, the methods used for measuring the PWTT delay rely on the patient having a unilateral stenosis. The disadvantage of this is that a proportion of the population will have bilateral stenosis and so the delay between legs could in many cases be minimal, leading patients to be misdiagnosed as healthy normals.

As previously discussed in section 4.3.2.1 a comparison of pulse timing, amplitude and shape characteristics was conducted by Allen et al (2005). The study compared three different pulse measurement techniques to assess and diagnose lower limb peripheral arterial disease. Pulse wave analysis extracted PPG pulse transit times measured at the toe; it also analysed pulse amplitude and shape characteristics. Normative ranges of these pulse characteristics were then calculated for healthy subjects and compared against patients with different grades of lower limb stenotic disease as referenced to the ankle brachial pressure index. The three different characteristics were then ranked in order of diagnostic performance, both for individual and bilateral great toe pulses.

This thesis does not measure the bilateral differences between pulse characteristics, but analyses individual pulse measurements. Therefore the results of the arterial study will be compared with the individual pulse measurements conducted by Allen et al (2005). Their results showed that shape index diagnostically performed the best on patients with an ABPI of <0.9, i.e. patients with low grade and high grade disease. This group comprised all patients in the study and achieved sensitivity and specificity scores of 88.9% and 90.6% respectively. Pulse transit time diagnostically performed the worst with sensitivities of 31.5% and specificities of 93.8%. If we compare a similar group from this thesis, i.e. the moderate, significant and occlusive groups together, Table 4 shows that area achieved sensitivities and specificities of 74% and 84% respectively, while PWTT scored 79% and 76% respectively. When both tests were combined sensitivity and specificity scores become 82% and 84% respectively. When the tests were repeated on patients with high grade disease, i.e. ABPI <0.5 Allen et al (2005) reported an increase in sensitivities and specificities for both shape index and PWTT. Shape index rose to 100% and 90.6% respectively and PWTT marginally to 45.5% and 93.8% respectively. Comparing this with the significant and occlusive disease group, Table 4 shows area sensitivity and specificity scores of 85%, and PWTT scores of 85% and 86% respectively. Again if both tests are combined sensitivity and specificity scores become 85% and 91% respectively.

The shape index used in the Allen et al (2005) study gave substantial agreement with ABPI, approximately 90% for all disease groups. The similar group in this thesis gave lower sensitivities and specificities scores of 82% and 84% respectively. Therefore in comparison, neither individual nor combined scores in this study match the accuracy as reported by Allen et al (2005). However, in their study, patients were assigned to the high or low level disease group according to their ABPI score. As discussed previously in section 3.2.6, evidence

suggests ABPI is biased towards more significant disease as compared to duplex ultrasound patient groups. Therefore it could be concluded that the moderate disease group in the Allen et al (2005) study contains patients with more advanced lower limb disease than the moderate group in this thesis. This could partly explain the higher sensitivity and specificity scores achieved in their study.

Minimal user effort and minimal time to acquire the signals was also of prime importance in this thesis, particularly if the system is to be used as a screening tool in a primary care setting. In terms of user effort, Allen et al (2005) calculated pulse wave transit times with reference to the ECG signal and so their technique requires the application of ECG leads to the patient. This can be cumbersome and requires additional time and training. Furthermore, signal acquisition takes 2.5minutes. In comparison, the techniques investigated in this study do not require the use of ECG leads for PWTT calculations and signal acquisition takes 10 seconds which is a significant reduction in time. Additionally, as discussed in 6.4 there is only a marginal decrease in sensitivity and specificity levels.

7 Venous Research

The following section describes the patients and methods used in the venous study, it explains the analysis techniques employed and presents the results.

7.1 Venous Patients and Methods

A total of 25 patients (14 men, 11 women, age range 44-89 yrs, mean age 63 years) with CVI were investigated. All the patients had deep venous insufficiency and a further number had additional superficial and or perforator incompetence. Patients had a range of signs and symptoms and a detailed CEAP classification for each patient can be seen in appendix B. A brief description follows: 2 patients had no signs of venous disease; 10 patients had telangiectasias or reticular veins; 9 patients had varicose veins; 12 patients had oedema; 11 patients had skin changes; 2 patients had healed ulcers and 2 patients had active ulcers. All patients had deep venous insufficiency; 16 patients had concurrent superficial and/or perforator insufficiency. All patients had reflux greater than 1 second and two of those had chronic obstruction. All patients had a duplex ultrasound scan to rule out significant arterial insufficiency.

The control group comprised 13 men and 11 women, age range of 22yrs-73yrs with a mean age of 50 years. These also had a duplex scan to rule out arterial and venous insufficiency.

Once the above knee and below knee data were transferred into Matlab, two separate groups were created. One group contained the healthy controls and the other the patients. The signals were first conditioned by removing the D.C offset from the raw PPG signal. It was

anticipated that the signals would be examined and analysed in both time and frequency domains. In doing so, this separated the analysis into two distinct sections; with the waveforms being treated and dealt with accordingly. The two sections will be explained in more detail below. A block diagram of the processing and analysis of the venous signals can be seen in Figure 58.

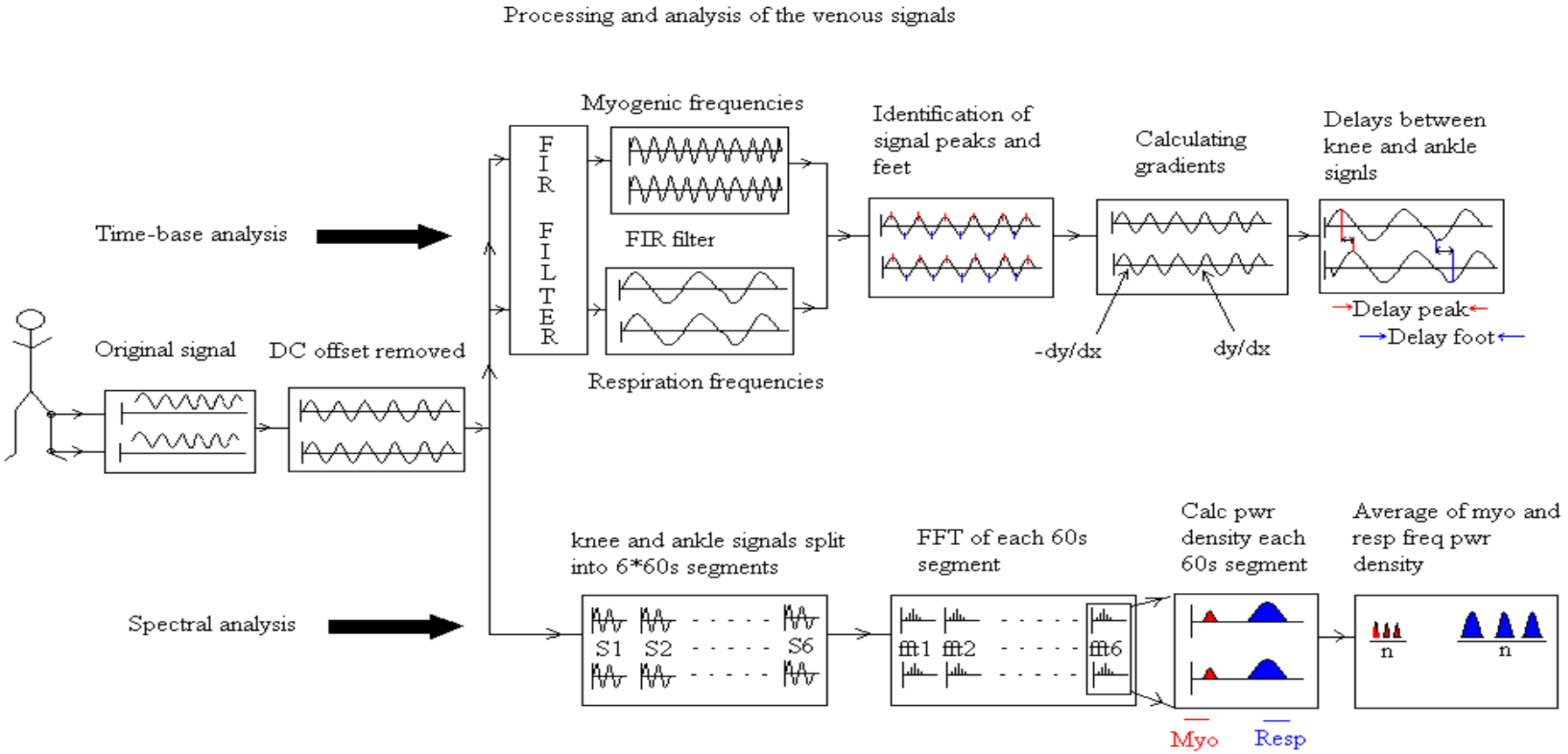

Figure 58 Processing and analysis of the venous signals

7.2 Time Base Analysis

Time base analysis was performed on two components of the PPG signal: the myogenic and the respiratory components-see sections 2.2.2 and 2.3 for an explanation of their origins. To isolate these components a 7000 order finite impulse response filter (FIR) was used. This would ensure a linear phase response. This was conducted firstly over the frequency range 0.06Hz to 0.12Hz (3.6cpm to 7.2cpm) to produce the myogenic coefficients, and then over the frequency range 0.15Hz to 0.4Hz (9cpm to 24cpm) to produce the respiratory coefficients. These coefficients were then used in the Filtfilt function to isolate the separate frequencies. The action of the filters described above removed the cardiac component that was present in the signal.

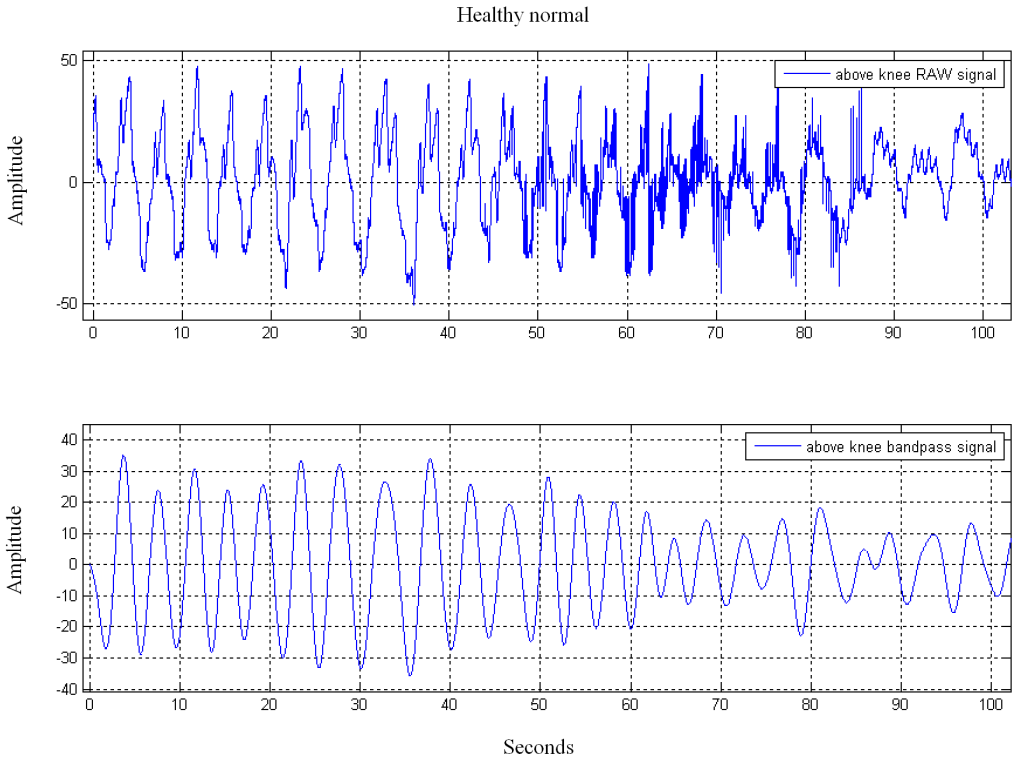

Figure 59 Comparison of RAW and filtered PPG signal (respiration)

The Filtfilt function produces a filtered signal with minimal phase distortion as described previously in 6.1.1. The top waveform in Figure 59 shows a 100 second segment sample of an above knee RAW unfiltered signal from a healthy control. The bottom waveform shows the same signal after it has been filtered at respiration frequencies. Figure 60 shows the result of the Filtfilt function at myogenic frequencies.

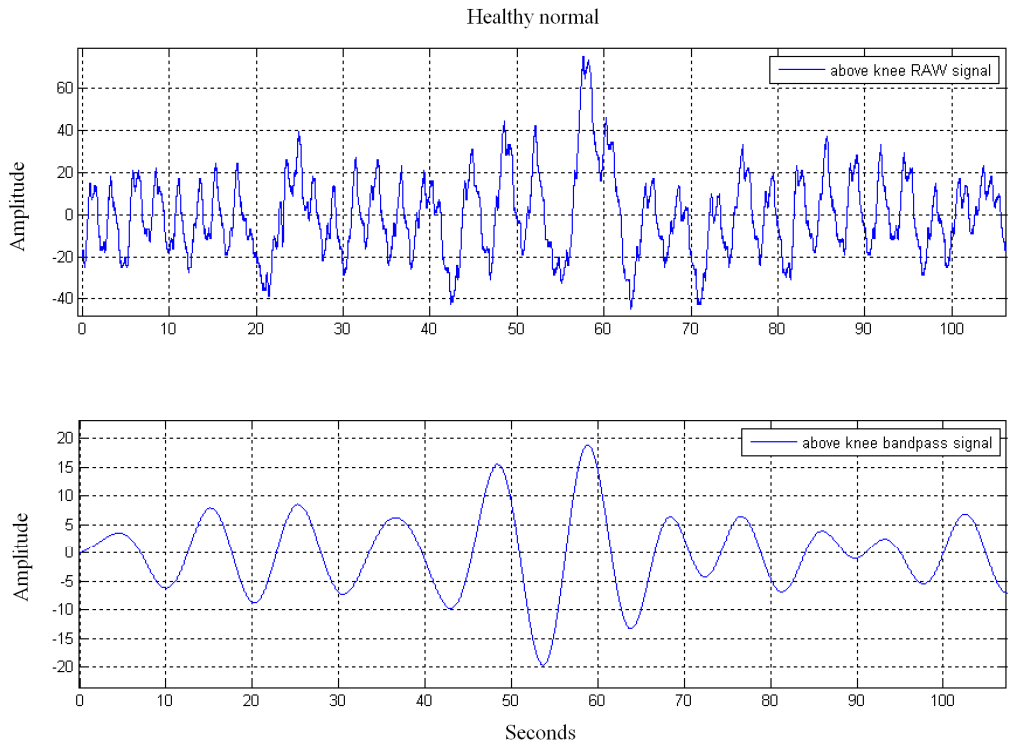

Figure 60 Comparison of RAW and filtered PPG signal (myogenic)

The next step in the programming was to identify the peaks and troughs of the filtered signal. The differential in successive points along the signal vector was calculated. The peak position of the waveform was stored if the differential changed from positive to negative and the trough of the differential changed from negative to positive. This process was repeated for the knee and ankle signals and both for myogenic and respiratory frequencies. These markers were then used to help identify any features of the signal which would differentiate the

different groups. Figure 61 shows an example of the identification of the peaks and troughs of a myogenic filtered waveform from above the knee of a healthy patient.

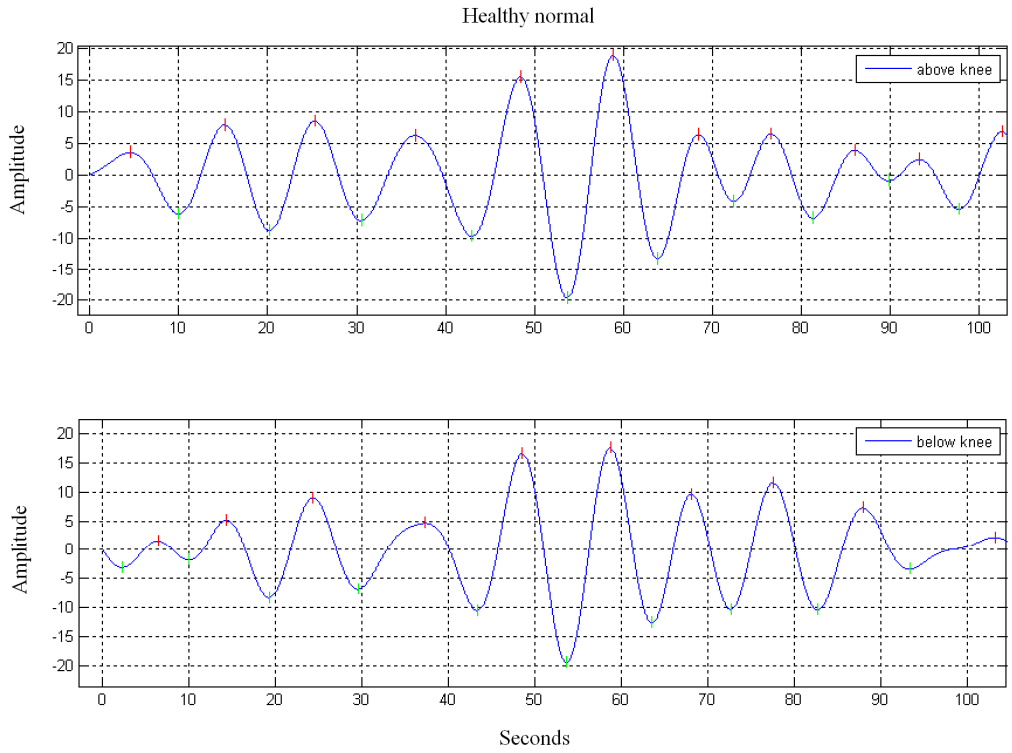

Figure 61 Identification of Peaks and troughs of the filtered waveform (Myogenic)

Next, a noise level threshold value was chosen based on the median amplitude of the pulse peaks and troughs. For each patient, a median amplitude value of all the signal peaks and troughs was calculated. The absolute value of the difference between these two median values was used as the median pulse height. A threshold value was then calculated by dividing this median pulse height by 100. Therefore any pulses of height less than one-hundredth would be excluded. This was done for each patient in each group, thereby only using pulses of adequate amplitude when investigating features of the signal.

Now that the different frequency components of the RAW signal could be isolated, and the peaks and troughs identified, different aspects of the filtered signals between the normal and patient groups could be analysed and compared.

As indicated above, the features investigated were separated into two main groups: time base analysis and spectral analysis. The time base features investigated were: The gradient of the leading and lagging edges; the time delays between above and below knee peaks and this was repeated for the troughs; the phase changes of troughs between groups and this was repeated for the peaks; the difference in the number of peaks above and below knee. The two main spectral features investigated were repeated for both myogenic and respiration frequencies: the power densities between healthy and patient groups; the power density ratio (resp/myo) between healthy and patient groups. An explanation of how each feature was derived and calculated is written below.

7.2.1 Gradient of the Leading and Trailing Edges in myogenic and respiration waveforms

Now that the peaks and troughs of the filtered waveforms have been identified, the pulses that make up the 6 minute signal can be separated into the leading and trailing edges. The leading edge was defined from the trough of the pulse to its peak, while the trailing edge was defined from the peak of the pulse to the following trough. The program ran through the control and patient groups, analysing both myogenic and respiration waveforms separately. Maximum and median gradients of the leading and trailing edges were calculated for each pulse of the 6 minute signal. From the results an overall maximum and median gradient could be calculated from the individual pulse gradients that would be representative of that person. A mean of the

maximum gradients was also calculated. This was performed for both above knee and below knee signals so that intra and inter comparisons could be made.

7.2.2 Delays between the above and below knee pulse peaks for myogenic and respiration signals

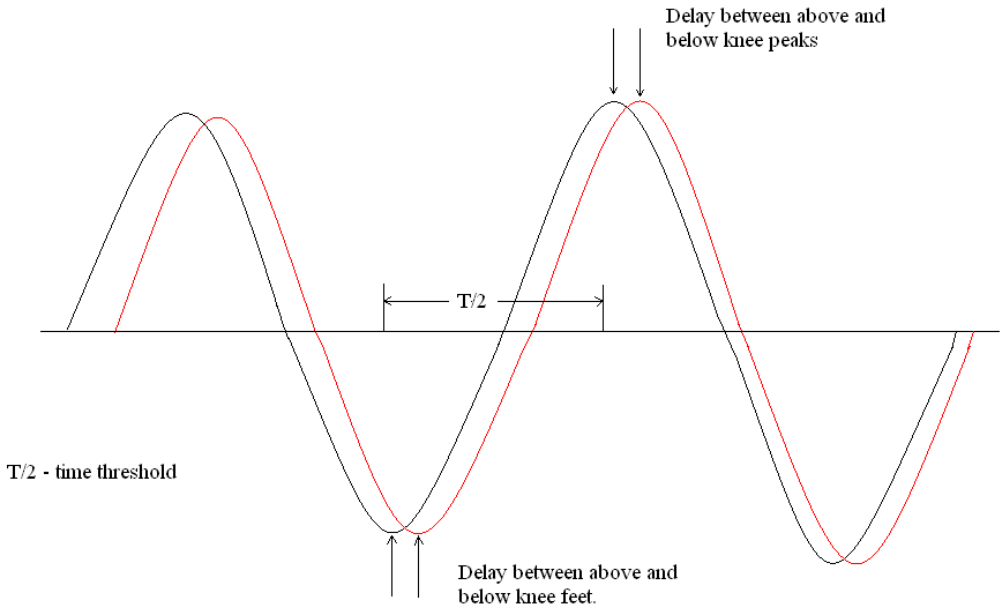

Figure 62 shows the delay between above and below knee pulse troughs and pulse peaks for signals in the same frequency band (i.e. myogenic or respiration band) and also the time threshold used.

The analysis was performed on both myogenic and respiratory bands. Because of the spread of frequencies within each band, time thresholds needed to be used so that only peaks within this time frame would be utilised to calculate the delays between the above and below knee signals Figure 62. These thresholds were determined on an individual by individual basis. To calculate the threshold the number of pulses over the entire 6 minute signal were counted. Next, the total was divided by 6 to give the number of pulses per minute (ppm). By dividing the ppm by 60 gave the frequency of signal, and from this the period of the signal was derived. This was finally divided by 2 to give half the period of the waveform (T/2). This

represented the time threshold for that subject and was used to match above and below knee peaks and troughs in time. If the time difference between two pulses was greater than the time threshold, then the pulses were not matched and therefore the delay between the peaks could not be calculated and the two pulses were ignored. Only when the time difference between two peaks were within the time threshold calculated for that individual, were they matched. Because the above knee and below knee peaks changed sometimes from leading to lagging, a positive and negative time threshold value was used. This ensured that only the correctly matched peaks from the above and below knee signals were utilised in the delay calculations.

The same process was carried out for calculating the delays between the above and below knee pulse trough.

7.2.3 Matched delays in Myogenic and respiration signals between the above and below Knee Peaks and Troughs

Now that the individual pulse peaks between the above and below knee signals had been matched and similarly the individual pulse trough between above and below knee, the next stage was to investigate if there was any correlation of these parameters between corresponding pulse trough and peak delays. To ensure that the delays in the pulse trough matched the delays in the pulse peaks, a second time threshold was set-up. This time threshold comprised a half time period plus a quarter time period calculated from the individual's myogenic or respiratory rate. In this way, the program ensured that any single pulse trough was matched with its own pulse peak, and not that of a later peak from a different pulse. The above and below knee signals were both investigated in this way. When the program established pulse troughs and pulse peaks were within the predetermined time

threshold, the delays between pulse troughs and the delays between pulse peaks for above and below knee could be calculated. Once the delays have been calculated for all the matched pulses from one individual, the above and below knee troughs delays were subtracted from the above and below knee peak delays so that the mean and median values of the aligned delays could be calculated. These values would be representative of an individual and therefore the control groups could be compared to the patient group.

7.2.4 Phase changes in myogenic and respiratory signals in above and below knee waveforms

The number of phase changes which occurred between the above and similarly for the below knee pulse peaks and above and below knee pulse troughs were determined from the delays computed from the previous aligned delay analysis. Each delay calculated between the peaks for each separate pulse of the six minute signal was examined to determine if the delay was positive or negative. The delay was calculated by subtracting the below knee peak time from the above knee peak time. The number of positive and negative delays was counted separately for the entire signal. The number of positive and negative delays counted in each signal was divided by the total number of pulses captured for the entire signal. This accounted for the variation in pulse numbers captured between individual subjects. The proportion in number of negative delays identified was subtracted from the proportion of number of positive delays identified and this difference represented the number of phase changes that occurred over a 6 minute period. As mentioned above, this method was performed for both troughs and peak delays over myogenic and respiratory frequencies.

7.2.5 Comparison of myogenic and respiration rates between above and below knee signals

The difference in the numbers of peaks between the above knee and below knee signals was calculated for both myogenic and respiratory waveforms and compared for control and patient groups.

7.3 Frequency Based Analysis

A signal describes how one parameter changes with another. A typical example would be a signal showing voltage varying with time at one particular frequency from an analogue electronic circuit. In biological signals, the parameter on the y-axis can be obtained from many sources such as a potential difference measured across ECG electrodes, pressure within a pneumatic cuff or the light intensity reflected from an infra-red signal incident on the tissue. The parameter which is mostly used for the x-axis is time. Signals that are recorded from the body are more complex in nature consisting of a number of different frequency components. These frequency components can be analysed using a mathematical technique developed some 300 years ago by Joseph Fourier. This technique is based on the principle that any continuous periodic signal can be represented by the sum of sinusoidal waves of different frequencies, called a Fourier series. In this way the signal is converted or transformed from the time to the frequency domain.

Fourier analysis assumes the signals are infinite in length; however biological signals are recorded over a predetermined time and so are finite in length. Furthermore, the signals are sampled and stored onto a computer for analysis off-line, i.e. after signal acquisition is complete. To get around this problem the Discrete Fourier Transform (DFT) was developed

which makes an approximation by imagining the original signal as repeating itself an infinite number of times. Therefore the signal appears periodic and infinite in length with a wavelength equal to that of the original signal. The DFT is calculated using an extremely fast algorithm called the Fast Fourier Transform (FFT). The transformed signal is then displayed with frequency on the x-axis and power of the frequency component on the y-axis, also known as the power spectrum (Figure 63).

Fourier analysis is best suited to signals whose frequency content does not change with time, also known as stationary signals. However, the frequency content of biological signals tends to vary with time due to the complex nature of human physiology. There are various techniques which can look at how the frequency components within the signal change with time such as complex demodulation (CDM) and Wavelet analysis and these will be touched upon later in this chapter. Nonetheless, the amplitude of the power spectrum can give us some insight into distribution of the frequency content over time. For example, any frequency that exists only for a short period of time will have a smaller power in the frequency domain compared to frequencies that last for a longer time. In this thesis, myogenic and respiratory frequency bands were analysed, but since the frequency bands are not of equal length (myogenic: 0.06-0.12 Hz; respiration: 0.15-0.4 Hz) then power densities were calculated so that the two frequency bands could be compared.

As mentioned above certain techniques can be employed to overcome to some degree this disadvantage. A technique known as windowing can be used that splits the signal up into smaller segments i.e. the windows, and an FFT calculated for each segment. By examining how the FFT changes from one window to the next, the variation in the frequency content of the signal can be examined. However there is a disadvantage with this method, which is

shorter signal acquisition times reduce the frequency resolution. Complex Demodulation is another technique which can overcome some of the difficulties with using Fourier analysis. Instead of analysing the whole spectra of frequencies, the technique focuses on a single frequency and how its amplitude and phase varies with time. There is still however a trade-off between resolution in the time and frequency domain. Wavelet analysis is a mathematical tool which splits the signal data into different size windows or wavelets; larger wavelets will only capture gross features in the signal where as smaller wavelets identify smaller features in the signal which occur over a shorter time scale. Wavelet analysis shows how the different frequency components in the signal change with time and a particularly well suited to study situations where the signal contains discontinuities and sharp spikes.

This part of the analysis used the windowing technique to split both the above and below knee 6 minute signals into 1 minute segments. Six minutes of data were acquired as this was the minimum length of time the venous unit recorded. As mentioned above this was performed so that any variation or change in the frequency content of the signal over the 6 minute period (in one minute segments) could be captured and analysed. By splitting the signal in this way a median value was calculated that represented the 6 individual 1 minute segments. This is not the same as a median value calculated over the entire 6 minute signal. Therefore it is a simple method which can capture any change in the frequency content of the signal. Before an FFT could be taken of the signals, a Hanning window was applied to each segment. The data points from each 1 minute segment were multiplied by an N-point Hanning window. In the time domain this reduces the amplitude of the signal from a maximum value at the centre to zero at the edges. The result is improved frequency resolution in the power spectrum. An FFT performed on data without a window results in smearing or leakage in the frequency domain. Using an appropriate window reduces these effects.

An FFT was then performed on each minute of the signal. Once this was completed for the above and below knee signals, the power density within the myogenic and respiratory bands could be calculated. This was achieved as follows: since the signal was sampled at a rate of 100Hz, each 60 second segment of signal contained 6000 data points; this gave a spectral resolution of 0.016Hz sample^{-1} (100Hz/6000). In order to isolate part of the spectrum that represents the myogenic band, lower and upper sample points needed to be calculated. The lower and higher sampling points for the myogenic bands were calculated as follows: given the sampling resolution of 0.016Hz sample^{-1} and the lower bandwidth point of 0.06Hz for myogenic frequencies, the lower sampling point was 0.06Hz/0.016Hz sample^{-1}. This gives a lower sampling point of 4. The upper sampling point is calculated in much the same way, but this time using the upper bandwidth point, 0.12Hz/0.016Hz sample^{-1}. This gives an upper sampling point of 7. The process was repeated for the respiratory part of the spectrum and this gave a lower respiratory sample point 9 and an upper sample point 24. Using these calculated sample points, bandwidths could be identified and subsequently power densities were calculated for each 1 minute segment. This was carried out for both myogenic and respiratory bands for the complete 6 minute signal. Furthermore, a power density index was calculated by dividing the respiratory power density with the myogenic power density. The regions of interest can be seen from Figure 63 which shows an example of the spectrum of the PPG signal, split into one minute sections, of a healthy individual above the knee. The relevant bandwidths from the graph are from, 4 cycles min^{-1} to 7 cycles min^{-1} (myogenic band), and from 9 cycles min^{-1} to 24 cycles min^{-1} (respiratory band).

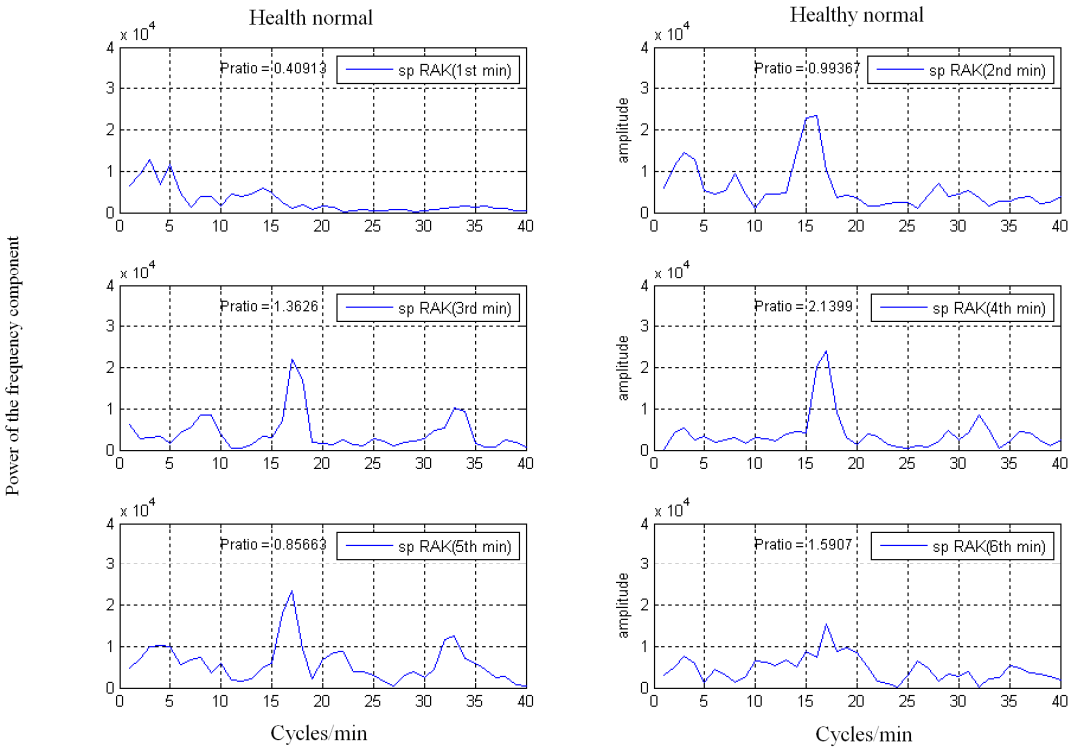

Figure 63 Spectral analysis of above knee PPG signal. The 6 minute signal has been separated into 1 minute sections starting with the 1st minute top left to the 6th minute bottom right.

7.4 Venous Results

The following section reports the results of investigations undertaken of the venous signals taken from above and below the knee. The signals from both sites were analysed in both time and frequency domains, and are reported separately.

7.4.1 Time Base Analysis

Time base analysis investigated the gradients, delays, number of peaks and phase changes of the signals within and between groups. Each analysis is reported separately with a table summarising the results. For clarity, the Q-Q plots and box plots of some results can be seen in appendix B.

7.4.1.1 Gradient of Leading and Trailing Edges

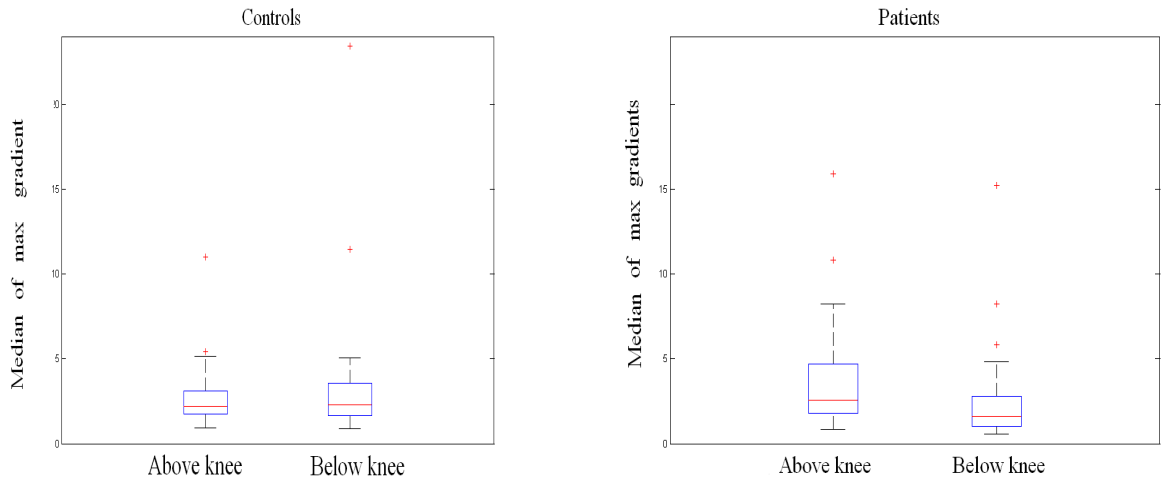

Figure 64 Gradient of leading edge at myogenic frequencies

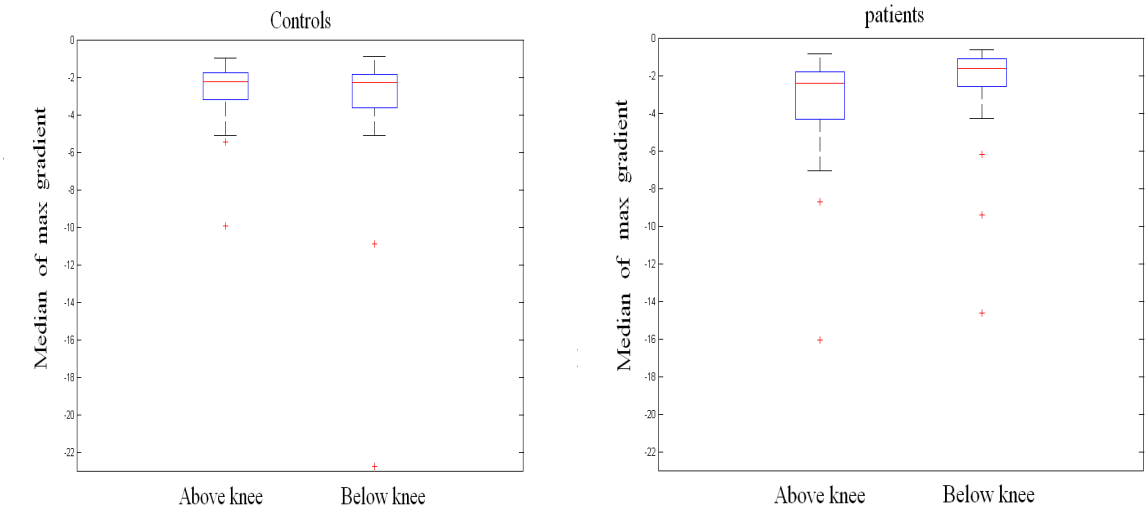

Figure 65 Gradient of trailing edge at myogenic frequencies

Figure 64 and Figure 65 show example box plots of the maximum gradients between the above and below knee signals for control and patient groups at myogenic frequencies. Similar

box-plots of gradient data at respiration frequencies can be seen in appendix B. The results for both myogenic and respiration frequencies are summarised in Table 11

		Myogenic		Respiration	
		p-value	null	p-value	null
Median of max grad	Leading	0.80	0	0.58	0
	Trailing	0.57	0	0.54	0

Table 11 Time base analysis within group comparisons for healthy controls between above and below knee signals

As can be seen from Table 11 there is no statistically significant difference in the median of the maximum gradients between the above and below knee leading or trailing edges at myogenic or respiration frequencies.

		Myogenic		Respiration	
		p-value	null	p-value	null
Median of max grad	Leading	0.06	0	0.12	0
	Trailing	0.04	1	0.11	0

Table 12 Time base analysis within group comparisons for patients between above and below knee signals.

The patient group shows statistically significant differences at the 5% and 10% levels between the above and below knee signals at myogenic frequencies. As indicated in Table 12, the most significant difference was seen for the trailing edge at myogenic frequencies, where there was a statistically significant difference in the median maximum gradients between the above and below knee signals at the 5% level. The least significant difference in gradients between above and below knee signals was the leading edge at respiration frequencies where there was a poor statistical difference.

		Myogenic				Respiration			
		p-value above kn	Null Above kn	p-value below kn	Null below kn	p-value above kn	Null Above kn	p-value below kn	Null below kn
Median of max grad	Leading	0.48	0	0.06	0	0.007	1	0.003	1
	Trailing	0.41	0	0.04	1	0.008	1	0.004	1

Table 13 Time base analysis for same-site comparisons between healthy controls and patients

Table 13 shows the results of the time base analysis for same-site comparisons between healthy controls and patients. Respiration measures in particular, show a statistically significant difference when comparing control and patient groups above and below the knee. As indicated the above knee and below knee median maximum gradient of the leading and trailing edges show a statistically significant difference at the 5% level. In contrast, the above knee measures show poor significance at myogenic frequencies, however, the median of the maximum gradients of the trailing edge below the knee shows a statistically significance at the 5% level and the leading edge above the knee at the 10% level. Boxplots representing the respiration frequency data can be found in appendix B.

7.4.1.2 Delays Between Above and Below Knee Signal Peaks and Troughs

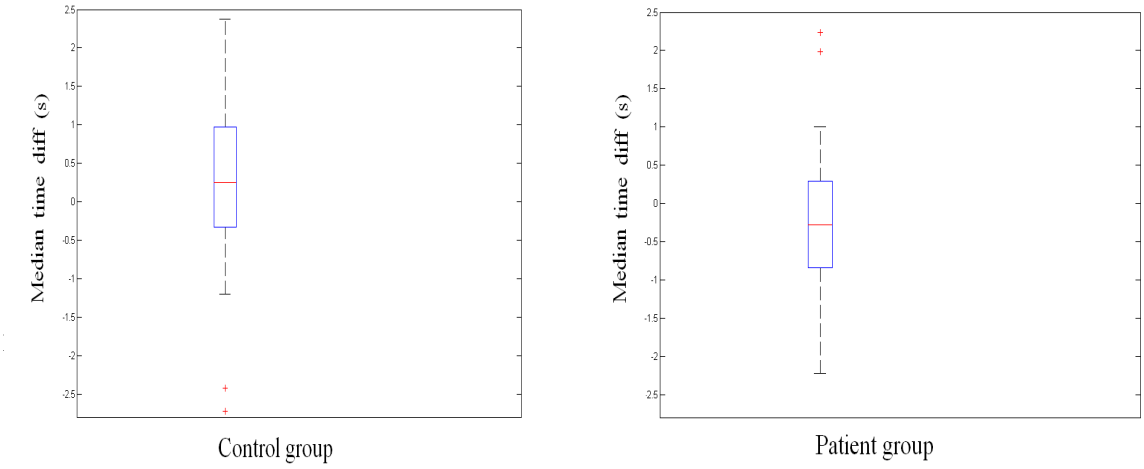

Figure 66 Delays in the above and below knee peaks at myogenic frequencies

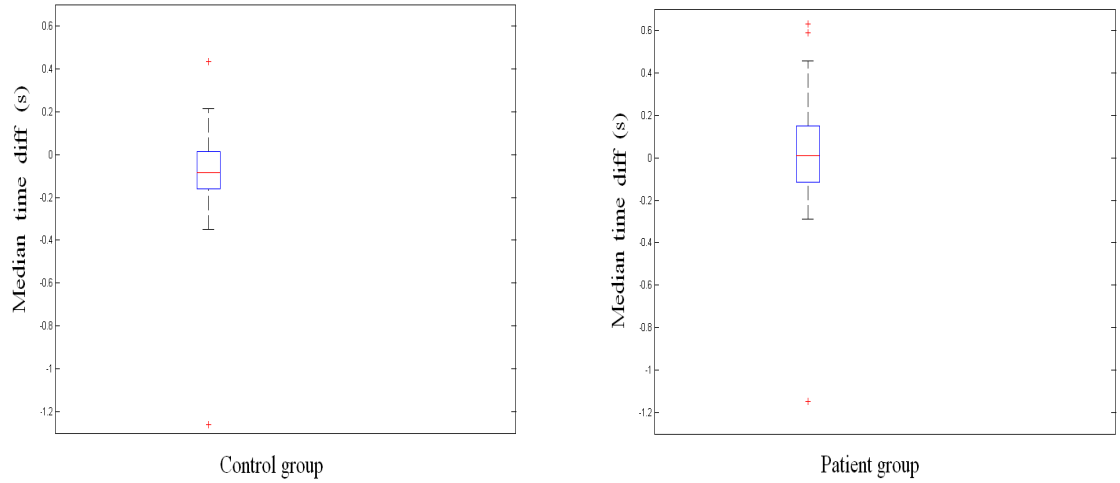

Figure 67 Delays in the above and below knee peaks at respiration frequencies

Figure 66 and Figure 67 show the delay in the peaks between the above and below knee signals for myogenic and respiration frequencies, for both the control and patient groups respectively. The corresponding delays for the pulse trough between the above and below knee signals can be found in appendix B.

7.4.1.3 Delays between the Matched above and below knee Signals Using Signal Peaks and Signal Troughs

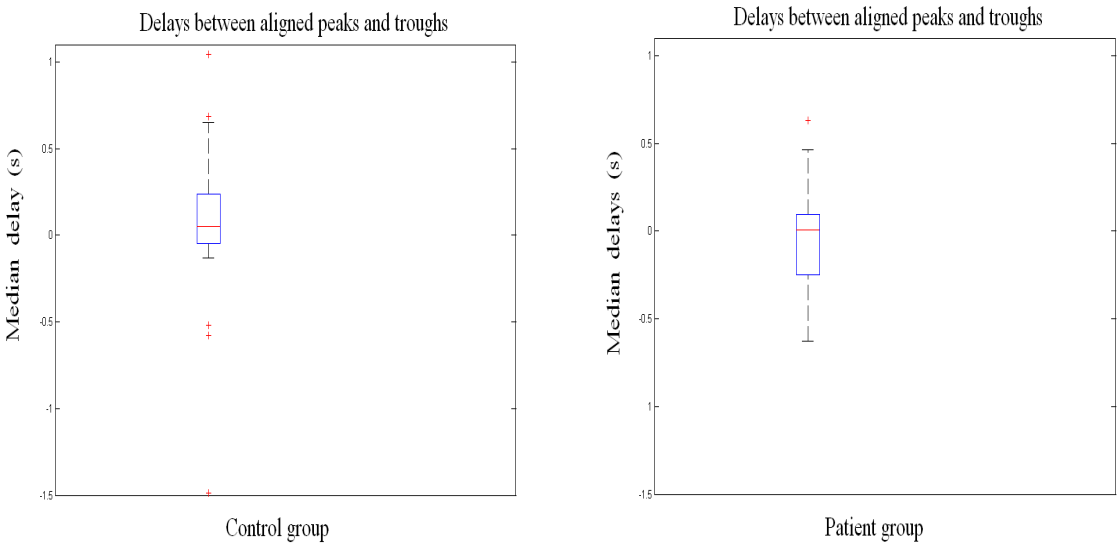

Figure 68 Delays between the matched signals at myogenic frequencies

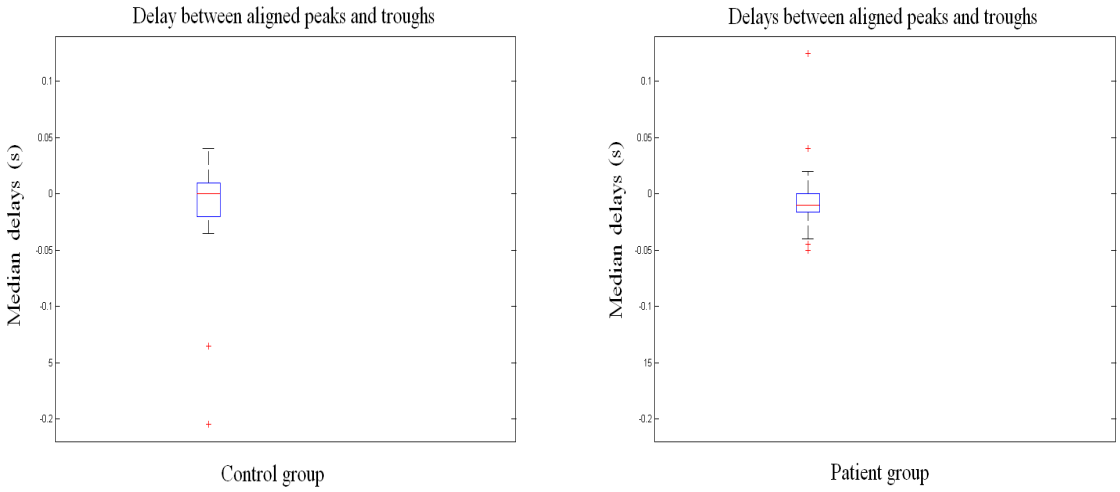

Figure 69 Delays between the matched signals at respiration frequencies

Figure 68 and Figure 69 show the delays between the matched signal peaks and signal troughs for the above and below knee signals at both myogenic and respiration frequencies

respectively. Control and patient groups are shown. A summary of the results for both the delay between above and below knee signals and the matched delays can be seen in Table 14

Median Delays	Myogenic		Respiration	
	p-value	Null	p-value	null
Peaks	0.07	0	0.09	0
Troughs	0.13	0	0.05	0
Matched peaks and troughs	0.23	0	0.49	0

Table 14 Delays in the peaks and troughs between healthy controls and patients

The median delays in the peaks and troughs at both myogenic and respiration frequencies show a level of statistical significance. With reference to Table 14, there was one test which showed significance at the 5% level, and this was seen between the delays in the troughs at respiration frequencies. Median delays between the peaks at myogenic and respiration frequencies showed statistically significant difference at the 10% level.

7.4.1.4 Number of Peaks Above and below knee

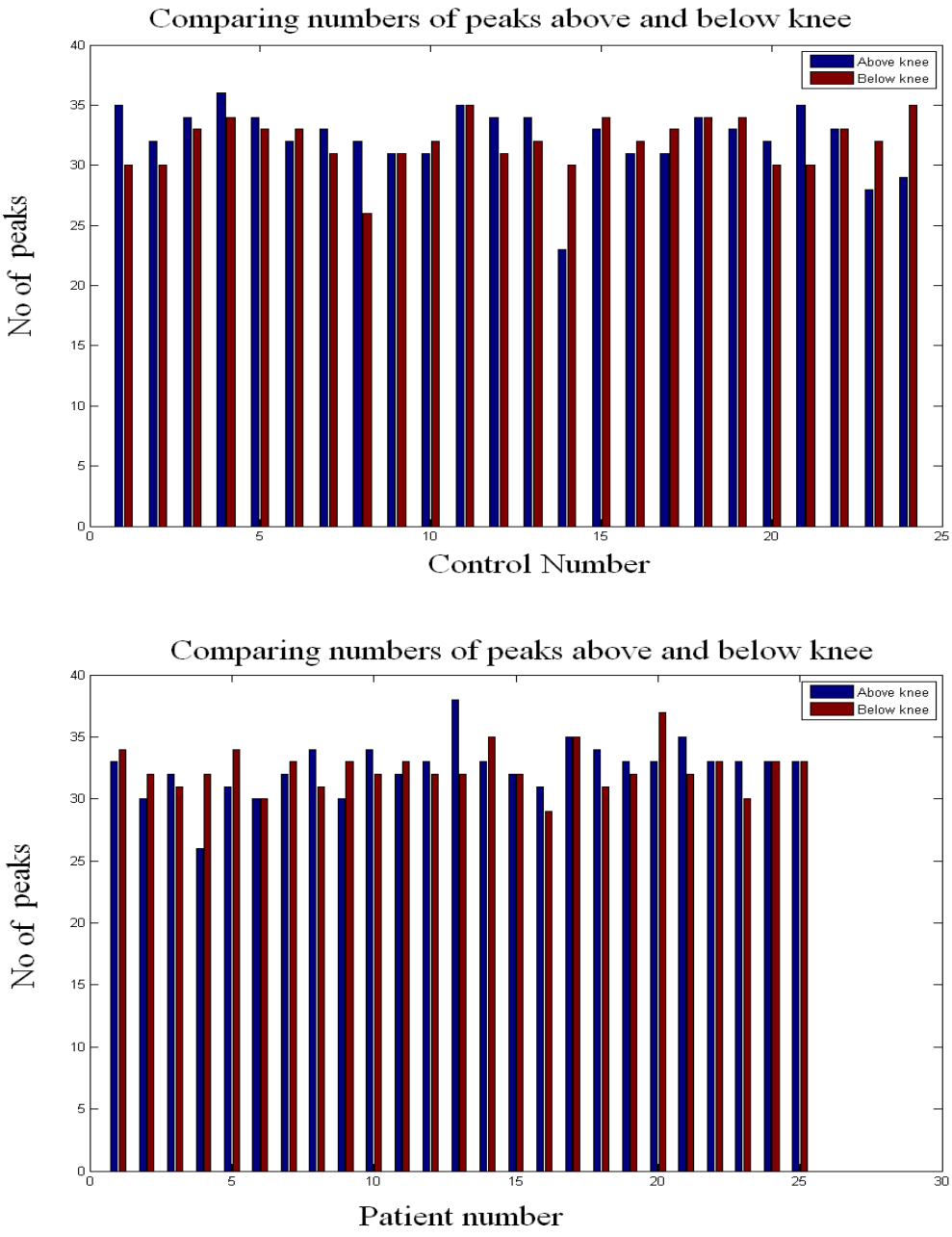

Figure 70 **Number of peaks above and below knee at myogenic frequencies for control and patient groups**

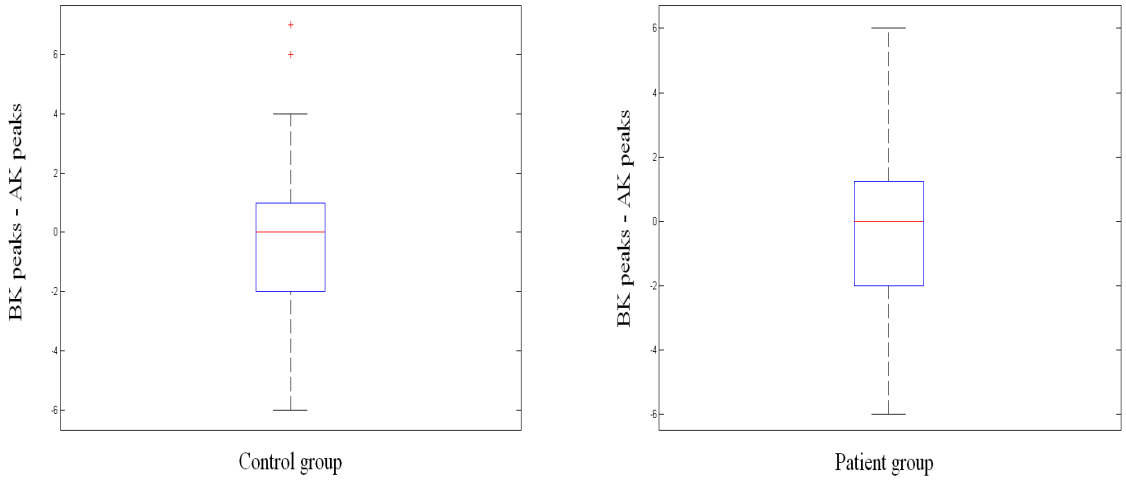

Figure 71 Difference in number of peaks between above and below knee at myogenic frequencies between healthy controls and patient groups

Figure 70 shows bar graphs of the number of peaks above and below the knee for the control and patient groups at myogenic frequencies. A box plot of the difference between the above and below knee signals for the control and patient group is shown in Figure 71. This is repeated for respiration frequencies and the results are shown in Figure 72 and Figure 73. Table 15 summarises the results and shows the statistical significance levels for the difference in above and below knee peak numbers over the six minute period, between control and patient groups at myogenic and respiration frequencies.

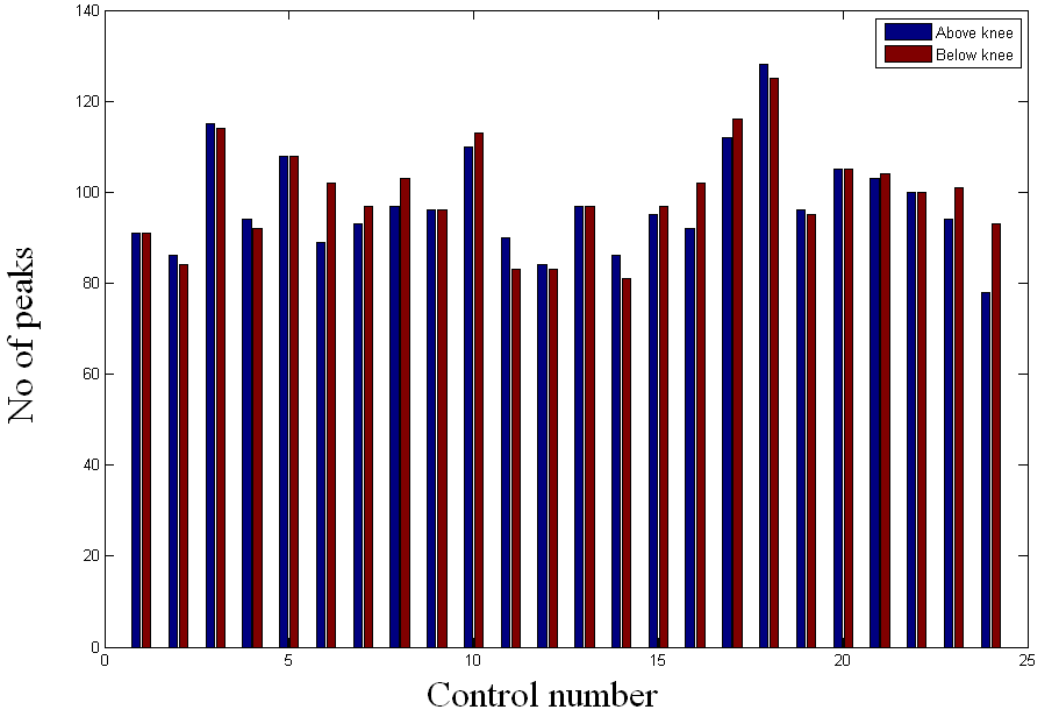

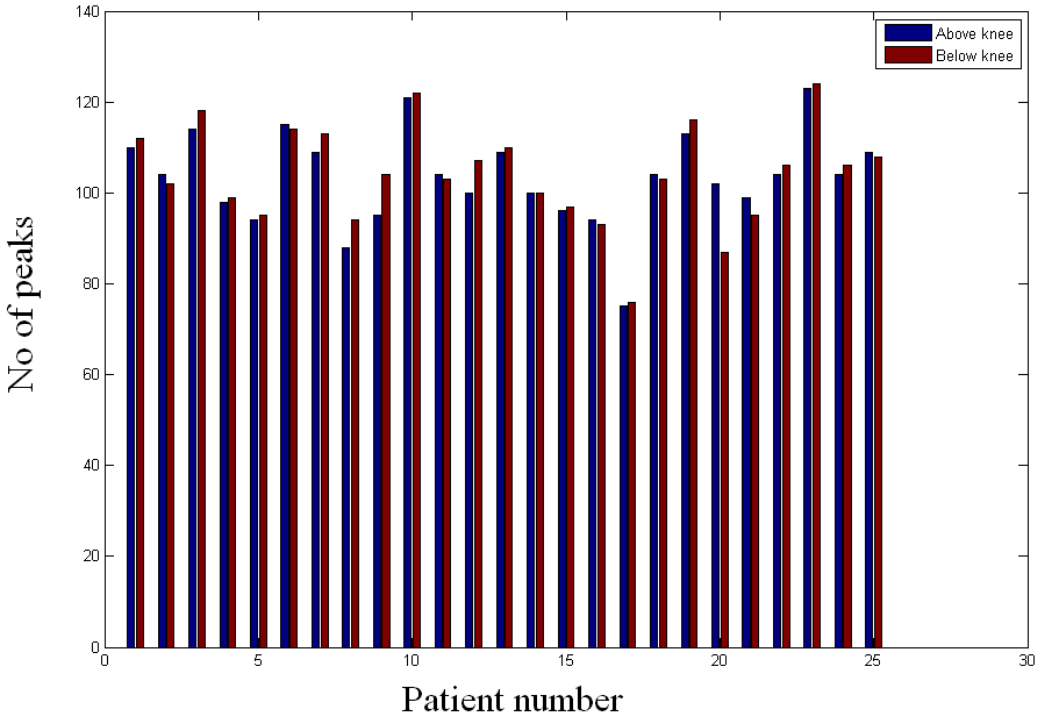

Figure 72 Number of peaks above and below knee at respiration frequencies between healthy control and patient groups

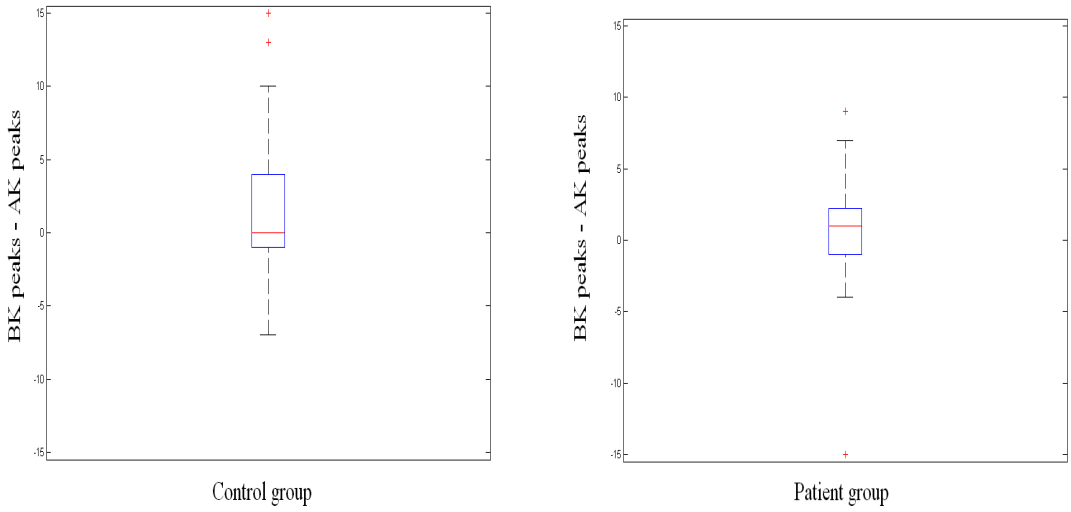

Figure 73 Difference in the number of peaks between above and below knee at respiration frequencies between healthy controls and patients

	Myogenic Frequencies		Respiration Frequencies	
Difference in peaks	p-value	Null	p-value	null
	0.77	0	0.83	0

Table 15 Shows results of the statistical test on the difference in peaks between control and patient groups for myogenic and respiration frequencies

7.4.1.5 Difference in the Proportion of Phase Changes between Above and Below Knee Signals

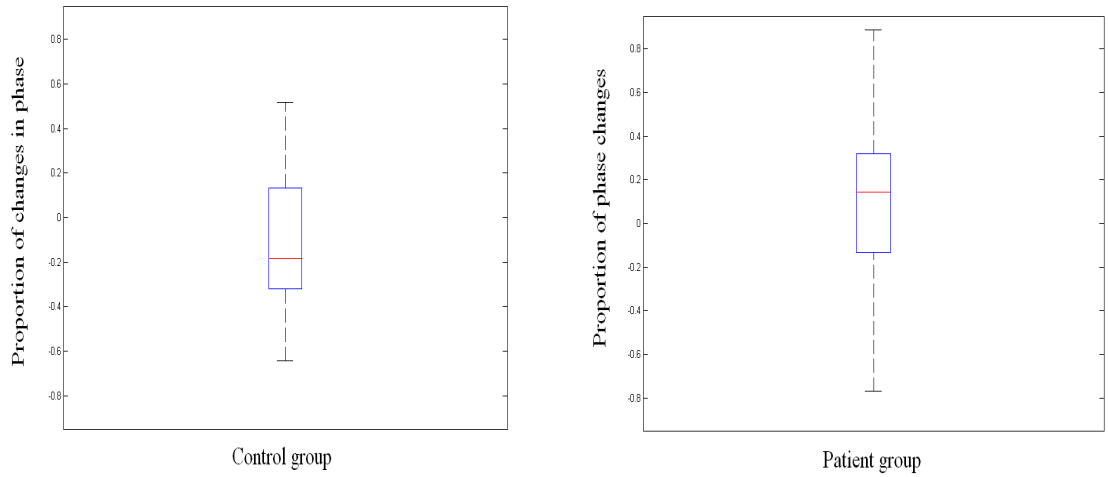

Figure 74 Difference in the proportion of total phase changes of pulse troughs between the above and below knee signals at myogenic frequencies

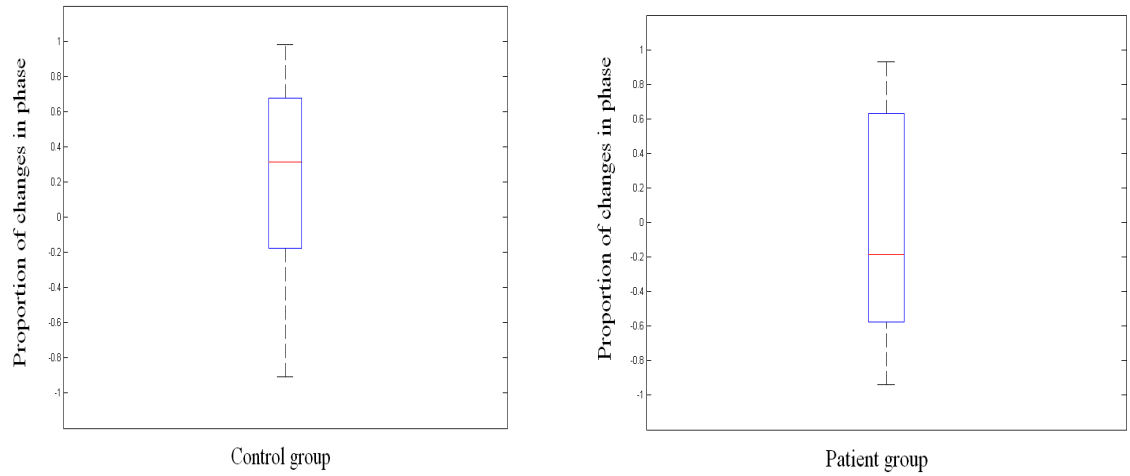

Figure 75 Difference in the proportion of total phase changes of pulse troughs between the above and below knee signals at respiration frequencies

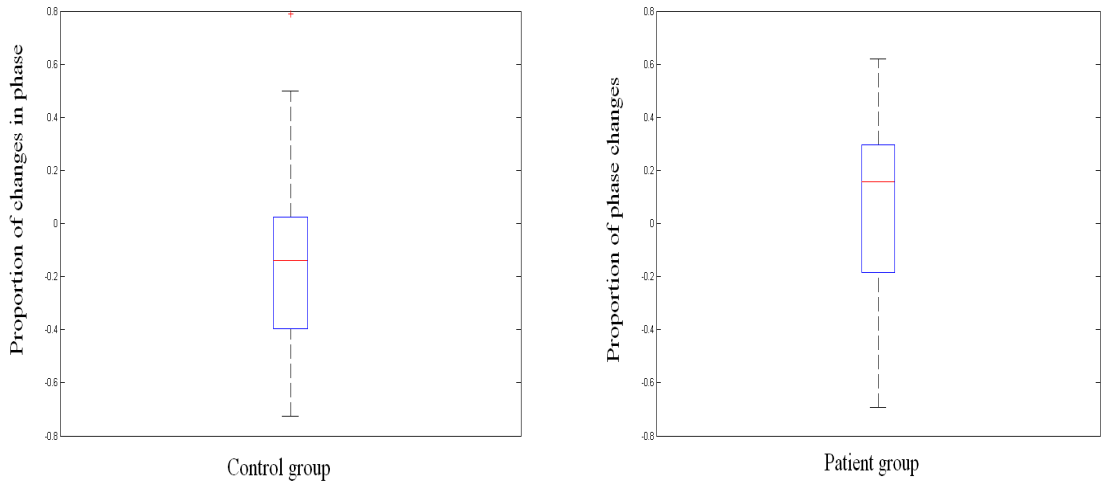

Figure 76 Difference in the proportion of total phase changes of pulse peaks between the above and below knee signals at myogenic frequencies

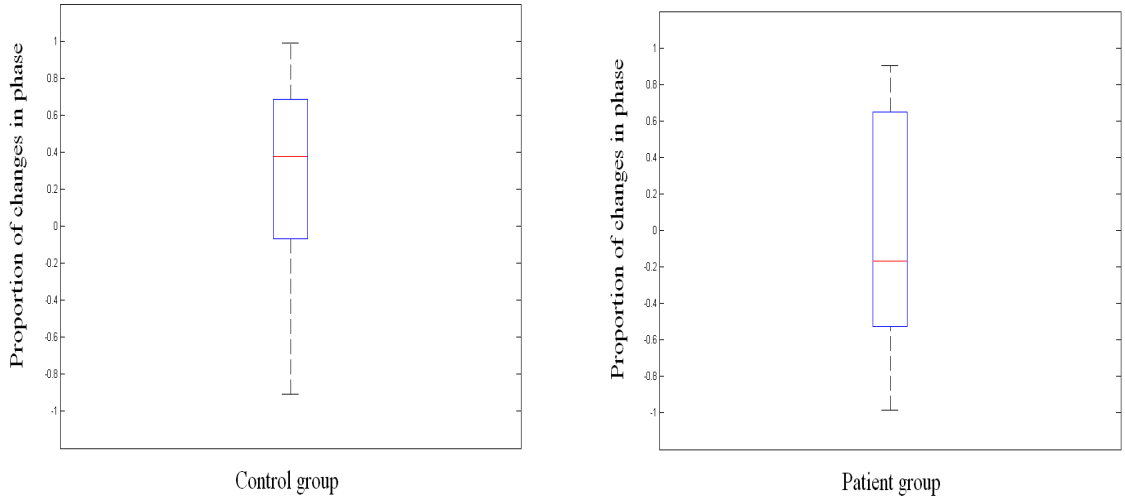

Figure 77 Difference in the proportion of total phase changes of pulse peaks between the above and below knee signals at respiration frequencies

Figure 74 and Figure 75 show box plots of the difference in the proportion of phase changes of the troughs between the above and below knee signals at myogenic and respiration frequencies respectively. Figure 76 and Figure 77 show the phase changes between the peaks for myogenic and respiration frequencies. Table 16 summaries these results. There is a statistically significant difference, at the 5% level, in the median of the phase changes of the pulse peaks and pulse trough between the control and patient groups at myogenic frequencies.

	Myogenic		respiration	
	p-value	Null	p-value	null
Peak phase change	0.03	1	0.23	0
Troughs phase change	0.02	1	0.18	0

Table 16 Phase changes of peaks and troughs between healthy controls and patients

QQ plots of the data for Table 16 can be seen in section appendix B

7.4.2 Frequency Analysis

First, frequency analysis calculates the above and below knee power density within the myogenic and respiration frequencies and compares the results between the control and patient groups. Second, the power density ratio is calculated (respiration density/myogenic density) from above and below knee signals and then compared between the control and patient groups. The results are presented below.

7.4.2.1 Power Density

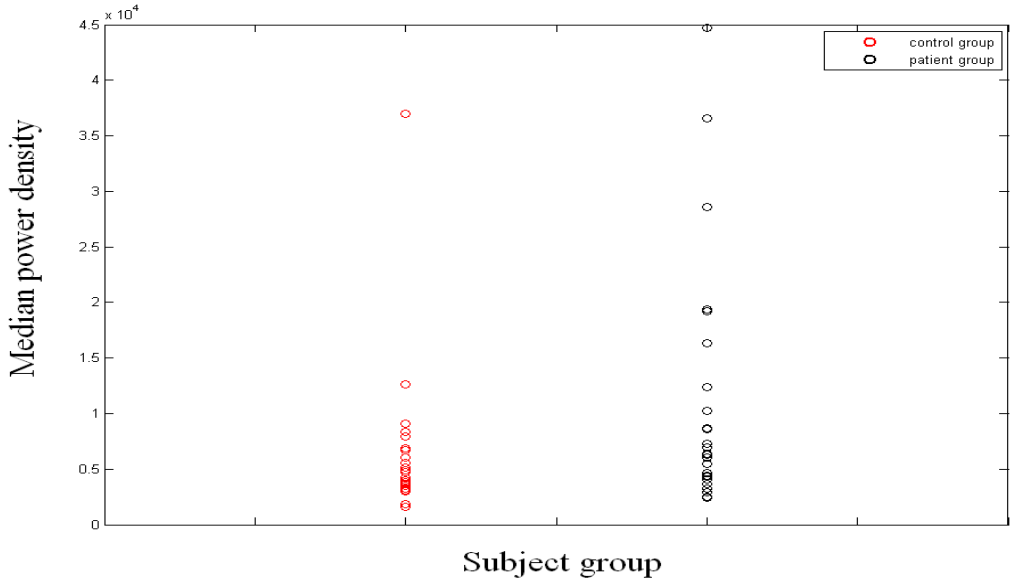

Figure 78 Above knee power density at myogenic frequencies

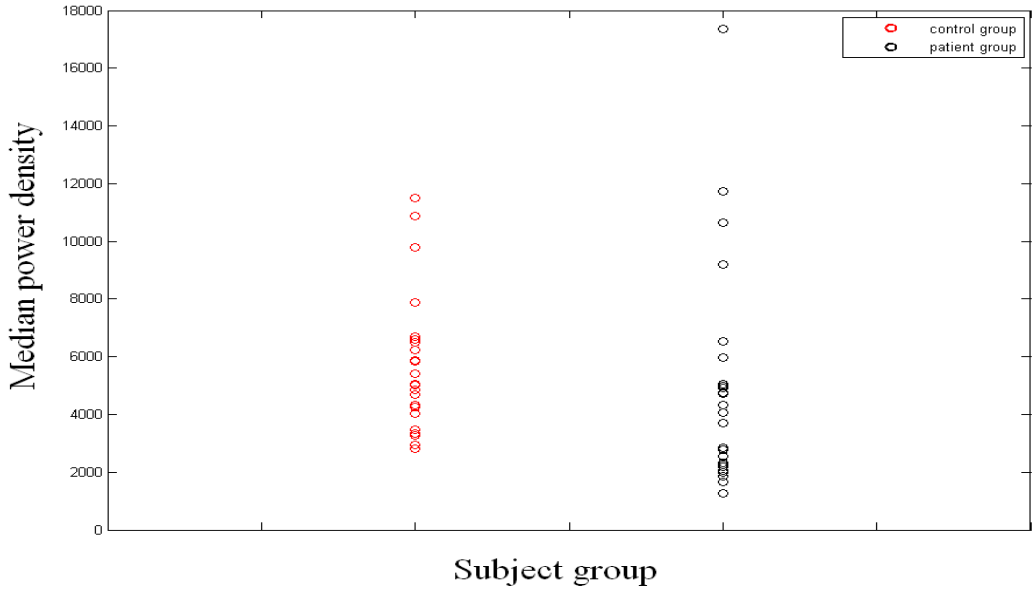

Figure 79 Above knee power density at respiration frequencies

Figure 78 and Figure 79 show scattergrams of the above knee power densities at myogenic and respiratory frequencies and Figure 80 and Figure 81 show the below knee power

densities at myogenic and respiration frequencies. The results of the statistical analysis performed on the two groups are reported in Table 17

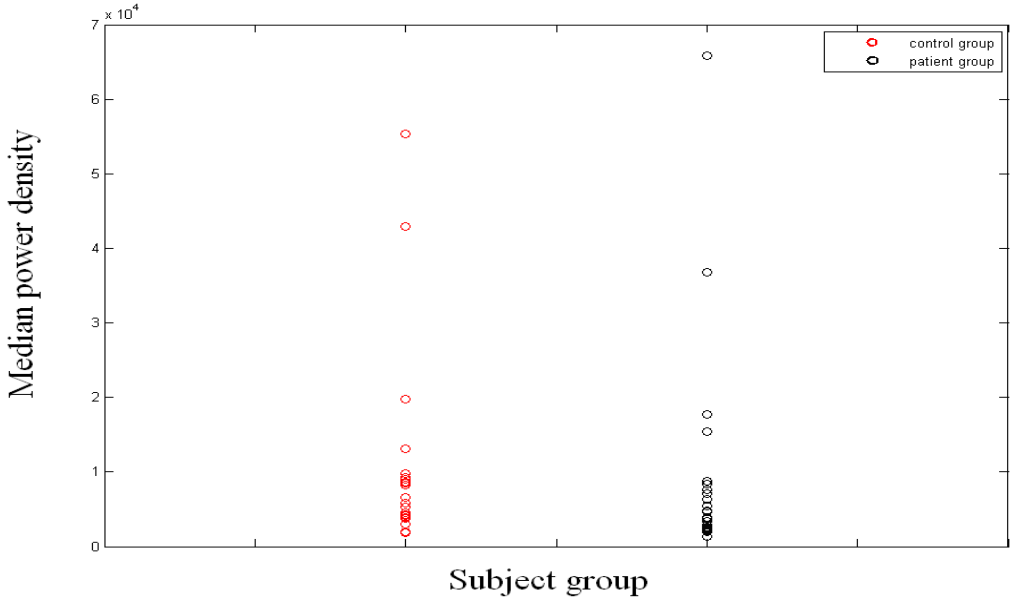

Figure 80 **below knee power densities at myogenic frequencies**

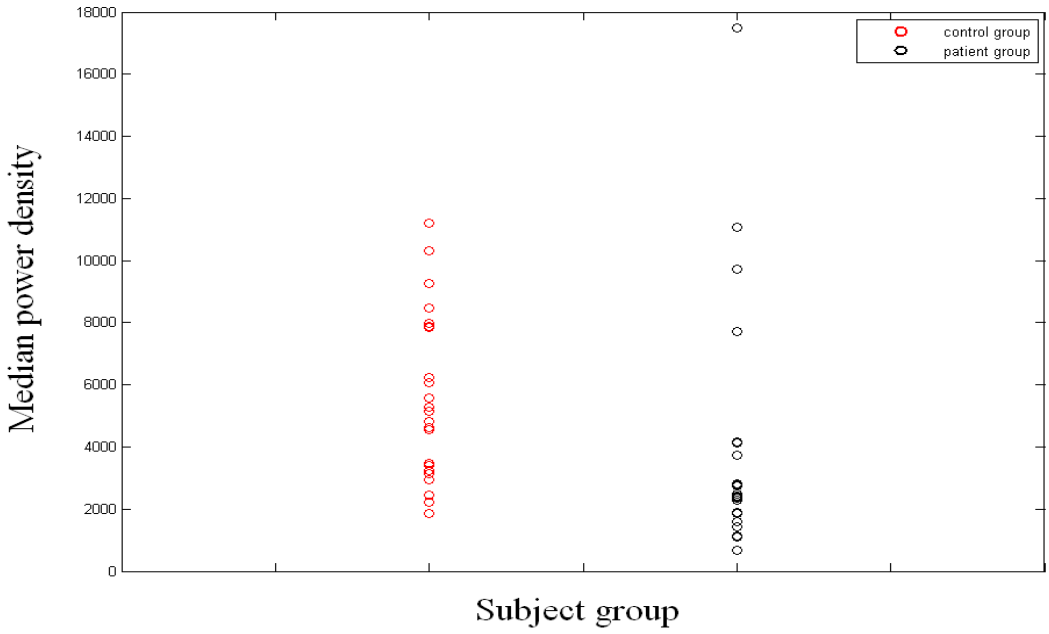

Figure 81 **below knee power densities at respiration frequencies**

7.4.2.2 Power Ratios

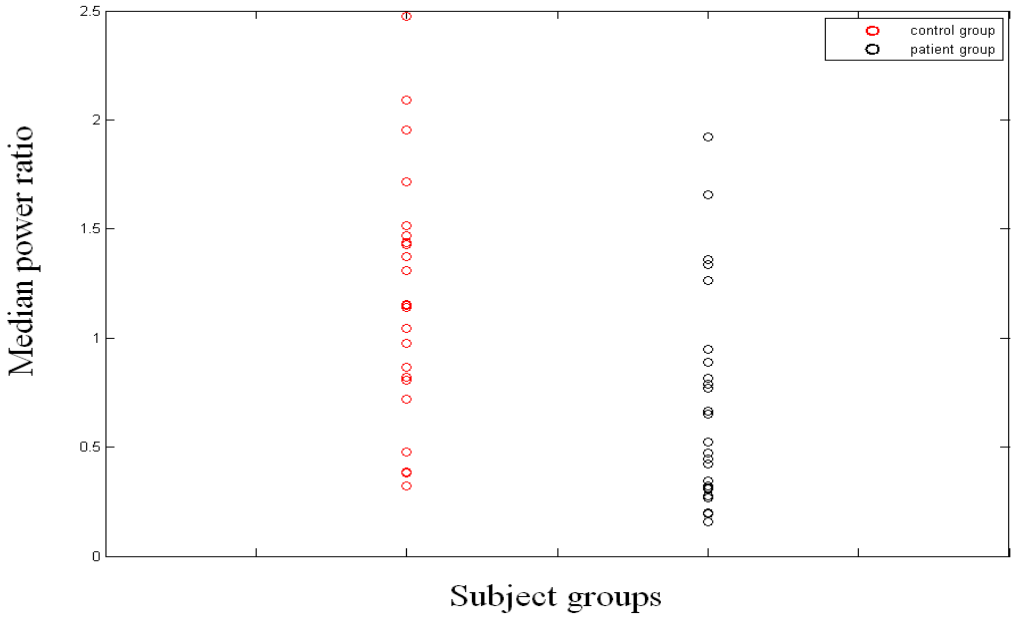

Figure 82 Above knee power ratios between control and patient groups

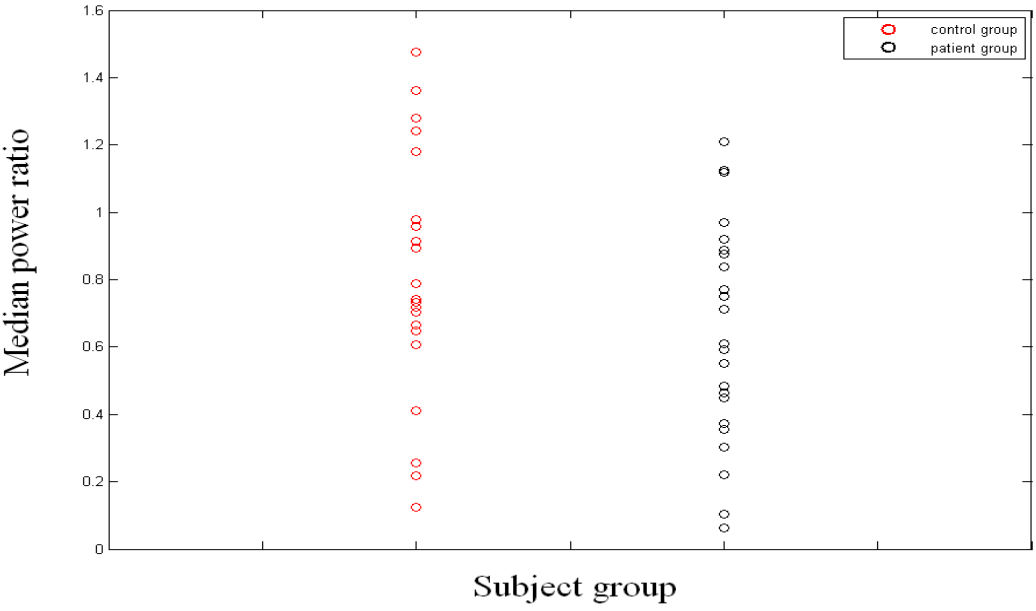

Figure 83 Below knee power ratios between control and patient groups

Figure 82 and Figure 83 show the scattergrams of the above and below knee power ratios for the control and patient groups respectively. The results of the statistical analysis for power density and power ratio analysis can also be seen in Table 17.

	myogenic		respiration		Resp/myo	
	p-value	Null	p-value	Null	p-value	null
Above knee	0.09	0	0.04	1	0.001	1
Below knee	0.1	0	0.002	1	0.16	0

Table 17 Frequency analysis of myogenic and respiration waveforms using power density results between healthy control group and patient group.

There are statistically significant differences between median power density values between control and patient groups at myogenic and respiration frequencies. As can be seen respiration p-values are significant at the 5% level above and below knee. Myogenic p-values are significant at the 10% level. The above knee power density ratio (resp/myo) is statistically significant at the 5% level above knee only.

A summary of the results of the statistical tests can be seen in Table 18 for each venous test parameter chosen. The table shows a yes or no whether the particular test was statistically significant at the 5% level.

Test	Group	Myogenic	Respiration	Resp/myo
Gradient	Control	no	no	n/a
	Patient	yes	no	n/a
	C and P	yes	yes	n/a
Delays	C and P	no	no	n/a
Num of peaks	C and P	no	no	n/a
Phase changes	C and P	yes	no	n/a
Power Density	C and P	no	yes	n/a
Power ratio	C and P	n/a	n/a	yes

C and P- controls and patients;
yes = statistically significant at the 5% level.

Table 18 Summary of the statistical significant results for the different venous parameters chosen

Time base and frequency analysis test results showed some statistically significant differences between the chosen test parameters within and between groups.

Time-base analysis of the signal gradients showed a 5% significant difference of the trailing edge at myogenic frequencies within patients. A significant difference was also demonstrated for the leading and trailing edge gradients between controls and patients, but this was only at respiration frequencies. Only the trailing edge gradient at myogenic frequencies was statistically significant at the 5% level.

The proportion of phase changes between the above and below knee signals at myogenic frequencies demonstrated a statistically significant difference at the 5% level, but not at respiration frequencies.

The results in the frequency domain analysis showed both above and below knee power densities at respiration frequencies to be statistically significant at the 5% level between controls and patient, but not at myogenic frequencies. Also power density ratio showed a strong statistical difference above the knee, but not below.

No significant difference at the 5% level either at myogenic or respiration frequencies was found for the delays in the above and below knee peaks and troughs. Similarly the difference in the number of peaks between above and below knee signals was not significant at myogenic or respiration frequencies.

In the next section the four statistically significant tests will be explored further for diagnostic accuracy. The results with their sensitivity and specificity scores are shown in Table 19.

7.4.3 Venous Diagnostic Accuracy

Since these methods of assessing vascular disease are intending to be used in a primary care setting, sensitivity and specificity scores are more relevant at evaluating the accuracy of the diagnostic test. Therefore, 4 of the tests from Table 18 i.e. gradient, phase changes, power density and power ratio that achieved a statistically significant difference of 5% between normal and patients had scatter plots and associated ROC curves calculated. Therefore sensitivity and specificity scores may be calculated. The scattergrams and ROC curves are shown below and then the sensitivity and specificity scores are shown in Table 19.

7.4.3.1 Gradient

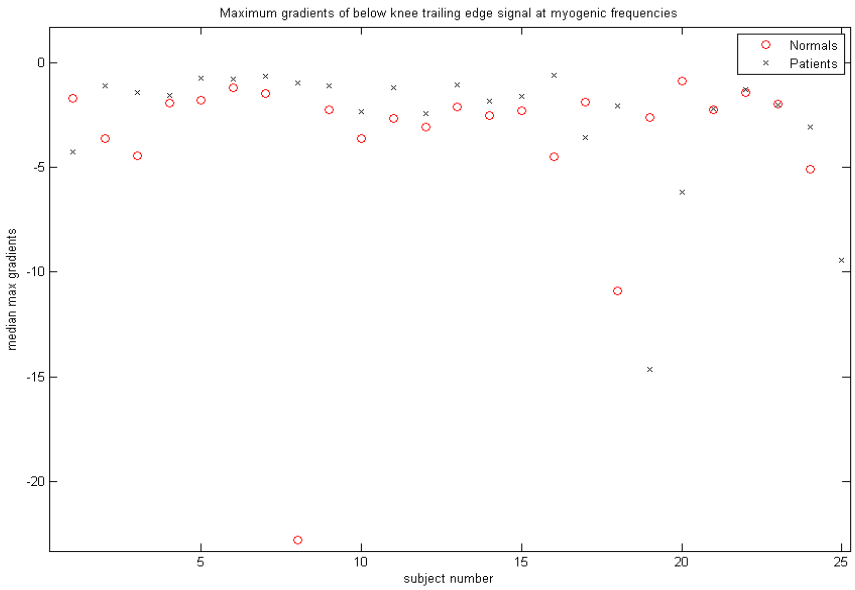

Figure 84 Scattergram of trailing edge gradient below knee at myogenic frequencies

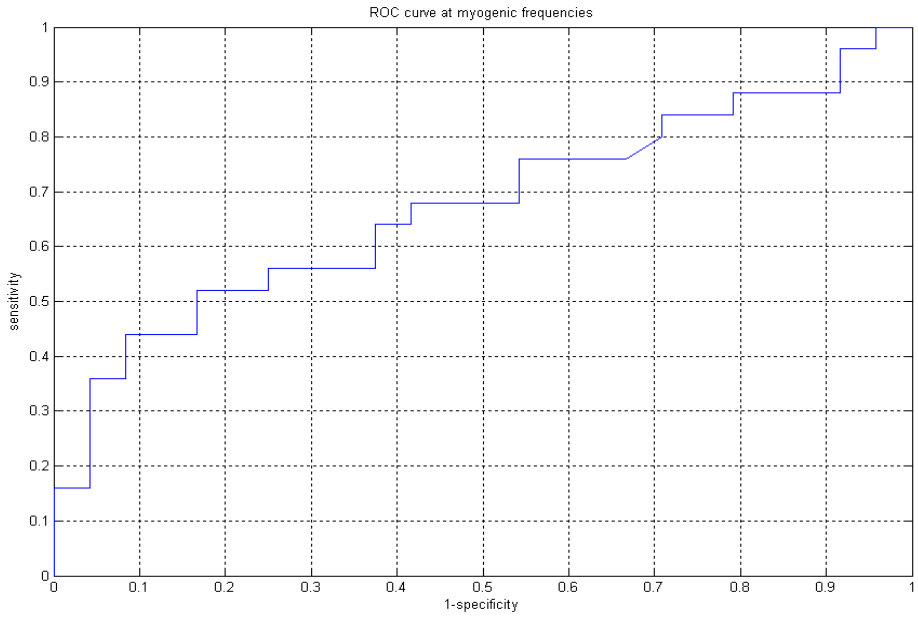

Figure 85 ROC curve of trailing edge gradient below knee at myogenic frequencies

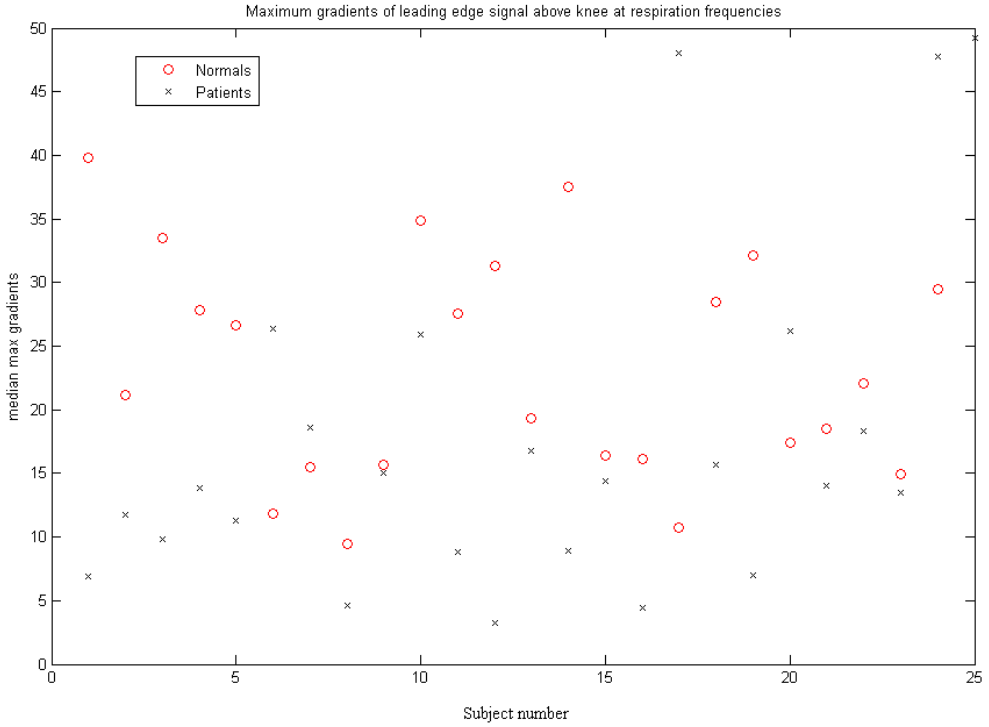

Figure 86 Scattergram of above knee leading edge gradient at respiration frequencies

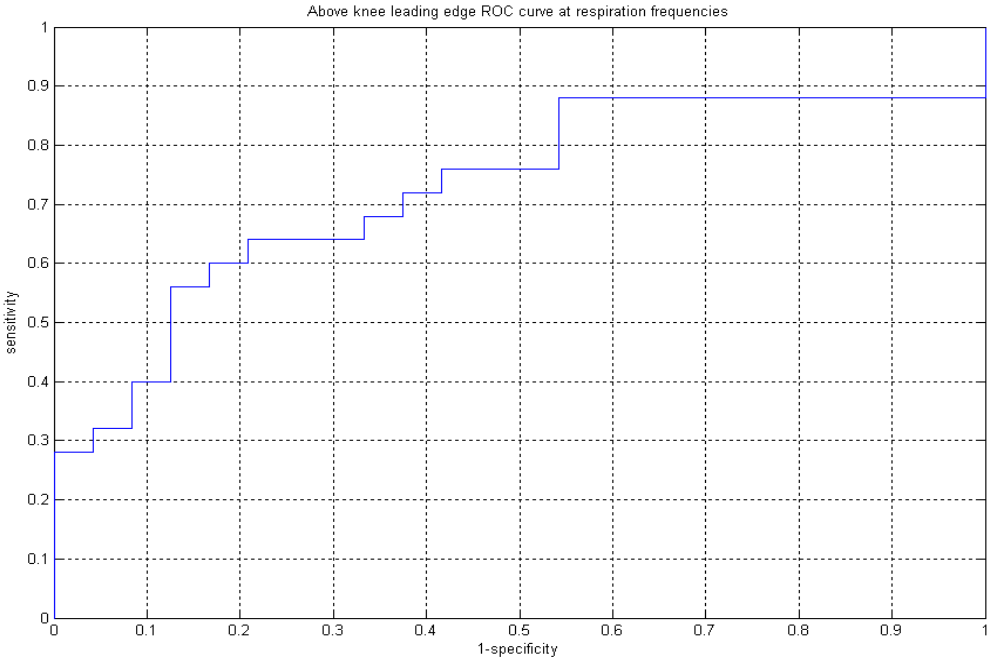

Figure 87 ROC curve of above knee leading edge gradient at respiration frequencies

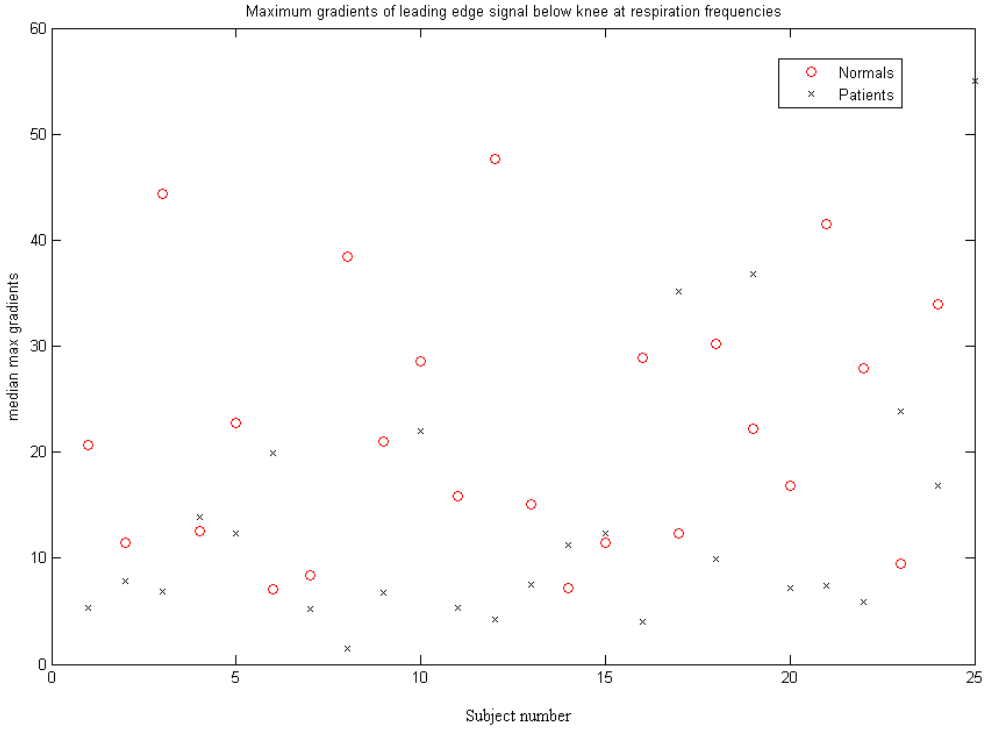

Figure 88 Scattergram of below knee leading edge gradient at respiration frequencies

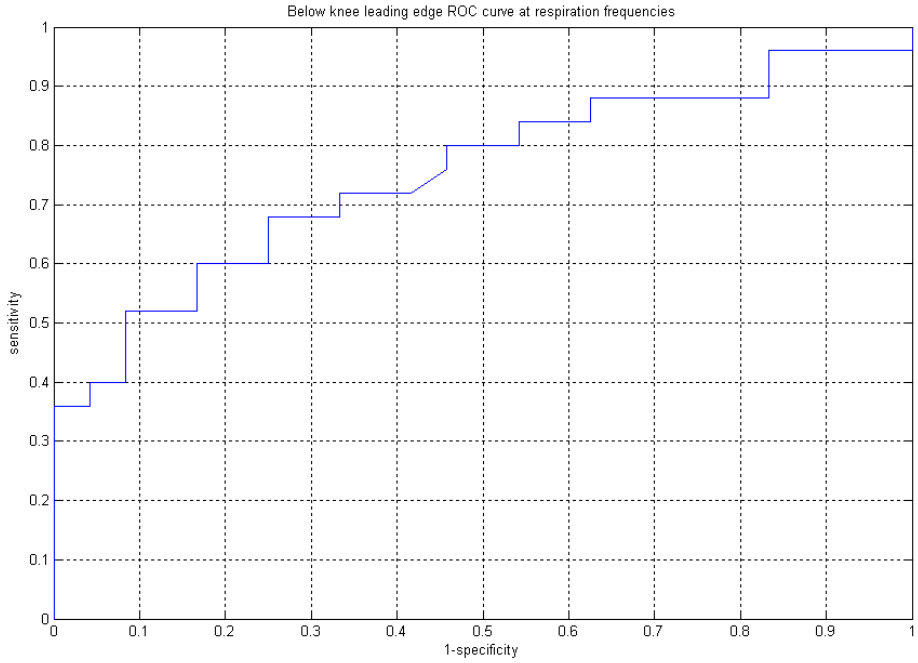

Figure 89 ROC curve of below knee leading edge gradient at respiration frequencies

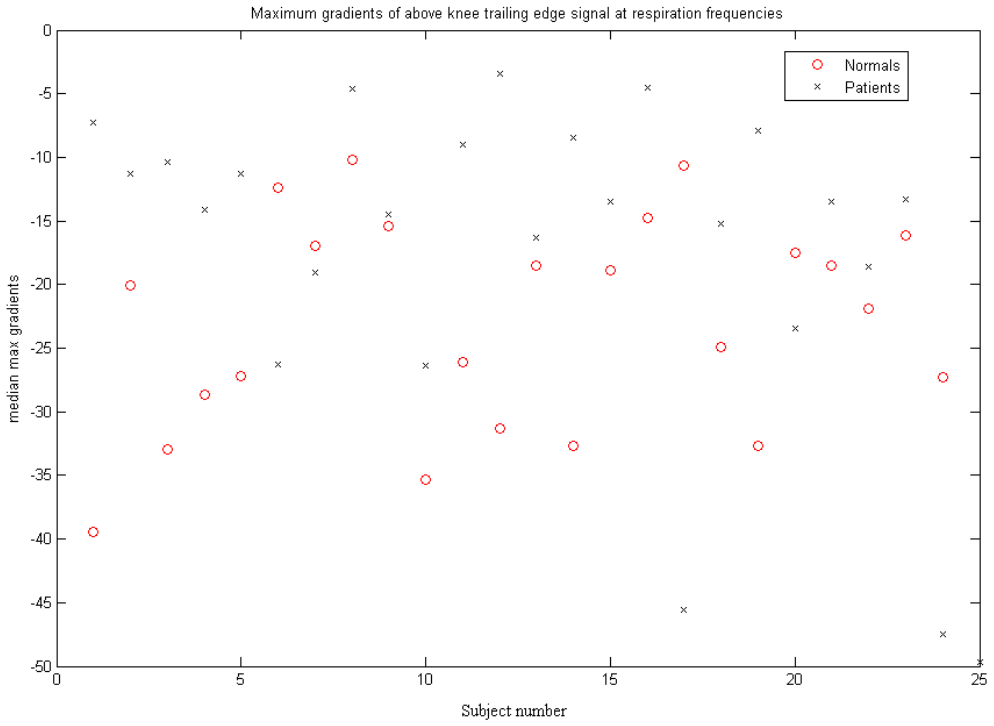

Figure 90 Scattergram of trailing edge above knee gradient at respiration frequencies

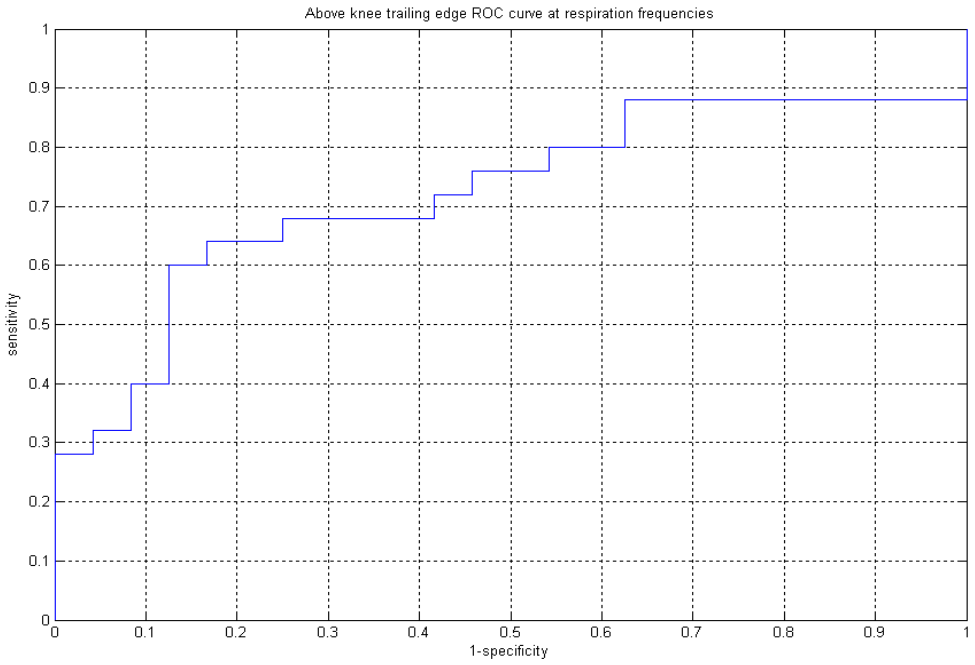

Figure 91 ROC curve of trailing edge above knee gradient at respiration frequencies

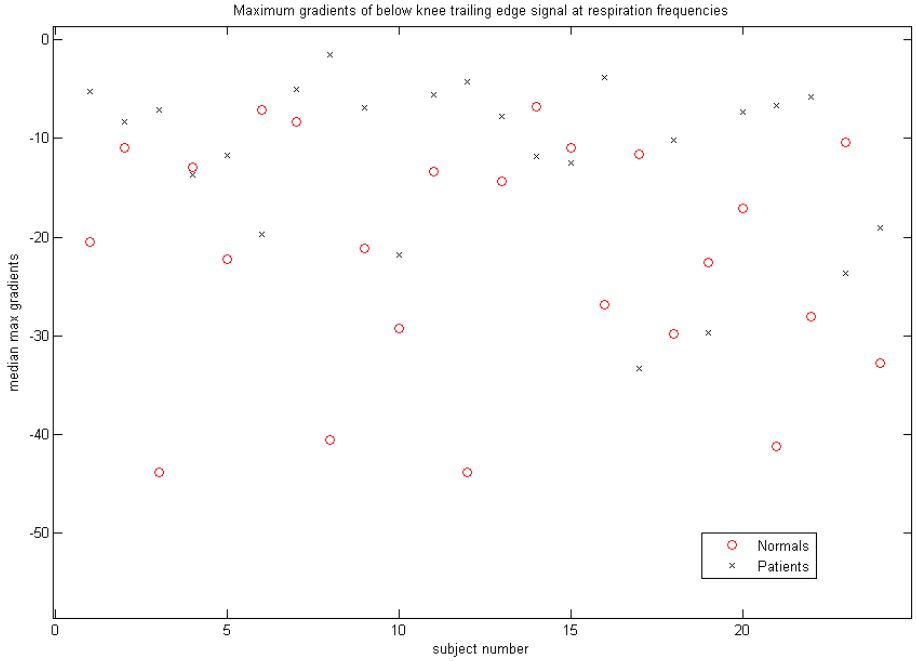

Figure 92 Scattergram below knee trailing edge gradient at respiration frequencies

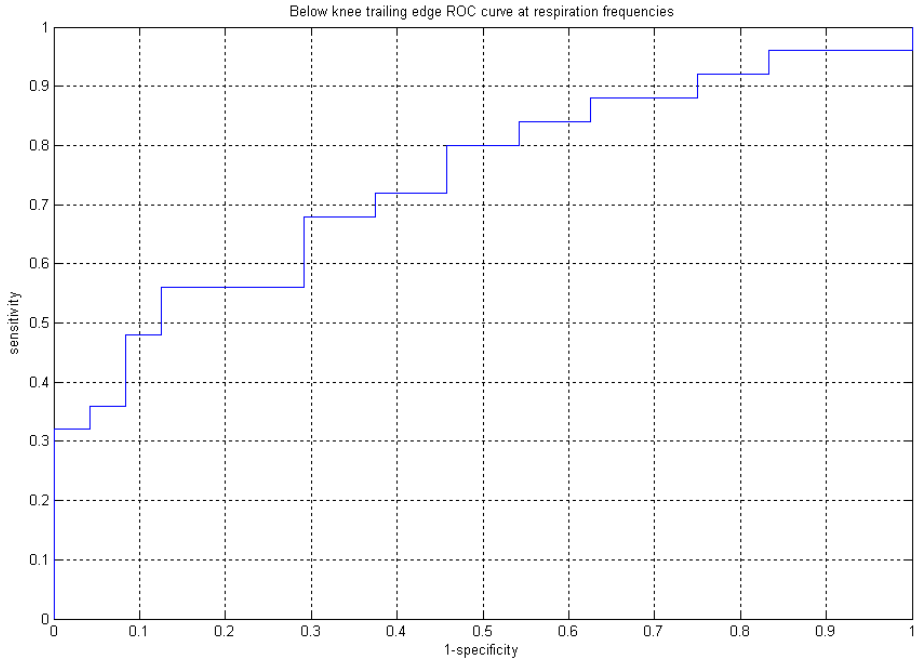

Figure 93 ROC curve below knee trailing edge gradient at respiration frequencies

7.4.3.2 Phase Changes

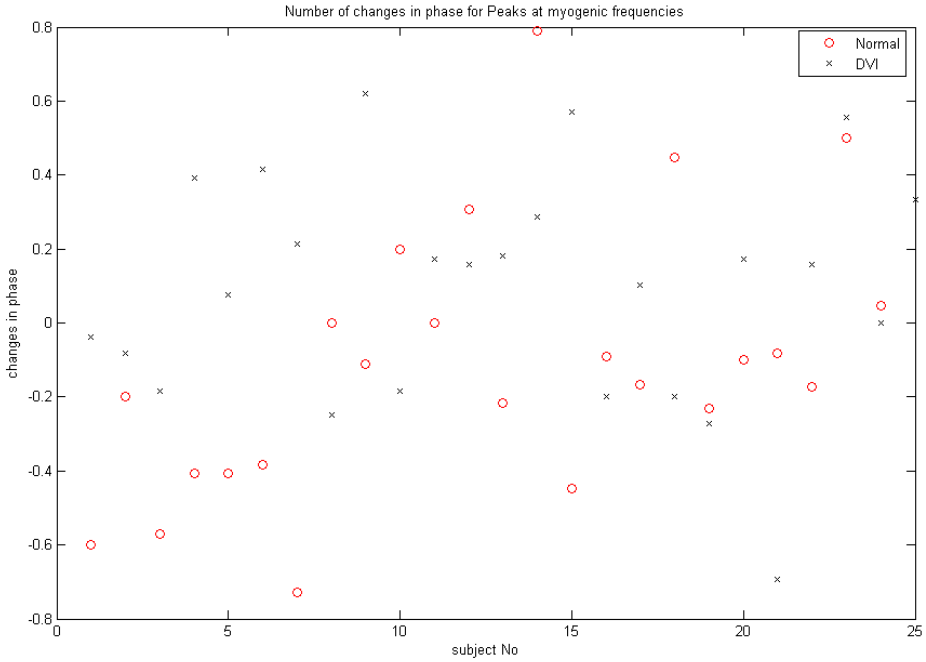

Figure 94 Scattergram of peak phase changes at myogenic frequencies

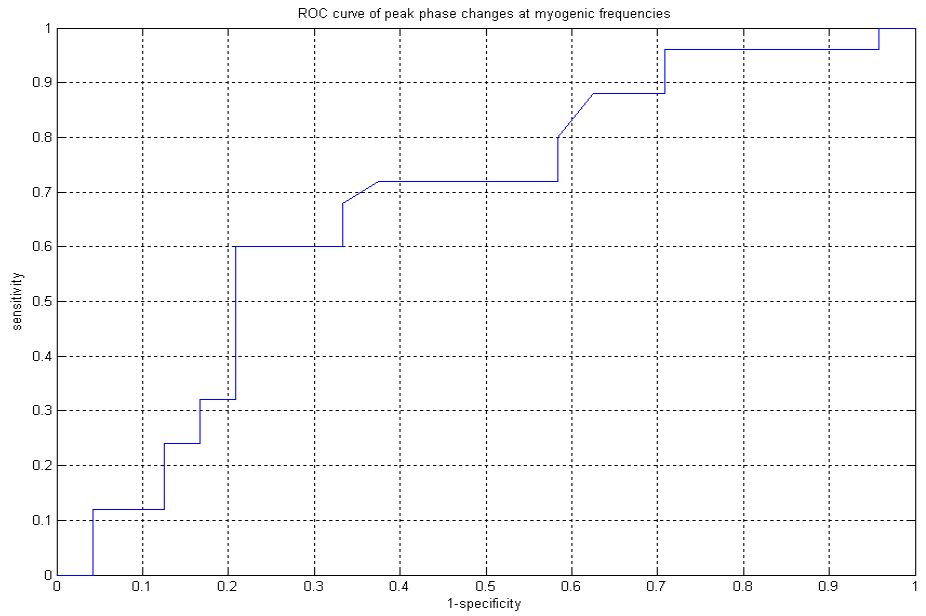

Figure 95 ROC curve of peak phase changes at myogenic frequencies

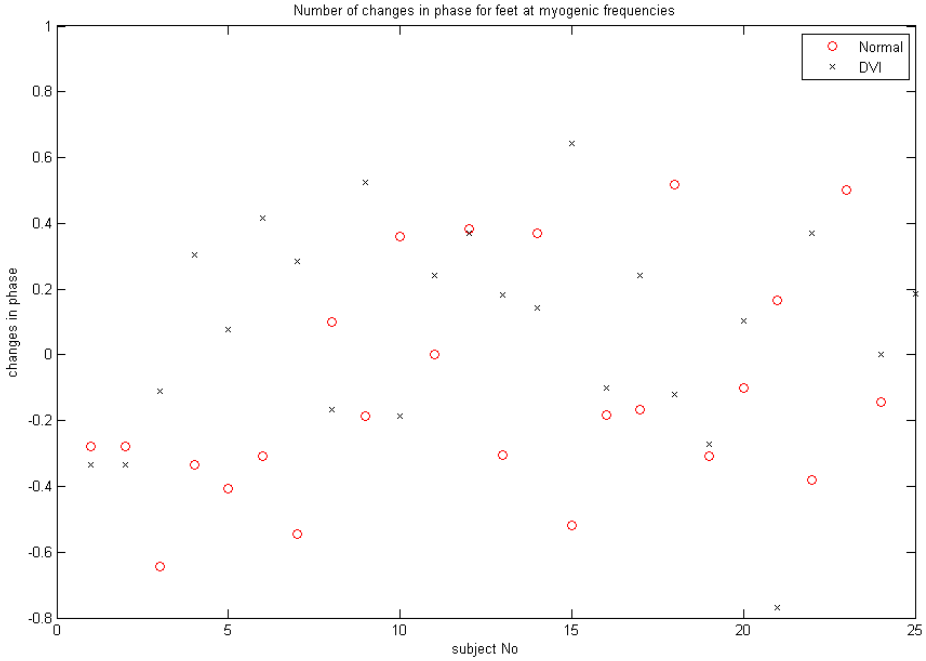

Figure 96 Scattergram of troughs phase changes at myogenic frequencies

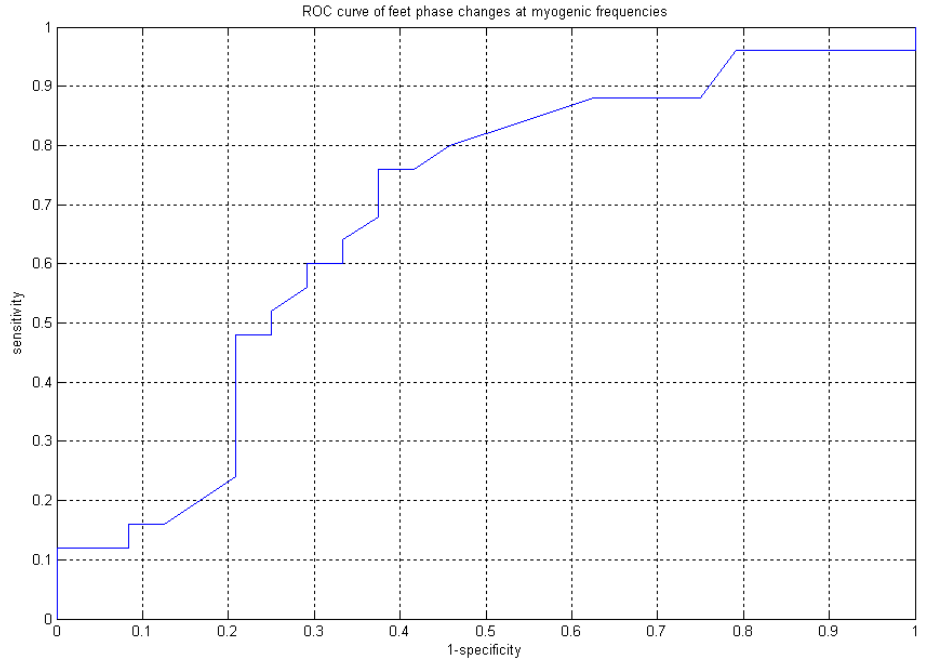

Figure 97 ROC curve of troughs phase changes at myogenic frequencies

7.4.3.3 Power Density

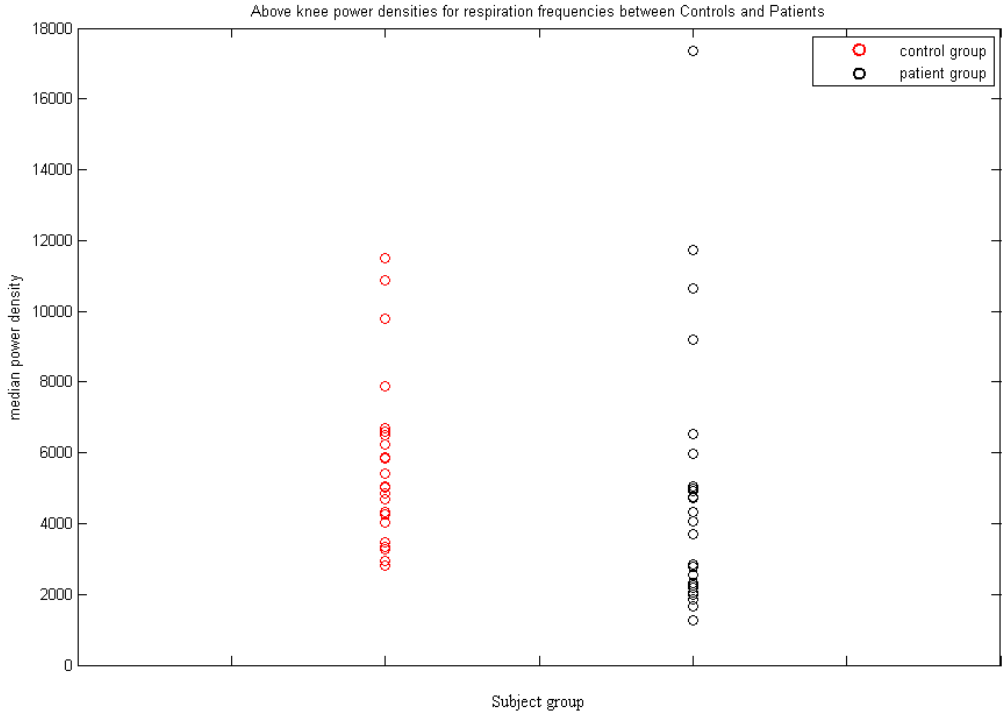

Figure 98 Scattergram of power density above knee at respiration frequencies

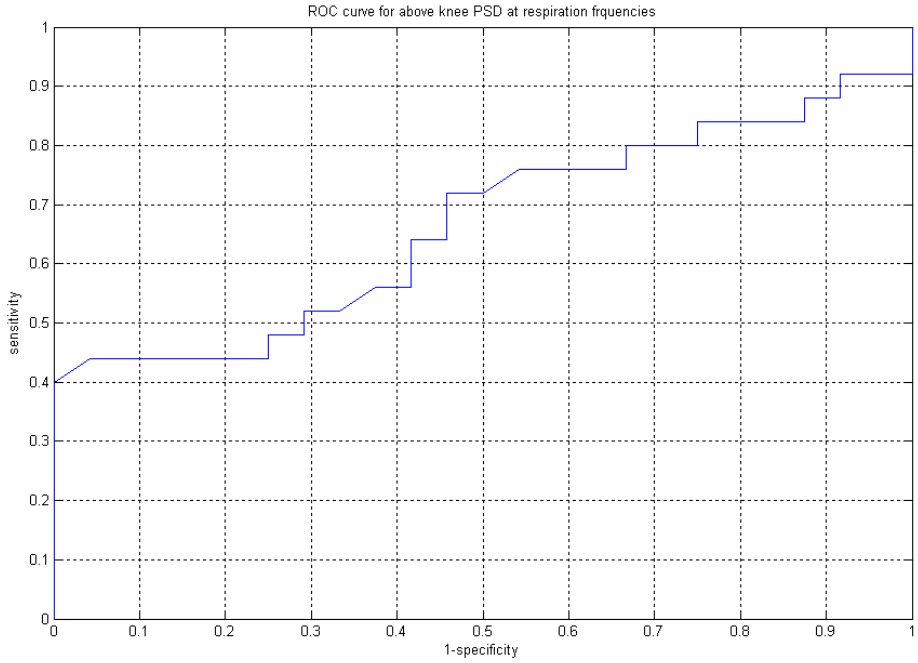

Figure 99 ROC curve of power density above knee at respiration frequencies

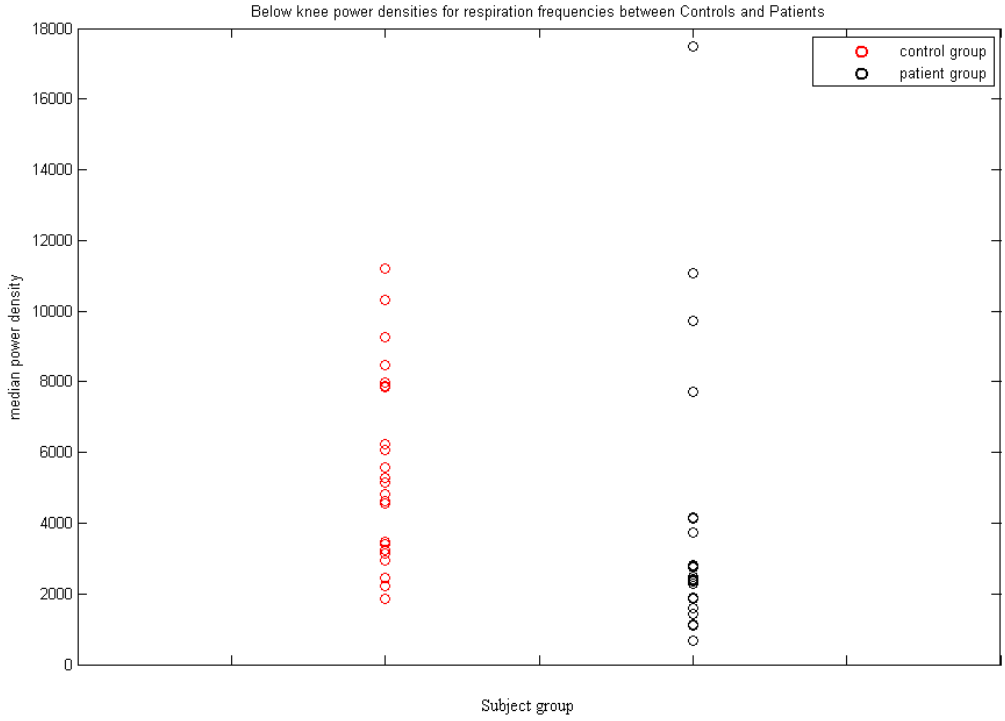

Figure 100 Scattergram of power density below knee at respiration frequencies

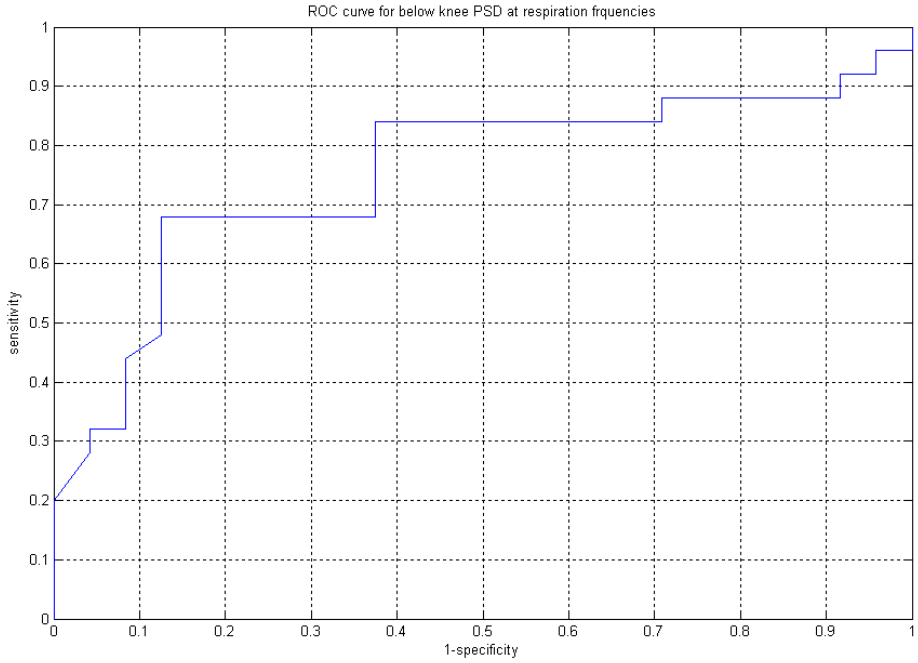

Figure 101 ROC curve of power density below knee at respiration frequencies

7.4.3.4 Power ratio

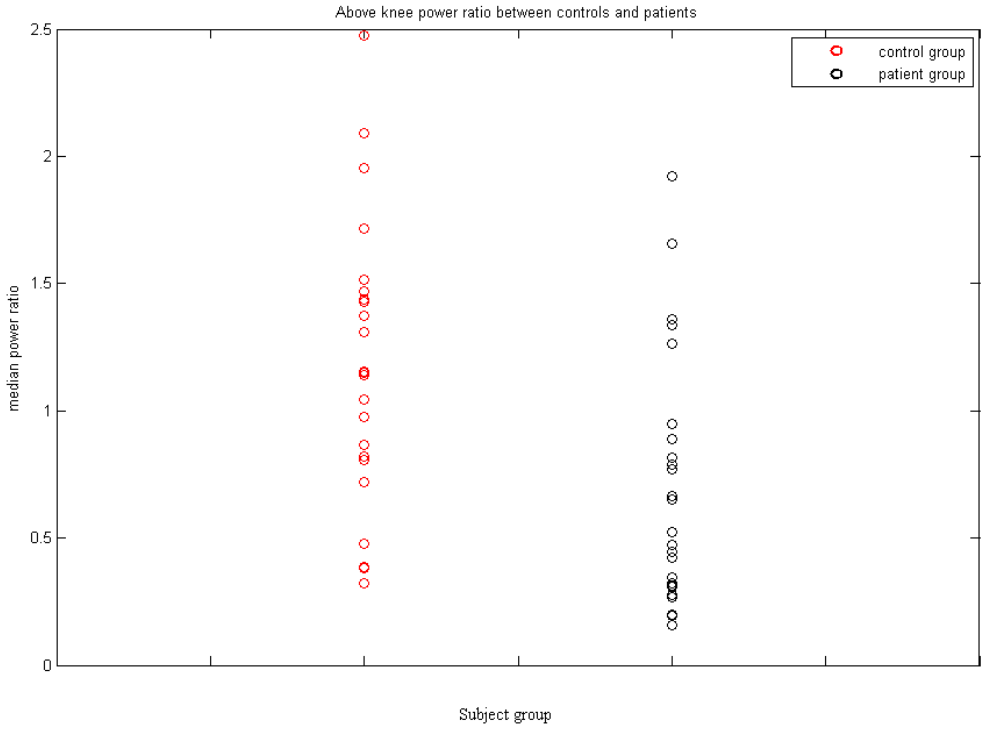

Figure 102 Scattergram of above knee power ratio

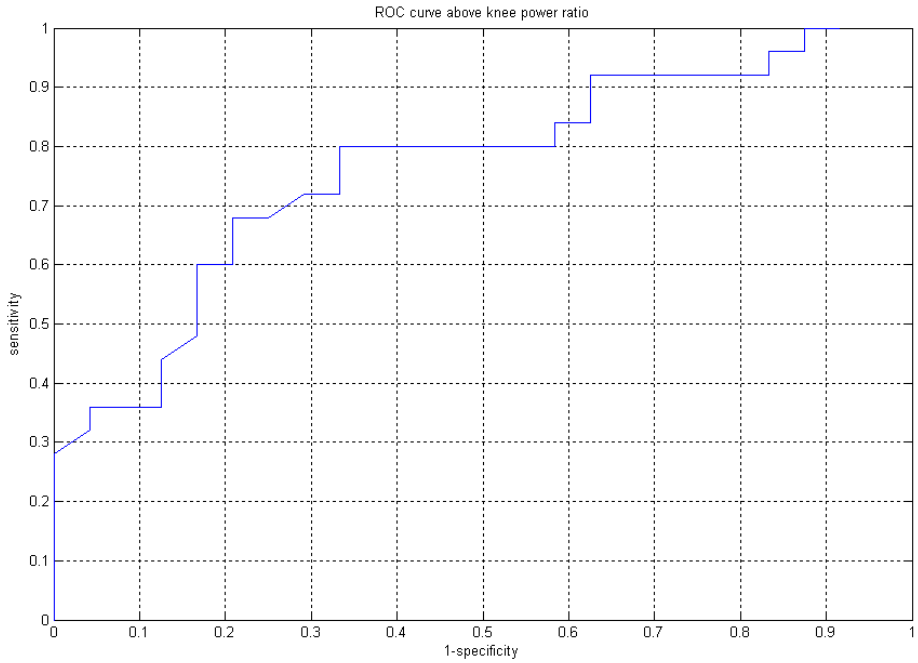

Figure 103 ROC curve of above knee power ratio

A summary of the sensitivity and specificity results for each of the statistically significant tests is shown in Table 19.

Test	Sens(%)	spec(%)	Parameter	freq
Gradient	51	80	TE BK	myogenic
	60	80	LE AK	respiration
	60	80	LE BK	respiration
	64	80	TE AK	respiration
	56	80	TE BK	respiration
Phase Changes	32	80	Peak	myogenic
	22	80	Trough	myogenic
Power Density	44	80	AK	respiration
	69	80	BK	respiration
Power ratio	60	80	AK	Resp/myo

TE-trailing edge, LE-leading edge, AK- above knee, BK-below knee

Table 19 Sensitivity and specificity scores of the 4 venous tests

Ideally a screening tool would have an accuracy of 100%, but in reality vascular screening tools, such as ABPI have sensitivities within 80% to 100%. One of the aims of the venous insufficiency test is to reduce the number of false positive scans being referred from primary care centres. Consequently a screening test with a high specificity is required. Therefore to ensure a fair comparison was made between the four different venous tests, a specificity of 80% was selected from the ROC curves and the equivalent sensitivity was then recorded as shown in Table 19. The table shows a range of sensitivities between 22%, when the phase of the pulse trough between above and below knee signals is used as a test at myogenic

frequencies and 69% when the power density of the below knee signal is used at respiration frequencies.

7.5 Venous Summary and Discussion

Five parameters of the venous PPG signal were investigated: the gradient of the leading and trailing edges of the signal, the delays between the above and below knee signal, the difference in the number of peaks above and below knee, the phase changes between the above and below knee signals and the power in the signal. Since these five parameters were analysed at myogenic and respiration frequencies and from behind the knee and also at ankle level, this produced 28 separate tests. Statistical tests were performed on all 28 tests and statistically significant differences were found between the control and patient groups for 10 of the 28 tests investigated.

These 10 tests were investigated further as a potential screening test for CVI. To test their accuracy, sensitivity and specificity scores were calculated. From this, the worst performing parameter was phase changes between the above and below knee signals which had a sensitivity and specificity scores of 22% and 80% respectively. The best performing parameter was the power density in the signal at ankle level at respiratory frequencies, with sensitivity and specificity scores of 69% and 80% respectively.

Other studies that investigated the effect of vasomotion in patients with CVI were Cheatle et al (1991); Chittenden et al (1992); Hafner et al (2009) Heising et al (2009). The two former studies both investigated laser Doppler flux (LDF) changes in amplitude and frequency at ankle level while patients were supine. They found that LDF was significantly higher in CVI patients than compared to normal healthy volunteers. As in this study patients remained

motionless throughout the experiment. However Chittenden et al (1992) used an electrophoresis technique to investigate the effect of increased temperature on vasomotive frequencies in normal skin and Cheatle et al (1991) raised the local skin temperature to 43 degrees centigrade and found that vasomotion frequency increased in controls but not in CVI patients.

Hafner et al (2009); Heising et al (2009) investigated differences in vasomotor activity between healthy and patients with CVI by analysing the LDF activity in myogenic, respiratory and cardiac bands. They found statistically significant differences in peak energy at all three frequency bands. This thesis also investigated myogenic and respiratory frequency bands in patients with CVI and found power density levels to be significantly different from healthy controls only at respiratory frequencies at both ankle and knee level. The author is unaware of any other studies that have investigated simultaneous measurement of vasomotive activity in patients with CVI at knee and ankle level. Additionally, investigating the shape of the venous signal also appears to be an innovative idea, particularly analysing the potentially difference in pulse shape parameters between the ankle and knee level venous signals at myogenic and respiratory frequencies.

8 Summary and Discussion

The final chapter of this thesis restates the research objectives and the remaining sections summarise the results and discuss their implications.

The initial objective was to identify optical and other methods of evaluating arterial and venous insufficiency. The methods kept four main key points in mind:

1) minimal operator effort
2) minimal patient effort
3) minimal cost
4) Minimal testing time

Optical and other techniques were investigated to determine the best method, in accordance with the key points above, for assessing peripheral vascular insufficiency. This was achieved by undertaking a literature search, and the results suggested that the best technical method for investigating arterial and venous insufficiency was optical technology. This addressed the cost objective, as simple optical devices are such as PPG are relatively cheap to purchase for a primary care centre. Currently however, the methods used to investigate vascular insufficiency, in particular venous insufficiency using optical technology, rely on patient movement or the use of cuffs and tourniquets to separate patients with vascular insufficiency from healthy controls. From the literature search, spectral and pulse shape analysis techniques were identified as potential methods of investigating vascular disease and reducing patient and operator effort, which were of primary concern.

These analysis techniques were then investigated further by comparing duplex ultrasound, used as the gold standard for identifying arterial and venous insufficiency with PPG measurements taken from various sites on the lower limbs. It was anticipated that the waveforms detected from these measurements would be altered in the presence of peripheral vascular disease

The drawback with current arterial and venous insufficiency testing methods such as duplex ultrasonography, ankle brachial pressure index (ABPI), arterial photoplethysmography (APPG), and venous plethysmography (VPPG) as screening tools is they all too some extent or other require: significant patient or operator effort, a relatively long testing time, or the purchase cost of the equipment is relatively expensive. The development of a screening tool that reduces these drawbacks, and informs the primary care clinician simply whether vascular disease is present or not would be of great benefit to the primary care centre.

Existing vascular tests aim to inform the clinician of the location, extent and severity of vascular disease present. This is the main diagnostic goal if a comprehensive picture of the patient's vascular condition is needed, but it is not necessarily required at the initial stages of the GP's clinical evaluation. The primary goal of a screening tool at this stage would be to indicate if the patient's signs and symptoms are vascular in nature. Further investigation of location, extent and severity of vascular disease can be performed more accurately in a specialist vascular clinic or by duplex ultrasound in hospital. Therefore the goal of this thesis is to supplement the GP's clinical assessment of a patient with potential vascular insufficiency and thereby giving the clinician more confidence in sending the patient for further appropriate clinical investigations.

Extensive research has been conducted into new techniques at analysing patient blood flow data and into new methods of screening patients for arterial and venous insufficiency, but as yet no one technique has become routine, or replaced the current testing methods in the primary care setting. If any screening technique is to replace or be comparable with an existing method, then either its accuracy should be as good as, if not better than the current system, or, if the decrease in accuracy of the new technique is acceptable, then it should be quicker and easier to use.

The methods used in this thesis for detecting arterial insufficiency do not rely on the application of ECG leads or on the use of cuffs. This study also included patients with diabetes which other studies have excluded, but make up a significant proportion of the vascular insufficiency population. Additionally, the use of duplex ultrasound in this study as a gold standard for the detection of arterial insufficiency, has allowed a more moderate group of patients to be analysed with PPG than has been accomplished previously, therefore potentially allowing for earlier identification of arterial disease. This technique also significantly reduces the signal acquisition time; previous methods have signal acquisition times of 2.5 minutes. In this study signals were acquired in 10 seconds with minimal reduction in sensitivity and specificity.

The objectives of the venous methodology primarily followed those of the arterial methods i.e. the use of a technology and methods that reduced: purchase cost, patient and operator effort and testing time. Spectral and time base analysis techniques were identified from the literature search as potential techniques for investigating CVI. The analysis determined 10 statistically significant test results. Subsequently sensitivity and specificity scores were

calculated for the 10 test identified and below knee power density at respiration frequencies had the highest score.

In its present form the arterial testing procedure takes 10 seconds to complete, with the patient supine and two probes placed on the index finger and toe, while the venous test requires 6 minutes to complete with the patient sitting and two probes placed behind the knee and at ankle level. This is not ideal for a single screening test as repositioning the sensors and patient between tests is not only inconvenient for patient and operator, but moving the patient between tests will affect vasomotive and sympathetic frequencies and require a further delay between tests. Therefore a test where the patient and probes remain in the same position between tests would be ideal. In addition, it would be advantages if the venous testing time could be reduced. A reduction in testing time of 1 minute could be feasible, as even at the lowest end of the bandwidth of respiration frequencies of 0.15Hz, there would still be approximately 9 respiration pulses to analyse. Further more the detection of acute deep vein thrombosis has intentionally not been included in this study. Additional work could include acute as well as chronic venous insufficiency, making these methods more comprehensive in their detection of vascular disease.

This thesis has identified a technology that is cost effective for a primary care centre to purchase as a screening tool for patients with vascular insufficiency. It has also identified techniques that can be used with this technology that requires minimal operator and patient effort. In doing so it has significantly reduced the testing time to identify patients with arterial insufficiency, with diagnostic accuracies only marginally lower than current testing methods. The test also has other advantages such as it does not require the application of ECG leads or pneumatic cuffs and could potentially aid the clinician in diagnosing patients with arterial

insufficiency at an earlier stage than other testing methods. A venous test has also been produced that can identify patients with CVI, with sensitivities and specificities of 69% and 80% respectively, that also does not require tourniquets or pneumatic cuffs or requires the patient to perform any physical task. Although not a comprehensive diagnostic tool, the optical technology used and the methods applied using this technology described in this thesis are a step forward to a usable clinical diagnostic vascular tool for use in a primary care setting.

9 References

Abbott G T, Diggory R T, and Harris I (1995) Comparison of Light Reflection Rheography with Ascending Venography in the Diagnosis of Lower Limb Deep Venous Thrombosis. British Journal of Radiology 68: 593-595.

Abramowitz H B, Flinn W R, and Bergan J J (1979) The Use of Photoplethysmography in the Assessment of Venous Insufficiency: A Comparison to Venous Pressure Measurements. Surgery 86: 434-441.

Allen J (2007) Photoplethysmography and its application in clinical physiological measurement. Physiological Measurement 28: 1-39.

Allen J, and Murray A (1993) Development of a Neural Network Screening Aid for Diagnosing Lower Limb Peripheral Vascular Disease from Photoelectric Plethysmography Pulse Waveforms. Physiological Measurement 14: 13-22.

Allen J, and Murray A (1995) Prospective Assessment of an Artificial Neural Network for the Detection of Peripheral Vascular Disease from Lower Limb Pulse Waveforms. . Physiological Measurement 16: 29-38.

Allen J, and Murray A (1999) Modelling the relationship between peripheral blood pressure and blood volume pulses using linear and neural network system identification techniques. Physiological Measurement 20: 287-301.

Allen J, and Murray A (2000a) Similarity in bilateral photoplethysmographic peripheral pulse wave characteristics at the ears, thumbs and toes. Physiological Measurement 21: 369-377.

Allen J, and Murray A (2000b) Variability of photoplethysmography peripheral pulse measurments at the ears, thumbs and toes. Institute of Electrical Engineers Procedings-Science Measurement and Technology 147: 403-407.

Allen J, and Murray A (2002) Age-related changes in peripheral pulse timing characteristics at the ears, fingers and toes. Journal of Human Hypertension 16: 711-717.

Allen J, and Murray A (2003) Age-related changes in the characteristics of the photoplethysmographic pulse shape at various body sites. Physiological Measurement 24: 297-307.

Allen J, Oates C P, Henderson J, Jago J, Whittingham T A, Chamberlain J, Jones N A G et al. (1996) Comparison of lower limb arterial assessments using colour-duple ultrasound and ankle/brachial pressure index measurements. Angiology 47: 225-231.

Allen J, Oates C P, Lees T A, and Murray A (2005) Photoplethysmography detection of lower limb peripheral arterial occlusive disease: a comparison of pulse timing, amplitude and shape characteristics. Physiological Measurement 26: 811-821.

Alnaeb M E, Crabtree V P, Boutin A, Mikhailidis D P, Seifalian A M, and Hamilton G (2007) Prospective Assessment of Lower Extremity Peripheral Arterial Disease in Diabetic Patients Using a Novel Automated Device. Angiology 58: 579-585.

Avolio A (2002) The Finger Volume Pulse and Assessment of Arterial Properties. Journal of Hypertension 20: 2341-2343.

Balthazar W F (1866) On the Use of the Sphygmograph in the Investigation of Disease. British Medical Journal: 275-278.

Barber R F, and Shatara F L (1925) The varicose disease. New York State Journal of Medicine 31: 574.

Baumbach P (1986) Understanding Transcutaneous pO_2 and pCO_2 measurements. (1^{st} edn) : Radiometer Copenhagen. pp.1-54.

Baxter G M, and Polak J F (1992) Lower Limb Colour Flow Imaging: A Comparison with Ankle Brachial Measurements and Angiography. Clinical Radiology 47: 91-95.

Bergan J J [ed.] (2006) The Vein Book. (1st edn.) London: Elsevier.

Bernardi E, and Prandoni P (2000) The Post-thrombotic Syndrome. Current Opinions in Pulmonary Medicine 6: 335-342.

Bernardi L, Radaelli A, Solda P L, Coats A J, Reeder M, Calciati A, Garrard C S et al. (1996) Autonomic control of skin microvessels: assessment by power spectrum of photoplethysmographic waves. Clinical Science 90: 345-355.

Bernstein E F [ed.] (1985) Non-invasive Diagnostic Techniques in Vascular Disease. (3rd edn.) Missouri: Mosby.

Blazek V, and Schultz-Ehrenburg U (1996) Quantitive Photoplethysmography. First edition ed. Dusseldorf: VDI Verlag.

Boggett D, Blond J, and Rolfe P (1985) Laser Doppler Measurements of Blood Flow in Skin Tissue. Journal of Biomedical Engineering 7: 225-232.

Bortolotto L A, Blacher J, Kondo T, Takazawa K, and Safar M E (2000) Assessment of Vascular Aging and Atherosclerosis in Hypertensive Subjects: Second Derivative of Photoplethysmogram Versus Pulse Wave Velocity. American Journal of Hypertension 13: 165-171.

Browse N L, Burnand K G, Irvine A T, and Wilson N M. (1999) Investigations of Venous Function. Diseases of the Veins. London : Arnold.

Burton A C (1939) The range and variability of the blood flow in the human fingers and the vasomotor regulation of body temperature. American Heart Journal 127: (3) 437-453.

Burton A C (1965) Physiology and Biophysics of the circulation. Chicago: Year Book Medical Publishers Incorporated.

Callejas J M, and Manasanch J (2004) Epidemiology of chronic venous insufficiency of the lower limbs in the primary care setting. International Angiology 23: 154-163.

Carter S A, and Tate R B (1996) Value of Toe Pulse Waves in Addition to Systolic Pressure in the Assessment of the Severity of Peripheral Arterial Disease and Critical Limb Ischemia. Journal of Vascular Surgery 24: 258-265.

Carter S A, and Tate R B (2001) The value of toe pulse waves in determination of risks for limb amputation and death in patients with peripheral arterial disease and skin ulcers or gangrene. Journal of Vascular Surgery 33: 708-714.

Challoner A V J, and Ramsay C A (1973) A Photoelectric Plethysmography for the measurement of Cutaneous Blood Flow. Physics in Medicine and Biology 19: 317-328.

Cheatle T R, Shami S K, Stibe E, Coleridge Smith P D, and Scurr J H (1991) Vasomotion in venous disease. Journal of the Royal Society of Medicine 84: 261-263.

Chittenden S J, Shami S K, Cheatle T R, Scurr J H, and Coleridge Smith P D (1992) Vasomotion in the leg skin of patients with chronic venous insufficiency. Vasa 21: 138-142.

Chowienczyk P J, Kelly R P, MacCallum H, Millasseau S C, Andersson T L G, Gosling R G, Ritter J M et al. (1999) Photoplethysmographic assessment of pulse wave reflection: blunted response to endothelium-dependent beta2-adrenergic vasodilation in type two diabetes mellitus. Journal of the American College of Cardiology 34: 2007-2014.

Criqui M H, Fronek A, Klauber M R, Barrett-Connor E, and Gabriel S (1985) The sensitivity, specificity and predictive value of traditional clinical evaluation of peripheral arterial disease: results from non-invasive testing in a defined population. Circulation 71: 516-522.

Criqui M H, Jamosmos M, Fronek A, Denenberg J O, Langer R D, Bergan J J, and Golomb B A (2003) Chronic Venous Disease in an Ethically Diverse Population. The San Diego Population Study. American Journal of Epidemiology 158: 448-456.

Cummins H Z, and Yeh Y (1964) Observation of Diffuse broadening of Rayleigh Scattered Light. Physical reveiw letters 12: 150-153.

D'Agrosa L S, and Hertzman A B (1967) Opacity Pulse of individual minute arteries. Journal of Applied Physiology 23: 613-620.

Dachun X, Jue L, Liling Z, Yawei X, Dayi H, Sherry L P, and Yunsheng M (2010) Sensitivity and specificity of the ankle-brachial index to diagnose peripheral arterial disease: a structured review. Vascular Medicine 15: 361-369.

Doobay A V, and Anand S S (2005) Sensitivity and Specificity of the Ankle-Brachial Index to Predict Future Cardiovascular Outcomes: A Systematic Review. Arteriosclerosis, Thrombosis, and Vascular Biology 25: 1463-1469.

Dorlas J C, and Nijboer J A (1985) PPG as a monitoring device in anaesthesia. British Journal of Anaesthesia 57: 524-530.

Erts R, Spigulis J, Kukulis I, and Ozols M (2005) Bilateral photoplethysmography studies of the leg arterial stenosis. Physiol Meas 26: 865-874.

Evans C J, Allan P L, Lee A J, Bradbury A W, Ruckley C V, and Fowkes F G R (1998) Prevalence of venous reflux in the general population on duplex scanning: The Edinburgh Vein Study. Journal of Vascular Surgery 28: 767-776.

Fowkes F G (1988) The measurement of atherosclerotic peripheral arterial disease in epidemiological surveys. International Journal of Epidemiology 17: 248-254.

Fowkes F G R (2004) Peripheral Vascular Disease. Chicago: Springer-Verlag.

Fronek A, Minn C, and Kim R (2000) Venous outflow and inflow resistance in health and venous disease.[erratum appears in J Vasc Surg 2001 Jan;33(1):208]. Journal of Vascular Surgery 31: 472-476.

Goetz R H (1945) The Rate and Control of the Blood Flow Through the Skin of the Lower Extremities. American Heart Journal: 146-182.

Hafner H M, Brauer K, Radke C, and Strolin A (2009) Non-Linear Analysis of Skin Blood Flow in Patients Suffering from Chronic Venous Leg Ulcers. Phlebology 38: 64-70.

Hall A C G J E (2005) Textbook of Medical Physiology. (11 edn). Portland: Saunders/Elsevier.

Harada R N, Katz M L, and Comerota A (1995) A noninvasive screening test to detect "critical" deep venous reflux. Journal of Vascular Surgery 22: 532-537.

Hashimoto J, Chonan K, Aoki Y, Nishimura T, Ohkubo T, Hozawa A, Suzuki M et al. (2002) Pulse Wave Velocity and the Second Derivative of the Finger Plethysmogram in Treated Hypertensive Patients: their Relationship and Associating Factors. Journal of Hypertension 20: 2415-2422.

Heising S, Haase H, Sippel K, Reidel F, and Junger M (2009) Cutaneous Vasomotion in Patients with Chronic Venous Insufficiency and the Influence of Compression Therapy. Clinical Hemorheology and Microcirculation 41: 57-66.

Hennerici M [ed.] (1998) Vascular Diagnosis with Ultrasound. Clinical References with Case Studies. (1st edn.) New York: Thieme.

Hertman A B, and Spealman C R (1937) Observations on the finger volume pulse recorded photoelectrically. American Journal of Physiology 119: 334-335.

Hertzman A B (1938) The blood supply of various skin areas as estimated by photoelectric plethysmography. Proceedings of the Society for Experimental Biology and Medicine. 38: 328-340.

Hertzman A B, and Dillon J B (1940a) Application of Photoelectric plethysmography in Peripheral vascular Disease. American Heart Journal 20 (6): 750-761.

Hertzman A B, and Dillon J B (1940b) Distinction between Arterial, venous and flow Components in Photoelectric Plethysmography in Man. American Heart Journal 130: 177-185.

Hertzman A B, and Randall W C (1948) Regional Differences in the Basal and Maximal Rates of Blood Flow in the Skin. Journal of Applied Physiology 1: 234-241.

Hertzman A B, Randall W C, and Jochim K E (1946) The Estimation of the Cutaneous Blood Flow with the Photoelectric Plethysmography. American Journal of Physiology 145: 716-726.

Holloway G A, and Watkins D W (1977) Laser Doppler Measurements of Cutaneous Blood Flow. The Journal of Investigative Dermatology 69: 306-309.

Hyndman B W, Kitney R I, and Sayers B M (1971) Spontaneous Rhythms in Physiological Control Systems. Nature 233: 339-341.

Jago J R, and Murray A (1988) Repeatability of peripheral pulse measurements on ears, fingers and toes using photoelectric plethysmography. Clinical Physics & Physiological Measurement 9: 319-330.

Jeong G Y, Yu K H, and Kim N G (2005) Continous Blood Pressure Monitoring Using Pulse Wave Transit Time. Kintex: 2-5.

Johnson J M, Taylor W F, Sheperd A P, and Park M K (1984) Laser Doppler Measurement of Skin Blood Flow Comparison with Plethysmography. Journal of Applied Physiology 56: 798-802.

Jones D P (1987) Medical electro-optics: Measurements in the Human Microcirculation. Physics and Technology. 18: 79-85.

Kahn S R, and Ginsberg J S (2004) Relationship between deep venous thrombosis and the post-thrombotic syndrome. Archives of Internal Medicine 164: 17-26.

Kamal A A R, Harness J B, Irving G, and Mearns A J (1989) Skin Photoplethysmography- A review. Computer Methods and Programs in Biomedicine 28: 257-269.

Kerstein M D, and Reis E D (2001) Lower extremity wounds. Journal of Wound Care 10: 395-404.

Lax H, Feinberg A W, and Blake J F (1955) Studies of the Arterial Pulse Wave: The Normal Pulse Wave and its Modification in the Presence of Human Arteriosclerosis. Journal of Chronic Disease 3: 618-631.

Levy B (2005) Berne & Levy Principles of Physiology. 4th ed. New York: Mosby.

Linberg L G, Ugnell H, and Oberg P A (1992) Monitoring of respiration and heart rates using a fibre-optic sensor. Medical & Biological Engineering & Computing 30: 533-537.

Maiman T H (1960) Stimulated optical radiation in ruby. Nature 187: 493-494.

Marinelli M R, Beach K W, Glass M J, Primozich J F, and Strandness D E (1979) Non-invasive testing vs clinical evaluation of arterial disease. Journal of the American Medical Association 241: 2031-2034.

McMahon M P, Campell S B, Shannon G F, Wilkinson J S, and Fleming S J (1996) A non-invasive continuous method of measuring blood volume during haemodialysis using optical techniques. Medical Engineering & Physics 18: 105-109.

Megnien J L, Simon A, Denarie N, Del-Pino M, Gariepy J, Segond P, and Levenson J (1998) Aortic Stiffening Does Not Predict Coronary and Extracoronary Atherosclerosis in Asymptomatic Men at Risk for Cardiovascular Disease. American Journal of Hypertension 11: 293-301.

Meissner M H, Moneta G, Burnand K, Gloviczki P, Lohr J M, Lurie F, Mattos M A et al. (2007) The hemodynamics and diagnosis of venous disease. Journal of Vascular Surgery 46: S4-S24.

Millasseau S C, Guigui F G, Kelly R P, Prasad K, Cockcroft J M, Ritter J M, and Chowienczyk P J (2000) Non-invasive Assessment of the Digital Volume Pulse: Comparison with the peripheral Pressure Pulse. Hypertension 36: 952-956.

Millasseau S C, and Kelly R P (2003) The Vascular Impact of Aging and Vasoactive Drugs: Comparison of Two Digital Volume Pulse Measurements. American Journal of Hypertension 16: 467-472.

Millasseau S C, Kelly R P, Ritter J M, and Chowienczyk P J (2002) Determination of Age Related Increase in Large Artery Stiffness by Digital Pulse Contour Analysis. Clinical Science 103: 371-377.

Millasseau S C, Ritter J M, Takazawa K, and Chowienczyk P J (2006) Contour analysis of the photoplethysmographic pulse measured at the finger. Journal of Hypertension 24: 1449-1456.

Murray A, and Marjanovic D (1997) Optical Assessment of Recovery of the Tissue Blood Supply After Removal of Externally Applied Pressure. Medical & Biological Engineering & Computing 35: 425-427.

Murray W B, and Foster P A (1996) The peripheral pulse wave: Information overlooked. Journal of Clinical Monitoring 12: 365-377

Nguyen T H (2005) Evaluation of Venous Insufficiency. Seminars in Cutaneous Medicine and Surgery 24: 162-174.

Nichols W W, and O'Rourke M F (2005) McDonald's Blood Flow In Arteries. 5th Edition ed. London: Hodder Arnold.

Nicolaides A N (2000) Investigation of chronic venous insufficiency: A consensus statement. Circulation 102: E126-163.

Nicolaides A N, and Miles C (1987) Photoplethysmography in the Assessment of Venous Insufficiency. Journal of Vascular Surgery 5: 405-412.

Nicolaides A N, and Zukowski M D (1986) The Value of Dynamic Venous Pressure Measurements. World Journal of Surgery 10: 919-924.

Nijboer J A, and Mahieu H F (1981) Photoelectric Plethysmography-Some Fundamental aspects of the Reflection and Transmission method. Clinical Physics & Physiological Measurement 2: 205-214.

Nilsson G E, Tenland T, and Oberg P A (1980a) Evaluation of a Laser Doppler Flowmeter for Measurement of Tissue Blood Flow. Institute of Electrical and Electronic Engineers Transactions on Biomedical Engineering BME-27: 597-604.

Nilsson G E, Tenland T, and Oberg P A (1980b) A New Instrument for Continuous Measurement of Tissue Blood Flow by Light Beating Spectroscopy. Institute of Electrical and Electronic Engineers Transactions on Biomedical Engineering BME-27: 12-19.

Nitzan M, Babchenko A, and Khanokh B (1999) Very low frequency variability in arterial blood pressure and blood volume pulse. Medical & Biological Engineering & Computing 37: 54-58.

Nitzan M, Babchenko A, Khanokh B, and Landau D (1998) The variability of the photoplethysmographic signal--a potential method for the evaluation of the autonomic nervous system. Physiological Measurement 19: 93-102.

Nitzan M, Khanokh B, and Slovik Y (2002) The difference in pulse transit time to the toe and finger measured by photoplethysmography. Physiological Measurement 23: 85-93.

Nitzan M, Turivnenko S, Milston A, and Babchenko A (1995) Low frequency variability in the blood volume and in the blood volume pulse measured by photoplehtysmography. Journal of Biomedical Optics 1: 223-229.

Norris C S, Beyrau A, and Barnes R W (1983) Quantitative Photoplethysmography in Chronic Venous Insufficiency: A New Method of Non-Invasive Estimation of Ambulatory Venous Pressure. Surgery 94: 758-764.

O'Rourke M F, Pauca A, and Jiang X J (2001) Pulse wave analysis. British Journal of Clinical Pharmacology 51: 507-522.

Oates C (2001) Cardiovascular Haemodynamics and Doppler Waveforms. First ed. London: Greenwich Medical Media.

Oliva I, and Roztocil K (1983) Toe Pulse Wave Analysis in Obliterating Atherosclerosis. Angiology 34: 610-619.

Ouriel K (2001) Peripheral arterial disease. Lancet 358: 1257-1264.

Ouriel K, McDonnell A E, Metz C E, and Zarins C K (1982) A critical evaluation of stress testing in the diagnosis of peripheral vascular disease. Surgery 91: 686-693.

Pasternak R C, Criqui M H, Benjamin E J, Fowkes F G R, Isselbacher E M, McCullough P A, Wolf P A et al. (2004) Atherosclerotic Vascular Disease Conference: Writing Group I: Epidemiology. Circulation 109: 2605-2612.

Rashid P (1996) The Effect of Probe Position, Calf Muscle Pump Function and Lipodermatosclerosis on Photoplethysmographic Venous Refilling Time. Phlebology 11: 137-140.

Riva C, Ross B, and Benedek G B (1972) Laser Doppler measurements of blood flow in capillary tubes and retinal arteries. Laser Doppler Measurements 11: 936-944.

Rosfors S (1990) Venous Photoplethysmography: Relationship Between Transducer Position and Regional Distribution of Venous Insufficiency. Journal of Vascular Surgery 11: 436-440.

Rossi M, Bertuglia S, Varanini M, Giusti A, Santoro G, and Carpi A (2005) Generalised wavelet analysis of cutaneous flowmotion during post-occlusive reactive hyperaemia in patients with peripheral arterial obstructive disease. Biomedicine & Pharmacotherapy 59: 233-239.

Rutherford R B [ed.] (1995) Vascular Surgery (4th edn). Philadelphia: W.B. Saunders Company.

Rutherford R B [ed.] (2005) Vascular Surgery. (6th edn.) Philadelphia: W.B. Saunders Company.

Scanlon V C (1997) Understanding Human Structure and Function. (1st edn) Philadelphia: Robert G. Martone.

Serup J, Jermec G B E, and Grove G L [eds.] (2006) Handbook of non-invasive methods and the skin. (2nd edn.) Florida: CRC/Taylor & Francis

Sherebrin M H, and Sherebrin R Z (1990) Frequency analysis of the peripheral pulse wave detected in the finger with a photoplethysmograph. Institute of Electrical and Electronic Engineers Transactions on Biomedical Engineering 37: 313-317

Shung K K (2006) Diagnostic Ultrasound Imaging and Blood Flow Measurements. Florida: Taylor and Francis.

Sinex J E (1999) Pulse Oximetry: Principles and Limitations. American Journal of Emergency Medicine 17: 59-66.

Smith R P, Argod J, Pepin J L, and Levy A (1999) Pulse transit time: an appraisal of potential clinical applications. Thorax 54: 452-457.

Smits G J, Roman R J, and Lombard J H (1986) Evaluation of Laser Doppler Flowmetry as a Measure of Tissue Blood Flow. Journal of Applied Physiology 61: 666-672.

Sproule M W (1997) The value of light reflection rheography as a screeing tool for DVT. The British Journal of Radiology 70: 782-785.

Stein R, Hriljac I, Halperin J L, Gustavson S M, Teodorescu V, and Olin J W (2006) Limitation of the resting ankle-brachial index in symptomatic patientswith peripheral arterial disease. Vascular Medicine 11: 29-33.

Stern M D (1975) In vivo evaluation of microcirculation by coherent light scattering. Nature 254: 56-58.

Stern M D, Lappe D L, Bowen P D, Chimosky J E, Holloway G A, Keiser H R, and Bowman R L (1977) Continuous measurement of tissue blood flow by laser Doppler spectroscopy. American Journal of Physiology 232: H441-H448.

Takazawa K, Tanaka N, Fujita M, Matsuoka O, Saiki T, Aikawa M, Tamura S et al. (1998) Assessment of Vasoactive Agents and Vascular Aging by the Second Derivative of Photoplethysmographic Waveform. Hypertension 32: 365-370.

Tanaka T, Riva C, and Ben-Sira I (1974) Blood velocity Measurements in Human Retinal Vessels. Science 186: 830-831.

Thomas P R S, Butler C M, Bowman J, Grieve N W T, Bennett C E, Taylor R S, and Thomas M H (1991) Light Reflection Rheography: an Effective Non-Invasive Technique for Screening Patients with Suspected Deep Vein Thrombosis. British Journal of Surgery 78: 207-209.

Tremper K K (1989) Pulse Oximetery. Chest 95: 713-715.

Ugnell H, and Oberg P A (1995) The time-variable photoplethysmographic signal; dependence of the heart synchronous signal on wavelength and sample volume. Medical Engineering & Physics 17: 571-578.

Ulrich Schultz-Ehrenburg V B (2001) Value of Quantitative Photoplethysmography for Functional Vascular Diagnostics. Skin Pharmacology and Applied Skin Physiology 14: 316-323.

Watkins D W, and Holloway G A (1978) An Instrument to Measure Cutaneous blood Flow Using the Doppler Shift of Laser Light. Institute of Electrical and Electronic Engineers Transactions on Biomedical Engineering BME-25: 28-33.

Weinman J, and Manoach M (1962) A photoelectric Approach to the Study of Peripheral Circulation. American Heart Journal 63: 219-231.

Williams P M, Barrie W W, and Donnelly P K (1994) Light Reflection Rheography: A Simple Method of Assessing Lower Limb Venous Filling. Journal of the Royal College of Surgeons of Edinburgh 39: 89-92.

Yao S T, Hobbs J T, and Irvine W T (1969) Ankle systolic pressure measurements in arterial disease affecting the lower extremities British Journal of Surgery 56: 676-679.

Yeh Y, and Cummins H Z (1964) Localised Fluid Flow Measurements with a He-Ne Laser Spectrometer. Applied Physics Letters 4: 176-178.

Arterial Appendix A

Patient Disease List

Patient No	Disease Severity score		Description of Disease 3=moderate, 4=significant, 5=occlusive	
	R	L		
3	3	4	Diffuse SFA disease bilaterally	
4		3	Diffuse mid to distal popliteal	
13	5	4	**R**-occluded SFA reconstitutes proximal popliteal **L**-SFA to popliteal diffusely narrowed	
18	4	4	Bilateral distal aorta stenosis	
25	3	4	Bilateral stenosis at bifurcation of CFA and SFA	
26	3		Distal SFA and adductor regions are moderately narrowed	
27	4	5	**R**- EIA origin stenosis **L**-The SFA-adductor occlusion. There is also a mid/distal popliteal stenosis	
28	3	4	Bilateral distal aorta and proximal CIA stenoses	
32	3		Stenosis at trifurcation level	
33	4		CIA origin stenosis. Small AAA	
34	3	3	Bilateral distal SFA to proximal adductor stenoses	
37	3	4	Bilateral mid SFA to proximal adductor stenoses	

39	3		Mid SFA stenosis	
43	5	5	Bilateral mid SFA to mid adductor occlusions	
45	4		Proximal EIA stenosis	
50	3	3	Bilateral mid SFA to proximal adductor	
63		5	7cm occlusion from SFA origin	
64		4	Distal SFA/proximal adductor stenosis and mid popliteal stenosis	
70		4	SFA/PFA bifurcation stenosis	
78	3		Distal SFA stenosis	
83	3		Distal SFA stenosis	
85	3	4	Bilateral EIA origin stenosis	
86	4		Proximal popliteal stenosis	
87	4	5	**R**-proximal SFA moderately narrowed, with a significant adductor stenosis **L**-SFA occludes 10cm from origin, reconstitutes adductor region	
88	5	4	R-SFA stenosis that occludes in distal SFA, reconstitutes adductor region L-Significant distal SFA stenosis.	
89	5	5	Bilateral SFA origin to distal SFA occlusions	
90	4	4	Bilateral distal aorta stenoses	
91	4	4	Bilateral distal SFA stenoses	

93		5	SFA origin to adductor occlusion	
94	3		SFA and PFA origin stenosis and a tight PTA stenosis	
95	4	5	**R**- moderate mid SFA and a significant distal SFA stenosis. **L**-3-4cm mid SFA occlusion. Also the ATA is occluded, reconstitutes ankle	
96	5		6cm AAA. SFA occluded from origin, reconstitutes in proximal popliteal	
97	5		PFA origin stenosis. SFA occluded with proximal popliteal reconstitution.	
98	4	5	**R**-SFA moderately narrowed with significant proximal and mid SFA stenosis **L**-SFA occludes from origin with adductor reconstitution	
99		3	Distal SFA stenosis	
100	4		CIA origin stenosis	
101		3	Distal SFA stenosis	
102	4		CIA origin stenosis	
103	5	5	R-Significant PFA origin stenosis. SFA to proximal adductor occlusion. L-CIA occluded. Significant mid SFA stenosis	
104	5		Below knee popliteal occlusion	
105		4	Proximal EIA stenosis	
106	5	5	**R**-Significant PFA SFA origin stenosis. SFA occludes 10cm from origin. Distal SFA reconstitution, but vessel reoccludes in adductor with above knee popliteal reconstitution **L**- SFA occluded throughout. Above knee popliteal reconstitution	

107		5	SFA origin to above knee popliteal reconstitution	
108		5	EIA and CFA occluded	
113	3		Distal SFA stenosis	
115		3	Mid SFA stenosis	

ROC Analysis to Choose Best Curve for PWTT and Area combined

Moderate Disease

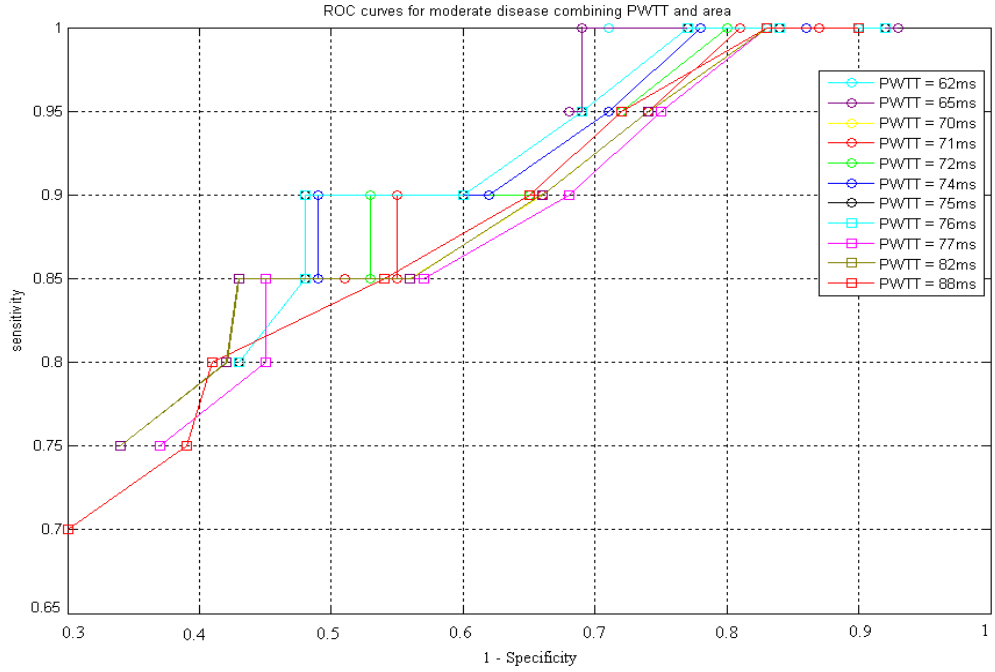

Significant Disease

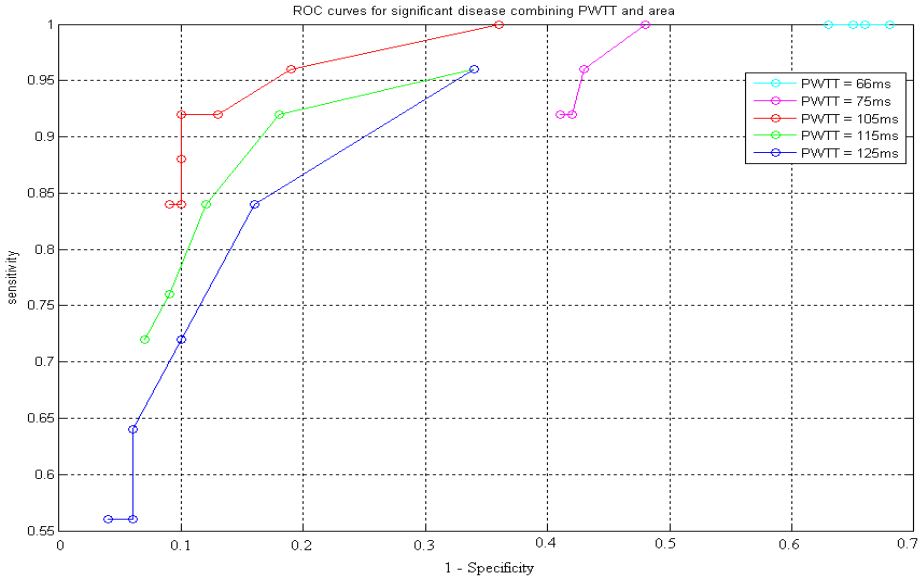

Occlusive Disease

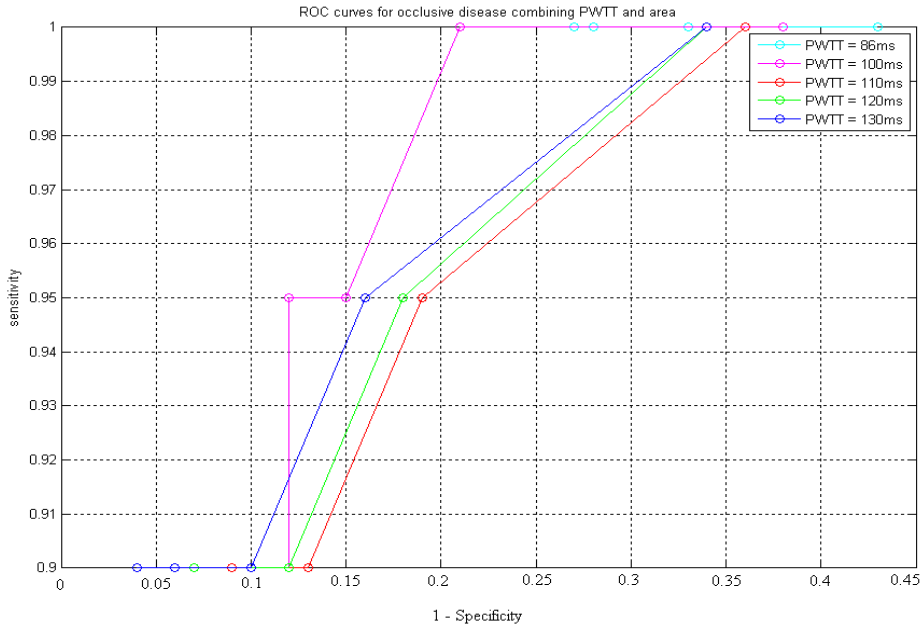

Significant and Occlusive Disease

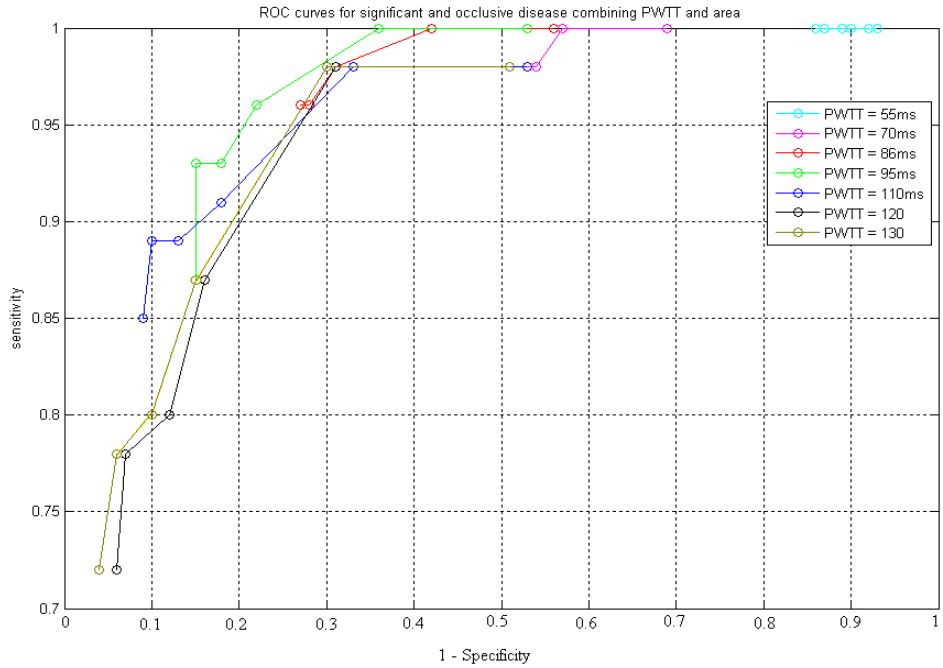

Moderate Significant and Occlusive Disease

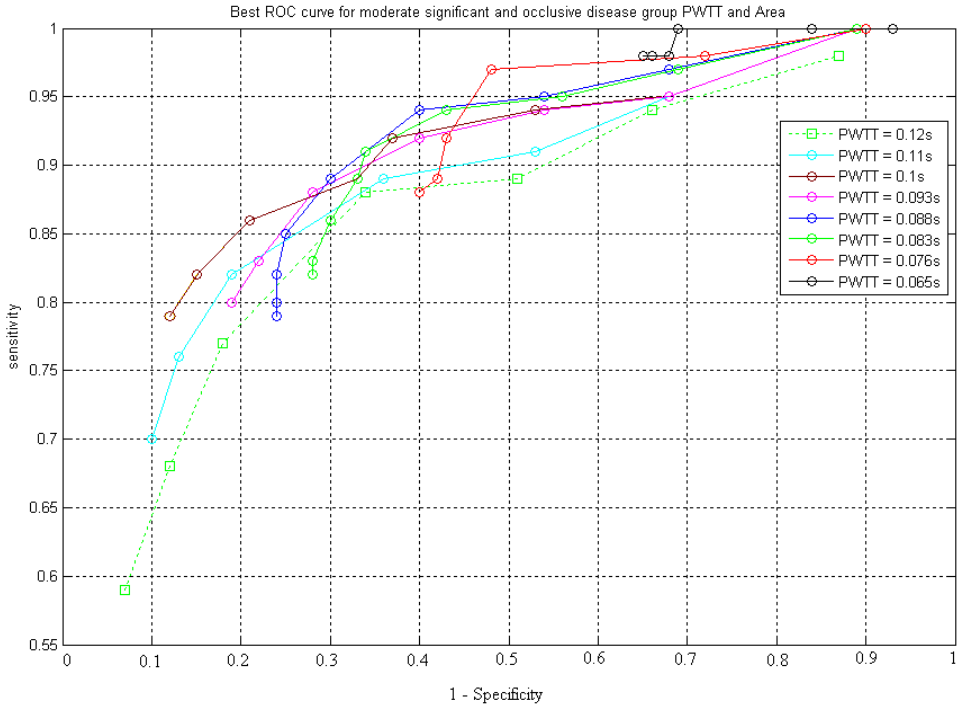

Venous Appendix B

Patient information and CEAP score

Pt no	Age	Legs R,L,B	clinical	etiologic	anatomical	pathophysiological	Sex
36(90)	76	R	3,s	s	d,p	r,13,14,15,18	M
2(34)	65	R	0,s	s	d	r:15(peroneal only)	F
13(47)	72	R	3,s	s	d	r14,15	M
14(48)	53	L	1,4,s	s	d	r11,13,14,15	M
15(49)	67	L	1,2,4	s	s,d	r2,3,15	F
16(51)	64	L	4,s	s	s,d	r3,4,14,15	M
17(52)	48	L	s	s	d	r14,15	F
18(53)	59	L	1,3,s	s	d	r14,15	F
19(54)	51	L	s	s	d	r13,14,15	M
20(56)	65	R	1	s	p,d	r1,14,15,18	M
21(57)	63	R	2,3,s	s	p,d	r,o,1(ankle),2,3(occluded),14,15,18(cockett II)	F
22(59)	48	L	s	s	s,d	r,o,4(phlebitis),13,14	F
23(60)	76	L	1,2,3,4a,6	s	s,d	r,5,14,15	M
24(65)	76	L	1,2,3,s	n	s,d	r,1,3,14,15,18	F
25(67)	44	L	2,4b,s	s	s,d	r,3,14,15,18	M
26(68)	49	L	1,3,4a,	s	d	r,14,15	M
27(70)	70	L	1,2(trough),3,4b,5,s)	s	p,d	r,1,13,14,15,18	F
28(72)	78	L	1,2,3,4,5,s	s	d,p,s	r,14,15,18	F
29(74)	72	L	3	p	d	r,14,15	M
30(75)	55	L	1,3,s	s	d	r,15	M
31(76)	49	R	3,4,s	s	s,d,p	r,3,13,14,15,18	M
32(81)	89	R	3,4,6,s	?	d,p	r,15,18	F
33(85)	74	R	2,4a	s?	s,p,d	r,2,3,14,15,18	M
34(89)	78	L	1,2,s	s	s,p,d	r,4,14,15,18	F
35(91)	46	R	2,3,s	s	s,p,d	r,14,15,18	M

CEAP Classification

The CEAP classification was created because of the need for a consistent approach to the evaluation of venous disease. It was produced by an international committee of clinical experts and is a comprehensive tool that organises the information into categories to provide a descriptive classification system. CEAP stands for Clinical, Etiological, Anatomical and Pathophysiological and forms a classification system that deals with all forms of chronic venous disorders. The full CEAP classification is shown below:

Clinical Classification

C0: No visible of palpable signs of venous disease
C1: Telangiectasia or reticular veins
C2: Varicose veins
C3: Oedema
C4a: Pigmentation and/or eczema
C4b: Lipodermatosclerosis and/or atrophie blanche
C5: Healed ulcer
C6: Active venous ulcer
S: Symptoms including ache, pain, tightness, skin irritation, heaviness, muscle cramps as well as other complaints attributable to venous dysfunction.
A: Asymptomatic

Etiologic Classification

Ec: Congenital
Ep: Primary
Es: Secondary (postthrombotic)
En: No venous etiology identified

Anatomic Classification

As: Superficial veins
Ap: perforator veins
Ad: Deep veins
An: No venous location identified

Pathophysiologic Classification

Basic CEAP:
Pr: Reflux
Po: Obstruction
Pr,o: Reflux and obstruction
Pn: No venous pathophysiology identified

Advanced CEAP

Same as basic, with the addition that any of the 18 named venous segments can be utilised as locators for venous pathology:

Superficial veins:

1. Telangiectasias/reticular veins
2. Long saphenous veins (LSV) above knee
3. LSV blow knee
4. Short saphenous vein (SSV)
5. Nonsaphenous veins

Deep veins:

6. Inferior vena cava
7. Common iliac vein
8. Internal iliac vein
9. External iliac vein
10. Pelvic: Gonadal, broad ligament veins, other
11. Common femoral vein
12. Deep femoral vein (profunda vein)
13. Superficial femoral vein
14. Popliteal vein
15. crural: anterior tibial, posterior tibial, peroneal veins (all paired)
16. Muscular: gastrocnemial, soleal veins, other

Perforator veins:

17. Thigh
18. Calf

Frequency Response of FIR Filter

Myogenic (0.06Hz to 0.12Hz) Filter Response

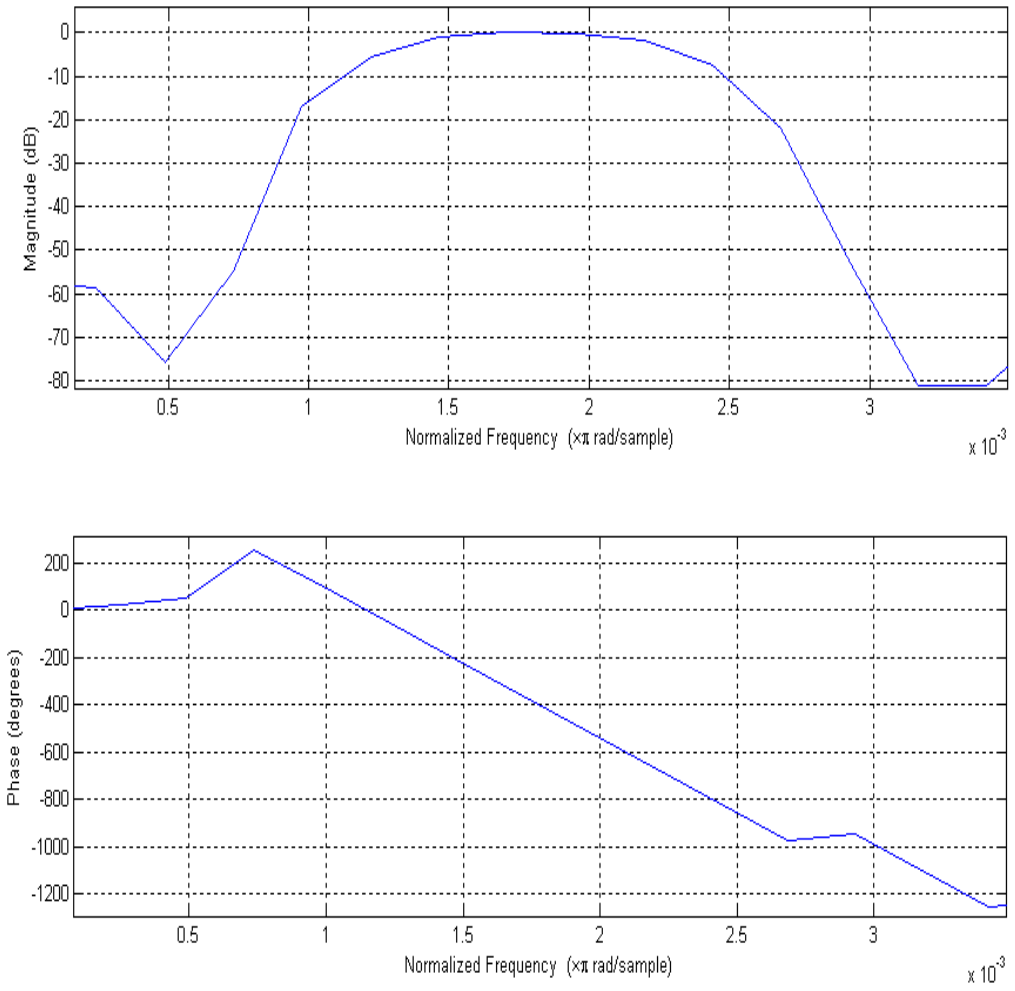

Figure 104 Magnitude and phase response of myogenic FIR filter

Respiration (0.15Hz to 0.4Hz) Filter Response

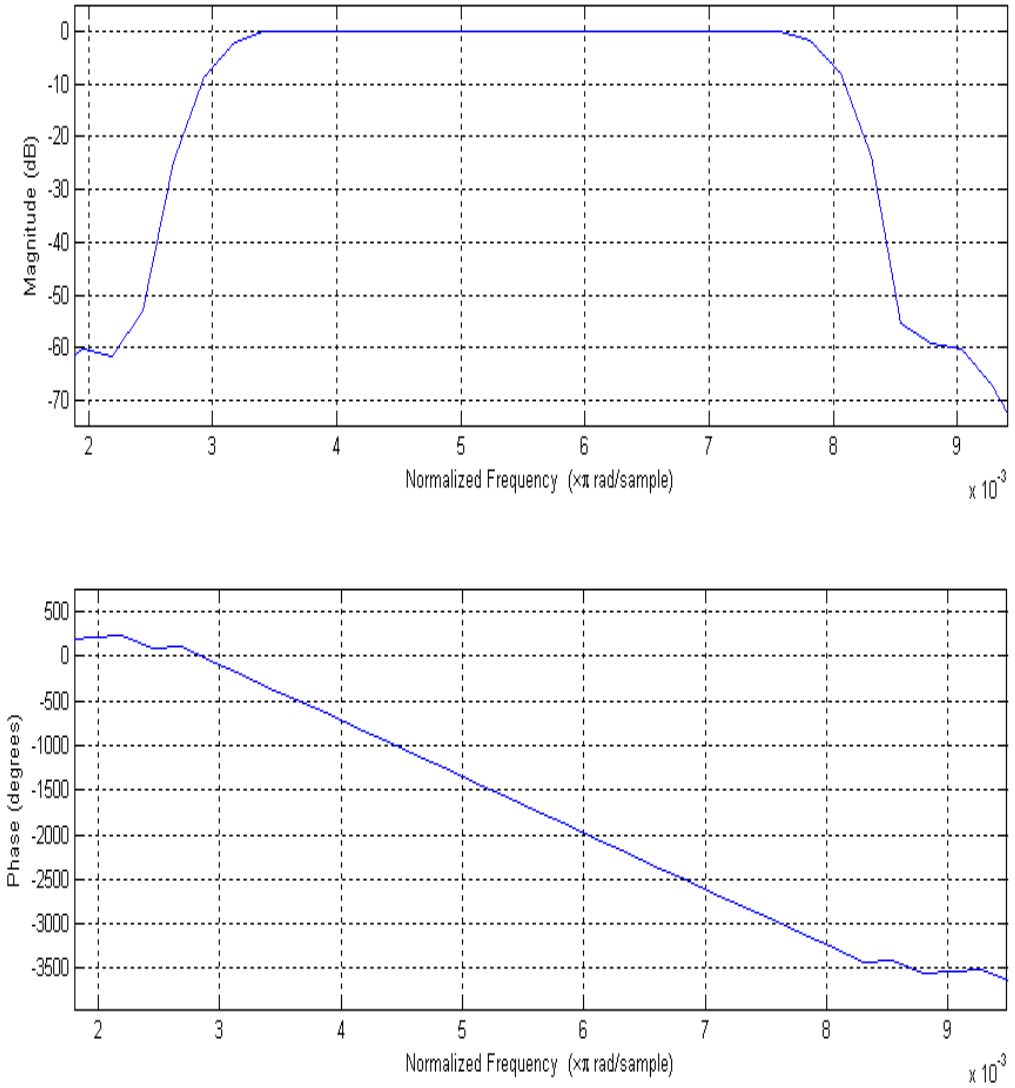

Figure 105 Magnitude and phase response of respiration FIR filter

Example QQ plots of Maximum Gradients for Above and Below knee Controls and Patients for Myogenic and Respiration Frequencies

Myogenic Frequencies

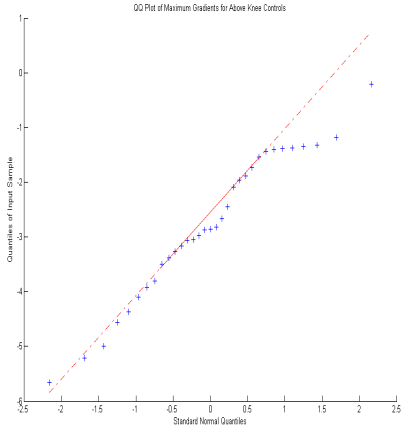

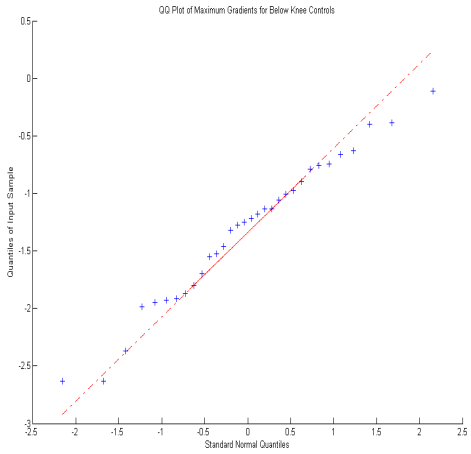

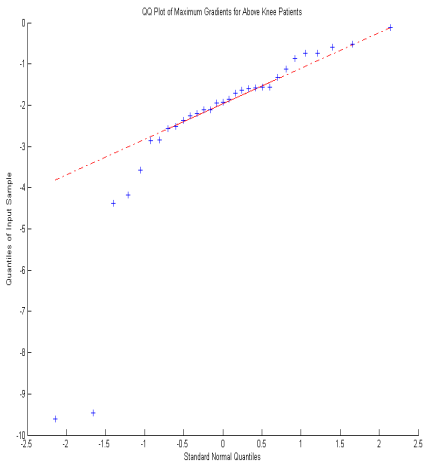

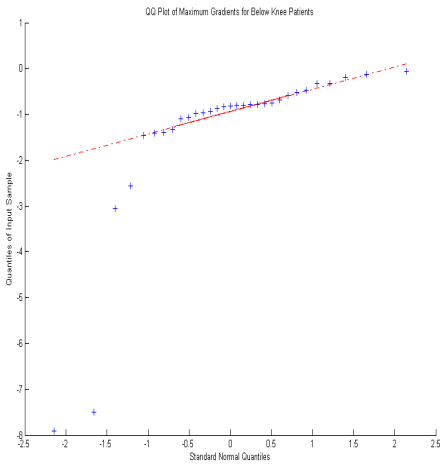

Respiration Frequencies

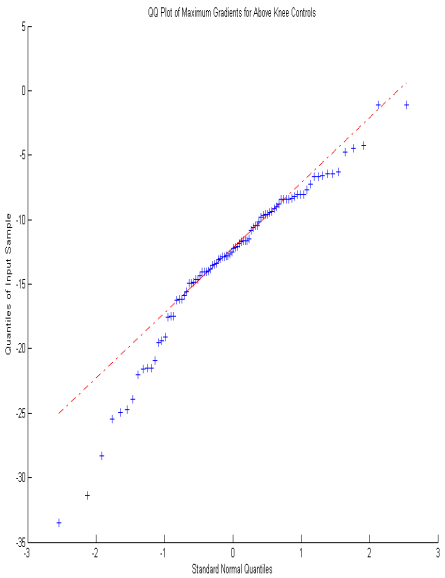

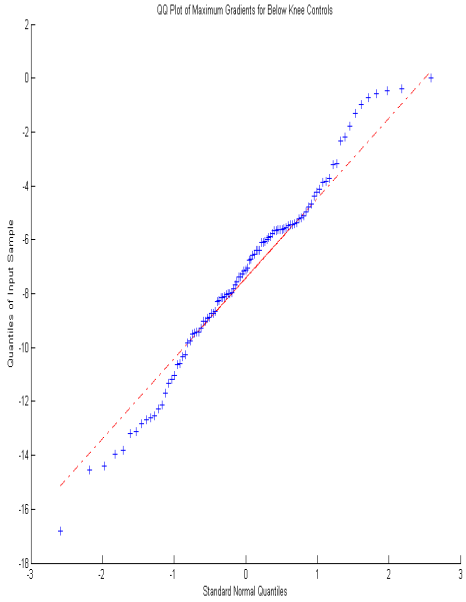

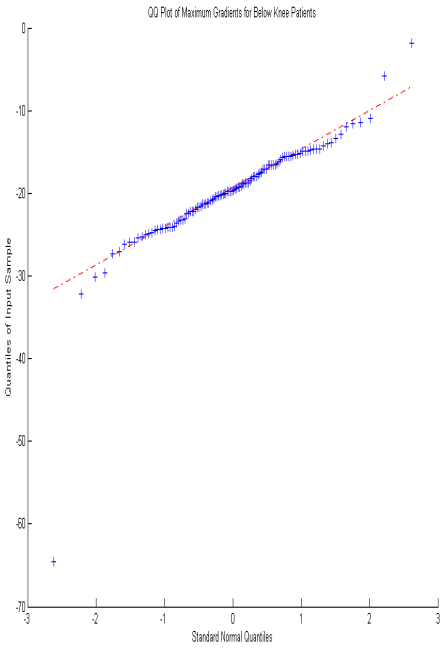

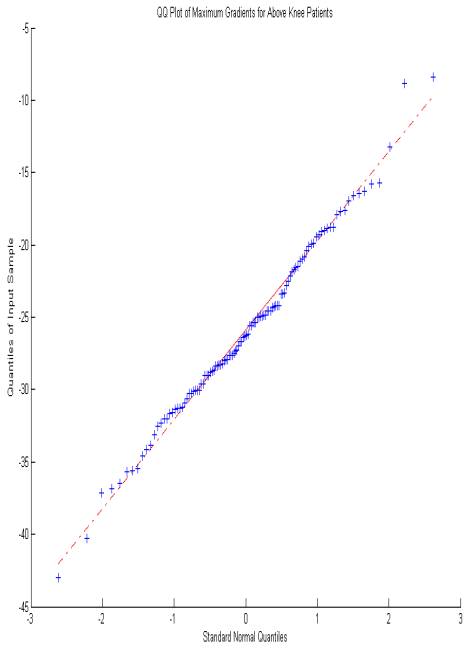

Q-Q Plots of Difference in Proportion of Total Number of Phase Changes in Troughs Between Above and Below knee

Myogenic Frequencies

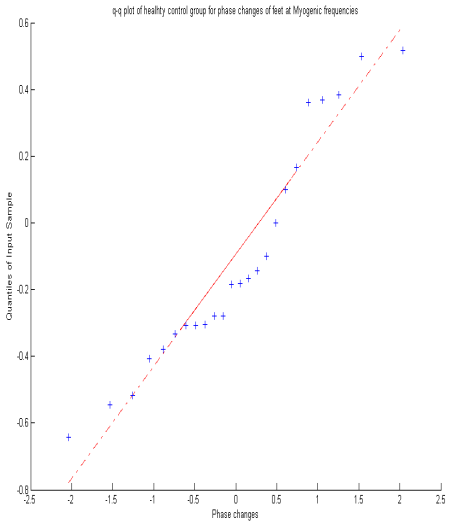

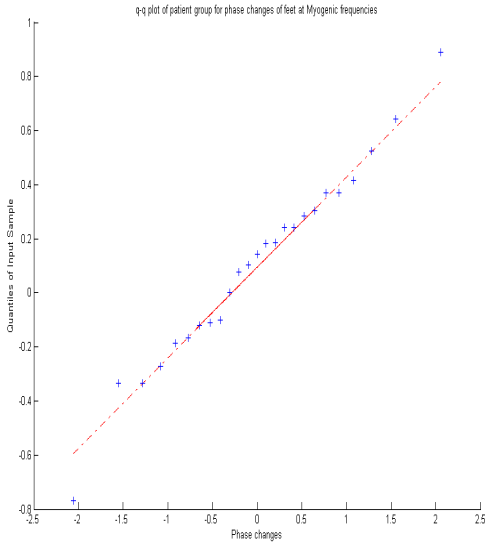

Respiration frequencies

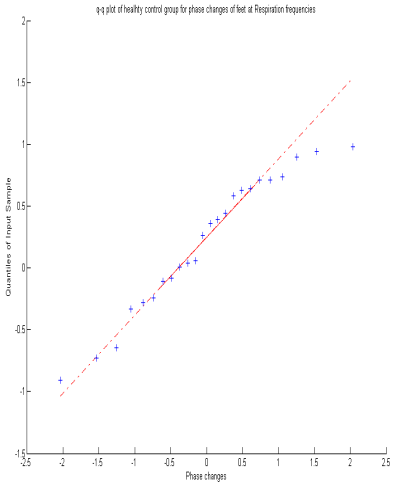

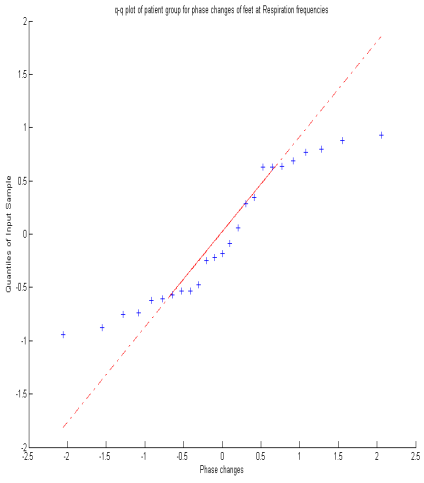

Q-Q Plots of Difference in Proportion of Total Number of Phase Changes in Peaks Between Above and Below knee

Myogenic Frequencies

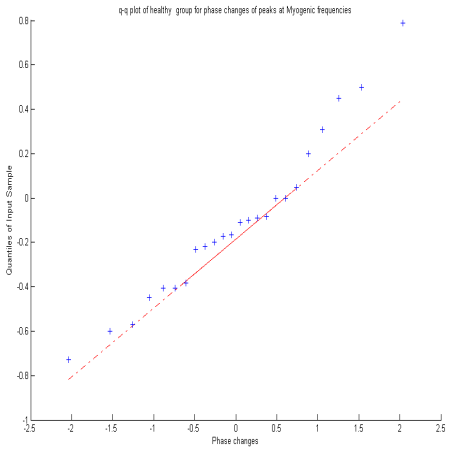

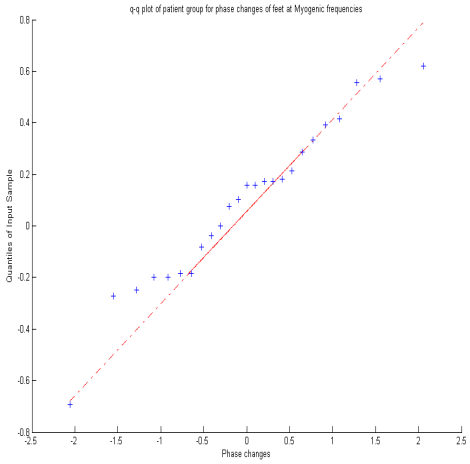

Respiration Frequencies

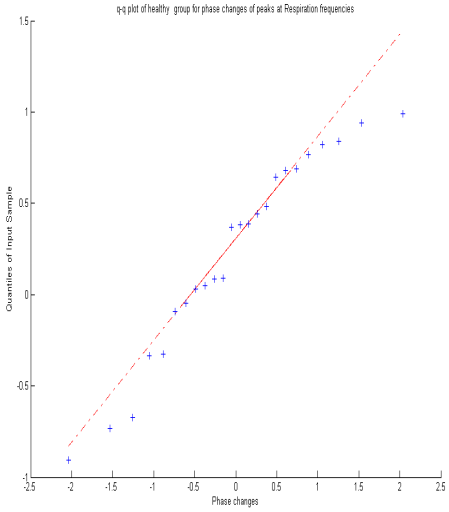

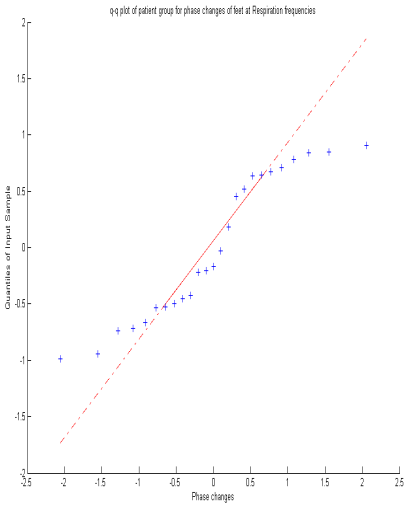

Box-plots of gradient data at respiration frequencies

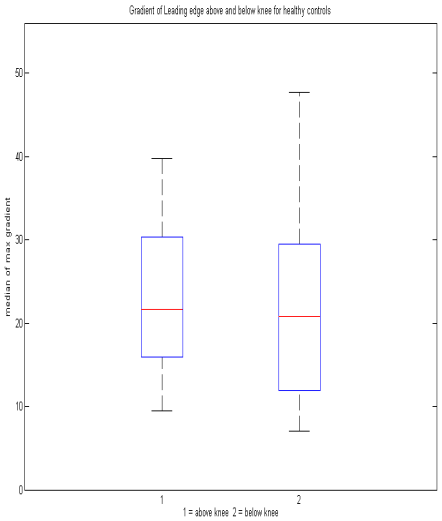

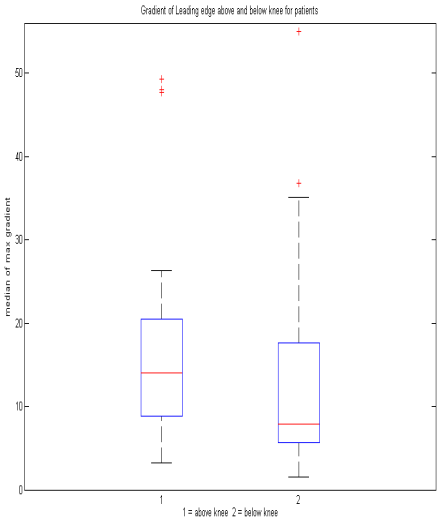

Gradient of leading edge at respiration frequencies

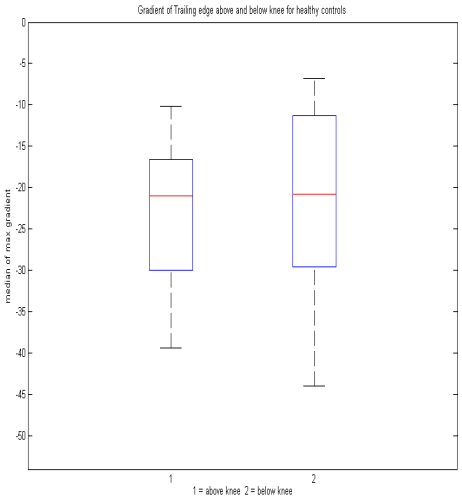

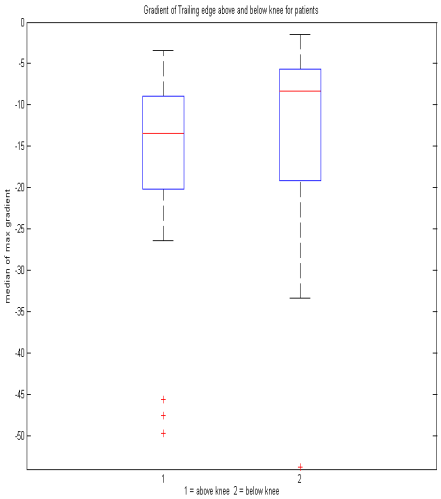

Gradient of trailing edge at respiration frequencies

Boxplot of delay data for signal troughs

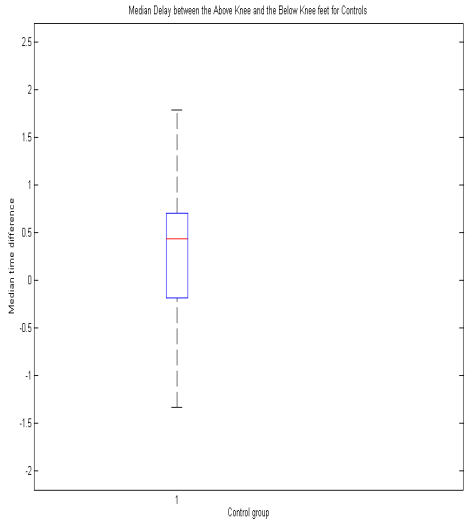

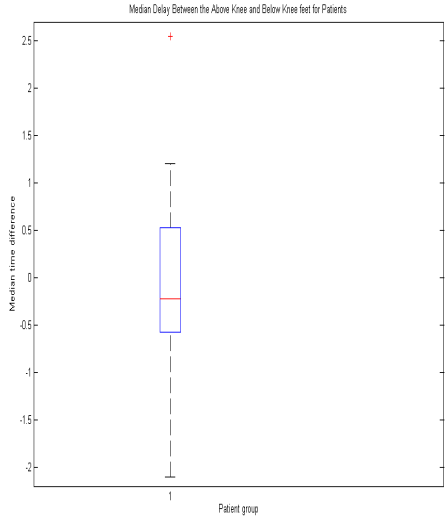

Delays between the above and below knee troughs at myogenic frequencies

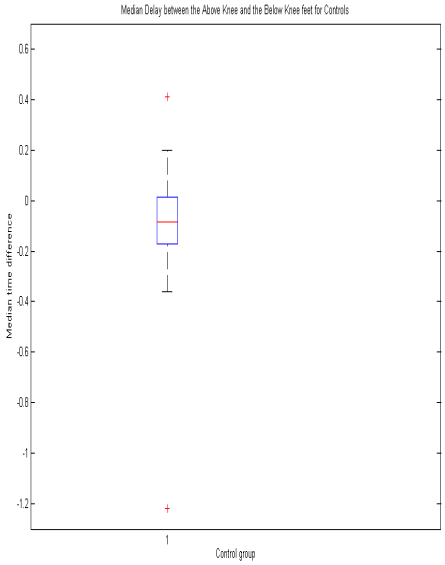

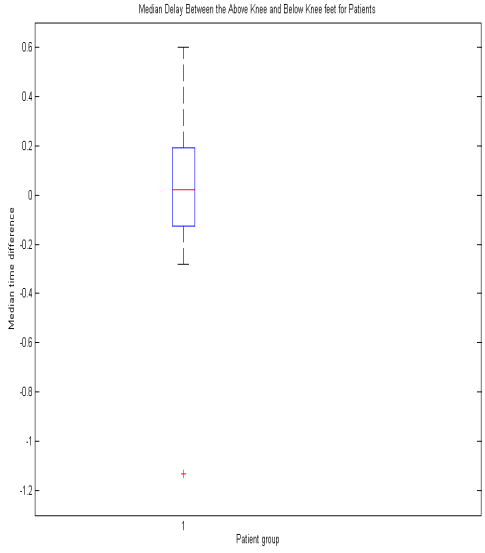

Delays between the above and below knee troughs at respiration frequencies

Appendix C

The following tables in appendix C show examples of some of the measurements from the arterial and venous groups.

List of PWTT and area measurements for arterial control group

Controls	PWTT (ms)	Normalised Area (a.u)
Pt0	120	5581
Pt0	106	5497
Pt2	103	4770
Pt5	82	4903
Pt6	56	3915
Pt6	53	4067
Pt8	56	4770
Pt9	68	4732
Pt10	85	5000
Pt10	68	4493
Pt11	56	4558
Pt11	62	4491
Pt12	69	4748
Pt14	56	4089
Pt14	57	3931
Pt16	68	4039
Pt17	90	5229
Pt19	74	4261
Pt19	60	4423
Pt20	68	4556
Pt21	68	4396
Pt22	74	4592
Pt23	88	4742
Pt23	76	4909
Pt24	73	4414
Pt24	76	4559
Pt30	56	4319
Pt30	65	4504
Pt31	96	4817
Pt31	71	4599
Pt35	94	4930
Pt36	88	4342
Pt36	65	4356
Pt40	42	4990
Pt40	115	5226
Pt42	94	6178
Pt44	33	4643
Pt46	72	4262
Pt48	76	4028
Pt48	71	4190
Pt49	121	4785
Pt56	68	4636

Pt56	58	4292
Pt61	96	4822
Pt62	77	4925
Pt62	80	4806
Pt66	43	4595

List of PWTT and area measurements for arterial patient group

Patients	PWTT (ms)	Normalised Area (a.u)
Pt3	95	4838
Pt4	172	5286
Pt25	71	4464
Pt26	130	4912
Pt28	73	4986
Pt32	113	4874
Pt34	110	4866
Pt34	90	4859
Pt37	103	4851
Pt39	65	4843
Pt50	83	4835
Pt50	82	4828
Pt78	63	4820
Pt83	150	4812
Pt85	117	4805
Pt94	134	4797
Pt99	73	4789
Pt101	77	4781
Pt113	71	4774
Pt115	124	4766
Pt3	115	4758
Pt13	106	4751
Pt18	170	4743
Pt18	209	4735
Pt25	110	4727
Pt27	161	4720
Pt28	209	4712
Pt33	157	4704
Pt37	117	4697
Pt45	131	4689
Pt64	147	4681
Pt70	67	4673
Pt85	117	4666
Pt86	124	4658
Pt87	73	4650
Pt88	128	4643
Pt90	159	4635
Pt90	151	4627
Pt91	110	4619
Pt91	52	4612
Pt95	68	4604
Pt98	145	4596
Pt100	119	4589

Pt102	138	4581
Pt105	106	4573
Pt13	147	4565
Pt27	223	4558
Pt43	148	4550
Pt43	133	4542
Pt63	196	4535
Pt87	149	4527
Pt88	95	4519
Pt89	242	4511
Pt89	204	4504
Pt93	114	4496
Pt95	118	4488
Pt96	331	4480
Pt97	211	4473

List of above and below knee median leading edge gradients at respiration frequencies for the venous control group

Controls	Above knee gradients (a.u)	Below knee gradients (a.u)
Pt4	40	21
Pt5	21	11
Pt6	33	44
Pt8	28	13
Pt9	27	23
Pt10	12	7
Pt11	15	8
Pt12	10	38
Pt3	16	21
Pt7	35	29
Pt92	28	16
Pt93	31	48
Pt94	19	15
Pt95	37	7
Pt96	16	11
Pt97	16	29
Pt99	11	12
Pt101	28	30
Pt102	32	22
Pt103	17	17
Pt104	19	42
Pt105	22	28
Pt106	15	10
Pt107	29	34

List of above and below knee median leading edge gradients at respiration frequencies for the venous patient group

Patients	Above knee gradients (a.u)	Below knee gradients (a.u)
Pt1	7	5
Pt2	12	8
Pt13	10	7
Pt14	14	14
Pt16	11	12
Pt15	26	20
Pt17	19	5
Pt18	5	2
Pt19	15	7
Pt20	26	22
Pt21	9	5
Pt22	3	4
Pt23	17	8
Pt24	9	11
Pt25	14	12
Pt26	4	4
Pt27	48	35
Pt28	16	10
Pt29	7	37
Pt30	26	7
Pt31	14	7
Pt32	18	6
Pt33	13	24
Pt34	48	17
Pt35	49	55

List of below knee power densities for venous control group

Controls	Below knee power density at respiration frequencies (a.u)
Pt4	5293
Pt5	3460
Pt6	9274
Pt8	2958
Pt9	5161
Pt10	1850
Pt11	2448
Pt12	11203
Pt3	4636
Pt7	6243
Pt92	6088
Pt93	8466
Pt94	3410
Pt95	2237
Pt96	4836
Pt97	7861
Pt0099	3135
Pt101	7995
Pt102	5563
Pt103	3241
Pt104	7875
Pt105	4543
Pt106	3150
Pt107	10325

List of below knee power densities for venous patient group

Patients	Below knee power density at respiration frequencies (a.u)
Pt1	1880
Pt2	1904
Pt13	2364
Pt14	2772
Pt16	2811
Pt15	3750
Pt17	2387
Pt18	679
Pt19	1418
Pt20	4143
Pt21	1107
Pt22	2291
Pt23	1859
Pt24	2797
Pt25	3730
Pt26	1150
Pt27	9719
Pt28	2424
Pt29	11061
Pt30	2497
Pt31	2743
Pt32	1601
Pt33	4161
Pt34	7728
Pt35	1880